Thermal techniques for characterizing building insulation materials

Hussein Hafudh Humaish

Thèse de Doctorat

Mention Sciences pour l'ingénieur

Spécialité génie civil

Présentée à **l'Ecole Doctorale en Sciences Technologie et Santé (ED 585)**

de l'Université de Picardie Jules Verne

Par

HUMAISH Hussein Hafudh

Pour obtenir le grade de Docteur de l'Université de Picardie Jules Verne

Etude de techniques de mesure pour la caractérisation thermique de matériaux isolants du bâtiment

Soutenue le 14 décembre 2016, après avis des rapporteurs, devant le jury d'examen :

M. M. El-GANAOUI	**Professeur, Université de Lorraine**	**Rapporteur**
M. E. ANTCZAK	**Professeur, Université d'Artois**	**Rapporteur**
M. O. QUEMENER	**Professeur, Université d'Évry-Val-d'Essonne**	**Examinateur**
M. T. LANGLET	**Professeur, Université de Picardie Jules Verne**	**Examinateur**
M. L. MARMORET	**Maître de Conférences, Université de Picardie Jules Verne**	**Co encadrant**
M. H. BEJI	**Professeur, Université de Picardie Jules Verne**	**Directeur de thèse**
M^{me} C. PELEGRIS	**Maître de Conférences, Université de Picardie Jules Verne**	**Invitée**

Doctoral thesis

In partial fulfillment of the requirement for the degree of doctor of

Picardie Jules Verne University (France)

Domain: Civil engineering

By

Hussein Hafudh HUMAISH

Thermal techniques for characterizing Building insulation materials

Defended, December 14th 2016 in front of the following committee:

M. M. El-GANAOUI	**Professeur, Université de Lorraine**	**Rapporteur**
M. E. ANTCZAK	**Professeur, Université d'Artois**	**Rapporteur**
M. O. QUEMENER	**Professeur, Université d'Évry-Val-d'Essonne**	**Examinateur**
M. T. LANGLET	**Professeur, Université de Picardie Jules Verne**	**Examinateur**
M. L. MARMORET	**Maître de Conférences, Université de Picardie Jules Verne**	**Co encadrant**
M. H. BEJI	**Professeur, Université de Picardie Jules Verne**	**Directeur de thèse**
M^{me} C. PELEGRIS	**Maître de Conférences, Université de Picardie Jules Verne**	**Invitée**

Abstract

This thesis is part of a long-term objective to determine in situ (and / or in use) the thermal properties of building insulation materials. We want to reduce the gap between the laboratory measurement and the actual performance of insulation in buildings walls. We have set two main objectives during this study:

1- To study the possibility of using a non-steady state hot probe for measuring thermal properties of insulants,
2- To study the thermal behaviour of insulation materials in use by using a guarded hot box. Climatic conditions in temperature and humidity close to real situations can be submitted supported by hot and cold cells.

This work has shown the interest of using thermal probe to characterize insulating materials. Guarded hot box is also interesting for studies in real conditions and to follow heat and mass transfer in buildings walls.

Résumé

Cette thèse s'inscrit dans un objectif à long terme de déterminer in situ (et/ou en usage) les propriétés thermiques des matériaux isolants du bâtiment. Notre objectif est de réduire l'écart entre la mesure en laboratoire et la performance réelle des isolants dans les parois de bâtiments. Nous nous sommes fixés deux objectifs principaux au cours de cette étude:

1- Etudier la possibilité d'utiliser la sonde cylindre à choc thermique pour la mesure des caractéristiques thermiques des matériaux isolants du bâtiment,
2- Etudier le comportement thermique d'un isolant en usage en utilisant un montage basé sur le principe de la boite chaude gardée. Cet équipement permet d'effectuer des études dans des conditions climatiques en température et en humidité proches de situations réelles supportées par l'enveloppe d'un bâtiment.

Ce travail a permis d'identifier des verrous lors de l'utilisation d'une sonde à choc thermique pour caractériser des matériaux isolants. Il a aussi montré l'intérêt de la boite chaude gardée pour effectuer des études dans des conditions réelles et pour étudier les transferts de chaleur et de masse dans les parois de bâtiments.

Acknowledgement

I am extremely grateful to the director of the laboratory LTI and director of my thesis Pr. Hassen Beji for his help, encouragement and patience throughout this period of research. Also I am extremely thankful for my assistant Supervisor Laurent Marmoret who under his supervision and teachings, I have improved as researcher and gained new insight.

Thanks also go to other members of the technical staff at laboratory for innovative technology in technology institute in universities of Picardie Jules Verne. Thank you all for your help, encouragement, and for simply making my time here doing a PhD a more interesting experience.

Special thanks for pr. Olivier Quemener and Mr. Yassine Rouizi (LMEE laboratory) in Evry University of Paris and Christine Pelegris (LTI, site of Saint Quentin).

I would like also to acknowledge the financial supporter of my PhD studies from the Ministry of Higher Education and Scientific Research (MOHESR) of my country, the Republic of Iraq and special thanks for Foundation of Technical Institutes (Al-Kut Technical Institute-Department of Surveying). Also I would like to express my special thanks to the Campus France to facilitate all the obstacles especially Mr. Adrien Chalançon.

Most especially to my big family, my lovely mother, father and brothers, and to my small family, my wonderful wife and my children, for their understanding and support.

Table of Contents

Nomenclature

S_v: Volumetric surface [m-1]

A_{sg}: Surface area [m²]

V: Volume [m3]

S_m: Specific surface [m². g-1]

K_A: Air permeability [m.s-1]

U: Thermal transmittance [W m-2.K-1]

R: Thermal resistance [m2.K.W-1]

C_p: Specific heat capacity [J.kg-1K-1]

t : Measuring time [s]

P_e: Electric power dissipated in the electric resistive circuit [W]

q: Heat flux actually passing through the sample [W]

r : Sensor radius [mm]

R_s : Radius of the probe [m]

R_c : Contact resistance (= 1/H) [m².K.W-1]

H: Conductance of the air gap [W.m-2.K-1]

M: Thermal mass of the probe [-]

T: Temperature [K]

Bi: Biot number [-]

F_o: Fourier number [-]

Q_{ts} : Heat transfer through test specimen [W]

Q_{in} : Total power input [W]

Q_p : Heat transfer parallel to test specimen [W]

Q_w : Heat transfer through metering box walls [W]

S : Surface area of the metering box [m²]

Q_c: Heat transfer through cold cell (from inside to outside) [W]

R_{ts}: test specimen thermal resistance [m² K/w]

A_{ts} : Test specimen area [m²]

$T_{hot\ ts}$: Hot side test specimen surface temperature [k]

$T_{cold\ ts}$: Cold side test specimen surface temperature [k]

f_{hot}: Hot surface flow [W/m²]

f_{cold}: Cold surface flow [W/m²]

d: Thickness of the wall [m]

t_{lag}: Time lag [-]

$t_{T-hot(\max)}$: The time that the hot surface temperature is being maximum [hr]

$t_{T-cold(\max)}$: The time that the cold surface temperature is being maximum [hr]

D_f: Decreament facto [-]

$T_{hot(\min)}$: Minimum hot surface temperature [K]

$T_{cold(\min)}$: Minimum cold surface temperature [K]

Greek symbols

$\boldsymbol{\rho_o}$: Bulk density [kg.m^{-3}]

$\boldsymbol{\rho_f}$: Density of the glass fibers [kg.m^{-3}]

$\boldsymbol{\mathcal{E}}$: Porosity [%]

$\boldsymbol{\rho_v}$: True density [kg.m^{-3}]

$\boldsymbol{\omega}$: Moisture content by mass [kg.kg^{-1}]

Θ: Volumetric water content [m^3.m^{-3}]

$\boldsymbol{\lambda}$: Thermal conductivity [W.m^{-1}K^{-1}]

$\boldsymbol{\lambda_{eff}}$: Effective thermal conductivity [W.m^{-1}K^{-1}]

$\boldsymbol{\sigma}$: Stefan–Boltzmann constant = $5.67\ 10^{8}$ [W/m$^{2}\cdot$K^{4}]

$\boldsymbol{\alpha}$: Thermal diffusivity [m².s^{-1}]

γ: Euler's constant (0.5772157…)

Ω: Inertia contrast [-]

Résumé de la thèse en français:

En France, le bâtiment est le premier consommateur d'énergie (43%) et produit un quart des émissions de gaz à effet de serre, avec un parc de bâtiments qui présente une consommation moyenne annuelle de 240 KWh d'énergie primaire par m² habitable. Les cibles visées, moins de 50 kWh/m², voire des bâtiments autonomes ou à énergie positive, constituent une des clefs permettant de réduire très sensiblement nos dépenses énergétiques, et de contribuer à la réduction des GES. Dans le domaine de l'efficacité énergétique du bâtiment, il est sans conteste que le premier geste pour limiter les déperditions d'un bâtiment est de bien isoler son enveloppe. Depuis les années 1970 et les crises énergétiques mondiales, les procédés de production et de mise en œuvre des isolants du bâtiment n'ont cessé d'évoluer. Ces améliorations ont été encouragées par les règlementations thermiques successives en France. Cependant on ne dispose que de peu de données sur le comportement en usage de ces isolants. L'essentiel de ces études ont été réalisées en laboratoire dans des caissons climatisés essayant de reproduire les conditions climatiques réelles supportées par l'enveloppe des bâtiments. Des logiciels, validés par ces données expérimentales, ont été développées ces dernières années pour l'étude du transfert couplé de chaleur et de masse. Ils ont le mérite d'apporter une meilleure connaissance du comportement de la paroi dans un temps long de plusieurs années. Mais ils ne fournissent pas d'informations sur les variations de propriétés thermiques des isolants dans le temps (étude de vieillissement). Lors des études in situ, des capteurs de température et d'humidité sont intégrés dans la paroi. On prévoit également parfois des suivis sur les flux de chaleur échangés entre les surfaces interne et externe de la paroi grâce à l'installation de fluxmètre. Cependant, on ne dispose pas de mesures en continu des caractéristiques thermiques de la paroi ou des matériaux composant cette paroi.

Cette thèse s'inscrit donc dans un objectif à long terme de déterminer in situ les propriétés thermiques des matériaux isolants des parois d'un bâtiment. Des études ont déjà montrées l'influence de la présence de l'humidité sur les propriétés thermiques (conductivité et diffusivité) des matériaux poreux du bâtiment et en particulier des isolants. Il est également à noter que pour atteindre les attentes des pouvoirs publics, et évidemment aussi des occupants des bâtiments, en termes de réduction des consommations énergétiques il est indispensable que l'isolant joue efficacement son rôle. Son pouvoir isolant ne doit pas être altéré dans le temps. Pour réduire le fossé qui existe entre la mesure en laboratoire et la

performance réelle en usage, nous nous sommes fixés deux objectifs d'études principaux dans la thèse d'Hussein Humaish :

1. *Evaluer la pertinence d'utiliser la sonde cylindre à choc thermique (thermal probe) pour la caractérisation thermique de matériaux isolants,*

Cette sonde est déjà utilisée lors de mesures in situ pour caractériser thermiquement des sols argileux ou des produits alimentaires par exemple. Cependant les fabricants de sondes contre-indiquent l'utilisation de leur matériel pour des matériaux poreux de conductivité thermique inférieure à 0.1 W/m.K (et donc pour les matériaux isolants). Durant ce travail, nous chercherons, tout d'abord, à comprendre cette restriction en identifiant les limites à partir de la théorie et de l'expérimentation. Puis nous tenterons de proposer des solutions innovantes pour la caractérisation des matériaux isolants. Deux axes d'innovation seront évalués:

a. La possibilité de faire évoluer la méthode mathématique de détermination de la conductivité thermique. Il est d'usage d'utiliser une régression linéaire cependant nous constaterons que la variation de la température de la sonde en fonction du logarithme du temps ne suit pas une évolution linéaire mais une sigmoïde pour les matériaux isolants. Nous chercherons également à déterminer simultanément la conductivité et la diffusivité thermiques par cette nouvelle méthode.
b. La possibilité de proposer une nouvelle sonde et une nouvelle procédure d'expérimentation. La composition de matériaux pour confectionner la sonde, la puissance d'alimentation, par exemple seront étudiés. Pour cela, nous ferons appel au logiciel Comsol Multiphysics® pour évaluer l'influence des paramètres qui ne sont pas accessibles expérimentalement.

2. *Evaluer les performances thermiques d'un isolant en utilisant un montage basé sur le principe de la boite chaude gardée dans l'objectif de reproduire les conditions climatiques réelles supportées par l'enveloppe d'un bâtiment*

Il est à noter qu'initialement l'objectif était d'intégrer une sonde à choc thermique dans la paroi mais le manque de temps ne nous a pas permis cette étude. En effet, la boite chaude gardée a été acquise par notre établissement en fin de la seconde année de la thèse d'Hussein. Donc après une phase préliminaire de validation de la boite chaude gardée avec la détermination de l'importance des différents flux (bilan thermique) dans la cellule chaude (Hot cell) puis dans la cellule froide (Cold cell), nous procèderons aux études suivantes :

a. Détermination de la résistance thermique en fonction de la température et de l'humidité du matériau. Ces mesures ont également été effectuées avec d'autres techniques de mesure (Hot Disc et plaque chaude gardée) de façon à valider notre méthode de caractérisation.
b. Détermination de la capacité calorifique en fonction de la température et de l'humidité du matériau. Pour cela, des fluxmètres ont été installés sur chacune des 2 surfaces d'échanges en contact avec la cellule chaude et la cellule froide de la boite chaude gardée.
c. Un cas simple de transfert de chaleur et de masse a été étudié expérimentalement. Puis les résultats ont été confrontés aux valeurs issues du logiciel WUFI® de façon à envisager des perspectives à ce travail.

La thèse d'Hussein est organisée en 5 chapitres. Les chapitres 4 et 5 décrivent les études permettant de répondre aux 2 objectifs précédemment cités. Au préalable, le chapitre 2 aura décrit les principes généraux des échanges de chaleur dans les isolants, les propriétés thermiques puis décrira les méthodes de caractérisation thermique utilisées dans cette étude ; la méthode de la sonde cylindrique à choc thermique et la boite chaude gardée. Le chapitre 3 présentera les principales caractéristiques physiques (morphologie, mécanique, hydrique) de la laine de verre utilisée lors de cette étude. Ces résultats sont extraits d'études déjà réalisées et publiées issues de la thèse de Fouzia Achchaq et de travaux réalisés par Laurent Marmoret lors de collaborations avec d'autres laboratoires universitaires français. Il nous a semblé important de choisir un matériau dont nous connaissons bien les caractéristiques physiques autres que thermiques.

Chapitre 2: Etat de l'art sur les techniques de caractérisation thermique des isolants du bâtiment

Dans un premier temps, les différents modes d'échange de chaleur (conduction, convection et rayonnement) ont été décrits. L'importance de chacun de ces modes d'échange a été discutée pour les matériaux isolants fibreux de façon à pouvoir mieux appréhender l'étude de la laine de verre lors de cette étude. Les techniques de caractérisation ont été classifiées en deux catégories suivant si elles appliquent le régime permanent (plaque chaude gardée et méthode fluxmétrique) ou le régime transitoire. Etant donné les objectifs à long terme de l'étude de déterminer les caractéristiques thermiques in situ, il est nécessaire de cibler des techniques de mesure intervenant durant le régime transitoire. En effet, seules ces techniques présentent une facilité d'emploi et de déplacement, une rapidité de mesure et de faible variation de température permettant de prendre en compte les effets de l'humidité par exemple et un coût réduit par rapport aux techniques du régime permanent. Ensuite, nous décrirons la théorie associée aux deux techniques de caractérisation en régime transitoire étudiées lors de ce travail : la sonde cylindrique à choc thermique et la boite chaude gardée.

La technique de la sonde cylindrique à choc thermique a évolué depuis un siècle. Des chercheurs ont commencé par étudier le fil chaud avant d'intégrer ce fil dans une sonde de façon à intégrer l'émission de chaleur mais aussi la mesure de température. En fonction des matériaux étudiés, la théorie a évolué en intégrant de nouvelles hypothèses et simplifications. Pour choisir une sonde adaptée aux matériaux étudiés, il est aujourd'hui impératif de respecter un ratio longueur sur diamètre de la sonde mais la principale hypothèse concerne la méthode d'analyse des résultats expérimentaux. En effet, de façon habituelle, la conductivité thermique est déterminée en utilisant une régression linéaire appliquée sur la cinétique représentant l'évolution de la température de la sonde en fonction du logarithme du temps. Il est alors nécessaire de définir un temps minimum de façon à éliminer les effets de la résistance de contact et un temps maximum évitant que le flux thermique atteigne les limites géométriques du matériau étudié (milieu semi-infini).

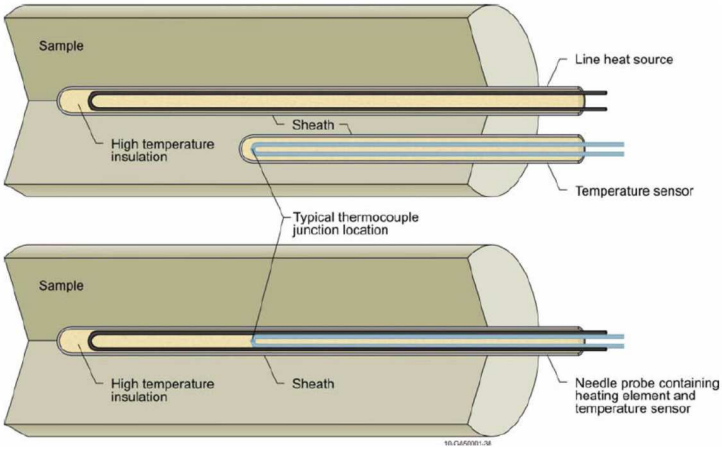

Les études issues de la technique de la boite chaude gardée sont moins anciennes même si la première manipulation date de 1930. Le principe général est d'émettre un flux de chaleur depuis la cellule chaude. Un gradient de chaleur est produit grâce à une autre cellule (dénommée cellule froide). Ces deux cellules sont séparées par la paroi à étudier. Il est possible d'instrumenter le montage de façon à évaluer l'importance des flux présents et ainsi d'établir un bilan thermique. Les différences entre les différents montages portent essentiellement sur les équipements techniques (résistances électriques de chauffage, groupe froid, ventilation pour homogénéiser les conditions d'ambiance en température et humidité) mais aussi sur la précision des capteurs de mesures (température, humidité). Il est à noter que le laboratoire a fait évoluer le montage de façon à le faire équiper d'une régulation en humidité dans chacune des cellules.

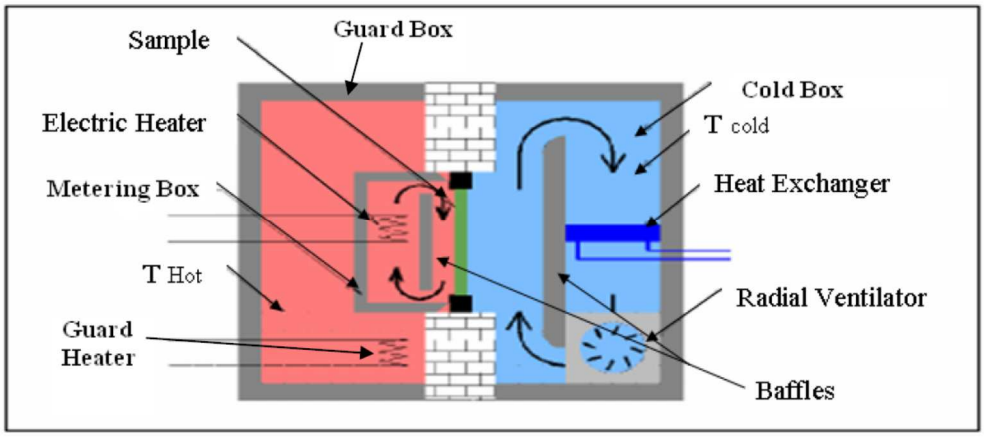

De nombreuses références bibliographiques sont insérées à la fin du chapitre permettant ainsi au lecteur d'approfondir les connaissances en fonction de ses attentes.

Chapitre 3: Principales charactéristiques thermophysiques de la laine de verre étudiée

Dans un premier temps, un état de l'art portant sur les isolants thermiques sera présenté précisant la classification et les applications dans le bâtiment. La méthode de fabrication de la laine fera l'objet d'une étude toute particulière. En effet, la laine choisie pour cette thèse n'est pas une laine de verre ordinaire. Elle a été développée dans les laboratoires de recherche d'ISOVER- Saint Gobain en appliquant une technique dénommée le crimping. Au cours de ce process, le matériau évolue (photos ci-après) jusqu'à parvenir à un assemblage de fibres non pas suivant des plans parallèles mais suivant une organisation des plans de fibres plus aléatoire. La structure de la laine est donc plus homogène dans les 3 directions de l'espace. On peut s'attendre à obtenir une résistance thermique similaire dans chacune des 3 directions de l'espace. Cela peut être important lorsque l'isolant doit traiter les pertes par les ponts thermiques dans les ossatures par exemple.

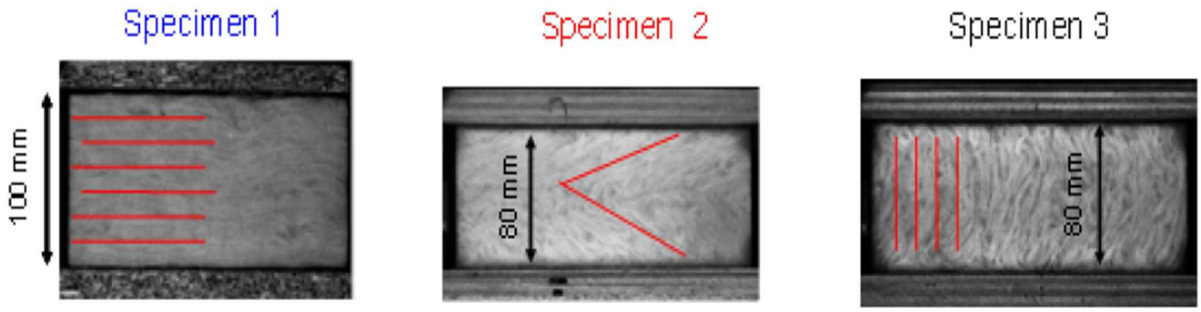

Au cours de la thèse d'Achchaq soutenue en 2008, la morphologie de ces laines a été étudiée à l'échelle microscopique à la plate-forme microscopie de l'Université de Picardie Jules Verne (UPJV). Des échantillons ont été étudiés par microscopie électronique à balayage (MEB, Quanta 200 FEG Environmental SEM/FEI). La pression de la cellule de l'échantillon a été réduite à environ 1 mbar pour l'étude des fibres seules et à 0,28 mbar pour l'étude des liants et des fibres. Une hétérogénéité de la structure et la distribution aléatoire des fibres dans la totalité du matériau ont été observées. L'hétérogénéité concerne aussi bien la géométrie des fibres (longueur et diamètre) que la taille des pores et les dépôts de liant. Couplé à un détecteur EDX, le MEB environnemental permet de déterminer la composition chimique des matériaux. L'approche suivie consiste à étudier une fibre de chaque laine sans son liant (non ensimée) puis le liant présent sous forme de goutte ou d'amas.

Lors de cette thèse mais aussi au cours de travaux de Laurent Marmoret en collaboration avec des laboratoires universitaires, il a été établi que la structure de la laine peut être considérée comme présentant une très forte porosité totale (> 95%), une division très fine (surface spécifique S_V = 0,2332 ±0,0120 $m^2.g^{-1}$) et une perméabilité intrinsèque très importante ($k \cong 4{,}5\ 10^{-10}\ m^2$). Ces caractéristiques morphologiques expliquent la faible adsorption de vapeur d'eau de la laine dans les domaines mono et multimoléculaires (la teneur volumique en eau inférieure à 0,1%) et la forte perméabilité à la vapeur d'eau (π_v = $5{,}84\ 10^{-11}\ kg.Pa^{-1}.m^{-1}.s^{-1}$).

La thèse d'Hussein a permis de caractériser thermiquement la laine par des mesures utilisant la technique dénommée de son nom commercial Hot Disc. Le laboratoire a fait l'acquisition de cette méthode au cours de la thèse. Cette méthode est installée dans l'équipe basée à l'IUT de Saint Quentin (02). Nous avons également réalisé des essais de caractérisation thermique à partir de la technique de la plaque chaude gardée à Amiens dans notre laboratoire. Ces mesures ont été réalisées en fonction de la température du matériau. Elles serviront par la suite à valider les résultats des mesures de sonde à choc thermique (chapitre 3) et de boite chaude gardée (chapitre 4). La méthode Hot Disc a été utilisée également pour déterminer la conductivité et la diffusivité dans des différentes directions afin de montrer l'effet du process dénommé Crimping. Il a été constaté une meilleure homogénéité des mesures suivant ces différentes directions.

Chapitre 4: Caractérisation thermique de la laine avec la sonde cylindrique

Ce chapitre concerne le premier objectif de la thèse d'Hussein. Un accord de coopération avec la société Hukseflux (Pays Bas) a permis de disposer de 2 sondes cylindriques de dimensions différentes mais également de pouvoir avoir accès à des informations techniques sur la fabrication des sondes. La sonde dénommée TP02 est la plus adaptée pour la caractérisation des isolants thermiques du fait d'un ratio longueur sur diamètre de 100 (alors que des travaux ont établi que pour éviter les pertes dans l'axe de la sonde il est nécessaire que ce ratio soit supérieur à 25). La composition et le fonctionnement de la sonde a fait l'objet d'une étude approfondie afin de justifier l'intérêt de choisir cette sonde. Lors de la thèse les mesures ont été réalisées avec l'appoint d'une interface de contrôle. Celle-ci n'est pas indispensable mais elle permet d'utiliser très rapidement la sonde et d'accéder à la mesure de la conductivité pour un non spécialiste de la thermique. Cependant, par cette interface, seuls 3 flux sont possibles (4.44, 2.64 et 0.87 W/m) et le temps de mesure est plafonné à 1500s (auquel il faut ajouter 1500 secondes supplémentaire pour atteindre l'équilibre thermique avant le début de l'essai).

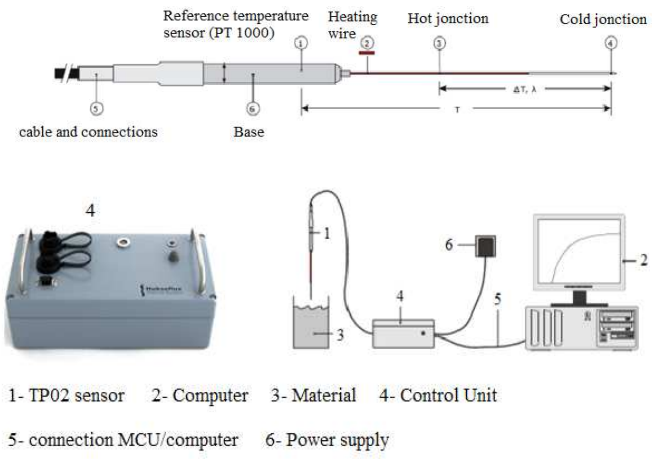

Sonde TP02 et interface de contrôle

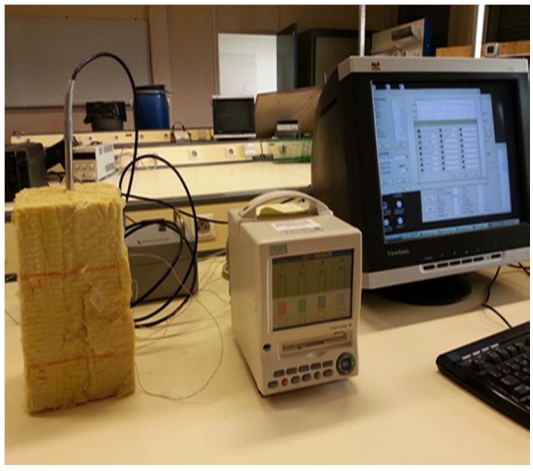

Image du montage expérimental

Dans un premier temps, Hussein a procédé au calibrage de la méthode en testant sur différents matériaux. La méthode a, tout d'abord, été validée sur le glycérol. La conductivité thermique de référence pour ce fluide est de 0.29 W/(m.k) alors que la mesure obtenue est, en fonction des réglages de puissances et de temps, comprises entre 0.28 et 0.31 W/(m.K). L'incertitude de mesure est de 3% en appliquant les valeurs données par le fabricant. Ensuite,

nous avons souhaité complexifier l'étude en considérant des milieux de porosité croissante. Des billes de verre de différents diamètres (2, 8 puis 10 mm) ont été utilisées de façon à faire varier la porosité totale de 36.5 à 41%. Nous avons alors constaté que les cinétiques des courbes exprimant la variation de la température de la sonde en fonction du logarithme du temps n'étaient pas toujours linéaires. Mais la théorie qui est associée à la méthode suppose dans une approximation linéaire aux temps longs qui n'est pas observée pour les billes de verre de 8 et 10 mm de diamètre. Il y a donc lieu de proposer des modifications pour que la sonde soit utilisable pour les matériaux d'une telle porosité.

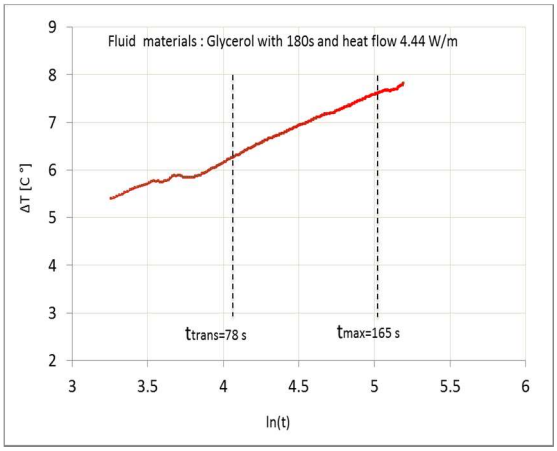

Cinétique pour le glycérol

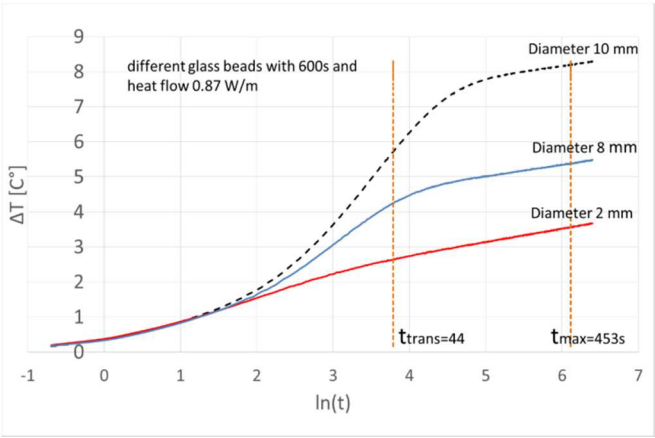

Cinétiques pour les billes de verre

Deux études ont été proposées.

- Dans un premier temps, une évaluation des erreurs associées au design de la sonde (dimension, composition) puis aux conditions d'essai (puissance, temps de mesure) sera réalisée. Cette étude doit aboutir à établir des améliorations pour in fine pouvoir réaliser ultérieurement une sonde mieux adaptée à la caractérisation des matériaux isolants. Nous avons simulé dans le logiciel Comsol Multiphysic® la sonde et son environnement afin de pouvoir faire varier des paramètres non accessibles expérimentalement.

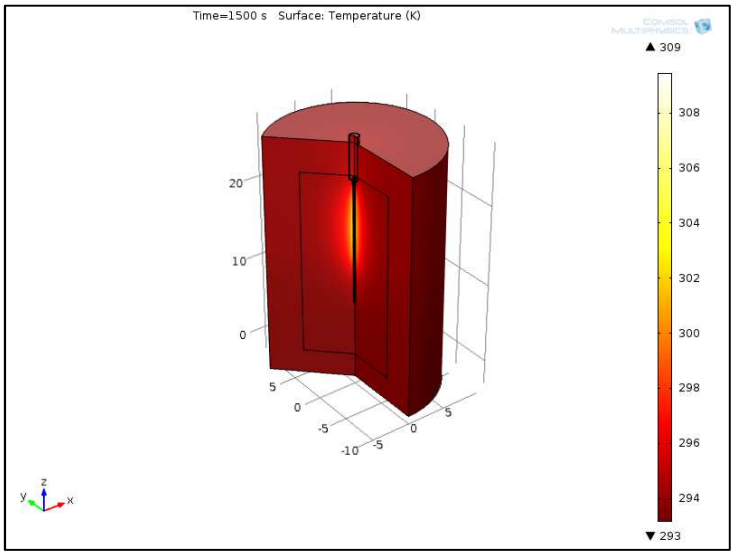

Image de la représentation de la sonde provenant de Comsol Multiphysic®

Nous avons pu constater qu'en diminuant la puissance d'alimentation, la cinétique de mesure devenait plus linéaire. Les conditions pour obtenir une conductivité thermique cohérente avec les valeurs de référence nécessitent des temps de mesure supérieurs à 1500s et un flux de chaleur inférieur à 0.1 W/m. Il a été également établi qu'une variation de température inférieure à 5°C entre le début et la fin de l'essai est indispensable à respecter. Ces conditions ne peuvent être obtenues avec l'interface de contrôle.

Le ratio longueur sur diamètre de la sonde est un élément important à considérer. Les figures suivantes présentent les isothermes obtenues par Comsol représentant les pertes par la base de la sonde et par l'autre extrémité axiale. Ces isothermes montrent que les températures à ces deux extrémités sont très importantes pour la sonde ayant un ratio de 25. Les pertes de chaleur par ces extrémités seront donc trop importantes pour ne pas les prendre en compte. Nous considérons qu'une valeur de 100 pour ce ratio est suffisante pour éviter les pertes de chaleur le long de l'axe de la sonde pour les isolants.

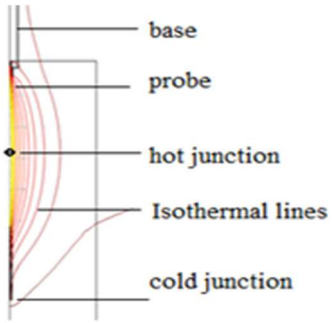

L/D ratio =100

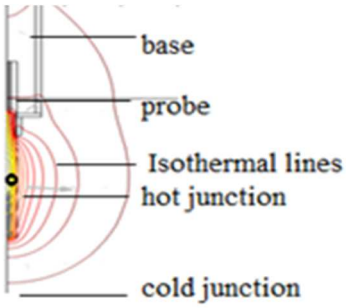

L/D ratio = 25

Au niveau du design, il est important de connaître l'exacte position des capteurs de température dans la sonde. Informations que nous n'avons pas pu obtenir avec précision du fabricant de la sonde. Le cuivre semble avoir des propriétés plus intéressantes que l'acier inoxydable pour l'émission de chaleur dans le matériau à étudier. Cependant, l'acier inoxydable a des propriétés stables dans le temps et est moins sujet à l'influence de la présence d'humidité à son contact.

Les effets associés à la résistance de contact semblent avoir une influence non négligeable. Mais ces effets dépendent du matériau étudié. La laine de verre, du fait essentiellement de sa forte porosité, présente une forte inflexion au début de la cinétique.

- Dans un second temps, un programme rédigé sous Matlab® a été développé de façon à prendre en considération la non-linéarité de la cinétique. Nous avons cherché à minimiser les hypothèses et simplifications dans les équations. Les techniques inverses visant à minimiser l'écart entre courbes expérimentales et valeurs simulées ont été appliquées.

Une étude de sensibilité des 3 paramètres considérés que sont la résistance de contact, la conductivité et la capacité calorifique a permis de montrer qu'aucune interaction n'existait entre eux. Il est donc possible d'appliquer les principes de la technique inverse sur ce problème. Les résultats du code de calcul Matlab sont cohérents avec les mesures expérimentales. Des améliorations sur le calcul numérique sont en cours dans le cadre d'une collaboration avec l'Université d'Evry.

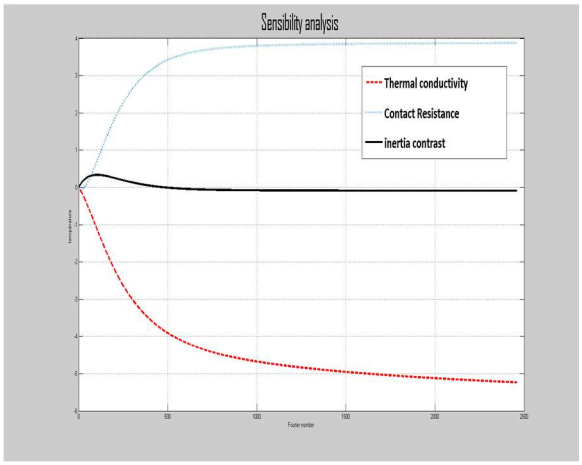

Etude de sensibilité des paramètres

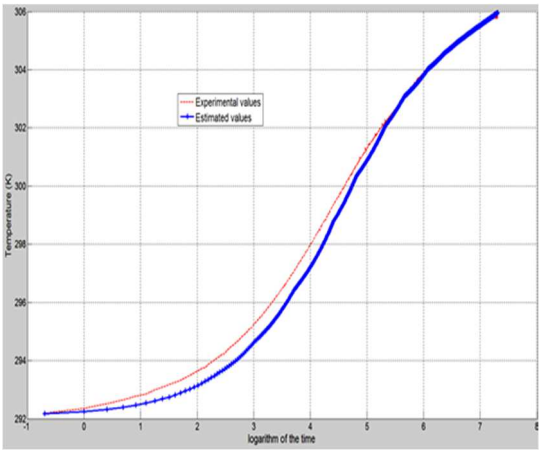

Résultats de la simulation

Chapitre 5: Etude du transfert de chaleur dans une paroi

Cette étude concerne l'objectif 2 de la thèse. Initialement nous souhaitions intégrer la sonde à choc thermique dans une paroi en reproduisant les conditions climatiques que subissent les enveloppes d'un bâtiment. C'est-à-dire que d'un côté de la paroi les conditions de l'ambiance intérieure (Cellule chaude et stable dans le temps) et de l'autre côté les conditions d'une ambiance extérieure (Cellule plus froide et évoluant sinusoïdalement dans le temps). Pour reproduire ces conditions, nous avons fait l'acquisition d'une manipulation dénommée Thermo 3R basée sur la méthode de la boite chaude gardée. Ces deux cellules encadrent la paroi à étudier. Connaissant le flux de chaleur émis dans la paroi (Q) il est possible de déterminer ses caractéristiques thermiques.

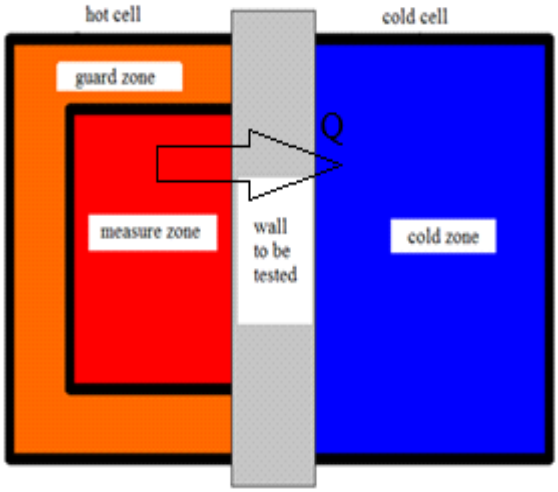

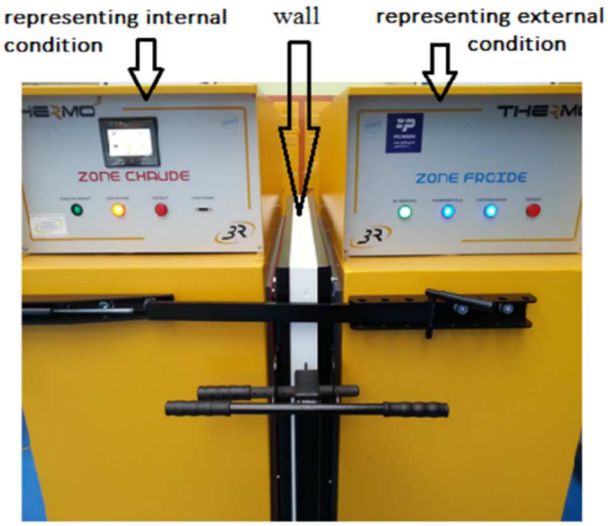

Schématisation du transfert de chaleur *Image de la boite chaude gardée*

La calibration de la manipulation constitue la première étape de l'étude. Dans ce cadre, nous avons cherché à établir un bilan thermique de la cellule chaude puis de la cellule froide.

La cellule chaude est composée d'une zone de garde et d'une zone dite de mesure. Nous avons établi le bilan thermique dans la zone de mesure à partir de la relation suivante :

$$Q_{ts} = Q_{in} - Q_p - Q_w$$

Où: Q_{ts} : le flux de chaleur transféré dans la paroi à étudier (W),

Q_{in} : le flux de chaleur total fourni par la résistance chauffante (W),

Q_p : le flux de chaleur dissipée par la paroi à étudier vers l'ambiance (W),

Q_w : le flux de chaleur transféré de la zone de mesure vers la zone de garde (W).

En positionnant des capteurs de température dans la paroi (sensor 2 sur la figure suivante) et en surface de la paroi (sensor 1), il a été démontré que le flux (Q_p) pouvait être négligé. Des tests ont également montré que le flux (Q_w) est important au début de l'essai mais lorsqu'un équilibre de température est obtenu (régime établi, cela se produit en général après une heure) la température de la cellule de mesure et de la zone de garde étant identique ce flux devient négligeable. De plus, connaissant la composition de la paroi nous avons calculé le flux (Q_w) et l'avons comparé à la valeur expérimentale. Il est donc possible de négliger ces deux flux (Q_p et Q_w) et de considérer la relation dans la cellule chaude : $Q_{ts} = Q_{in}$.

Dans la cellule froide, le groupe froid (flux Q_c) apporte un flux supplémentaire. Ce flux a des effets sur le flux traversant la paroi à étudier (Q_{ts}) et sur le flux dissipé dans le laboratoire par les parois de la cellule froide ($Q_{w'}$).

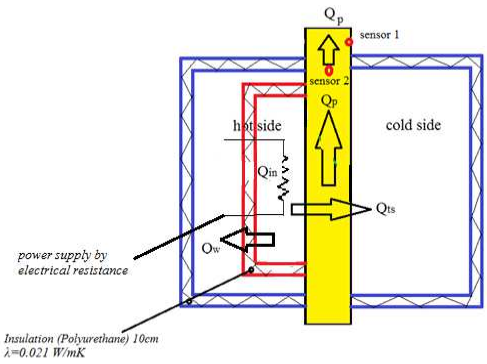

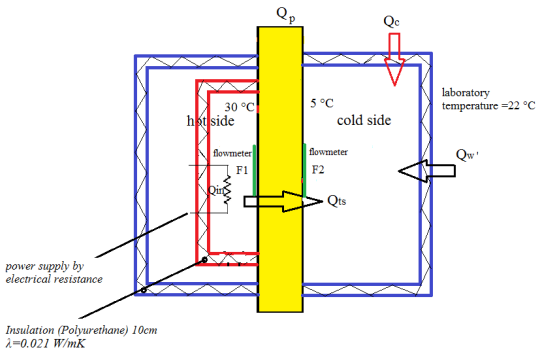

Schématisation des flux dans la cellule chaude *Schématisation des flux dans la cellule froide*

Nous avons étudié le cas où le groupe froid est éteint (Q_c=0 W) puis lorsque le groupe est allumé. Dans ce dernier cas si la température de la cellule froide doit être maintenue à 5°C, il a été montré expérimentalement que la puissance émise par le groupe ne peut être négligé car elle équivaut à 1W pour une puissance transmise par la paroi (Q_{ts}) de 2.6W. Nous avons constaté également que l'équilibre de température (régime établi) est atteint plus rapidement lorsque le groupe froid est allumé.

A présent, connaissant la valeur du flux de chaleur transféré dans la paroi il est possible de déterminer sa résistance thermique. Des mesures à différentes températures et pour différentes humidités ont été réalisées. Nous avons constaté une bonne cohérence avec les mesures issues d'autres techniques (Hot Disc et plaque chaude gardée). La température du matériau considérée diffère suivant les techniques. Pour la plaque chaude gardée comme pour la boite chaude gardée, elle correspond à la moyenne des températures de surfaces alors que pour la Hot Disc le matériau étant dans une étuve, c'est la température de réglage de cette

étuve qui est relevée et donc la température peut être considérée comme locale (au niveau de la sonde). La cellule chaude est réglée à 30°C et la cellule froide à 20°C et les réglages en humidité sont 0, 50, 75 et 95%.

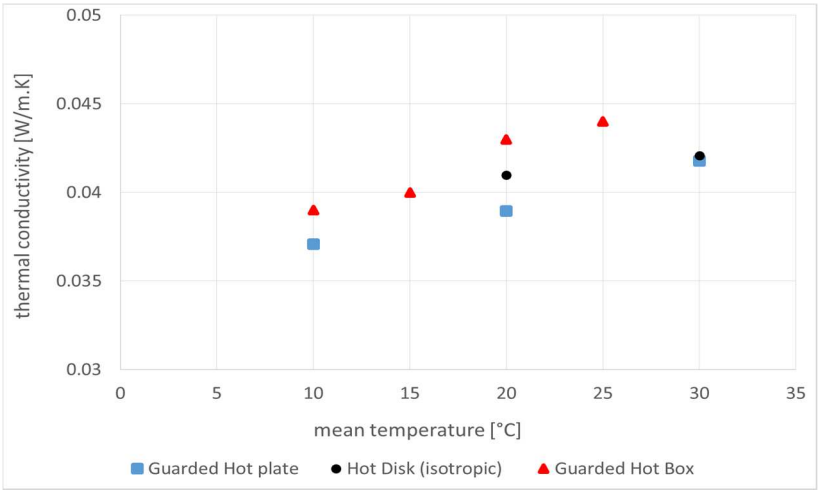

Effet de la température

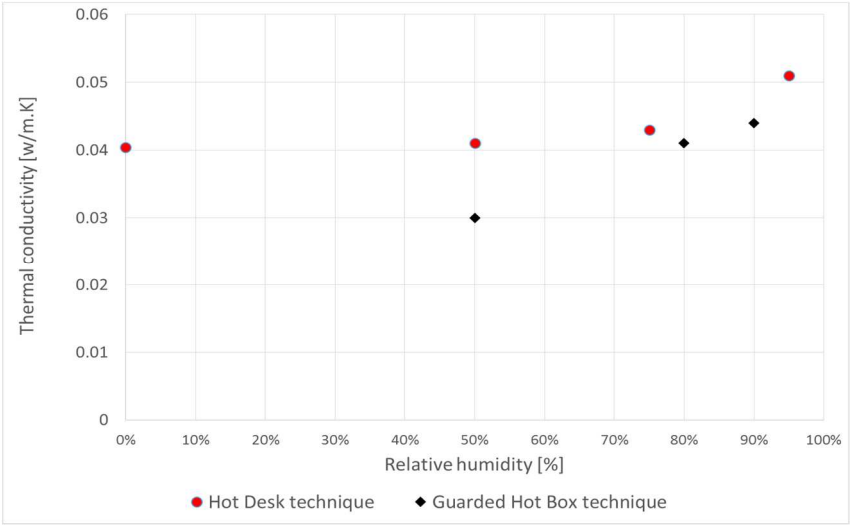

Effet de l'humidité

Nous avons ensuite cherché à définir une méthode pour déterminer la capacité calorifique de la paroi dans la boite chaude gardée. Des fluxmètres ont été installés sur chacune des 2 faces de la paroi à étudier. Nous avons montré qu'à l'équilibre thermique, il est possible d'accéder à la capacité calorifique C_p par la relation :

$$C_p = \frac{\int_0^t (f_{hot} - f_{cold})dt}{\rho.d.\Delta T}$$

où: C_p: capacité calorifique du matériau (J/kg.k)

f_{hot}: flux de chaleur (mesuré par le fluxmètre) provenant de la cellule chaude (W/m²)

f_{cold}: flux de chaleur (mesuré par le fluxmètre) provenant de la cellule froide (W/m²)

ρ: masse volumique du matériau (kg/m3)

d: épaisseur de la paroi (m)

ΔT: gradient de température entre les deux cellules (K)

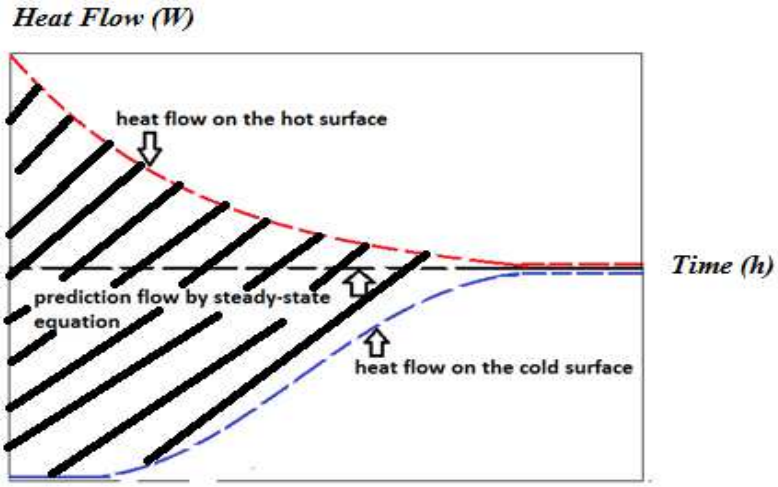

L'aspect original de la démarche concerne le calcul de l'intégrale pour déterminer la capacité calorifique. Il est possible de calculer cette intégrale en déterminant l'aire de la zone hachurée sur la figure précédente. Pour ce faire, expérimentalement, un fluxmètre a été positionné sur chaque surface de la paroi à étudier (au centre de celle-ci, voir figures suivantes) en contact avec les cellules du GHB. Une soustraction entre les mesures de ces 2 fluxmètres permet de calculer la puissance stockée par le matériau. Il est nécessaire d'attendre le régime permanent et donc que les puissances mesurées soient identiques pour arrêter l'essai.

Matériau étudié

Fluxmètre positionné sur la paroi

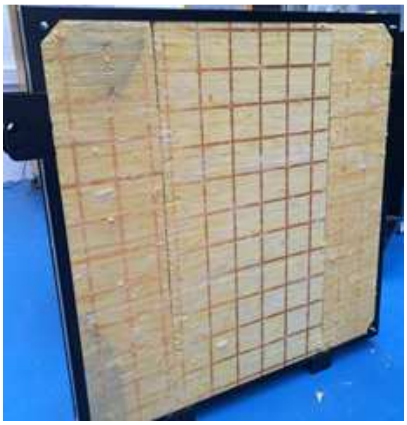

Paroi étudiée

La figure suivante (à gauche) présente le résultat d'un essai avec la cellule chaude régulée à 30°C et la cellule froide à 20°C. On constate sur la figure de droite que des oscillations

apparaissent sur le flux mesurée par le fluxmètre positionné en contact avec la cellule chaude. Le groupe froid étant atteint, ces oscillations sont dues aux relances thermiques de la résistance chauffante dans la cellule chaude pour maintenir la température. La figure de droite est obtenue pour une température de cellule chaude égale à 50°C (et non 30°C comme sur la figure de gauche). La température de la cellule froide est toujours de 20°C.

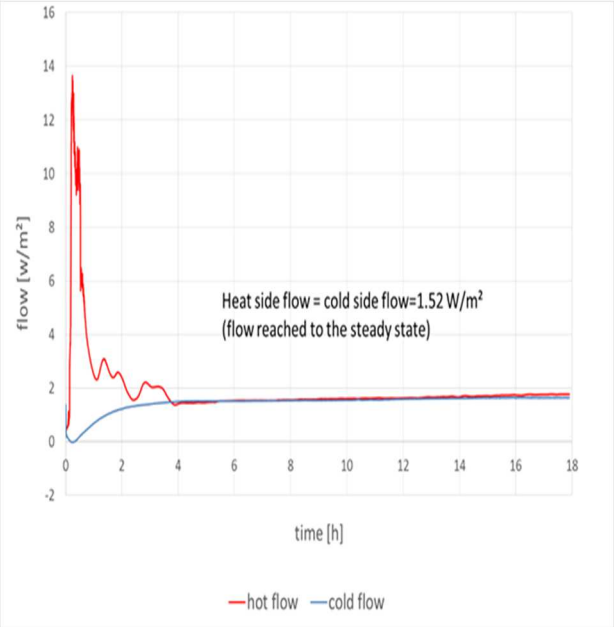

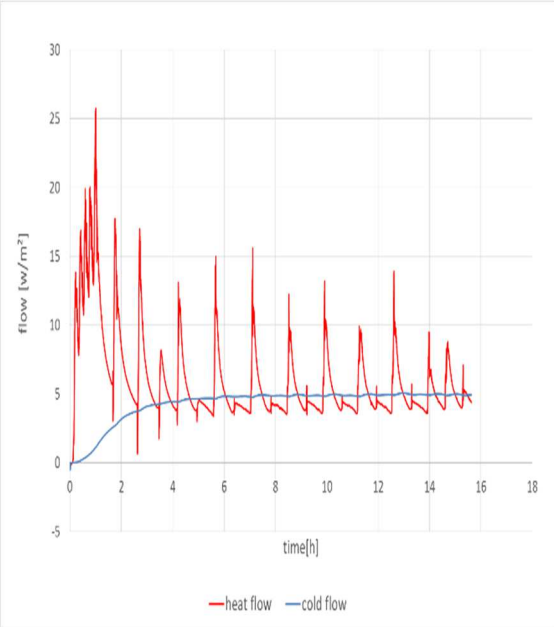

La figure suivante reproduit les mesures des fluxmètres au contact des cellules froides uniquement. On constate qu'en faisant varier la température de la cellule chaude (la température de la cellule froide reste à 20°C le gradient de température change) deux paramètres évoluent. D'une part, le flux augmente ce qui est logique puisque le gradient de température augmente. D'autre part, le temps nécessaire pour l'établissement du régime permanent augmente avec cette température.

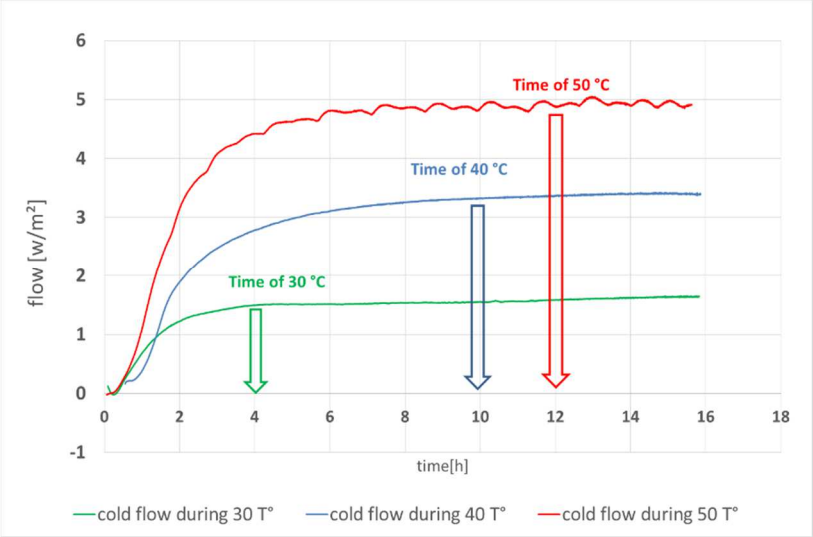

Nous avons testé la formule suivante pour déterminer ce temps :

$t = \frac{d^2}{\alpha}$ Où d représente l'épaisseur [m] et α la diffusivité thermique [m²/s] du matériau.

Nous avons comparé ces valeurs calculées avec la valeur obtenue par lecture sur les graphes (comme sur la précédente figure). On constate que les résultats de calcul ne sont pas concluants. La formule ne semble pas prendre en compte l'influence de la température bin que nous ayons modifié la valeur de la diffusivité avec la température suivant nos résultats expérimentaux. Mais la diffusivité évolue peu avec la température à la différence de ce temps d'établissement du régime permanent.

La capacité de stockage thermique de la paroi peut être également étudiée par d'autres paramètres. Il est possible de définir un temps exprimant le décalage entre les températures dans la cellule chaude et dans la cellule froide. Ce temps est dénommé 'time lag (t_{lag})' dans la thèse. Un autre paramètre exprime l'amortissement des amplitudes de température entre les 2 cellules. Ce paramètre est dénommé 'damping' ou 'decrement factor (D_f)'. L'inertie provoquée par les caractéristiques thermiques de la paroi peut être plus facilement appréhendée à travers la définition de ces paramètres. Les formules sont :

$t_{lag} = t_{T-hot(\max)} - t_{T-cold(\max)}$

$D_f = \frac{A_h}{A_c} = \frac{T_{hot(\max)} - T_{hot(\min)}}{T_{cold(\max)} - T_{cold(\min)}}$

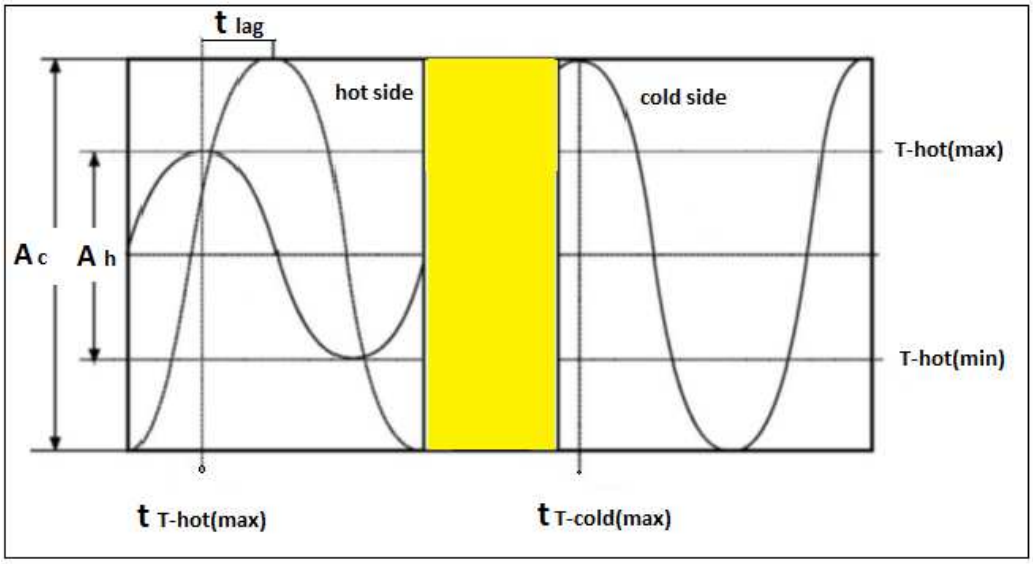

En comparant nos résultats, issus de l'expérimentation, avec ceux de la littérature, on constate que les résultats pour le 'time lag' sont cohérents mais les résultats du 'decrement factor' ne le sont pas.

Epaisseur (cm)	Résultats expérimentaux		Résultats d'Asan [littérature]	
	Time lag (h)	Decrement factor (-)	Time lag (h)	Decrement factor (-)
5	4.8	0.18	5.1	0.20
7.5	5.1	0.17	5.5	0.15
10	5.9	0.14	6.4	0.10

Dans une dernière partie de ce chapitre, le logiciel WUFI a été utilisé pour étudier le comportement de la paroi intégrant des sollicitations en température et en humidité. La notion de temps est capitale puisqu'il est impossible expérimentalement d'effectuer des études sur des temps de plusieurs années dans le cadre d'une thèse ce qui est très facile avec ce logiciel. La paroi étudiée comprend deux couches de laine de verre de 25 mm d'épaisseur chacune. Un paragraphe est consacré aux données introduites dans le logiciel. Les valeurs expérimentales de caractérisation morphologique, hydrique et thermique de la laine de verre ont été insérées dans la base de données du logiciel.

Dans un premier temps, nous avons cherché à valider les résultats du logiciel avec nos valeurs expérimentales. Cette procédure de validation a été effectuée sur un temps d'études de 1 jour (24h). Initialement la paroi est régulée à 20°C et 80% d'humidité relative.

La procédure de validation effectuée, nous avons testé la paroi dans différentes conditions afin d'évaluer les risques de condensation. En particulier, nous avons étudié l'influence de la température initiale (10, 20 et 30°C) avec une humidité de 80%.

Notre volonté en utilisant le logiciel WUFI était aussi d'évaluer la pertinence de l'utiliser pour montrer l'importance des propriétés thermiques. Celles-ci évoluent en fonction de l'humidité. Nous avons cherché à voir s'il est possible de faire évoluer ces propriétés dans le temps en cas de vieillissement du matériau.

En conclusion, ce travail a permis des avancées très intéressantes dans l'utilisation d'une sonde à choc thermique pour caractériser des matériaux isolants mais aussi la pertinence de la boite chaude gardée pour effectuer des études dans des conditions proches de situations réelles en température et en humidité.

En ce qui concerne la sonde à choc thermique, la méthodologie habituelle pour déterminer la conductivité thermique n'est pas applicable pour les matériaux isolants. En effet, il est d'usage de disposer d'une fonction linéaire entre la température et le logarithme du temps afin d'appliquer la relation mathématique pour déterminer la conductivité thermique. Cependant, dans le cas des isolants, cette fonction est de type sigmoïdale. Il a donc été décidé d'orienter l'étude suivant deux directions :

- La relation linéaire est obtenue avec des approximations qui sont discutables pour les matériaux isolants. Donc il a été décidé d'effectuer un ajustement entre résultats expérimentaux et une relation mathématique qui n'a pas fait l'objet de simplifications. Nous avons utilisé un programme Matlab et appliqué les techniques inverses pour résoudre le problème. Les résultats sont intéressants. Nous pouvons déterminer simultanément la conductivité thermique et la diffusivité thermique. Cette étude va se prolonger de façon à améliorer l'ajustement et réduire les écarts entre résultats expérimentaux et valeurs du modèle.
- Le design de la sonde n'est pas optimal pour la mesure sur des matériaux isolants. Nous avons donc développé une étude en utilisant le logiciel Comsol Multiphysics de façon à évaluer la pertinence du choix de la société Hukseflux avec qui nous avons collaboré pour cette étude. Les choix peuvent concerner la composition et les dimensions de la sonde. Nous avons également utilisé le logiciel pour tester l'influence de la puissance d'alimentation de la sonde et les caractéristiques thermiques du matériau à tester.

En ce qui concerne la boite chaude gardée, nous avons disposé tardivement (en 2nde année) de l'appareillage. De ce fait les objectifs d'étude ont été réduits. Nous souhaitons initier des études pour maîtriser le fonctionnement de l'appareillage et déterminer les caractéristiques thermiques (conductivité et capacité calorifique) Cependant, nous ne disposons pas assez de temps pour introduire la sonde à choc thermique et effectuer des essais pour connaitre les propriétés en usage et non dans des méthodes de caractérisation de laboratoire. Donc au cours de cette thèse nous avons étudié :

- La détermination de la résistance thermique sous différents gradients de température et pour différentes humidités dans les cellules chaude et froide.
- La détermination de la capacité calorifique par la méthode des fluxmètres en fonction également de la température et de l'humidité. Cette méthode nécessitant l'établissement du régime permanent nous avons essayé de trouver un calcul pour définir préalablement à l'essai le temps nécessaire pour l'établissement de ce régime. Les paramètres « time lag » et « decrement factor » caractéristiques de la capacité de stockage de la paroi ont été définis. Une étude comparative avec des résultats issus de la littérature a également été effectuée pour vérifier la validité de nos résultats. Enfin, nous avons utilisé le logiciel WUFI pour étudier le comportement de la paroi soumise à des variations en température et en humidité et ainsi se rapprocher des conditions expérimentales dans les cellules froide et chaude de la boite chaude gardée.

Chapter 1 : Introduction

1-1 Preface

The world currently faces its greatest challenge ever in diminishing natural resources and increase pollution, now the largest environmental problem is the atmosphere, where the accumulation of greenhouse gases that cause climate change. The latest report of the International Panel on Climate Change (IPCC) declares that the increasing carbon dioxide in the atmosphere is the main cause of climate change [1]. IPCC explains that by 2020, the amount of CO_2 emissions from building energy use can be reduced by 29% without additional cost by using existing technology. The main sector to emit CO_2 in Europe is buildings, besides to transport and industry. Thermal insulation gives us the greatest potential saving of CO2 compared to other building efficiency measures [1] (figure 1-1).

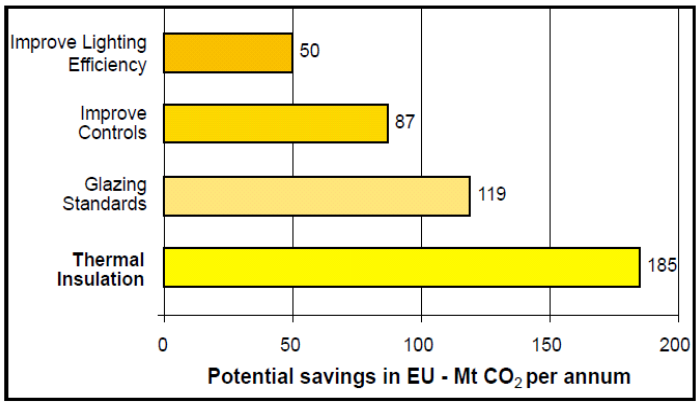

Figure 1-1: saving of CO2 by thermal insulation compared with other building efficiency measures [1] (2002)

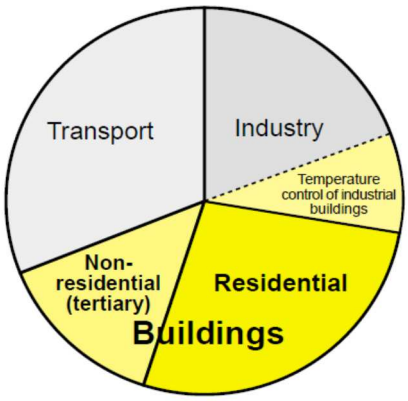

Figure 1-2: Buildings are responsible for 50% of Europe energy use [2] (1998)

50% of European energy is dedicated to buildings, and 40 to 60% of this is heating energy [2] (figure 1-2). We can reduce this consumption for new building by good design and optimum levels of insulation, but for existing building it requires renovation insulation and glazing. The amount of energy required to cool and heat a building depends on how their structures are thermally designed. The thermal performance of building is determined by the thermal characteristics of the materials and how to install these materials in the elements of buildings according to the direction of heat transfer. The quantity of energy saved and the efficiency of insulations are influenced by type of insulation material used, construction techniques, position of materials and its thickness. Europe is now moving to upgrading the level of thermal insulation systems in buildings. In addition, a number of countries move strongly to

the assessment of building materials according to Environmental Product Declaration and Life Cycle Assessment of the product.

Reducing the fundamental mechanisms of heat transfer process (conduction, convection and radiation) is a priority during manufacturing [3]. An understanding of the thermal properties of insulation materials (thermal conductivity, specific heat capacity and thermal diffusivity) is very important to decide which material is best for buildings insulation. Thermal performance of insulants is determined from thermal resistance (R-value or its inverse U-value). Having low U-values is considered the most important factor. But Thermal storage and longevity of U-values should be also important parameters. Thermal resistance value (R-value) changes over time. There are many factors that influence on the performance of insulation materials cause failure risk on long-term performance. The most important of these risks are the moisture, air movement and interstitial condensation. Durability of insulants depends also mainly from strength (compressive, flexural, and tensile), dimensional stability and chemicals and biological agents. Materials of animal origin are one of the oldest thermal insulation materials. Besides the natural products and during the industrial revolution many artificial materials were also developed, now more than 95% from insulation is artificial materials [4]. Glass and stone wool represent over 50% of the EU market. They had several advantages more than the natural materials (durability, acoustic insulation, and fire and water resistance).

1-2 Aims and methodologies of this work

The object of this work is to assess the interest of using new methods to test thermally insulation materials. Stafford et al. [5] have shown that differences between designed and measured in-situ thermal material performance of more than 20% common and of more than 100% in some cases. The actual performance is worse than was predicted. Moreover, as life of buildings can be reached to 500 years, more research is required to determine long-term performance of insulants by in situ measurements. So, there is a need of developing new methodology to reduce the performance gap between design and real energy performance of building and to studied aged materials in situ.

The first aim of this work is to study performance and limit of using a non-steady state hot probe (TP02 Hukseflux®) to determine thermal characterizations in the case of insulation materials. TP02 technique is usually used for soil characterization, powder and fluid but it is not currently used for buildings materials. It is well-adapted to determine in situ thermal performance. This probe can also take into account the effect of moisture content

because it needs short time (10 minutes) and low flow (less than 1 Watt) in comparison with steady state techniques. In laboratory conditions, guarded hot plate apparatus (a steady state technique) is better considered to assess the thermal performance of a sample of a building material or construction element.

But, before this work, TP02 Hukseflux® like other non-steady state probes (NSSP) is considered not adapted to characterize insulation materials. In the TP02 user guide manual, Hukseflux restraints the use of their probe to a range of thermal conductivity between 0.1 and 6.0 $W.m^{-1}.K^{-1}$ and defines an expected accuracy at 20 degrees of ± (3% + 0.02) $W.m^{-1}.K^{-1}$. The fixed accuracy of 0.02 doesn't allow insulation material characterization with usual thermal conductivity of 0.04 $W.m^{-1}.K^{-1}$. Pilkington [6] justify this restriction because he observed that the kinetic, in the case of insulant, representing non-linear temperature gradient against the logarithm of time. For powder, fluid and soil, a linear temperature gradient is obtained. The so-called long term approximation equation, that can be considered the traditional process, can be applied to determine thermal conductivity. We will show that for insulation materials traditional linear process can't be applied because of the S-shaped temperature gradient kinetic. So, during this work, we have purposed two study cases to improve the NSSP methodology for insulation materials (figure 1-3):

- **To develop a new mathematical analysis by considering the entire S-shaped curve and not only its linear part.** The necessity of developing a new methodology has been described in a publication [1]. Matlab program has been developed by applying mathematical inverse technique principles. This work has been published already [2]. This methodology allows also to determine simultaneously thermal conductivity and thermal diffusivity. Hot disc and guarded hot plate methods have been used to validate experimental measurements by this innovative method with NSSP. Validation of thermal characterization by thermal probe technique has been done by using Hot Disc technique that allows the simultaneous determination of thermal conductivity and diffusivity. Hot Disk technique has been also used during this work to study effect of anisotropic structure composed of pores and fibers. The effect of the direction of the flux is also studied and published [3].

[1] H. Humaish, B. Ruet, L. Marmoret, H. Beji , Assessment of long time approximation equation to determine thermal conductivity of high porous materials with NSS probe, Journal of Sustainable Construction Materials and Technologies, Volume 1, pp 1-15, 2016

[2] L. Marmoret, H. Humaish, H. Beji, New methodology to determine thermal properties of building insulation materials with cylindrical hot probe, International Journal of Thermal Sciences (THESCI)

[3] L. Marmoret, H. Humaish, A. Perwuelz, H. Beji, Anisotropic Structure of Glass Wool Determined by Air Permeability and Thermal Conductivity Measurements, Journal of Surface Engineered Materials and Advanced Technology, Volume 6, pp 72-79, 2016.

- **To improve the design of the probe for characterizing insulation materials.** COMSOL® multiphysics axisymmetric 2D model has been used to study the influence of characteristics of the probe (materials, sensors, powers…) that can't be accessible experimentally. For example, the effect of length to diameter ratio and materials of components of hot wire of the probe has been presented during colloquium [4 and 5]. Long term objective is to develop a new probe specially adapted for insulation materials thermal characterization.

[4] B. Ruet, H. Humaish, L. Marmoret, H. Beji, Assessment of thermal probe technique for determination of effective conductivity of building insulation materials, in proceeding of the 20th European Conference on Thermophysical Properties (ECTP), Porto, Portugal, 2014.

[5] H. Humaish, B. Ruet, L. Marmoret, H. Beji, Thermal characterization of highly porous materials by the hot wire method, in proceeding of the French Thermal Society (SFT) congress, La Rochelle, France, 2015.

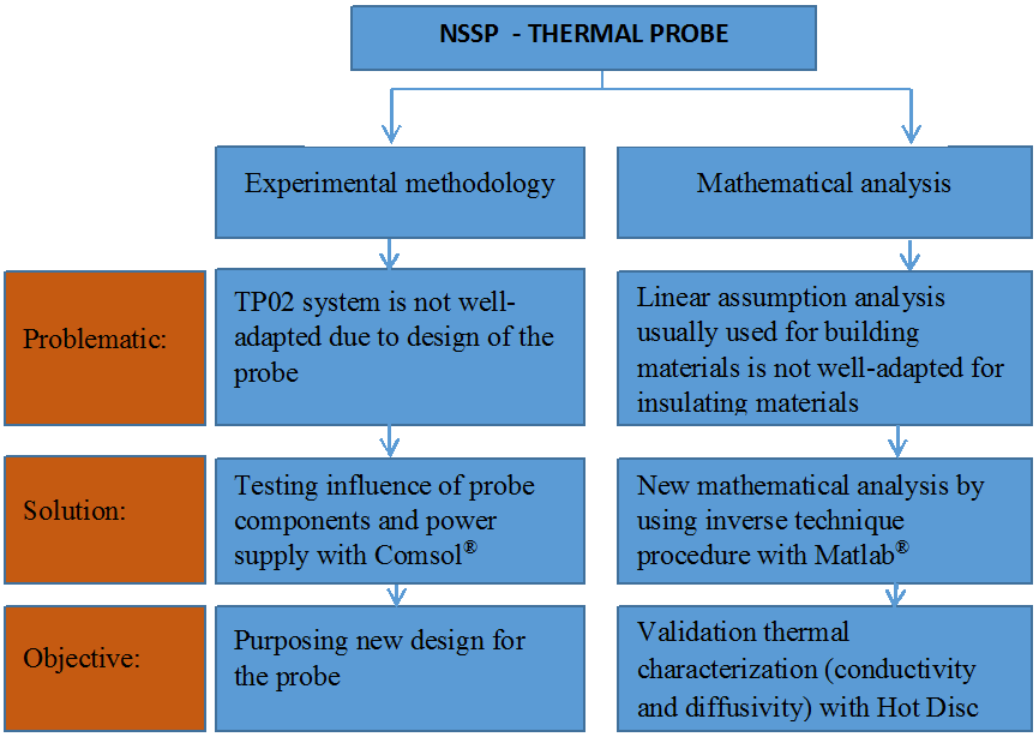

Figure 1-3: study steps with thermal probe

The second aim of this work is to study thermal performance of a glass wool in realistic climatic building envelopes conditions. Building envelopes are subjected to thermal and hydric stresses that are not constant during days and seasons. In situ measurements are difficult (and often impossible) to control one-self due to coupled effects of heat and mass transfer coming from environment (sun, wind, rain,…). Such as dynamics solicitations in temperature and humidity are difficult to reproduce in laboratory. Guarded Hot Box (GHB) apparatus can be considered as an interesting help to create realistic climatic conditions. Due to the fact that a GHB has been bought during this work (second year of this work), we can't define objectives requiring too long time like moisture effect and the durability of insulants. So, during this work, we have fixed the following objectives:

- **Determination of thermal resistance of a glass wool wall against temperature gradient.** These values can be also obtained by guarded hot plate and hot disc techniques during steady state conditions. So a comparison has been done in order to validate measurements. It can be considered as preliminary step to take control of the apparatus.

- **Determination of thermal storage capacity of the glass wool wall against temperature and humidity gradients.** During transient or un-steady state conditions, thermal properties of materials like specific heat capacity, diffusivity and effectivity can be determined. An interesting flowmeter method already used in laboratory on guarded hot plate method has been adapted on GHB method. Thermal balance calculation must be undertaken to evaluate the importance of various heat flow inside GHB apparatus. These thermal properties can be also compared with Hot Disc results. Time delay and damping have been also determined to characterize thermal storage capacity of glass wool wall.

- **Study of heat and mass transfer (in simple cases) and a comparison with Wufi® data.** Temperature and humidity gradients regulated in each cell of GHB can generate moisture transfer, air movement and superficial or interstitial condensation. To study these phenomena, WUFI® can be considered a well-adapted software. A comparison of results from GHB (experimental) and WUFI® (simulated) have been investigated.

1-3 Structure of thesis

This thesis is presented in five chapters:

Chapter 2: The thesis starts with a literature review of thermal characteristics of insulation materials (thermal conductivity, thermal resistance, specific heat capacity and diffusivity). It focuses on transient techniques and especially on probe method and hot disk method. Steady state techniques (heat flowmeter technique and guarded hot plate technique) are also presented.

Chapter 3: It focuses on building insulation materials and classification of these materials according to the origin of basic materials and practical applications. It will describe the life cycle of insulation materials and physical characteristics. The insulation material we use during this work is a glass wool which has been submitted to a crimping process. Morphological characteristics (density, porosity and specific surface) and basic principles of hydric properties of this material have been presented. Thermal characterisation of insulation materials that obtained by guarded hot plate (steady state) and hot disk (transient state) have been determined during this work have been presented also.

Chapter 4: This chapter describes the use of a Non Steady State Probe (NSSP) technique so-called TP02 Hukseflux®. It focuses on the experimental results for different materials starting by glycerol (fluid material) and then after the study of different insulation materials such as vermiculite, extruded polystyrene and glass wool. Ordinary procedure of treatment needs to apply linear assumption on the experimental kinetic reflecting the temperature increase against the logarithm of time. But in the case of insulation materials, kinetic is not linear. So, new mathematical methodology using inverse technique and requiring Matlab® program has been developed. Comsol Multiphysics® simulation has been used to study the influence of parameters such as the components of the probe (composition, size ...), the contact resistance and the thermal properties of materials on the non-linear S-shaped form of the kinetic.

Chapter 5: This chapter focuses on the experimental heat transfer study inside insulation materials by using guarded hot box (THERMO 3R). After presented the calibration of hot cell and cold cell, experimental results for thermal resistance against temperature, thickness and humidity have been determined. Thermal inertia has been studied by using flowmeter method and the determination of parameters such as time lag and decrement factor. Tests for studied heat and mass transfer by simulation with WUFI software have been presented.

Chapter 6: presents the conclusions of this work, and makes suggestions for future work.

References

[1]: Insulation for Sustainability, XCO2 conisbee Ltd, Consulting engineer, 1-5 Offord Street London N1 1DH, UK, E: mail@xco2.com W: www.xco2.com

[2]: Based on Assessment of Potential for the Saving of Carbon Dioxide Emissions in European Building Stock. Report to EuroACE by Caleb Management Services, Report is available on www.euroace.org, referred to as CALEB 1, May 1998.

[3]: Turner, W.C. Energy Management Handbook. Lilburn, Ga.: Fairmont Press. 2001.

[4]: Dávid Bozsaky, The historical development of thermal insulation materials, Department of Architecture and Building Construction, Széchenyi István University, H-9026 Gy˝or, Egyetem tér 1., Hungary 2011.

[5]: Stafford, A., Johnston, D., Miles-Shenton, D., Farmer, D., Brooke-Peat, M., Gorse, C., 2014. Adding Value and Meaning to Co-heating Tests. Struct. Surv. 32, 331–342. Doi: 10.1108/SS-01-2014-0007, 2014.

[6]: Pilkington B, In situ measurements of building materials using a thermal probe, phD, University of Plymouth, England, 2008.

Chapter 2 : Literature review on thermal testing methods

2-1 Introduction

There are four modes of heat transfer in a fibrous material: (1) Conduction through the solid medium, i.e. the fibers, (2) conduction through the gas medium, i.e. the air trapped between the fibers, (3) convection due to the air in the space between the fibers and (4) radiation interchange between fibers and air. Convection is caused by the air molecule's movement.

Heat transfer in the conduction phase in insulation materials (fibrous materials) occurs as a result of the solid conduction and gas conduction.

The convection in insulation materials can be divided into two cases: the convection inside the cells pores and the convection through the material on a macroscopic scale. According to the literature, heat transfer by convection can be neglected within a fibrous material, thus the heat transfer takes place just by radiation and conduction in these materials. Bhattacharyya in 1980, [1], showed when the sample is placed in a temperature between from - 41 C° to 88 C° , the convection can be negligible in a porous fibrous materials because the convective heat flow is less than 1% of the total. Stark and Fricke (1993) [2] said that the natural convection is generally negligible on fibrous insulation samples with densities equal to or greater than 20 kg/m3. While Daryabeigi in 2002, [3], said the natural convection is not a procedure for heat transfer in fibrous insulation materials with densities equal to or greater than 24 kg/m3. Du et al. in 2008 [4], proved that the samples with porosities less than 0.992, the convection is generally negligible on fibrous insulation.

The electromagnetic radiation in insulation materials tends to transfer the heat by radiation. The net radiation is the difference between the radiation in two surfaces hot and cold. The thermal conductivity by radiation (λR) is coming from the radiation transmission reflected and scattered by the fibrous structure, the fiber radiation dependent on the absorbance and emittance of the fiber and the thermal difference between fibers [5].

There are different techniques to characterize thermal properties for insulation materials: steady-state techniques (guarded hot plate method and guarded hot box method) and transient techniques (probe method and hot disk method). The steady-state techniques suffers from major drawbacks. It requires a long time to establish a steady-state temperature gradient

across the sample, and a large temperature gradient. A large sample size is also required, and the contact resistance between the thermocouple and the sample surface is considered as a major source of error. Transient techniques (probe method and hot disk method) are distinguished mainly by the short time and by the low flow in comparison with steady-state technique.

This chapter focuses on the thermal characteristics (thermal resistance, specific heat capacity and thermal diffusivity) of insulation materials and the techniques that used to measure these characteristics. It discusses the steady state techniques and transient state techniques and describes in details probe method and hot disk method (transient technique) that are used in the experimental.

2-2 Thermal characteristics and heat transfer in a wall

2-2-1 thermal conductivity and thermal resistance

One of the most important characterisation of the insulation materials is thermal conductivity. The thermal conductivity of a material represents the quantity of heat that passes through the thickness per unit area per second with one degree difference in temperature between the faces. The heat flow is moving the heat from the high temperature place to low temperature place to reach the equilibrium. Ideally, discrete analysis based on characterization of each fiber, interstitial materials and interface conditions provide the most representative system. The number of fibers, the complexity of the microscopic structure and the interactions between the components make the discrete analysis very expensive and sometimes impossible. One way to overcome the difficulties is to determine a hypothetical homogeneous material equivalent. The properties of this equivalent material are denoted as “effective material properties”. Some properties as the effective density or effective specific heat can be determined by some form of averaging values of each component. The effective thermal conductivity not only depends on the properties of each component but is also function of the shaping process. The method consists of the development of empirical models or rigorous numerical simulations using generally the finite element method or analytical models.

The effective thermal conductivity can be likened to three forms of heat transport in insulation materials; conduction through solid, conduction during gas phase and radiation within pores as:

$$\lambda_{eff} = \lambda_{solid} + \lambda_{gas} + \lambda_{rad} \quad (2\text{-}1)$$

Where λ_{eff}: effective thermal conductivity (W/m.K), λ_{solid}: The conductivity for solid conduction (W/m.K), λ_{gas}: The conductivity for gas conduction (W/m.K), λ_{rad}: The conductivity for radiation.

The part of the thermal conductivity due to the direct conduction in fibers and at the contact between the fibers is generally small for high porosity materials. In general the biggest of these parts is the solid conduction (figure 2-1). Due to the very small dimensions of the cavities the air's movement between the fibers is practically negligible, heat transfer of convection is minimal and can therefore be omitted from the calculations. Insulation materials have small amount of structural solid with highly porous. The importance of the radiation will increase in a material with a small amount of solid [6]. Then the optimum point for insulation materials is summation of the radiation and solid conduction if we considered the gas conduction for conventional insulation materials is constant.

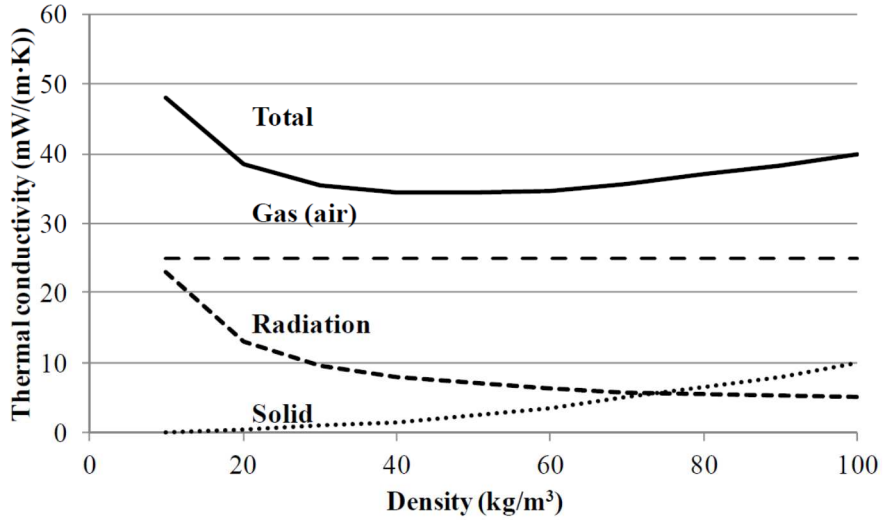

Figure 2-1: Thermal conductivity in porous materials [6]

Thermal resistance (R) of the insulant can be calculated from thermal conductivity by:

$$R = d\ /\lambda \qquad (2\text{-}2)$$

The UNI EN ISO 6946 [7] describes a method for calculating the thermal resistance and thermal transmittance of building elements based on the electrical analogy (figure 2-3). The theory indicates that the total strength of the wall is equal to the sum of the resistances of each layer that constitutes it (figure 2-2). This is what we will check through the experimental tests.

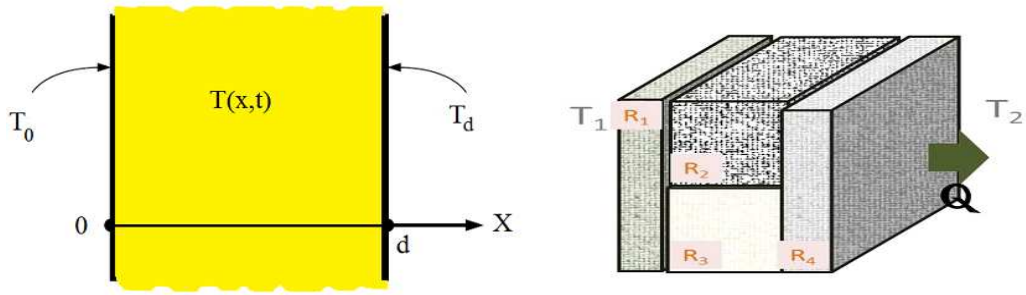

Figure 2-2: Thermal transmittance of building elements based on the electrical analogy

$$q = \frac{(T_o - T_d)}{R} . A \qquad (2\text{-}3)$$

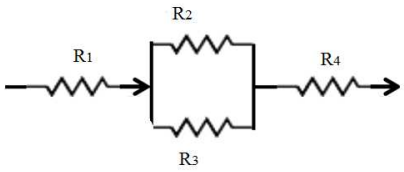

Figure 2-3: Electrical analogy for the heat transfer through wall

Where:

R: Thermal resistance (m^2.K/W)

d: Thickness of the wall (m)

The thermal performance of any wall is highly dependent on the amount of insulation installed. Other factors such as air leakage, installation defects and moisture content can have also a great influence. U-value is an effective factor for describing the thermal performance of the walls [8]. Decreasing this factor indicates good insulation for walls. U-value is useful to predict behaviour wall layers and measurement of this value helps in achieving energy conservation in walls.

2-2-2 *Specific heat capacity*

Specific heat capacity represents the ability of the materials to store or absorb the thermal energy. It is also the energy required to raise one degree variation of temperature of the unit mass of the material. There are two types of specific heat; specific heat capacity at constant volume C_v, and specific heat capacity at constant pressure C_p. The energy storage in the material during steady state conditions can be determined from the expression:

$$C_p = \frac{q}{\rho.V.\Delta T} \qquad (2\text{-}4)$$

Where:

C_p: Specific heat capacity of the sample at constant pressure
q: Heat flow (w)
ρ: Density of the sample (kg/m^3)
ΔT: Differences of temperature between two surface of the wall (K)

Equation (2-4), representing the ability of the wall to store the energy which depends on the properties of the material ($\rho, C_p \; and \; d$) where ΔT (is condition of the material and not from the properties). The insulating materials should had a high specific heat capacity that mean it should have a high capacity to retain heat.

Building materials absorb energy slowly and hold it for much longer periods of time than do less massive materials. This delays and reduces heat transfer through a thermal mass building component. Mass is another important characteristic that affects the thermal performance of construction assemblies. Heavy walls, roofs, and floors have more thermal storage than light ones. Thermal storage both delays and dampens heat transfer (Figure 2-4).

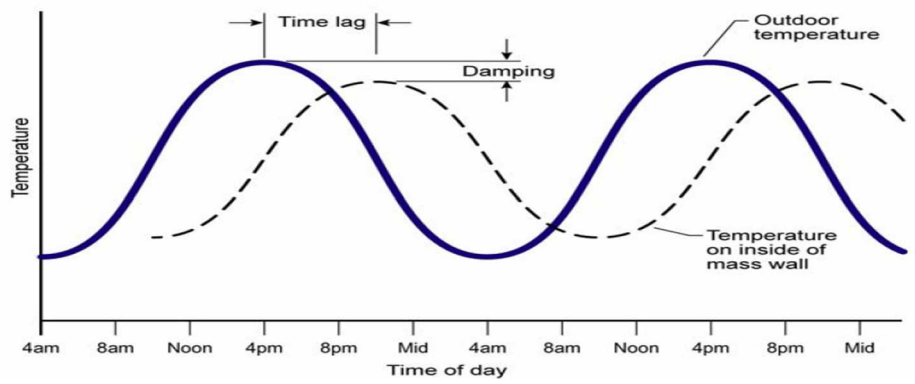

Figure 2-4: Effect of thermal storage

It may be noted that the steady state method does not account for the effect of heat capacity of building materials. The *ASHRAE Standard 90.1–Energy Standard for Buildings Except Low-Rise Residential Buildings*, the *International Energy Conservation Code*, and most other energy codes recognize the benefits of thermal mass and require less insulation for mass walls. Thermal resistance (R-values) and thermal transmittance (U-factors) do not take into account the effects of thermal mass, and by themselves, are inadequate in describing the heat transfer properties of construction assemblies with significant amounts of thermal mass.

2-2-3 Thermal diffusivity

The thermal diffusivity is representing fast propagation of heat through the material. Thermal diffusivity refers to the distribution of the temperature in the material during non-steady state (transient condition). Thermal diffusivity is a function for heat conduct and heat store and allows to compare the ability of materials to conduct and store thermal energy. It is expressed in m^2/s and it is measured in compliance with ISO 22007-1.

$$\alpha = \frac{\lambda}{\rho \, .C_p} \qquad (2\text{-}5)$$

Where:

α: Thermal diffusivity
λ: Thermal conductivity
ρ: Density
C_p: Specific heat capacity of the sample at constant pressure.

Thermal conductivity and thermal transmittance are used to define the insulation properties in steady state. Thermal transmittance, also known as U-Value, is the steady state heat flow passing through a unit surface area induced by a 1 K difference of temperature expressed in W/m^2K. It takes into account conductive heat transfer and also convective and radiative heat transfers. Thermal transmittance U-Value can be measured with the hot-box method [9] and can also be estimated with the ISO 6946 calculation method.

For the unsteady the most used parameter is the thermal diffusivity α. Several comparative studies demonstrated that the calculated U-values are usually lower than the measured ones.

The following paragraph will present steady state and transient methods to determine thermal characteristics of insulation materials.

2-2-4 Conduction heat transfer in a plane wall

The conduction heat transfer in a plane wall is described by the one-dimensional transient heat conduction equation:

$$\frac{\partial}{\partial x}\left[\lambda \frac{\partial T}{\partial x}\right] = \rho C \frac{\partial T}{\partial t} \quad (2\text{-}6)$$

Whereλ, ρ and C are the thermal conductivity, density and specific heat capacity of the wall material. The wall exchanges heat by convection from surface of the wall to ambient.

To determine the time constant, usually we consider lumped system assumption. Heat transfer into the wall during dt is equal to the increase in the energy of the wall during dt:

$$hA_s(T_\infty - T)dt = \rho CV dT \quad (2\text{-}7)$$

$$\frac{d(T-T_\infty)}{T-T_\infty} = -\frac{hA_s}{\rho CV}dt \quad (2\text{-}8)$$

Integrating from t=0 at which $T=T_0$ to any time t at which T=T(t) gives:

$$ln\frac{T(t)-T_\infty}{T_0-T_\infty} = -\frac{hA_s}{\rho CV}t \quad (2\text{-}9)$$

Taking the exponential, we obtain:

$$\frac{T(t)-T_\infty}{T_0-T_\infty} = e^{-\frac{t}{\tau}} = e^{-F_0} \qquad \text{où } \tau = \frac{\rho CV}{hA_s} \quad (2\text{-}10)$$

Where F_0 is the Fourier's number (this parameter will be described in more details in §2-4-3).

Thermal time constant (τ=TTC) is a measure of time it takes heat to propagate through the wall and is a kind of "effective" thermal insulating capability. TTC can be also defined as the sum of the heat capacity of a layer and the cumulative thermal resistance up to layer.

$$\text{TTC} = \sum_i^n \rho_i \, C_{pi} L_i \, R_{0-i} \tag{2-11}$$

Thermal time constant is effective during determination place of the insulation material in the building envelope in external or internal (higher TTC mean lower the overall heat transfer through the structure). The value of this time is depends on the thermal capacity and thermal resistance of the materials.

The lumped system provides great convenience in heat transfer analysis but criteria must be respected to use it. Characteristic length (L_c) is defined as V/A_s. So Biot number (B_i) can be determine from characteristic length as:

$$B_i = \frac{convection\ at\ the\ surface\ of\ the\ wall}{conduction\ within\ the\ wall} = \frac{hL_c}{\lambda} \tag{2-12}$$

The lumped system is applicable if $B_i \leq 0.1$

To determine time to reach the steady state, it is possible to consider 5τ to have 99% of the steady state (figure 2-5).

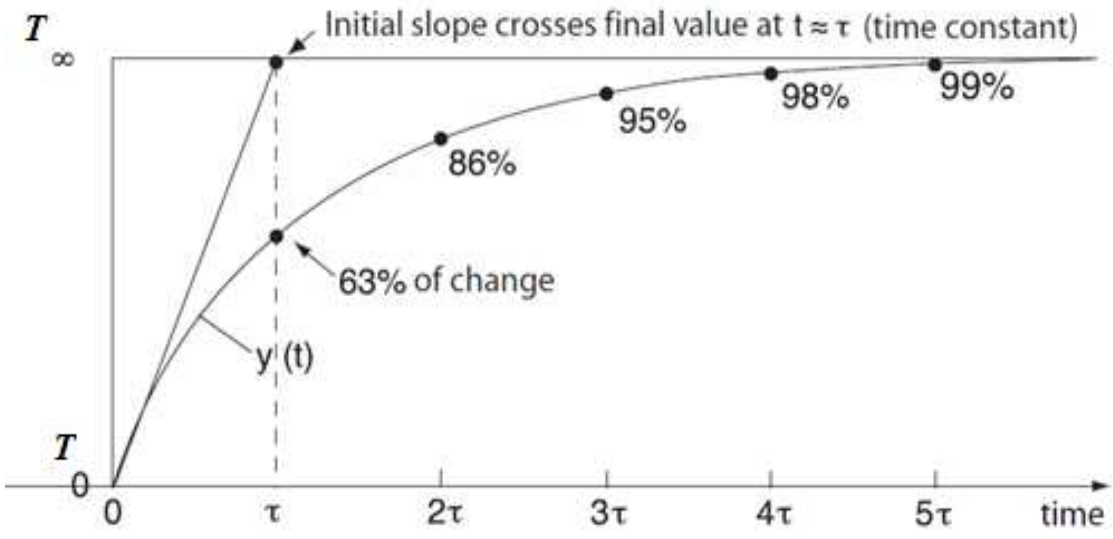

Figure 2-5: Transient heat flow

2-3 Thermal technique of characterization

There are two methods to measure thermal conductivity of insulation materials: steady state methods and transient state methods.

Under steady state conditions (figure 2-6), heat flow through element is constant during time. Temperatures in each point of components layer are only function of its thermal resistance. Time lag and heat storage are not an issue. The steady state method depends on the Fourier law of heat conduction and suffers from major drawbacks. It requires a long time to establish a steady-state temperature gradient across the sample and a large temperature gradient. A large sample size is also required, and the contact resistance between the thermocouple and the sample surface is considered as a major source of error. One of the common widely of steady state methods is Guarded Hot Plate (GHP) technique which is suitable for homogenous materials.

Under unsteady state (transient) conditions (figure 2-7), heat flow through the element is not constant. Temperatures in each point of the layer depend on time, thermal resistance and thermal capacity of this element and solicitations. Transient state method depends on the procedure of applying constant heat flux through the sample which must be in thermal equilibrium initially. Rapid results are one of the main advantages of these methods besides possibility used in situ.

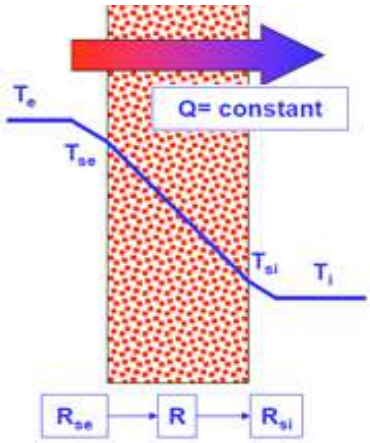

Figure 2-6: Steady state conditions

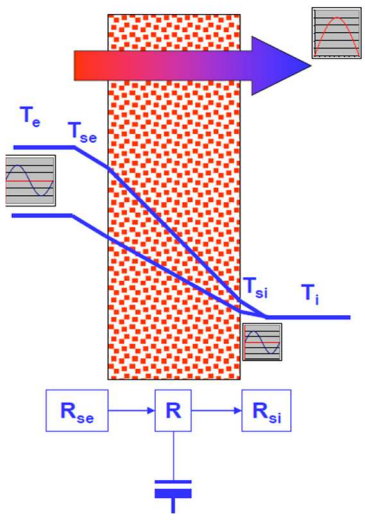

Figure 2-7: unsteady state conditions (transient)

2-3-1 Steady state techniques

This is the most common method for the measurement of thermal conductivity of insulation materials. It is suitable for dry homogeneous materials in slab forms. Under steady state condition, the rate of flux through unit area for each temperature gradient is constant and perpendicular to the isothermal surface of the sample. Thermal conductivity for homogeneous sample is calculated by:

$$\lambda = \frac{q.d}{A.(T_{h-}T_c)} \tag{2-13}$$

Where:

λ : Thermal conductivity (w/m.k)
q : Rate of heat flux (w)
d : Thickness of the sample (m)
A : Area measured on the a selected isothermal surface (m²)
T_h : Temperature of the hot surface (k)
T_c : Temperature of the cold surface (k)

Usually the heat flux is determined by the measurement of a power emitted in an electrical heater divided by the area of the sample. Generally, the value of thermal conductivity is related to the average temperature of the hot surface and cold surface.

2-3-1-1 Heat flow meter (HFM) technique

A heat flux meter (HFM) is located between the guard plate and the heater, it allows to control the temperature difference between the two pieces (figure2-8). The heat flux is obtained by the so-called (hybrid method) [10] as shown in figures 2-9.

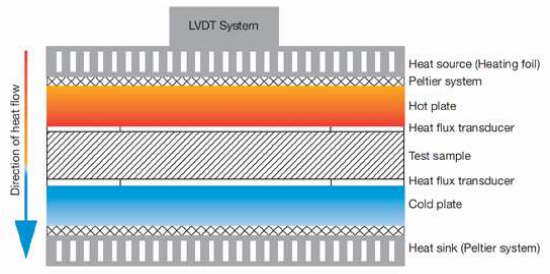

Figure 2-8: scheme of heat flux meter

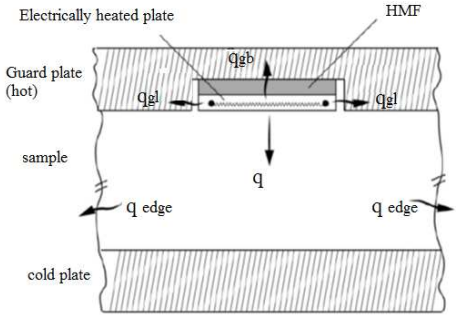

Figure 2-9: heat flux by hybrid method [10]

At steady state the heat balance on the heater plate expressed by:

$$P_e = q + q' \quad (2\text{-}14)$$

Where:

P_e: The electric power dissipated in the electric resistive circuit
q: The heat flux actually passing through the sample
q': Parasite (leak) heat fluxes defined as:

$$q' = q_{gb} + \sum_{i=1}^{4} q_{gl,i} + \sum_{i=1}^{4} q_{edge,i} \quad (2\text{-}15)$$

Where:

q_{gb} : the back heat flux going to the guard plate through the HFM
$\sum_{i=1}^{4} q_{gl,i}$: the heat flow passing to the guard plate laterally through the gap
$\sum_{i=1}^{4} q_{edge,i}$: the edge loss

The ideal vertical flow that produced by the heater leaves the sample through its edges, all the parasite heat fluxes depends on the gradient temperature between the guard plate and the heater plate as well as the temperature of the edge of the sample during the test.

When the edge of the sample is fully insulated and the temperature is the same in the guard and measurement plate, it can be assumed that all the electrical power transmitted in the heater flows vertically through the sample.

So the electric power is equal to the heat flux actually passing through the sample as defined in equation:

$$P_e \backsimeq q \quad (2\text{-}16)$$

During appropriate designs, q' is typically less than 0.5% of q [11].

2-3-1-2 Guarded hot plate (GHP) technique

A sample of material is placed between two plates. One plate is heated and the other is cooled. The thickness of the sample and the heat input to the hot plate are used to calculate thermal conductivity. During Guarded Hot plate the heat flow is steady-state in one direction. The test is applying according to the American Society for Testing Materials (ASTM) Standard ASTM 1977-71, ASTM 1977-85 and ASTM 177-97 [12]. The most adapted technique for insulation materials (American ASTM C 177-97 and European ISO 8302 Standards) is guarded hot plate (GHP) which takes into account the total heat transfer is the

steady-state method [13]. The guarded hot plate like others steady-state methods suffers from major drawbacks. Guarded hot plate is suitable for dry homogeneous samples in slab forms. Heat flow in the steady-state method (guarded hot plate) transfer in one direction.

Van Dusen in 1920 used guarded hot plate to measure thermal conductivity for insulation materials [14]. Van Dusen and Finck in 1928 constructed a version of guarded hot plate that continued to work for a long time [15]. The value of thermal conductivity collected from this apparatus was in agreement with real value. Robinson, H. E., and T. W. Watson in 1951 carried out some experimental tests to measure thermal conductivity for the cork board [16]. GHP apparatus has been improved with much better designs and reductions of operating costs of buildings. Then, data on thermal conductivities of insulating and building materials have significantly been more accurate in technical journals and handbooks. Inter-laboratory comparisons agree to within ±3% of the values of thermal conductivity and thermal resistance of the insulating materials [17].

There are many designs for a GHP Apparatus with different standards. The main are single sample parallel plate method (figure 2-10) and twin sample parallel plate method (figure 2-11).

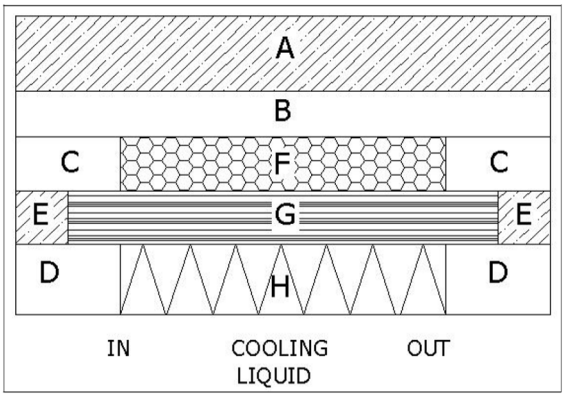

Figure 2-10: Single sample parallel plate method (A,E : insulation; B,C,D : guard heater; F: main heater; G: sample; H: cooling liquid)

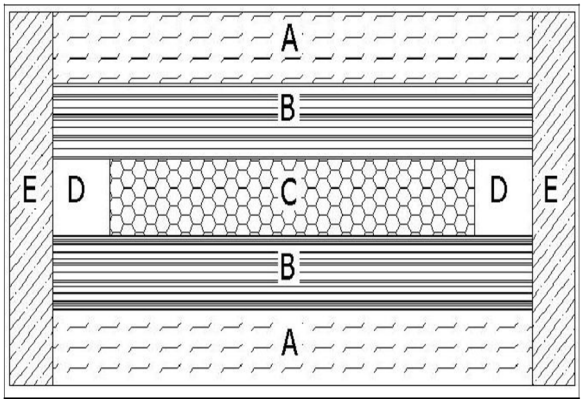

Figure 2-11: Twin sample parallel plate method (A: cold plate; B: sample; C: main heater; D: guard heater; E: insulation)

The heat source (F on figure 2-10 and C on figure 2-11), the sample (G on figure 2-10 and B on figure 2-11) and the heat sink (H on figure 2-10) are placed in contact with each other. Thermal guard (B, C and D) on figure 2-10 and D on figure 2-111 reduced the effect of climatic (temperature and humidity) environment. We consider the ideall approach that no heat leakage occurs from source, sample or sink boundaries. So, the measured heat input is fully transferred across the sample. The thermal conductivity is determined from the

measurement of the amount of heat input required to maintain the steady-state temperature profile across the test specimen and temperature of the heating and cooling plate. After steady state has been established, the thermal conductivity can be calculated from the heat input Q, the temperature differential across the sample (T1 - T2), and the sample thickness (Δ x) and heat transfer area of the sample (A).

$$Q = -\lambda A \frac{T_1 - T_2}{\Delta x} \quad (2\text{-}17)$$

Since steady state conditions may take several hours to develop, this method is unsuitable for use with material in which moisture migration may take place. The method has been used for measuring the thermal conductivity of dried materials.

2-3-1-3 Guarded Hot Box (GHB)

Hot Box is used to test the thermal properties of an individual material or a composition of materials in multilayer walls or cavity walls in buildings besides to measure frequently windows structures [18]. The measurement is done during the heat transfer through the materials. After completing this operation and collecting all the information the heat transfer coefficient or a U-value for that material or thermal resistance can be obtained [19]. Moisture transfer during the test specimen can also be tested by controlling the relative humidity and the temperature on the two sides of the sample [20]. Hot boxes also used to evaluate the thermal properties of building components had been calculated [21].

There are two groups from hot boxes; Calibrated Hot Box (CHB) and Guarded Hot Box (GHB), each group consists of different design used around the world.

First: Calibrated Hot Box (CHB) group

The first Calibrated Hot Box (CHB) was design in 1970 by Mamow [22] (figure 2-12).

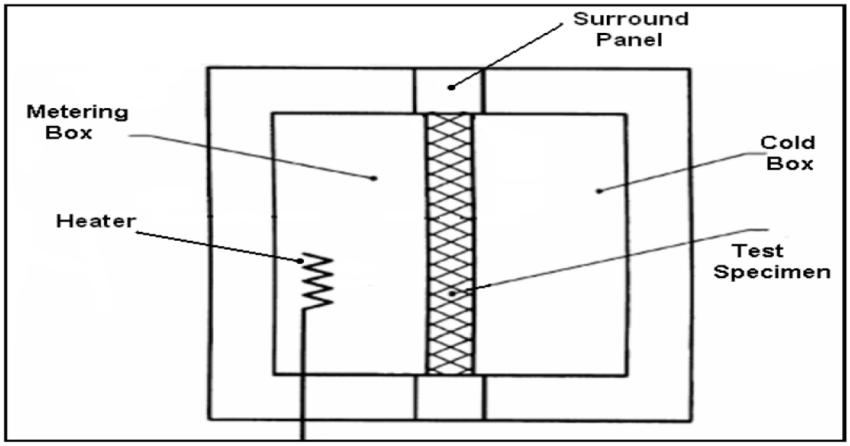

Figure 2-12: Calibrated Hot Box [22]

Simple Calibrated Hot Box (CHB) [23] consists of two chambers, the metering box representing the indoor environment and the cold box representing the outdoor environment [24]. The walls of the chambers are very thick to keep loss at a minimum and made from a material with a very high thermal resistance. The thickness of the surround panel is changed according to the standard Calibrated Hot Box (CHB). The test specimen is fixed between the two chambers and the energy flow transfer through the test specimen from hot chamber to cold chamber. The main objective of the hot chamber is to provide a controlled temperature, appropriateness wind velocity and heat flow through the specimen. The cold chamber contents the refrigeration system.

Second: Guarded Hot Box (GHB) group

The first Guarded Hot Box (GHB) was designed in 1930 to test more than 120 different wall [25]. The metering box in the Guarded Hot Box (GHB) existing inside guarded box to reduce heat loss and to keep same temperature in the metering box and guarded box, this is the difference between Guarded Hot Box (GHB) and Calibrated Hot Box (CHB) [19]. Guarded Hot Box (GHB) is suitable to test full-scale systems because it measured the total heat transfer through a complete test specimen [26]. It's more accurate but it has one insufficiency that it takes smaller test specimen than Calibrated Hot Box (CHB).

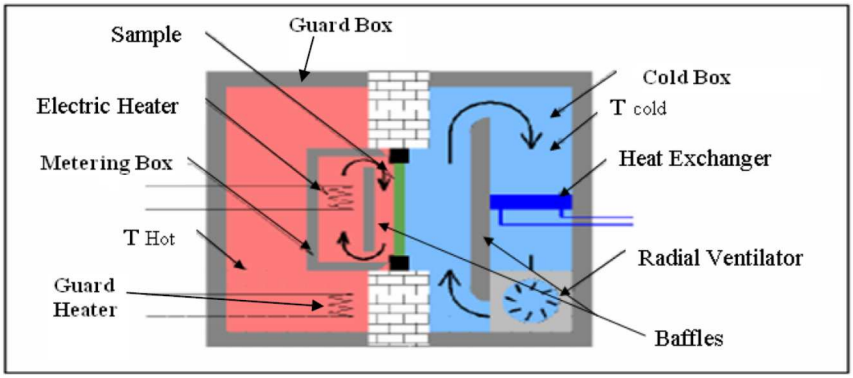

Figure 2-13: Guarded Hot Box (GHB) [27]

Figure (2-13) [27] illustrates the conventional Guarded Hot Box (GHB) which is similar to the Guarded Hot Box (GHB) described by Versluis [28], Kosney [29] and Nussebaumer [30]. The National Research Council Canada [31], built Guarded Hot Box (GHB) to test skylight windows with alternative designs, this is what made it possible to alternative designs to build Guarded Hot Box (GHB).

Other type of Guarded Hot Box (GHB) has been used in 2002 at University of Ulster to test the insulating properties of evacuated glazing. This kind of Guarded Hot Box (GHB) was designed and built according to the BS EN ISO 8990 [32]. The walls of metering box was constructed from plywood, a 20 W heater was used to heat the metering box and four electric fans fixed to eliminate static air pockets. Two baffles were installed parallel to the test specimen and behind the heater to eliminate the radiative exchange with the box walls. The guard box was built with of 150 mm Styrofoam insulation to keep the air temperature difference between the guard box and the metering box less than 0.1 °C as shown in figure (2-14) [33].

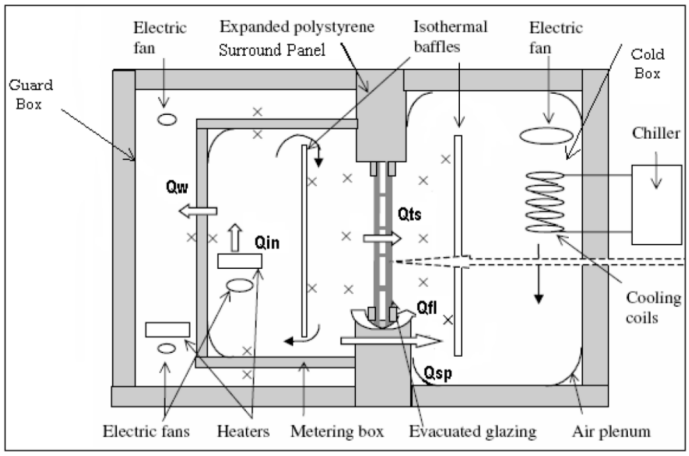

Figure 2-14: Cross section of Guarded Hot Box (GHB) [33]

2-3-2 transient techniques

As mentioned previously, heat flow through the sample during transient state condition is not constant and the sample must be in thermal equilibrium initially. The main advantage of transient techniques are rapid results (short time test) and possibility used these techniques in situ. Transient methods are suitable for materials have high moisture contents, a brief review of main transient technique is provided on table 2-1 [34] with Standard ASTM or ISO and capabilities / limitations.

Technique	Capabilities and limitations	Standard
Hot wire	- Suitable for liquids, powders and dielectric materials. - Not suitable for anisotropic materials. - Applicable for $\lambda < 15$ W/mK - Temperature range (20 °c to 1500 °C). - Long sensor, and consequently, long sample.	ASTM C1113/C1113M-09
Hot strip	- Suitable for solids and fluids with low elec. cond. - Capable of measuring (λ, α and C_p) - Long sensor, and consequently, long sample.	
Transient plane source (TPS)	- Suitable for solid, liquids and powders - Capable of measuring (λ, α and C_p). - Suitable for both isotropic and anisotropic materials. - Compact sensor, and consequently, small sample.	ISO22007-2
Laser flash	- Suitable for homogenous, isotropic and opaque solids. - applicable for α from 0.1 to 1000 mm^2/s - temperature range (75 K to 2800K)	ASTM E1461-13
3ω	- suitable for electric solids - for measuring thermal conductivity λ - temperature range (30 K to 750 K)	
Differential photoacoustic	- For measuring thermal conductivity λ of thin films.	
Pulsed phtothermal displacement	- For measuring thermal diffusivity α of solids.	
Thermal-wave	- For measuring thermal diffusivity α of high temperature Superconductors. -Temperature range (10 K to 300K)	

Table 2-1. Summary of capabilities and limitations of available transient techniques [34]

This study is focused on Hukseflux TP02 probe (Hot wire technique) and hot disk (Transient plane source) during the experimental tests for insulation materials due to the low cost, short time and possibility to use these methods in situ.

2-4 Probe technique

To access thermal characteristics of insulation materials, in situ measurements, and not just in laboratory conditions, can be considered an important issue. To determine these characteristics in situ, only the transient techniques are possible because of their quick measurement, their portability and their relative low cost. They are also interesting because of the low power they need making possible the study of moisture content influence. This technique is considered non-destructive method to evaluate thermal properties for insulation materials. The building insulation materials such as glass wool vary when transferred from the site to the laboratory due to the change of the conditions, therefore the transient technique (probe method) is used to overcome these restrictions in situ. Moreover, the steady state techniques such as guarded hot plate commonly used in the laboratory measurements required long time to achieve thermal properties.

2-4-1 Development stages of probe method

The development of probe method over several stages:

First: the nineteenth century (measuring thermal conductivity for gases)

Josef Stefan in 1872 [35], [36]; measured the thermal conductivity of air with an instrument called (Diathermometer), this was the first instrument to measure the thermal conductivity of gases. The value of the thermal conductivity agreed values at approximately the same temperature by 3 %. Stefan measured the thermal conductivity for gases by using similar technique and published his results in 1875 [37], [38].

Schleiermacher in 1888 [39] measured the thermal conductivity for gases by using a platinum hot wire (0.4 mm diameter and 320 mm length) into the center of the glass cylinder of 24 mm diameter.

Second: Twentieth century (measuring thermal conductivity for fluid and solid)

Weber in 1917 [40] modified method of Scheiermacher and proposed vertical instrument which is consist of platinum wire (0.4 mm diameter and 545 mm length) placed in side 23 mm diameter glass tube .he measured the thermal conductivity for some gases values was Close to current values.

Bertil Stâlhane and Sven Pyk[41] use of the transient hot-wire technique, for the first time in 1931, they employed this technique in order to measure the thermal conductivity of solids and powders (and some liquids),the hot wire was made from constantan (very low temperature coefficient of resistance). The work of Stâlhane and Pyk was improved by Eucken and Eglert in 1938 [42], they designed an absolute transient hot-wire instrument for low temperatures with using the 0.1 mm diameter platinum wire.

Van der Held and van Drunen in 1949 [43], Van der Held and et al 1953 [44] used a 0.3 mm diameter manganese, with 0.1 mm diameter copper/constantan thermocouple (placed together in a glass vessel) to obtain the thermal conductivity of aggressive liquids.

Hooper and Lepper in 1950 [45] used Aluminium probe with a steel tip (475 mm long by 5 mm diameter) to overcome Problems faced by the guarded hot plate method (moist and undisturbed) of samples.

Blackwell and Misener in 1951 [46] suggested simplifying assumptions of Hooper and Lepper and they used probe 800 mm long by 40 mm diameter to reduce error levels from axial and end losses. Blackwell carried out in 1952 other calculation about the radial and axial heat flow [47] then put equation to obtain the minimum probe length to radius ratio $L/r>[\alpha.t/0.0632r^2]^{0.5}$ and published theoretical solution for his work in 1954 [48].

Gillam et al. [49] in 1955 practice the ideas of Stâlhane and Pyk, Eucken and Englert to manufacture a simple apparatus of lower uncertainty, 0.3% for liquids and solids to obtain the temperature from the wire's resistance, they used a 0.1 mm platinum wire.

Jaeger in 1956 [50] described the contact resistance between the probes having big diameter (30 mm to 40 mm) and the medium (dry rock) as equal to the thermal resistance of 1mm air. After that, in 1959, Carslaw and Jaeger [51] developed a classical mathematical solution to obtain the thermal conductivity of the sample being measured.

Grassman and Straumann [52] in 1960 published a transient hot-wire apparatus for gases and solids, and Haupin [53] an instrument for solids in which a thermocouple placed in the centre of the sample is heated with alternating current expressible both as heat source and thermometer.

Turnbull [54] in 1962, compute the thermal conductivity of molten salts in the liquid and solid states, and of organic silicates. He used a 0.1 mm-diameter platinum wire, of 10 cm length, putting in the sample, was heated by direct current. The thermal conductivity was obtained uncertainty of 3%. Horrocks and McLaughlin [55] in 1963 used four terminal transient hot-wire instrument for finding the thermal conductivity of liquids, with an uncertainty of 0.25%. They used a 60 μm-diameter platinum wire of 15 cm length.

Mittenbühler [56], in 1964 used a heating wire of one metal with a thermocouple welded to the heating wire in the form of a cross in order to determine the thermal conductivity of solids. The temperature rise generated by heating power is used to find the thermal conductivity. The developed method formed the basis of methods for a German [57] and a European [58] standard in use today.

Four years later, in 1968, Burge and Robinson [59] suggested another four-terminal transient hot-wire instrument for gases employing lower times. The line source consisted of a 0.7 mm diameter, 20.6 cm length wire. They measured the thermal conductivity of He, Ne, Ar and their mixtures. Hayashi et al. [60] also used a four-terminal transient hot-wire instrument, but to measure the thermal conductivity of solids up to 1200 o C.

In 1971, Davis et al. [61] proposed a very small 6.2 μm-diameter and 1.3 cm-length platinum transient hot wire. They used a digital voltmeter (HP 2402A, 40 measurements/s) Instead of the photographing galvanometer spots or using chart recorders.

Work of Haarman [62], [63], in 1971 was the most important because he used an automatic Wheatstone bridge to measure the resistance difference of two wires. The bridge was able to determine the time required for the resistance of the hot wire. This bridge is used to reduce the duration of each experimental run and for elimination on the effect of arising from convection. Alloush et al. [64], in 1982 proposed using the wires are made from tantalum to measure the thermal conductivity of electrically conducting liquids

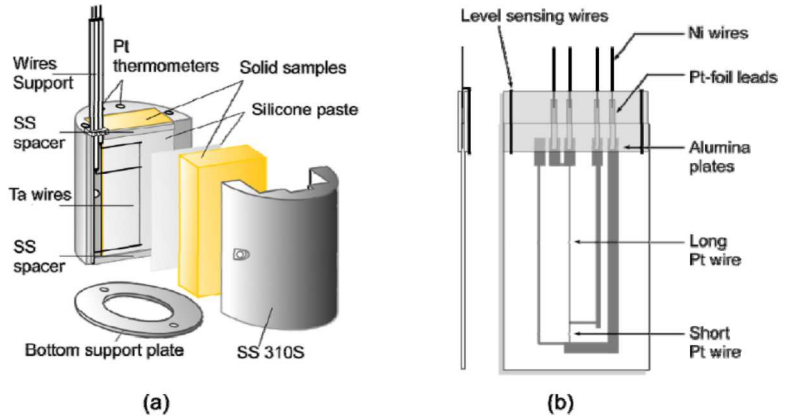

Figure 2-15: some transient hot wire instruments for solids [65 and 66]

Figure (2-15) shown some transient hot wire instruments for solids. Design (a) shown two tantalum wires are placed inside a soft silicone layer to avoid air gaps and make the contact excellent [65], has been achieved 1 % uncertainty by this way. Design (b) was the same but the two wire placed between soft alumina layers which became solid by fire under pressure [66].

In the transient hot wire method (THWM), the line heat source and the temperature sensor are separated where the position of the temperature sensor at a radial distance from the heat source, as shown in the figure (2-16) (top) [67]. While in the probe method the needle probe containing heating element and temperature sensor. The temperature sensor is separated by a medium with good electrical insulation, as shown in figure (2-16) (bottom) [67].

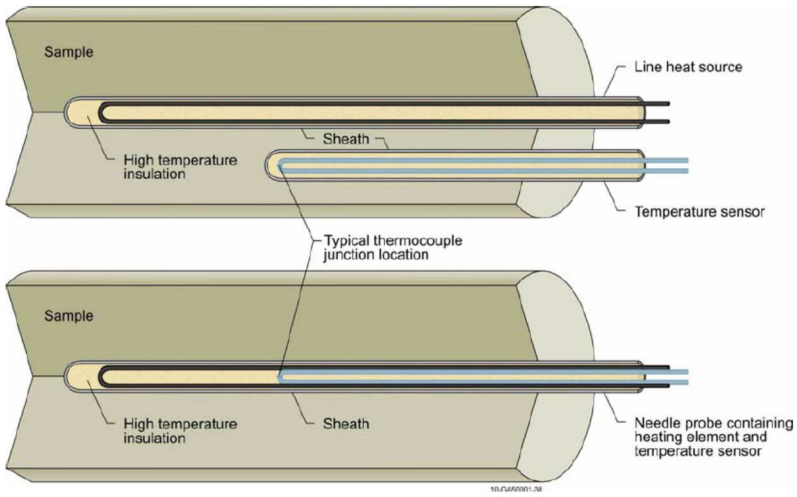

Figure 2-16: the details of the temperature sensor and the line heat source for transient hot wire method (top) and needle probe method (bottom) [67].

According to the number of needle, there is different type of probe such as:

First: Single Needle Probe

De Vries and Peck [68] designed thermal conductivity probe (TCP) as shown in Figure (2-17), the capillary glass is covered heating wire.

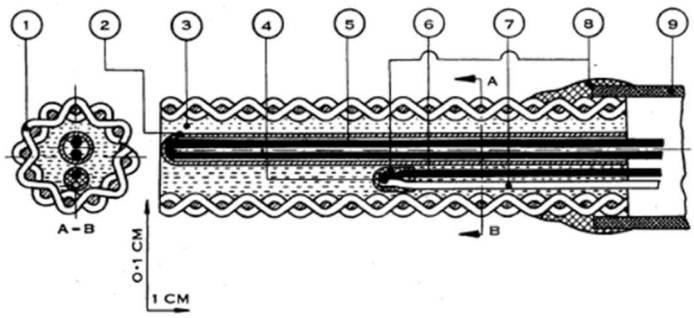

Figure 2-17: Radial and longitudinal cross sections of a TCP. 1, Monel gauze (filled with paraffin wax); 2, glass capillary; 3, paraffin wax; 4, thermojunction; 5, heating wire; 6, constantan wire; 7, copper wire; 8, insulating cover; 9, plastic socket. (Adopted from [68])

Another (TCP) designed from electrical heating coils as shown in Figure (2-18) [69], the steel and epoxy is embedded in the rod whose length is 20cm and the length of heating wire is 5 cm.

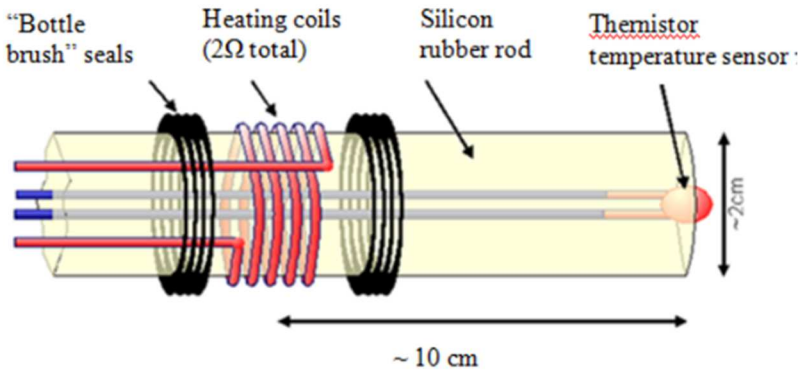

Figure 2-18: Another TCP design. [69]

Second: Multi Needle Probe

This kind of thermal conductivity probe has more than one needle altogether as shown in Figure (2-19). According to Bristow *et al*. [70], from this type of the probe it is possible to obtain thermal properties, water content and electrical conductivity of the sampling porous medium. Two needles are used to measure the thermal properties and water content and the

other needles are used to measurements of the electrical conductivity of the sampling porous medium.

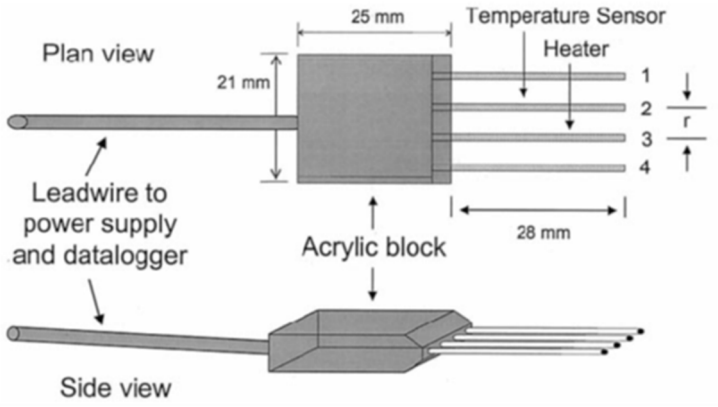

Figure 2-19: A multi-needle TCP design (Adopted from [70])

2-4-2 Theory of the thermal probe

The non-steady state probe (NSSP) method for thermal conductivity measurement assumed an infinitely long line heat source inserted in an infinite and homogeneous medium and is expressed by the general Fourier equation:

$$\frac{\partial T}{\partial t} = \alpha \nabla^2 T \qquad (2\text{-}18)$$

Subject to the initial condition: at $t \leq 0$, $\Delta T(r, t) = 0$

For boundary condition:

at r = 0 and $t \geq 0$, $\lim_{r \to 0} \left[\frac{rdT}{dr}\right] = -\frac{Q}{2\pi\lambda}$ (2-19)

at r = ∞ and $t \geq 0$, $\lim_{r \to \infty} [\Delta T(r, t)] = 0$ (2-20)

The temperature response of the heat source over time with heat is maintained at a constant rate can be described by Carslaw and Jaeger solution [51]:

$$\Delta T = -\frac{Q}{4\pi\lambda} Ei\,[u] \qquad (2\text{-}21)$$

Where :$u = \frac{r^2}{4\alpha t}$ (2-22)

The exponential integral function (E_i) can be expressed by a series expansion [71]:

$$-E_i(-u) = \int_u^{\infty} \left[\frac{e^{-u}}{u}\right] du \quad (2\text{-}23)$$

Where $-E_i(-u) = -\gamma - ln(u) - \frac{(u^2)}{2.2!} + \frac{(u^3)}{2.3!} - \frac{(u^4)}{2.4!} + \cdots$ (2-24)

Carslaw and Jaeger [51] found solutions for equation (2-18) after considering the assumptions of constant heat flow (Q), constant thermal properties, negligible the heat conduction in the radial direction and negligible thermal mass of the heater.

$$\Delta T = -\frac{Q}{4\pi\lambda}\left[-\gamma - ln(u) - \frac{(u^2)}{2.2!} + \frac{(u^3)}{2.3!} - \frac{(u^4)}{2.4!} + \cdots\right] \quad (2\text{-}25)$$

For small *u* value (equivalent to the large values of time), the terms after logarithmic term can be neglected and the temperature change can be approximated by:

$$\Delta T = \frac{Q}{4\pi\lambda}\left[\left[ln\left(\frac{t_2}{t_1}\right)\right] + B\right] \quad (2\text{-}26)$$

Where $B = ln\left\{\frac{4\alpha}{r^2}\right\} - \gamma + \frac{2\lambda}{rH}$ (2-27)

With *H* the air gap thermal conductance.

If the early time data are ignored, a graph of ΔT against *ln (t)* becomes straight line with a slope equal to$\frac{Q}{4\pi\lambda}$, then the two points define a straight line and the thermal conductivity could be found from:

$$\lambda = \frac{Q}{4\pi}\left[\frac{ln(t_2/t_1)}{T(t_2) - T(t_1)}\right] \quad (2\text{-}28)$$

The thermal conductivity can then be determined from the slope (Q/4πλ). The intercept B (equation 2-26) should determine the thermal diffusivity whether the approximation at long times is satisfied but also whether the conductance H of the air gap (the inverse of the contact resistance) is known. In practice, the value of H varies greatly depending on the quality of the contact with the surrounding material requiring a preliminary calibration [72]. Moreover there is a gap between the experimental results and the values from equation (2-28) which allow just the determination of thermal conductivity and not determinate thermal diffusivity.

The materials of more importance regarding building energy efficiency are insulations with typical thermal conductivities in the range 0.02–0.08 Wm^{-1} K^{-1}. When measuring these lower thermal conductivity materials with commercially available thermal probes, it has been found that, although the results have excellent levels of repeatability, they rise over time during the

measurement. The results obtained with the hot wire techniques were 13-15% higher than with guarded hot plate technique for bulk densities below 25 kg.m^{-3} (or porosities > 99%). Batty et al. [73] considered that this may be due to the layered structure of the material giving rise to increased thermal conduction in the planes parallel to the fibre layers. The steady state technique usually assumes that heat flows predominantly across these planes whereas the hot wire loses heat radially.

Batty et al [73] notes that this S-shaped curve appears not only for moist materials but more generally for mineral wool insulation (19.7 kg.m^{-3}) even if these materials are dried. Even if hot wire and thermal probe techniques are considered by Hust and Smith in 1989 [74] suitable to determine thermal conductivity of insulation materials (fibre glass insulation, extruded and expanded polystyrene, paraffin wax), Hukseflux actually considers that TP02 technique is not appropriated for characterization of insulation materials (or high porous materials). Hukseflux restraints the use of their probe to a range of thermal conductivity between 0.1 and 6.0 W.m^{-1}.K^{-1} and defines an expected accuracy at 20 degrees of ± (3% + 0.02) W.m^{-1}.K^{-1}. The fixed accuracy of 0.02 doesn't allow insulation material characterization with usual thermal conductivity of 0.04 W.m^{-1}.K^{-1}. Pilkington et al. [75] confirm this point and conclude that the probe technique is unsuitable for materials with thermal conductivity less than 0.07 W.m^{-1}.K^{-1} because of the nonlinear temperature increase against the logarithm of time.

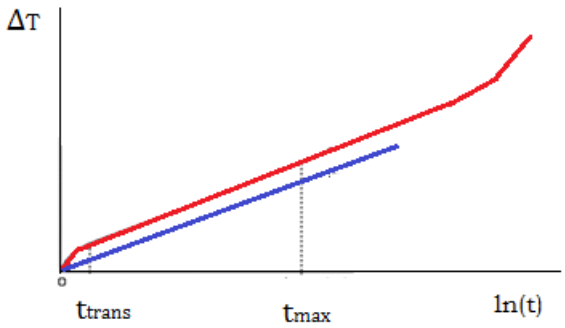

Figure 2-20: variation of temperature against natural logarithm

For short time (< t_{trans}): an initial phase after heating is happening due to the heating through the probe materials. This period is caused by the thermal capacity of the probe, contact resistance and a thermal imbalance between the temperature of the probe and the material

(figure 2-20). It depends on the thermal properties of the probe and its surrounding medium. Vos [76] defined the duration of this nonlinear transition period by:

$$t_{trans} = \frac{50.(R_S)^2}{4.\alpha} \quad (2\text{-}29)$$

Where Rs is the radius of the probe.

For long time (> t_{max}): this nonlinearity can be attributed to the axial losses at the end of the probe and heat exchange with the surrounding atmosphere (when the heating reaches the outer limits of the material). Vos [76] established time t_{max} by:

$$t_{max} = \frac{0.6\,(r-R_S)^2}{4.\alpha} \quad (2\text{-}30)$$

Where r is the sample radius.

2-4-3 Non dimensional parameters

2-4-3-1 Biot number (Bi)

Biot number (Bi) represents the ratio between thermal resistance by conduction and thermal resistance by convection at the surface of the probe. Bi number can be defined from the ratio of the time characteristics by conduction ($t_{cd} = \frac{R_S^2}{a}$) and by convection ($t_{cv} = \frac{\rho.c_p.R_S}{H}$). Bi number can also be determined by using λ the thermal conductivity ($W.m^{-1}.K^{-1}$), V_s the volume (m^3), A_s the external surface (m^2) and l_s the length (m) of the probe. Characteristic length (l_c) of the probe is defined for a lengthy cylinder (l_s>>>>R_s) as $l_c = R_s$:

$$Bi = \frac{\frac{V_S/A_S}{\lambda.A_S}}{\frac{1}{H.A_S}} = \frac{H.l_c}{\lambda} = \frac{R_S}{\lambda.R_c} \quad (2\text{-}31)$$

From this definition of the Biot number, 3 interesting cases can be studied:

- Bi<0.1: Thermal resistance of the probe is lower than thermal resistance of the material. This media can be considered as thermally thin. Material is heating uniformly without temperature gradient (so called zero gradient method). Surface resistance limits heat conduction through the medium.
- 0.1<Bi<100: Thermal flow is limited by the conduction (case of Fourier condition).
- Bi>100: Temperature is applied on the external surface (case of Dirichlet condition) so $H \to \infty$ and $Bi \to \infty$. Heat conduction inside the media is lower than at the external surface of the probe, so temperature gradients are important inside the media. The media can be considered as thermally thick.

The probability of probe contact with local fibres is relatively high because the probe is pushed into such an insulant and creating its own bore hole. Fibre / probe thermal contacts should be better than those between the fibres. The contact resistance of the glass fibre insulant with the probe was considered by Batty et al. [5] to be relatively small compared with thermal resistances provided by the insulant.

2-4-3-2 Fourier number (F_o)

The Fourier number determines the ratio of the heat conductive through the medium and heat stored:

$$F_o = \frac{\frac{\lambda.A}{l_c}\Delta T}{\frac{\rho.c.V}{t}\Delta T} = \frac{a.t}{l_c^2} = \frac{a.t}{R_s^2} \quad (2\text{-}32)$$

F_o<<1: Case of semi-infinite medium, low propagation of heat through the medium,

F_o>>1: Fast propagation of heat through the medium

2-4-3-3 Inertia contrast (Ω)

Inertia contrast represents the ratio between heat capacity of the material (S_m) and heat capacity of the probe (S_s). Considering ρ_s the density and C_s the specific capacity of the probe

$$\Omega = \frac{S_s}{S_m} = \frac{\pi.R_s^2.\rho_s.C_s}{S_m} \quad (2\text{-}33)$$

2-5 Hot Disk technique (HD)

Hot disk (HD), a transient technique [77], is distinguished mainly by the short time and by the low flow in comparison with a steady-state technique (GHP). Al-Ajlan [78] and Coquard et al. [79] have already validated the HD technique for the study of low-density thermal insulators. It is worth to be mentioned that the accuracy and short test time are the main advantage of the hot disk (HD). Bouguerra et al [80] used transient plane source technique to measure measurement of thermal conductivity, thermal diffusivity and heat capacity of highly porous building materials, ethylene tetrafluoroethylene sheets (ETFE). Al-Ajlan [78] used transient technique (TPS) to investigate thermal conductivity for different insulation materials (Extruded polystyrene, Polyurethane board, Perlite -loose fill- and rock wool) that are used in hot climate. He showed that thermal conductivity for insulation materials increased with temperature. In general hot desk (TPS) method is able to analyze the thermal transport properties of anisotropic materials counter to other methods that supposes homogeneity of the materials.

The Hot Disk thermal constant analysis is used to measure thermal properties for different materials such as liquids, solids and powders. It's based on the theory of the transient plane source (TPS) according to the ISO 22007-2. The TPS probe contains a sensor that is used as both a heat source for increasing the temperature of the sample and a resistance thermometer for registration the time.

When amount of power is passing through the wire or strip, the temperature is increased and thus the resistance will change in the wire or strip. The thermal characteristics (thermal conductivity, thermal diffusivity and thermal capacity) can be calculated during the increase of the temperature sensor with the time as shown in the figures (2-21).

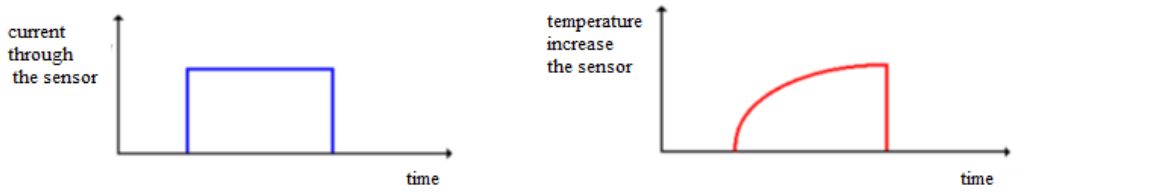

a- *Current through the sensor in TPS method*

b- Temperature increase of the sensor in TPS method

Figure 2-21: current and temperature through the sensor in TPS method

The sensor is put between two pieces of the sample or insert into the sample, the constant temperature differences applying by good contact between the surface of the sample and sensor (figure 2-22). The sample size must be more than the distance that has to be reached by heating from the sensor. This distance is called (probing depth) and depend on the sample thermal diffusivity and measuring time as in equation:

$$D = 2(\alpha . t)^{1/2} \qquad (2\text{-}34)$$

Where:

D : probing depth [mm]

α : Thermal diffusivity in [mm^2/s]

t : measuring time in [s]

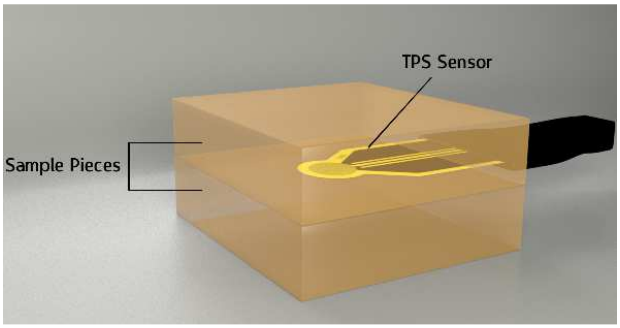

Figure 2-22: position of the sensor of TPS method between sample pieces

The measurement time during the test must be carefully chosen based on the diffusivity and the sample size. The width of the sample must be more than twice probing depth plus the sensor diameter and the thickness of the sample more than probing depth. This condition is very important to avoid the heat wave reaches the sample boundary during the measurement time. Other requirement must be check to obtain better measurement such as total time characteristic (dimensionless) [81] as in equation:

$$0.3 \leq \alpha . t/r^2 \leq 0.8 \quad (2\text{-}35)$$

Where:
r : Sensor radius [mm]

Selecting correct experimental setup parameters is very important to obtain accurate results. Other parameters effect on the results is the constant heat power, as we know the thermal conductivity of the materials affected by how much power should be used. Insulation materials that have low thermal conductivity need small power, in mW range, while metal materials that have high thermal conductivity need to use high power. For unknown samples starting by low power to avoid damage the sensor.

The assumption that the Hot Disk consists of a certain number of concentric ring heat sources, located in an infinitely large sample, was used to describe Hot Disk behaviour and to solve the equation of heat conduction. The increase in Hot Disk resistance is a function of time when it's electrically heated [82]:

$$R(t) = R_0[1 + \Omega\{\Delta T_i + \Delta T_{ave}(\tau)\}] \quad (2\text{-}36)$$

Where:

R_0 : is the resistance of the disk just before it is being heated (at time t = 0).
Ω : is the temperature coefficient of the resistivity (TCR).
ΔT_i : is the constant temperature difference that develops almost momentarily over the thin insulating layers which are covering the two sides of the hot disk sensor material (nickel) and which make the hot disk a convenient sensor,
ΔT_{ave} : is the temperature increase of the sample surface on the other side of the insulating layer and facing the hot disk sensor (double spiral).

The temperature increase recorded by the sensor is then obtained:

$$\Delta T_{ave}(\tau) + \Delta T_i = [\{R(t)/R_0\} - 1]/\Omega \quad (2\text{-}37)$$

Where:

ΔT_i : representing the contact between the sensor and the surface of the sample,
ΔT_i : Equal to zero for the perfect contact and become constant after short time
Δt_i is estimated as:

$$\Delta t_i = \delta^2 / \alpha_{\ i} \quad (2\text{-}38)$$

δ : is the thickness of the insulating layer of the sensor.
$\alpha_{\ i}$: is the thermal diffusivity of the layer material.

The time-dependent temperature increase is obtained by the theory as:

$$\Delta T_{ave}(\tau) = \left[\frac{P_0}{\pi^{\frac{3}{2}}\ r.\lambda}\right] D(\tau) \quad (2\text{-}39)$$

Where:
P_0 : Total output of power from the sensor [W]
r : Overall radius of the disk [mm]
λ : Thermal conductivity of the sample that is being tested [W/m.K]

$D(\tau)$: is a dimensionless time-dependent function which is found by:

$$\tau = \left(\frac{t}{\Theta}\right)^{1/2} \quad (2\text{-}40)$$

Where:
t : is the time measured from the start of the transient recording [s]
Θ : is the characteristic time defined as:

$$\Theta = r^{\,2}/\alpha \quad (2\text{-}41)$$

r : is the overall radius of the disk [mm]
α : Thermal diffusivity of the sample [mm²/s]

Conclusion of this chapter talks about the techniques used to measure thermal properties of insulation materials. It has been discussed the two techniques (steady state and transient state) and explain by details the types of each techniques and the advantage and disadvantage. Its focus on the probe method due to its low cost and short time during the test besides possibility use this method in situ. It explains the guarded hot box that use to test the thermal properties of an individual material or a composition of materials in multilayer walls.

References chapter two

[1]: Bhattacharyya RK., Heat-transfer model for fibrous insulations. In: McElroy DL, Tye RP (Eds), Thermal Insulation Performance, ASTM STP 718 (pp. 272 − 286). Philadelphia, PA: American Society for Testing and Materials. 1980.

[2]: Stark C, Fricke J, Improved heat-transfer models for fibrous insulations. International Journal of Heat and Mass Transfer, 36, 1993.

[3]: Daryabeigi K., Heat transfer in high-temperature fibrous insulation. Paper presented at the 8th AIAA/ASME Joint Thermophysics and Heat Transfer Conference, St. Louis USA. AIAA paper 3332, 2002.

[4]: Du N., Fan J., Wu H., Optimum porosity for fibrous porous materials for thermal insulation. Fibers and Polymers, 9: 27 − 33. (2008).

[5]: Bankvall **C**., Heat transfer in fibrous materials, Journal of Testing and Evolution, Vol.1, N°3, pp 235-243, 1973.

[6]: Simmler, H., Brunner, S., Heinemann, U., Schwab, H., Kumaran, K., Mukhopadhyaya, P., Quénard, D., Sallée, H., Noller, K., Kücükpinar- Niarchos, E., Stramm, C., Tenpierik, M. J., Cauberg, J. J. M., and Erb, M., Vacuum Insulation Panels. Study on VIP-components and Panels for Service Life Prediction of VIP in Building Applications (Subtask A): IEA/ECBCS Annex 39 High Performance Thermal Insulation (HiPTI), 2005.

[7]: NF EN ISO 6946, Composants et parois de bâtiments - Résistance thermique et coefficient de transmission thermique - Méthode de calcul, Juin 2008.

[8]: Schumacher, C.J., Temperature Dependence of R-values in Polyisocyanurate Roof Insulation, Building Science Info Sheet 502, BuildingScience.com, Somerville, MA, 2013.

[9] : A review of unconventional sustainable building insulation materials Sustainable Materials and Technologies Volume 4, Pages 1–17, July 2015.

[10]: Leong WH, Hollands K., Brunger A., On a physically-realizable benchmark problem in internal natural convection. Int J Heat Mass Tr 41(23):3817–3828, 1998.

[11]: International standard, ISO 8302, thermal insulation - determination of steady-state thermal resistance and related properties, 1991.

[12]: ASTM. a. C 177-97, Standard test method for steady state heat flux measurements and thermal transmission properties by means of the guarded-hot-plate apparatus. Annual Book of ASTM Standards, (04.06), 2000.

[13]: T Kobari, J. Okajima, A. Komiya, S. Maruyama, Development of guarded hot plate apparatus utilizing Peltier module for precise thermal conductivity measurement of insulation materials, International Journal of Heat and Mass Transfer Volume 91, pp 1157–1166, 2015.

[14]: Van Dusen, M. S., the thermal conductivity of heat insulators, the American society of heating and ventilating engineering (26): 385-414; also the American society for refrigerating engineering (7): 202-231, 1920.

[15]: Van Dusen, M. S. and Finck, J. L., heat transfer through insulating materials, the American institute for refrigerating (17): 137-150, 1928.

[16]: Robinson, H. E. and T. W. Watson. Inter laboratory comparison of thermal conductivity determinations with guarded hot plates. ASTM STP 119, pp. 36-44. 1951.

[17]: Robert R. Zarr, William Healy, James J. Filliben, Daniel R. Flynn; Design Concepts for a New Guarded Hot Plate Apparatus for Use Over an Extended Temperature Range; Building and Fire Research Laboratory and Manufacturing Metrology Division from National Institute of Standards and Technology, Gaithersburg, MD, 20899-8632 and 20899-8220 and MetSys Corporation, Millwood, VA 22646-0317, USA, 2002.

[18]: Yuan S., Experimental and Analytical Heat Transfer analysis For a calibrated Hot Box and Fenestration System, *University of Massachusetts Amherst. UMI No.3027279,* 2001.

[19]: Curcija D. PHD, Trends and developments in Window Testing Methods, University of Massachusetts, Centre for Energy Efficiency and Renewable Energy.

[20]: Burch D.M., Zarr R.R., Fanney A.H "Experimental verification of a moisture and heat transfer model in the hygroscopic regime" *Thermal performance of exterior envelopes of Building VI, Cleawater Beach FL. pp273-282,* 1995.

[21]: Rose J, Svendsen S. (2004) "Validating Numerical Calculations against Guarded hot box Measurements" *Nordic Journal of Building Physics Vol.4, 2004.*

[22]: Mumaw, J.R., Thermal Research Facility- A large calibrated Hot box For horizontal Building Elements". *Thermal Insulation Performance, ASTM STP 718, D.l. McElroy and R.T. Tyre, Eds. American society for testing and materials, pp. 195-207, 1980.*

[23]: BS EN ISO 8990, Thermal Insulation – Determination of steady state thermal transmission properties- Calibrated and Guarded hot box, 1996.

[24]: Gao Y., Roux J.J., Teodosiu C., Zhao L.H., Reduced linear steady state model of hollow block walls validation using hot box measurements. *Energy and Buildings 36, pp. 1107-1115, 2004.*

[25]: Zarr,R.R (2001) "A History of Testing Heat Insulators at the National Instituteof Standards and Technology" *ASHRAE Transactions 2001, V. 107, Pt.2., June 2001.*

[26]: Desjarlais A.O., Tye R. P. (1989) "The Thermal Performance of Reflective Insulation Materials and Systems with Vertical Heat Flow: a parametric study, *Thermal conductivity 21: The 21st International Thermal Conductivity Conference, October 15 – 18, Lexinton Kentucky, pp. 291 -309, 1989.*

[27]: Guarded Hot Box Image. Website: www.zebayern.comga

[28]: Velersluis R. MSC. Oversloot F.P. (2005) "Calibration of the TNO Guarded hotbox as specified by BS ISO 12567-1, *Netherlands Organisation for Applied Scientific Research,* 2000.

[29]: Kosney J, Dejarlais A. and Christian J. "Whole rating /Label for Structural Insulated Panels, Steady State Thermal Analysis" *Oak Ridge National Laboratory Building Technology Centre*, 1999.

[30]: Nussbaumer T., Bundi R., Tanner, Ch, Muehlebach H., Thermal Analysis of a Wooden Door System with Integrated Vacuum Insulated Panels, *Energy and* Buildings *37, 1107-1113, 2005.*

[31]: Elmahdy, A.H.; Haddad, K., Experimental procedure and uncertainty analysis of a guarded hotbox method to determine the thermal transmission coefficient of skylights and sloped glazing, *ASHRAE Transactions, v. 106, pt. 2, pp. 601-613, 2000.*

[32]: Fang Y, An experimental and theoretical investigation into the design, development and performance of evacuated glazing, *PhD thesis, the University of Ulster, Northern Ireland, UK*, 2002.

[33]: Fang Y., Eames P.C., Hyde T.J., Norton B. (2005)"Complex multimaterial insulating frames for windows with evacuated glazing" *Solar Energy 79, pp. 245-261, 2005.*

[34]: M. Ahadi, M. Andisheh-Tadbir, M. Tam, M. Bahrami, An improved transient plane source method for measuring thermal conductivity of thin films: Deconvoluting thermal contact resistance, International Journal of Heat and Mass Transfer 96, 371–380, 2016.

[35]: J. Stefan, Math. Naturwiss. Kl. Abt. II **65**, 45, 1872.

[36]: J. Stefan, Sitzungsberichte der Kaiserlichen Akademie der Wissenshaft **72**, 69, 1875.

[37]: *Air Products Material Safety Data Sheets* (https://apdirect.airproducts.com/msds/)

[38]: M.J. Assael,W.A.Wakeham, ThermalConductivity and Thermal Diffusivity,Chap. B3.5, in *Handbook of Experimental Fluid Mechanics*, ed. by C. Tropea, A.L. Yaril, J.F. Foss. (Springer, Berlin), pp. 133–147, 2007.

[39]: A. Schleiermacher, Ann. Phys. Chem. **270**, 623, 1888.

[40]: S. Weber, Ann. Phys. **359**, 437, 1917.

[41]: B. Stâlhane, S. Pyk, Teknisk Tidskrift, 61:389, 1931.

[42]: A. Eucken, H. Englert, Z. fur die gesamte Kalte-Industrie 45:109, 1938.

[43]: E.F.M. van der Held, F. G. van Drunen, Physica 15:865, 1949.

[44]: E.F.M. van der Held, J. Hardebol, J. Kalshoven, Physica 19:208, 1953.

[45]: Hooper FC, Lepper FR, *Transient heat flow apparatus for the determination of thermal conductivities,* Transactions American Society of Heating and Ventilation Engineers v .56, pp.309-324, 1950.

[46]: Blackwell JH, Misener AD, *Approximate Solution of a Transient Heat Flow Problem,* Proc. Phys. Soc. A 64, pp.1132-1133, 1951.

[47]: Blackwell JH, *Radial-axial heat flow in regions bounded internally by circular cylinders,* Canadian Journal of Physics, v.31 , nr.4, pp.4 72- 479, 1953.

[48]: Blackwell JH, *A transient-flow method for determination of thermal constants of insulating materials in bulk. Part 1-Theory,* Journal of Applied Physics, v.25, n.2, pp.137-144, 1954.

[49]: D.G. Gillam, L. Romben, H.-E. Nissen, O. Lamm, Acta Chemica Scandinavica 9:641, 1955.

[50]: Jaeger JC, *Conduction of heat in an infinite region bounded internally by* a *circular cylinder of* a *perfect conductor,* Australian J. Phys. v.9, pp.167-179,1956.

[51]: H.S. Carslaw, J.C. Jaeger; *Conduction of Heat in Solids, 2nd Ed*.; Oxford University,

London; 1959.

[52]: P. Grassman, W. Straumann, Int. J. Heat Mass Transfer 1:50, 1960.

[53]: W.E. Haupin, W. E., Am. Ceram. Soc. Bull. 39:139, 1960.

[54]: A.G. Turnbull, J. Chem. Engin. Data 7:79, 1962.

[55]: J.K. Horrocks, E. McLaughlin, Proc. Roy. Soc. A273:259, 1963.

[56]: A. von Mittenbühler, Ber. Dtsch. Keram. Ges. 41:15, 1964.

[57]: Testing of Ceramic Materials: Determination of Thermal Conductivity up to 1600o C by the Hot-Wire Method. Thermal Conductivity up to 2 W/m/K (Deutsches Institut für Normung DIN 51046, 1976.

[58]: Methods of Testing Dense Shaped Refractory Products. Part 14: Determination of Thermal conductivity by the Hot-Wire (Cross-Array) Method (European Committee for Standardization, EN 993-15, 1998.

[59]: H.L. Burge, L.B. Robinson, J. Appl. Phys., 39:51, 1968.

[60]: K. Hayashi, M. Fukui, I. Uei, Mem. Fac. Ind. Arts, Kyoto Tech. Univ. Sci. Tech., 20:81, 1971.

[61]: P.S. Davis, F. Theeuwes, R.J. Bearman, R.P. Gordon. 1971. "Non-steady-state, Hot Wire, Thermal Conductivity Apparatus," J. Chem. Phys., 55:4776, 1971.

[62]: J.W. Haarman, *Physica* 52**:**605, 1971.

[63]: J.W. Haarman, Ph.D thesis, Technische Hogeschool Delft, Netherlands, 1969.

[64]: A. Alloush, W.B. Gosney, W.A. Wakeham, Int. J. Thermophys. 3:225, 1982.

[65]: M.J. Assael, K.D. Antoniadis, K.E. Kakosimos, I.N. Metaxa, Int. J. Thermophys. 29:445, 2008.

[66]: M.V. Peralta-Martinez, M.J. Assael, M. Dix, L. Karagiannidis, W.A. Wakeham, Int. J. Thermophys. 27:353, 2006.

[67]: Brandon S. Fox “In-pile thermal conductivity measurement methods for nuclear fuels” Utah State University, Logan, Utah, 2010.

[68]: D. A. De Vries, and A. J. Peck, On The Cylindrical Probe Method of Measuring Thermal Conductivity With Special Reference To Soil; Division of Plant Industry, C.S.I.R.O, Deniliquin, N.S.W; 1957.

[69]: Australia,http://www.geosci.monash.edu.au/heatflow/chapter4.html, Faculty of Science, Building 20, Clayton Campus, Monash University, July 18, 2013.

[70]: K. L. Bristow, G. J. Kluitenberg, C. J. Goding, and T. S. Fizgerald; A small multi-needleprobe for measuring soil thermal properties, water content and electrical conductivity; Computer and Electronics in Agriculture, 31, p.265-280; 2001.

[71]: Abramowitz M, Stegun I, Handbook of Mathematical Functions with Formulas, Graphs and Mathematical Tables, Chapter 5, 9th Dover Printing, 10th GPO Printing Ed., Dover, 1964

[72]: Achard G., Roux J.J, Sublet, J.C “Description d’une sonde de mesure des caractéristiques thermiques des couches superficielles du sol. Résultats d’une campagne de mesures”, Revue Générale de Thermique, N° 267, pp 177-188, 1984.

[73]: W.J Batty, P.W O'Callaghan, and S.D Probert, Assessment of the thermal-probe technique for rapid, accurate measurements of effective thermal conductivities, Applied Energy, Vol. 16, pp. 83-113, 1984

[74]: Hust, JG, Smith, OR, lnterlaboratory comparison of two types of line-source thermal-conductivity apparatus measuring five insulating materials, National Institute of Standards and Technology, Report N. 89/3908, for U.S Dept. of Energy, Oak Ridge National Laboratory, 1989.

[75]: Pilkington B, In situ measurements of building materials using a thermal probe, phD, University of Plymouth, England, 2008.

[76]: Vos B, Analysis of thermal-probe measurements using an iterative method to give sample conductivity and diffusivity data, Appl. Sci. Res., pp. 425–438, 1955.

[77]: Y. He, Rapid thermal conductivity measurement with a hot disk sensor, Part 1: Theoritical considerations. Thermochimica Acta, 436, 1-2, pp 122-129, 2005.

[78]: S.A. Al-Ajlan, Measurements of thermal properties of insulation materials by using transient plane source technique, Applied Thermal Engineering, 26, pp 2184–2191, 2006.

[79]: R. Coquard, D. Baillis, D. Quenard Experimental and theoretical study of the hot-ring method applied to low-density thermal insulators, International Journal of Thermal Sciences, 47, pp 324–338, 2008.

[80]: A. Bouguerra, A. Ait-Mokhtar, O. Amiri, M.B. Diop, measurement of thermal conductivity, thermal diffusivity and heat capacity of highly porous building materials using

transient plane source technique, international communication in heat and mass transfer, 1065-1078, 2001.

[81]: V. Bohac, M.K. Gustavsson, L. Kubicar, S.E. Gustafsson, Parameter estimations for measurements of thermal transport properties with the hot disk thermal constants analyzer, Review of Scientific Instruments 71 (6), 2452–2455, 2000.

[82]: Hot disk thermal constants analyzer: Windows 95/98 Version 5.0. Instruction Manual, Hot disk AB, 1999.

Chapter 3 : Thermophysical characterisation of crimped glass wool

3-1 Introduction

A Mineral wool (glass wool), as a material used in the insulation of buildings, it's made from fibers and binders. There are repetitive patterns from the fibers across the panels according to a preferred orientation during their manufacture. The fibre mat with different texture is processed before the curing stage to produce a structure endowing the material with a higher mechanical strength. As a result, the elastic response of the finished product and its load bearing capacities are very sensitive to crimping process. This chapter focuses on the insulation materials and crimped glass wool that is used in this work. The physical characteristics (density, porosity and specific surface), hydric characteristics and thermal characteristics has been described.

3-2 Insulation materials

Using thermal insulation in buildings helps in reducing energy and the fossil fuel, saves operating cost, reduces emitted pollutants, improve the periods of indoor thermal comfort especially in between seasons, and reduce disturbing noise from neighbouring spaces or from outside, in addition to Economic benefits and Environmental benefits. Thermal insulation does not always have the same efficiency for all types of buildings. The efficiency of insulation is influenced by the following factors: the building component to be insulated (wall, roof and floor), the building type (function, size and shape) and climatic conditions of the building site. The energy consumption in heating constitutes the bulk of the energy used in Europe, both in the housing sector or the commercial sector (figures 3-1 and 3-2) [1].

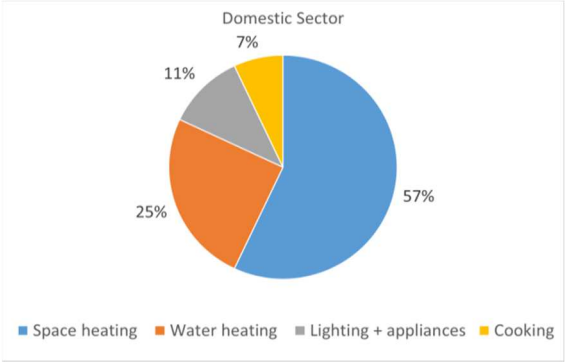

Figure 3-1: energy consumption in European for domestic sector [1]

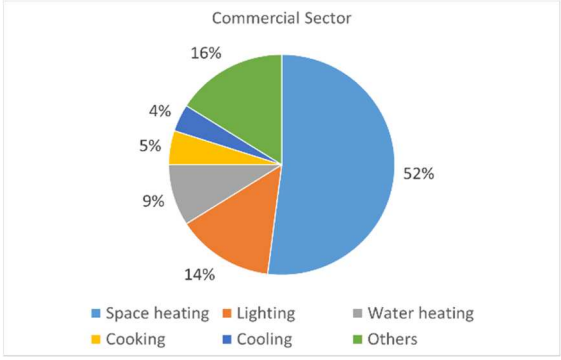

Figure 3-2: energy consumption in European for commercial sector [1]

To be defined as insulation materials, building materials must have, according to European standards (EN13162 to EN13171), a declared thermal resistance higher than 0.15 m².K/W or a declared thermal conductivity lower than 0.10 W/(m.K) at a measuring temperature of 10 °C. The main requirement for thermal insulation is to provide important resistance to the flow of heat through the insulation material (figure 3-3). To achieve this, the insulation material must reduce the rate of heat transfer by conduction, convection and radiation. Figures (3-4 and 3-5) [2] show the different between the uninsulated and insulated wall.

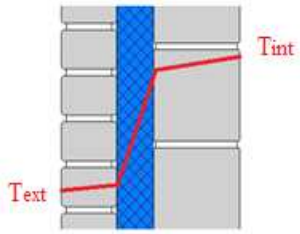

Figure 3-3: Temperature gradient in a wall

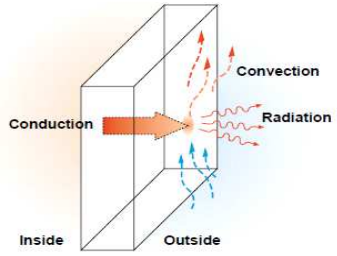

Figure 3-4: uninsulated wall [2]

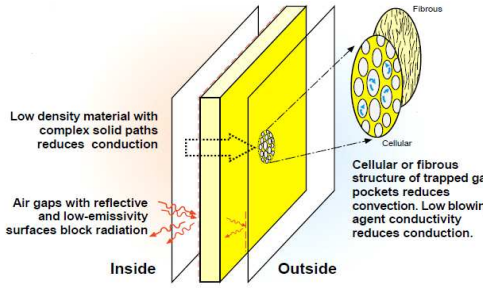

Figure 3-5: insulated wall [2]

3-2-1 Classification of insulation materials

Thermal insulation products for buildings have been classified (table 3-1) according to the origin of basic materials (oil-based, mineral-based or biomass-based) and form (fibre, foam or other) [3].

Origin form	Oil-based	Mineral-based	Biomass-based	Mixed
Fiber	Polyester fiber Other plastic fiber	Glass wool Stone wool Slag wool	Wood fiber and wool Cellulose / Cotton / Flax / Hemp / Sheep wool	
Foam	Expanded polystyrene Extruded polystyrene Polyurethane Polyisocyanurate Phenolic	Expanded perlite Cellular glass Calcium silicate Expanded vermiculite Expanded clay		
Other	Polyethylene	Aerogel	Expanded cork Feather Straw Strawboard	Reflective (foil) Insulation Vacuum insulation panels Expanded polystyrene mortar Hemp lime composite

Table 3-1: Classification of insulation materials [3]

Table (3-2) shows the practical application options of the different product varieties of insulating materials [4].

Materials	Density [kg/m^3]	Fire class MEN-EN13501	Flocks	Panels	Rolls	Injectable foam	Granules
Inorganic: fibrous							
Glass wool	12-150	A1	×	×	×	-	-
Rock wool	25-200	A1	×	×	×	-	-
Inorganic: cellular							
Calcium Silicate	200-240	A1	-	×	-	-	-
Foam glass	100-200	A1	-	×	-	-	-
perlite	32-176	A1	-	×	-	-	×
Vermiculite	64-130	A1	-	×	-	-	×
Organic-petrochemical: cellular							
Expanded polystyrene (EPS)	10-80	E-F	-	×	-	-	×
Extruded polystyrene (XPS)	15-85	E-F	-	×	-	-	-
Phenol formaldehyde (PF)	35-40	B-D	-	×	-	-	-
Polyurethane (PUR)	30-160	D-F	-	×	-	×	-
Polyisocyanurate (PIR)	28-40	D-F	-	×	-	-	-
Urea formaldehyde (UF)	15	D-E	-	-	-	×	-
Organic-renewable: fibrous							
Cellulose (paper wool)	30-70	E	×	×	-	-	-
Coconut	140	E	-	×	-	-	-
Flax (flax wool)	28	C	-	×	×	-	-
Hemp (hemp wool)	30-42	E	-	×	×	-	-
Recycled cotton	18	E	×	×	×	-	-
Sheep wool	25-60	E	-	×	×	-	-
Wood wool	55-140	E	-	×	-	-	-
Organic-renewable: cellular							
Expanded cork	100-120	E	-	×	-	-	×

Table 3-2: practical application options [4]

Glass wools are selected because of their price (less than 10 Euros per m²) but also because of fire resistance (classified A1) and their multi-use applications (flocks, panel and rolls). Inorganic insulation materials (glass wool and stone wool) represent over 50% of the EU market. Expanded and extruded polystyrene, polyurethane and polyisocyanurate make up the major part of rest of the market. Only a very small fraction (maximum 6%) is biomass based. Of this latter fraction wood fibre materials (including cellulose) are most common (table 3-3) [5].

Insulation materials	Western Europe	Central and East of Europe
Glass wool	39.5%	12.9%
Stone wool	16.1%	47.7%
Expanded polystyrene (EPS)	21.9%	28.7%
Extruded polystyrene (XPS)	8.3%	7.4%
Polyurethane / polyisocyanurate (PUR / PIR)	8.0%	2.1%
Others	6.2%	1.2%

Table 3-3: European market shares in 2008 of different types of thermal insulation for buildings [5]

More than 35% of heat loss in buildings occurs through walls and 25% of heat is lost through the roof. Insulating the loft and flat roof is a simple and effective way to reduce heat loss and reduce the cost (table 3-4). The insulation materials are added beneath the floorboard to reduce scape of heat. More than 15% of heat is lost through the floors, the roofs insulation are implemented underneath of the suspended floor or on the solid floors under the floorboard.

	Facades						Roofs					Floors			
	New constructions				Existing structures		New constructions			Existing structures		New constructions		Existing structures	
Material	Cavity wall	Wet render systems	Dry cladding systems	Timber frame construction	Cavity wall	Instruction the inside	Pitched roof	Flat roof	Prefab roof element	Pitched roof	Flat roof	Wooden floor	Concrete floor	Wooden floor	Concrete floor
Inorganic: fibrous															
Glass wool															
Flocks	×	-	-	×	×	-	-	-	-	×	-	-	-	×	-
Panels	×	×	×	×	-	×	×	×	×	×	×	×	×	×	×
Rolls	-	-	-	×	-	×	×	×	×	×	×	×	×	×	×
Rock wool															
Flocks	×	-	-	×	×	-	-	-	-	×	-	-	-	×	-
Panels	×	×	×	×	-	×	×	×	×	×	×	×	×	×	×
Rolls	-	-	-	×	-	×	×	×	×	×	×	×	×	×	×

Table 3-4: Application of inorganic insulation materials [4]

3-2-2 Life cycle of insulation materials

Life of buildings can reach to 500 years. The life cycle of thermal insulation materials follows generally these phases: raw materials phase (raw material extraction and processing, processing secondary material input and transport the materials), production phase (storage, production and packaging), use phase (distribution and use) and disposal phase (end-of-life) [6]. There are many factors that influence the performance of insulation materials which cause failure risk on long-term performance (Figure 3-6). The moisture considered is the biggest risk influence on the long-term performance of insulation materials where build-up of moisture tends to increase thermal conductivity of insulation materials especially in fibrous materials (may be damage fabric of insulant). Air movement on the surface of the fibres may tend to leakiness and be attacked by vermin spread of mold and rot. Vapour diffusion through the building envelope is due to vapour pressure gradient between two sides. Vapour diffusion can produce interstitial condensation against the amount of vapour humidity, pressure and temperature in different sides, composition of a wall, floor or ceiling and types of surface and painting [7]. More research in this sector is required to determine long-term performance of insulants.

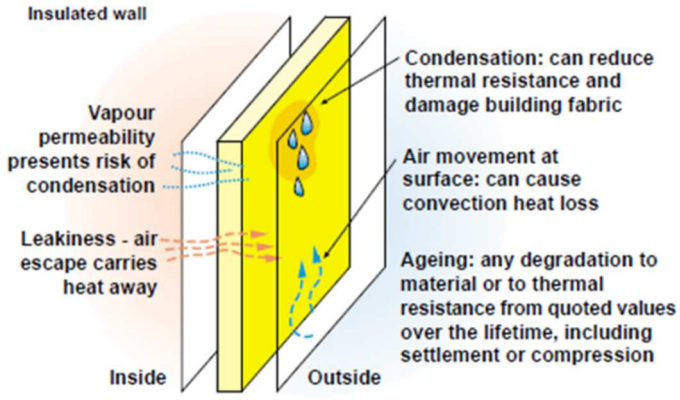

Figure 3-6: Risk of moisture (condensation and vapour permeability) [2]

3-2-3 Physical characteristics

Physical characteristics of insulation materials depend on the types of fibers. Table (3-5) compare physical characteristics of natural wools and synthetic expanded polystyrene (EPS). Origin of natural fibers can be animal for sheep wool, vegetal for flax wool and mineral in the case of glass wool. Materials have been selected for their similar density (20-30 $kg.m^{-3}$). Life

time and resistance to temperature (combustion point) are more important for natural wools. In terms of hydric characteristics, EPS is less permeable to vapour (μ- factor important) and is less subject to vapour absorption (hygroscopic capacity is small) compared to sheep and flax wools.

Glass wool is non-combustible (fire classification A1), has a lower thermal conductivity and is quite not sensible to vapour absorption (hygroscopic capacity is quite null). But, glass wool is also characterized by a less specific heat capacity than other materials.

Material	Density [kg/m^3]	Life time	Combustion point [°C]	Fire resistance classification	Hygroscopic capacity [%]	μ-Factor	Thermal conductivity [W/m.K]	C_p [J/kg.K]
Sheep wool	25	>100	600	B2	33	1-2 * 4-5 **	0.033	1720
Flax wool	32	100	570	B2	20	1-2	0.040	1550
Glass wool	22	100	600	A1	< 0.1	1-2	0.034	799
EPS	15	70	360	B1	1.1	20-90	0.040	1500

*sheep wool insulation Ltd., Ireland (DIN52615), **Doschawole, the Netherlands (DIN52615) [8]

Table 3-5: properties of insulation materials [8]

3-3 Crimped Glass wool

Glass wool, as a material used in the insulation of buildings, was invented in 1938 at the USA. It is used around the world in homes, commercial and industrial buildings for thermal insulation. It is made from sand and glass recycled then melted the blended in 1450 °C and spun into a fibrous mat and bound together by resin (Figure 3-7) [9].

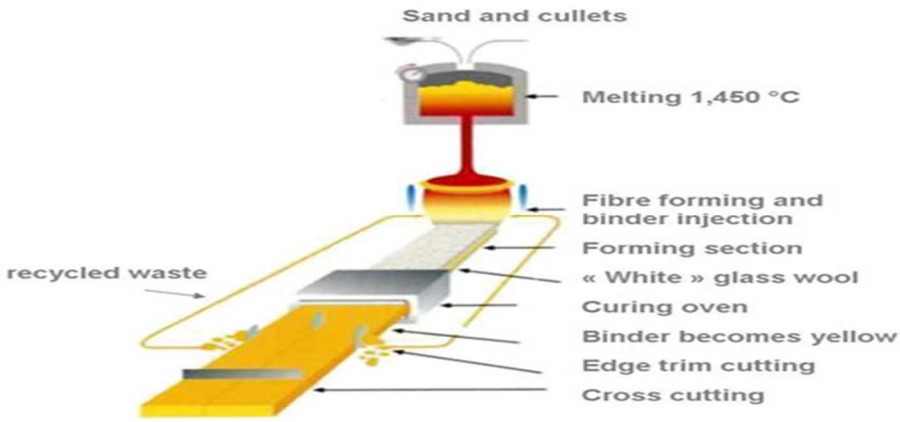

Figure 3-7: Manufacturing of glass wool [9]

The molten glass flows over a rotating disk in high speed in the form of fine fibers, then the glass streams flowing through channels in platinum through a stretching plate then the mats of fibers is form as shown in figure 3-8 [10].

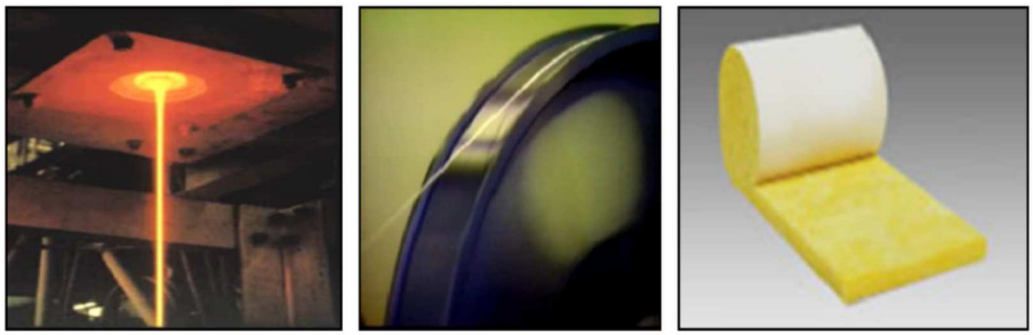

a- molten glass *b- fiber* *c- put roller*

Figure 3-8: form of the mats of fibers [10]

Glass fibres used in the fibre reinforcements, glass type E (standard), glass type C (corrosion resistant) and glass type A/R (alkali-resistant use with concrete) are classified in 3 categories. Type E is usually chosen for insulation materials because of electrical properties (resistivity of about 1015 Ω.cm) and its mechanical properties similar to those of the steel or aluminium with a lower density [10].

3-3-1 Crimping process

A Mineral wool is a cellular solid made of fibres with micrometric diameter and millimetric or centimetric length. These fibres are sprayed with a binder and cured in an oven for freezing the arrangement of the fibres and hence providing some elasticity. Glass wool denoted L1 is object of this study. L1 has been already studied by Achchaq [11] which studied mainly its hydric behaviour and compare properties with a hemp insulation material. Panels of 60 x 125 x 10 cm affected to thermal and noise insulation of sloped roofs are used. The repetitive patterns across the panels suggested that the fibers were prepared according to a preferred orientation during their manufacture. In fact, this pattern is obtained by “Crimping” process (figure 3-9) developed by Isover-Saint Gobain to increase the mechanical performances. The fibre mat with different texture (figure 3-10) is processed before the curing stage to produce a structure endowing the material with a higher mechanical strength. So a better mechanical behaviour is obtained due to a more favorable fibre orientation. As a result, the elastic response of the finished product and its load bearing capacities are very sensitive to this crimping process.

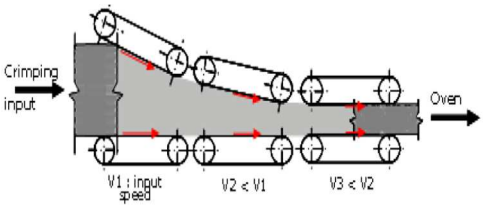

Figure 3-9: Compression process [12]

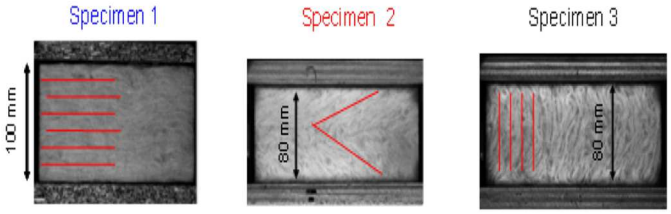

Figure 3-10: Different texture of glass wool obtained [12]

3-3-2 Microscopic analysis

The microscopy platform of University of Picardie Jules Verne (UPJV) has studied the morphology of these wools [13] at the microscopic scale. Samples were studied by scanning electron microscopy (SEM, Quanta 200 FEG SEM Environmental). The sample cell pressure was reduced to about 1 mbar for the study of single fibers and 0.28 mbar for studying binders and fibers. Scanning electron microscopy (SEM) shows heterogeneity and the random distribution of fibers, whatever the place of sampling within the materials. The heterogeneity concerns also the geometry of fibers since their dimensions (length and diameter) are variable (Figure 3-11). In addition, the presence of binders in the form of droplets and clusters could be observed. A more detailed observation allowed seeing that binder is distributed fairly regularly along the fiber (Figure 3-12).

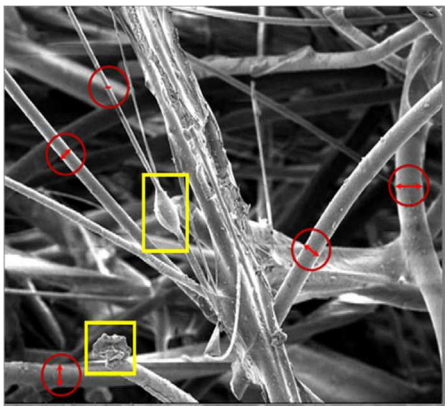

Figure 3-11: Components of the mat: fiber, binder, cluster [13]

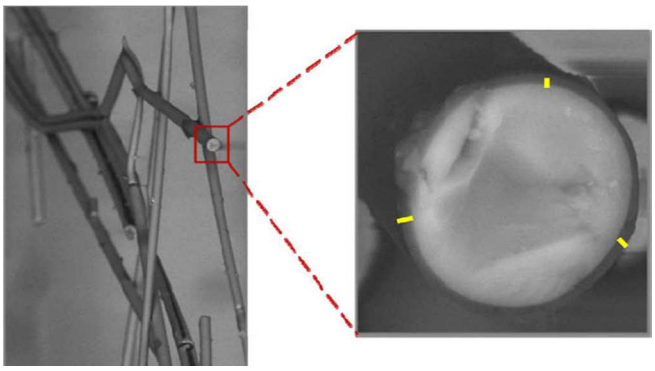

Figure 3-12: Magnification of a mineral fiber section and visualization of its coating [13]

Given that the SEM is coupled with a detector EDX, an attempt to determine the composition of glass wools could be envisaged, in order to carry out their analyses. In a first step, one fiber without its binder, then, an area rich only in binder (droplet or cluster) and finally, one

fiber coated with binder have been analysed. L1 Glass wool mainly contents silicon (Si), sodium (Na), calcium (Ca) and potassium (K).

As the distance of penetration of the electron beam in the material is limited to 1 µm and the average thickness of the binder is estimated at about 500 nm. Therefore, the detection of the elements concerns mainly the binder and only a small part of the glass fiber. This is the reason why the content of silicon is now lower than the value obtained. The contents of the other elements (sodium, calcium, etc.) increase because they are better seen by the beam.

Thermogravimetric analysis (TGA) has been used to determine the degradation temperatures of the binders of glass fibers and the amount of water surrounding adsorbed by the surface fibers. Two-step combustion in air of the coated glass fibers caused by the samples losing weight in response to heating can be observed. For L1 specimen, the slightly initial weight loss from 100 up to 210 °C is due to evaporation of the adsorbed moisture. The second severe weight loss (210–550 °C) is due to comprehensively decomposition of binders of the samples. As the onset of degradation temperature are very close to each other, hence neither of the binders, whatever their chemical compositions, contribute to the improvement of thermal stability of the materials. A release of water, constituent of the glass, could be considered. Therefore this thermogravimetric method does not distinguish between free water of bound water.

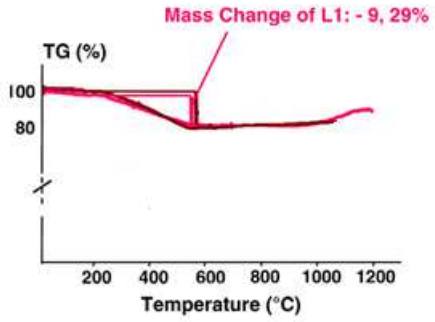

Figure 3-13: TGA thermograms of L1 samples in thermal and hydric equilibrium.

The DSC tests were carried out only on the samples in thermal and hydric equilibrium. The variation of the heat capacities ΔCp and glass transition temperature Tg of L1 specimen is shown in (figure 3-13). The thermal capacity Cp of a material is its ability to store heat. Then, more Cp is high, the higher the material can store a large amount of heat. If the values of the thermal capacity obtained for the binders ($\Delta Cp = 0.221\ Jg^{-1}K^{-1}$ for L1) are compared to the glass ($Cp = 0720\ Jg^{-1}K^{-1}$), the cellulose wadding ($Cp = 2\ Jg^{-1}K^{-1}$), or air values ($Cp = 1\ Jg^{-1}K^{-}$

[1]) [11], one realizes the very minor role they play in the thermal inertia of the glass wools. Also, the melting temperature of a glass, depending on its composition, varies between 1400 and 1600 °C. Generally, the glass transition of a glass expresses the transition from the cooled-liquid to the glass itself when its viscosity reaches 1013 poises. For temperatures above Tg, the liquid phase predominates. Below it is a glass. So, the glass transition temperatures observed are too weak to concern the glasses of the fibrous insulating materials (figure 3-14). Indeed, for the same heating rate, the onset of glass transition temperature of L1 occurs at 152, 5 °C. Therefore, the glass transition observed is about the binders.

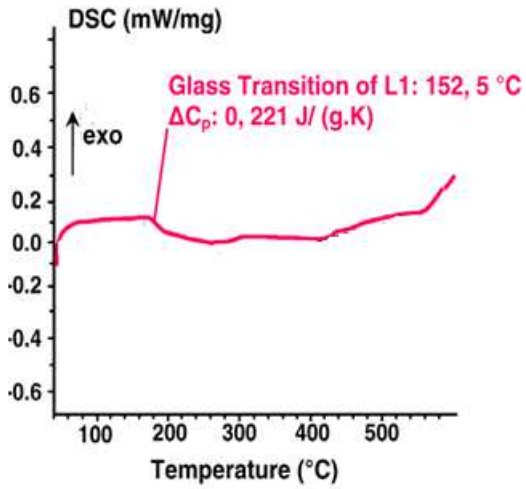

Figure 3-14: Schematic DSC curves of L1 sample

3-3-3 Morphological characteristics

3-3-3-1 density and porosity

The **bulk density** ρ_0 may be determined using the following relationship:

$$\rho_0 = \varepsilon_s \rho_f = (1-\varepsilon)\rho_f \quad (3\text{-}1)$$

Where ε_s and ε represent the porosity of solid and solid and gas respectively. ρ_f is the density of the glass fibers (from 2500 to 2800 $kg.m^{-3}$, function of the type of fiber). To determine the total porosity, gravimetric is the most usual method. The sample is generally subjected to vacuum pressure before immersing it inside distilled water. The validity of this method can be discussed for the fibrous insulation. High porosity makes it impossible to keep water on and the presence of this water in the fibrous medium causes swelling of the structure.

A comparison of results from gravimetric (previous method) and helium pycnometer (more used in chemistry) has been undertaken. Pycnometric method requires knowledge of the true density (ρv) of the material. The porosity is then calculated by the following equation:

$$\varepsilon = \frac{\rho_v - \rho_o}{\rho_v} \tag{3-2}$$

Samples are dried in an oven at a temperature of 40°C for 3 hours. The mass of the samples is obtained using a Mettler Toledo (LJ16). This balance enables also to check the water content of the materials. The bulk density ρ_0 is calculated from the mass of a known volume of material. The true density ρv is determined by a helium pycnometer (AccuPyc 1330). Helium is an inert gas to the fibrous structure. Fibers are inserted into a cylindrical cell volume (V=10 cm^3). This volume is chosen in order to respect representative volume element (RVE) of material determined here primarily from the dimension of the fibers. Total porosity of the wool L1 can be obtained by helium pycnometer measurement and gravimetric method. Good coherence between these methods can be observed (Table 3-6) taking into account accuracy showing that gravimetric method usually used in civil engineering laboratory is reliable. Porosity is very important (more than 95%) for these two glass wools.

Sample	Technique of measurement	Bulk density ρ_0 [kg.m^{-3}]	True density ρ_v [kg.m^{-3}]	Total porosity ε [%]
L1 wool	pycnometer	68,6 ± 2,2	2620 ± 70	97,4 ± 1,1
L1 wool	gravimetric	79,0 ± 3,1		96,9 ± 1,8

Table 3-6: Densities and total porosity of glass wool

3-3-3-2 Specific surface

The specific surface area (S_v) represents one of the most important parameter to study the heat and mass transfer. The specific volumetric surface (S_v), is determined by different method such as BET method, which is based on adsorption of gas on a surface. It is a cheap, fast and reliable method to measure specific volumetric surface (S_v). There are other method like Single point measurement, Flow deflection measurement and Gravimetric measurement can be used.

Specific surface (S_m) expresses the degree of division of the solid phase. For heat and mass transfer, a shape with higher specific surface value is more efficient. For a given volume (V) (or material mass), different geometric shape generate different amounts of surface area (A_{sg})

by which to interact with the environment. Volumetric surface (S_v) and specific surface (S_m) can be determined as:

$$S_v = \frac{A_{sg}}{V} = S_m \, \rho_o \quad (3\text{-}3)$$

Where S_v: Volumetric surface [m^{-1}], A_{sg}: Surface area [m^2], V: Volume [m^3], S_m: Specific surface [$m^2 . g^{-1}$]

The specific surface area (Marmoret et al [14]) is determined experimentally by a specific equipment (ASAP 2020, Micromeritics). Material is brought into contact with measuring cell containing krypton gas. Krypton is selected in order to be inert against fibrous medium. In the case of low gas contents (<0.35-0.40), molecules of krypton is strongly adsorbed in a monomolecular layer. By applying the BET method, the specific surface area is obtained. This value is important for L1 wool (S_V = 0.2332± 0.0120 $m^2.g^{-1}$) showing that the medium is finely divided. However, the coefficient C determined by the BET method is high. (Marmoret et al [14]) conclude that krypton molecule may not be the most suitable. Using the assumption of an equivalent insulating medium consisting of fibers of the same diameter (D_f) having the same surface area, it is possible to define the average fiber diameter from the usual equation: $D_f=4/S_V$. Fiber diameter can be extracted from this equation to 7.2± 0.5 μm. Compared to value obtained by SEM images statistical analysis (14 ± 6 μm) an important difference is obtained. Considering that industrial process make identical fiber diameter, only ten fibers are selected for statistical analysis. But manufacturer has confirmed the use of recycled fiber of various diameters that confirm the need of using more than 10 fibers for statistical analysis and can explain the difference.

The **intrinsic permeability** of the material is determined from air permeability test (TEXTEST FX 3300) [14]. In a previous work, we have observed dissolution of the binder has been observed due to the non-inert capacity of fiber material with water. So water permeability test can't be used [5]. Standard originally defined for textile fabrics (ISO 9237, 1995 F) has been followed to determine air permeability. Samples previously conditioned in an atmosphere of 20°C and 65% relative humidity are subjected to 200 Pa pressure gradient. Pressure gradient ΔP (Pa) ranging from 1 to 2000 Pa is applied on a finite surface sample A (20 cm^2) with thickness L (1 cm). When the flow q ($m^3.s^{-1}$) through the sample becomes constant, the air speed (ms^{-1}) is calculated by:

$$U_D = \frac{q}{A} = k_A . \frac{\Delta P}{L} = k_A . i \quad (3\text{-}4)$$

The **air permeability** k_A ($m.s^{-1}$) is measured in three directions as described in (Figure 3-15). $k_{A//1}$ and $k_{A//2}$ are representative of the permeability in the direction of lamination of the layers of fibers ($k_{A//1}$ being parallel to the fibers and $k_{A//2}$ being perpendicular to the fibers). $k_{A\perp}$ corresponds to the measurement in the perpendicular direction to the bedding plane and corresponds to the direction of heat flow in building use. The AF anisotropic factor is determined by the ratio of air permeability in both directions:

$$AF = \frac{k_{A//}}{k_{A\perp}} \tag{3-5}$$

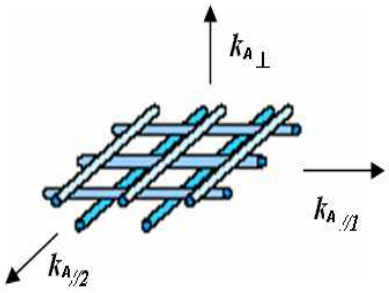

Figure 3-15: Air permeability and positioning bedding planes

The air permeability by using five samples has been determined. Results are presented in (Figures 3-16) with respect of 5% uncertainty defined in standard ISO 9237. Air permeability in three directions of the medium has been performed according to (figure 3-15). As linear relationship is observed between air speed and pressure gradient, Darcy's law can be applied.

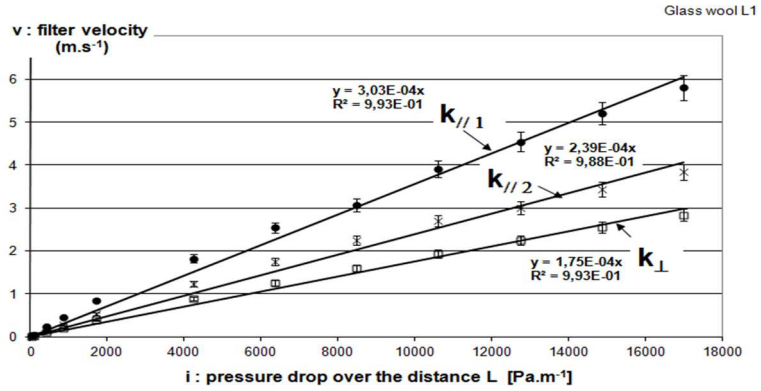

Figure 3-16: glass wool L1 air permeability

Table 3-7 presents air permeability values for L1. Compared to glass wool of the same density, conventional air permeability is given at 5.10^{-9} m². So, common glass wool is ten

times more permeable than L1. This can be due to the "crimping" process to manufacture the glass wools [15]. Air permeability is more important for L1 whatever the direction of the flow (perpendicular or parallel). This remark is coherent with porosity values. For a given material, the air permeability is lowest in the direction perpendicular to the stratification (i.e. in the effective direction of use of the glass wool) and highest in the flow directions parallel to the stratification plane. The highest value being measured in the direction along the fiber length (kA//1). A large difference is observed between kA//1 and kA//2, even if it is generally admitted they are usually equivalent. An anisotropy factor (AF) of 2 is usually observed in common glass wools. In the case of our materials, lower AF values are obtained, ranging from 1.37 to 1.73 (Table 3-7). These lower values can be assigned to the "crimping" industrial process described by the manufacturer [16]. The intrinsic permeability (k, in m²) is calculated from the air permeability kA using the following equation:

$$k = K_a . \frac{\eta}{\rho . g} \qquad (3\text{- }6)$$

Where η is the dynamic viscosity ($1.81.10^{-5}$ Pa.s), ρ the density of air (1.2 $kg.m^{-3}$) and g is the acceleration due to gravity (9.81 $m.s^{-2}$).

	Glass wool L1	AF	
k//1 (m²)	$4.66.10^{-10}$	$AF_1 = \frac{k_{A//1}}{k_{A\perp}}$	1.73
k//2 (m²)	$3.67.10^{-10}$	$AF_2 = \frac{k_{A//2}}{k_{A\perp}}$	1.37
k⊥ (m²)	$2.69.10^{-10}$		

Table 3-7: Intrinsic permeabilities (k) and anisotropic factor (AF)

3-3-4 Hydric characterization

Sorption isotherm (Marmoret et al [17]) has been obtained by following the mass of initially dry 2.5 × 2.5 × 2.5 cm dimension samples placed in a desiccator with 21.5°C temperature and constant relative humidity defined by the used of saturated salt solution (Table 3-8). Equilibrium is established when samples are subjected to mass variation less than 0,001g. Once equilibrium is reached, the present relative humidity is changed by higher percentage of relative humidity. The operation is repeated up to reach 100%, this is called adsorption process. The uncertainty on the relative humidity required by a salt is between 1 and 2%.

Possible variations in partial pressure of water vapor at the interface solution/sample are considered negligible.

Saturated salt solution	Relative humidity (%) at 23°C
Potassium hydroxide (KOH)	8
Sodium fluoride (NaF)	57
Sodium chloride (NaCl)	75
Potassium chloride (KCl)	84
Potassium sulfate (K2SO4)	97

Table 3-8: Saturated salt solutions

The measurements [18] of adsorption isotherms were performed in laboratory conditions at 23 ± 1°C. The samples were placed in desiccators with different solutions (table 3-8) to simulate different values of relative pressures. The initial state was dry material (*mo*) after maintained samples in an oven at 80 °C. The mass of samples was measured until the steady state value of the mass was achieved (mw). Then, the equilibrium moisture content by mass (ω in $kg.kg^{-1}$) was calculated according by gravimetric method:

$$\omega = \frac{m_w - m_O}{m_O} \tag{3-7}$$

The **volumetric water content (θ)** can be calculated with $\theta_l = (\rho_l / \rho_o).\omega$ where ρ_l and ρ_o are densities of water and material respectively. The experimental results on the equilibrium volumetric moisture content against relative pressures are given in (Figure 3-19). According to IUPAC classification [15], these **sorption curves** are classified as type II. This type corresponds to non-porous or macroporous media. The curves obtained for the glass wool L1 specimen. Three clearly defined regions can be distinguished. For $0<\varphi<0.8$, in the adsorptionally bound moisture region (with mono on the part ① and multi-molecular layer on part②), the amount of water adsorbed is very small. Volumetric water content doesn't exceed 0.1. In the capillary bound moisture region ($\varphi>0.8$), the increase of volumetric water content is important. For example, at $\varphi=0.90$, volumetric moisture content is (0.34) for L1. The water content difference cannot be only assigned to the experimental error [18] which doesn't exceed 5%.

The sorption curve for the glass wool L1 has been investigated also by using guarded hot box (THERMO 3R) and use glass wool wall as a sample with dimension (120 ×120) cm with thickness (5 cm) to study the behaviour of sorption curve during different percentage of

humidity. it's very difficult to obtain relative humidity for the all the wall during the test due to the difficulty of the weight of the wall model, therefore we obtain the relative humidity by depending on the model taking the dimensions (12 ×12) cm with the same thickness (5 cm) which has been put inside the cold cell parallel to the main wall (figure 3-17). The weight of the sample has been recorded by using balance PGW 753e with accuracy 0.001 g (figure 3-18).

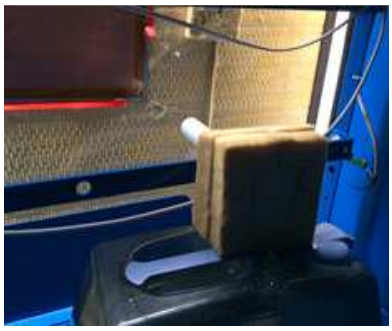

Figure 3-17: Model of sample wall

Figure 3-18: Balance used in weight

First, the sample has been put in the oven at 60 °C for 30 day to obtain dry weight (zero humidity) before paced it in the cold cell of guarded hot box. Second, the temperature of the two cell has been selected (30 °C for the hot cell and 5 °C for the cold cell). Thirdly, the humidity was maintained constant in the two cells (hot and cold) at 60% to stabilize the humidity in the whole wall. When the humidity has been stabilized, cold cell humidity has been changed to 80% and to 90% to record the humidity of the sample in each case. After weight the sample during each case, the humidity has been obtained and the sorption curve for the glass wool has been draw as shown in figure (3-19).

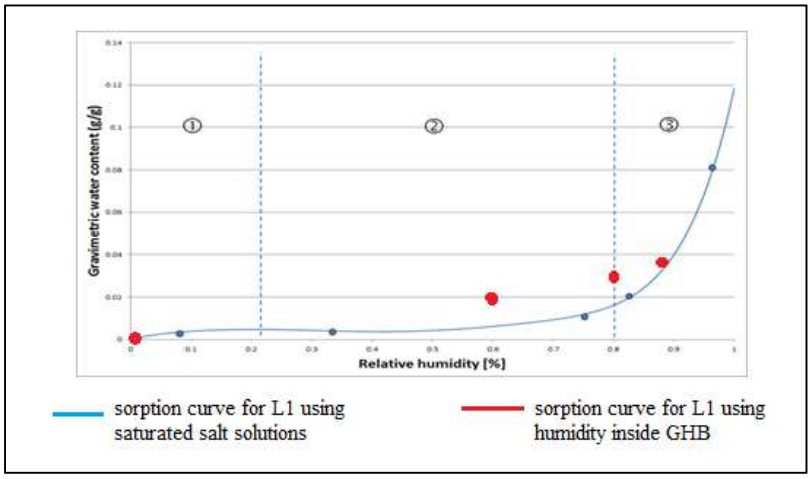

Figure 3-19: Sorption curve for glass wool L1 by saturated salt solutions and humidity of GHB.

The **water vapor permeability** has been determined (Gintronic gravitest) following the A-Type status of NF EN ISO 12572. The NF EN ISO 12572 specifies the number of samples: at least five if the material surface exposed to the lower stream is less than 500 cm², which is our case. A-Type condition corresponds to gradient pressure obtained with 0% humidity inside the cup (CaCl2 salt) and 50% humidity in the chamber. The climatic chamber temperature is regulated at 23°C±2°C. The principle is to seal specimens at the top of the test cup containing a desiccant or a salt thereof to obtain a specific humidity at a temperature fixed on one side of the specimen. The other face is exposed to a moist atmosphere different from that inside the cup. The indoor humidity is always lower than the humidity of the room atmosphere. The device measures the mass change over time when the steam flow is constant. Depending on the parameters of temperature, humidity, pressure, mass change over time and the area of material exposed to the test, one can determine the equivalent air thickness Sd (m) and water vapor diffusion factor μ (-) using the following equation for a thick material (m):

$$S_d = \mu\ d \qquad (3\text{-}8)$$

Vapor permeability is carried on 5 samples of 18 mm thick L1 glass wool. The material is sealed above the test cup containing either a saturated aqueous solution or a desiccant. All is placed in a test chamber regulated in temperature and humidity inside the vapor permeability-meter. Tests are performed in dry cup method with 23°C temperature and relative humidity gradient obtained with 0 ± 3% on the dried surface and 50 ± 3% on the other face (condition A of the standard). The test cup dry informs on the low moisture materials performance when moisture transfer is dominated by vapor diffusion. Measurement results are summarized in (Table 3-9). It should be noted that due to the definition of the equivalent thickness of air Sd (m), when Sd is low then water vapor permeability is high. Compared with different materials such as vapor barrier (Sd ≥ 18 m) or OSB3 panel of 15 mm thickness (Sd: 3.2 m), the air thickness Sd for L1 wool is very low and therefore the vapor permeability is very high. Using the definitions and Sd of vapor diffusion factor μ, it is possible to determine the permeability to water vapor wool: $\pi v=5.84\ 10^{-11}$ $kg.Pa^{-1}.m^{-1}.s^{-1}$. This value can be compared to the concrete ($\pi v=6.24.10^{-12}$ $kg.Pa^{-1}.m^{-1}.s^{-1}$). It should be noted that in literature, wool permeability is considered equal to $\pi v = 1.5\ 10^{-10}$ $kg.Pa^{-1}.m^{-1}.s^{-1}$ two times lower than our value. This difference can be assigned to treatments introduced during the crimping process.

Sample	Mean temperature (°C)	Mean Humidity (%)	Air speed (m/s)	Atmospheric pressure (mbar)	mass speed coefficient ($g.(m^2.24h)^{-1}$)	Air Thickness S_d (m)	Deviance Ecart-type S_d (m)
Laine L1	23,0 ±0,5	50,0 ±3	0,3	1011,18	348,64	0,057	0,002

Table 3-9: Air thickness for L1 wool

3-3-5 Thermal characterization

Thermal characteristics for crimped glass wool has been done by different techniques, transient technique by using hot disk method (TPS 2500) and steady state technique by using guarded hot plate (TLP 500 X1).

3-3-5-1 Thermal characterization by hot disk method (TPS 2500)

The Hot Disk thermal constants analysis based on the theory of the transient plane source (TPS) according to the ISO 22007-2. It's distinguished mainly by the short time and by the low flow in comparison with steady state techniques. TPS have different sizes of sensors and sensor element is made of a 10 μm thick electrically conducting Nickel foil in the style a double spiral. The Nickel foil is covered by two layers of polyimide (Kapton) in order to supply electrical insulation and to increase mechanical strength. The tests were carried out by using Hot Disk (TPS 2500), with rang (0.005 to 500 W/mK) for thermal conductivity, (0.1 to 100 mm^2/s) for thermal diffusivity and up to 5 MJ/m^3K for specific heat capacity. Accuracy of Hot Disk (TPS 2500) for thermal Conductivity better than 5% and Reproducibility is typically better than 1%. Duration of the test the samples in Hot Disk (TPS 2500) is ranges (1 to 1280 seconds).

Before starting the experimental tests we must select the correct experimental setup parameters to obtain accurate results. The most important these parameters are heating power, measurement time and sensor radius.

During the experimental tests using (TPS 2500), the heating power fed from the sensor is constant. The thermal conductivity of the materials is affected by amount of the heat power used. Insulation materials need small heat power while the other materials such as metals

need high heat power. Selection of the correct amount of heat power during the test gives accurate results, moreover the high heat power may damage the sensor.

The measurement time is influenced by thermal diffusivity of the materials and the probing depth as expression in equation (2-34).

The probing depth must be in the range of the sensor diameter that means the thermal penetration depth must not reach the outside boundaries of the sample during the experimental time. During the experimental tests we must make sure that the sample with more than two time the probing depth plus the diameter of the sensor and the sample thickness should be more than probing depth.

Hot Disk probe is placed between two pieces of same wool to be tested or after incision the sample with a cutter (figures 3-20 and 3-21). One of the features of the transient techniques over steady state techniques is that it can overcome the influence the contact resistance.

Al-Ajlan [19] and Coquard et al. [20] have already validated Hot Disk technique for the low-density thermal insulators thermal characterization.

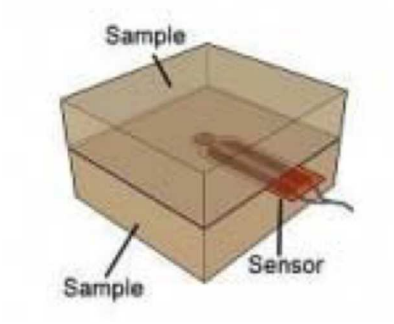

Figure 3-20:Scheme of sensor inside the sample

Figure 3-21:Image of the sensor inside sample

Experimental measurement

Our test was divided for two types isotropic and anisotropic for two samples of glass wool. For isotropic test thermal properties for the specimen was measured with different thee direction (X, Y and Z) by changing the site of the sensor every time according to the side of the sample and different temperature temperatures of 40, 30, 20 and 10 °C. Temperature 10 °C obtained during measuring the sample out of the laboratory. For anisotropic test thermal properties was measured axial and radial for different temperature of 40, 30, 20 and 10 °C.

First experimental: Isotropic measurement in different direction

Hot Disk bulk isotropic module has been used to determine thermal conductivity. TPS source (Hot Disk probe reference: 4922) characterized by a diameter of 14.61 mm has been selected. The output power and measuring time are equal to 40 mW and 160s respectively in order to produce a large range of viable data points and a large temperature gradient to ensure the accuracy of the measurement. Note that International Standard ISO 22007-2 recommended 0.1 W. We have chosen to reduce this flow to 40 mW in order to obtain an increased temperature near 1°C (exact value obtained is 0.46°C) which is well adapted for insulation materials. Results are obtained for a characteristic time of 0.353 s and a probing depth of 17.4 mm which respect semi-infinite assumption. Tests are carried out by using Hot Disk (TPS 2500).

The test has been applied for sample of dimensions (100×100×100) mm at temperature (20 °C) for three directions (X, Y and Z) to evaluate thermal conductivity in order to evaluate the isotropic (figure 3-22). Stratification planes of fibers have been pointed out in order to indicate the different structures of the glass wool in each direction (figure 3-23).

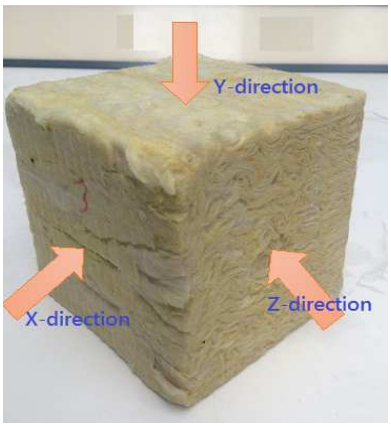

Figure 3-22:X, Y and Z-directions of the flow

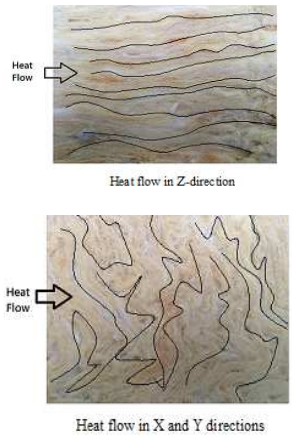

Figure 3-23:Effect of crimped process

Probe sensor can be inserted in the 3 directions X, Y and Z. Experimental values in the direction X and Y are closed themselves (table 3-10). Values in the Z-direction are bigger than the other ones. In the first case (X and Y directions), probe is inserted perpendicular of the stratification plane of fibers instead of in the second case (Z-direction) probe is parallel.

	X-direction	Y-direction	Z-direction
L1 glass wool	λ_X=0.03807	λ_Y=0.03914	λ_Z=0.04098

Table 3-10: Thermal conductivity [W. (m.K)-1] by using HD technique in different directions.

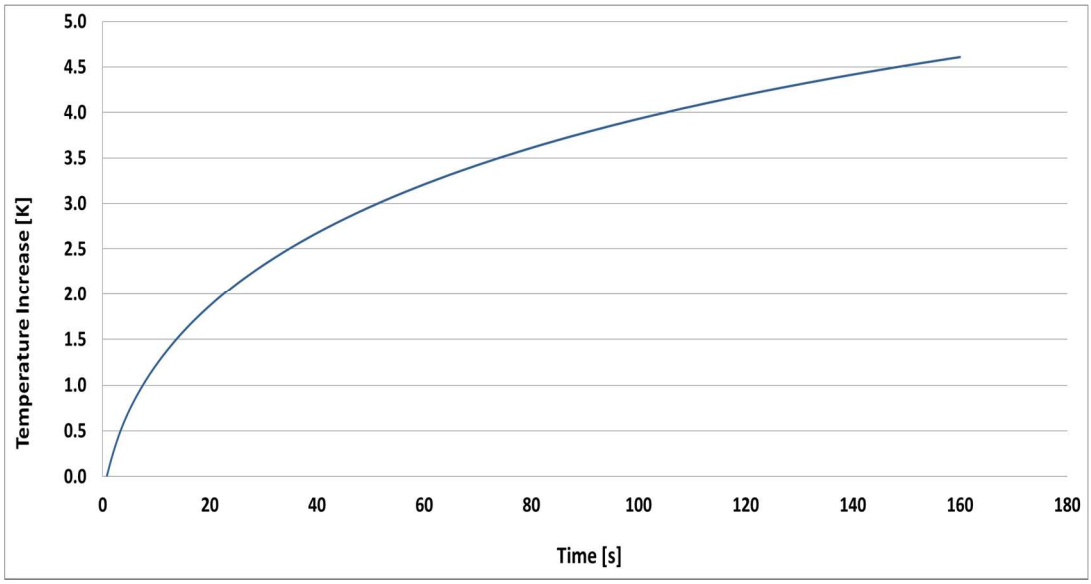

Figure 3-24: transient curve for the isotropic experimental measurement

The variation of the temperature during the experimental time as shown in the figure (3-24) in less than (5 K) and this agrees with requirement of (TPS 2500), typically 2-5 K. the calculated probing depth of 17.4 mm is less than the available probing depth (20 mm), in other words the heat wave does not reach to the boundaries of the materials during the experimental. Also the total characteristic time is (0.353 s) in the range of 0.33 to 1.0 according to the (TPS 2500) requirements.

The transient curve shown increase variation of temperature with the time of the experimental, we note the sharp initial variation of temperature due to the insulation of the sensor and the contact resistance between the sensor and the sample.

Second experimental: Isotropic measurement in different temperature

Hot Disk bulk isotropic module has been used to determine thermal conductivity in different temperature. TPS source (Hot Disc probe reference: 4922) characterized by a diameter of 14.61 mm has been selected with output power and measuring time are equal to 40 mW and 160s respectively. Before starting the measurements the sample is placed in an oven figures (3-25 and 3-26) to obtain stabilized temperature inside the material during the test. This temperature is followed by thermocouples sensors (T-type). This procedure is repeated for successive mean sample temperatures of 40, 30 and 20 °C.

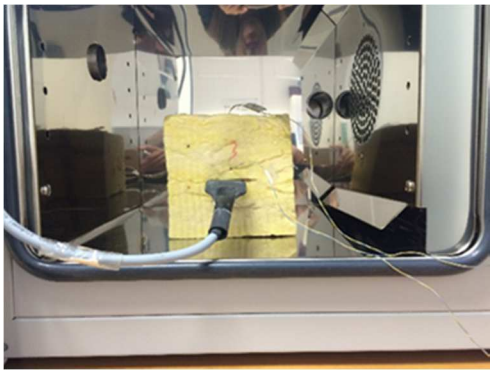

Figure 3-25: sample inside the oven

Figure 3-26: Oven and data logger

Experimental results coming from Hot Disk technique have been inserted in the figure 3-27. Measurement error bars of 5% for HD (ISO 22007-2 standard) have been added in order to establish the coherence of these results.

Thermal conductivity (λ) against sample mean temperature (T_m) have been presented. Linear variation is observed in the temperature domain from 10 to 40°C with a very good regression squared (R-squared>90%). Hot Disk curve is also coherent taking into account the measurement error. Hot Disk bulk anisotropic module methodology uses to determine thermal conductivity by HD method can now be considered validated.

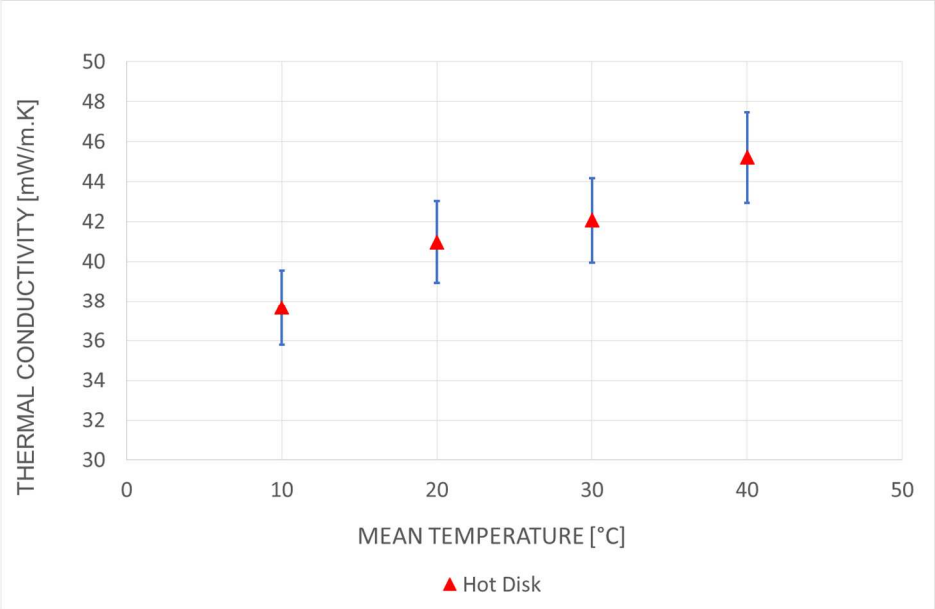

Figure 3-27: Hot Disk experimental values for glass wool

Anisotropic measurements

Hot Disk bulk anisotropic module has been used to determine axial thermal conductivity and radial thermal conductivity. TPS source (Hot Disc probe reference: 4922) characterized by a

diameter of 14.61 mm has been selected. The output power and measuring time are equal to 40 mW and 160s respectively in order to produce a large range of viable data points and a large temperature gradient to ensure the accuracy of the measurement.

Axial thermal conductivity was measured in the direction of the thickness while radial thermal conductivity was measured in the plane of the sample as shown in the figures (3-28 and 3-29).

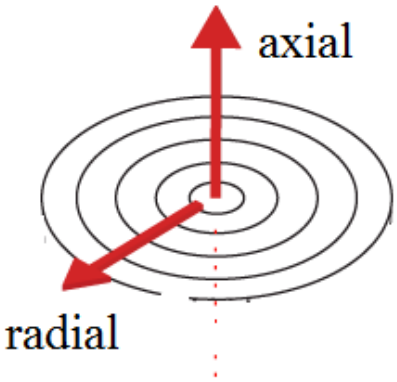

Figure 3-28: scheme for axial and radial flux

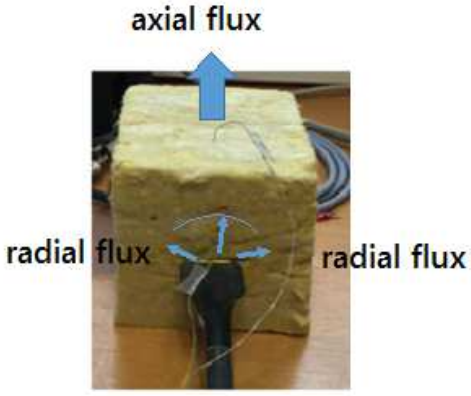

Figure 3-29: image of the sample during test

Experimental results coming from Hot Disk technique for anisotropic measurements have been inserted in the (figure 3-30). Measurement error bars of 5% for HD (ISO 22007-2 standard) have been added in order to establish the coherence of these results.

Axial and radial thermal conductivity (λ) against sample mean temperature (T_m) have been presented. Linear variation is observed in the temperature domain from 10 to 40°C with a very good regression squared (R-squared>90%) for axial thermal conductivity. Hot Disk curve is also coherent taking into account the measurement error. For figure (3-28) we note the effect of the variation of temperature on the axial thermal conductivity apparent more than radial thermal conductivity.

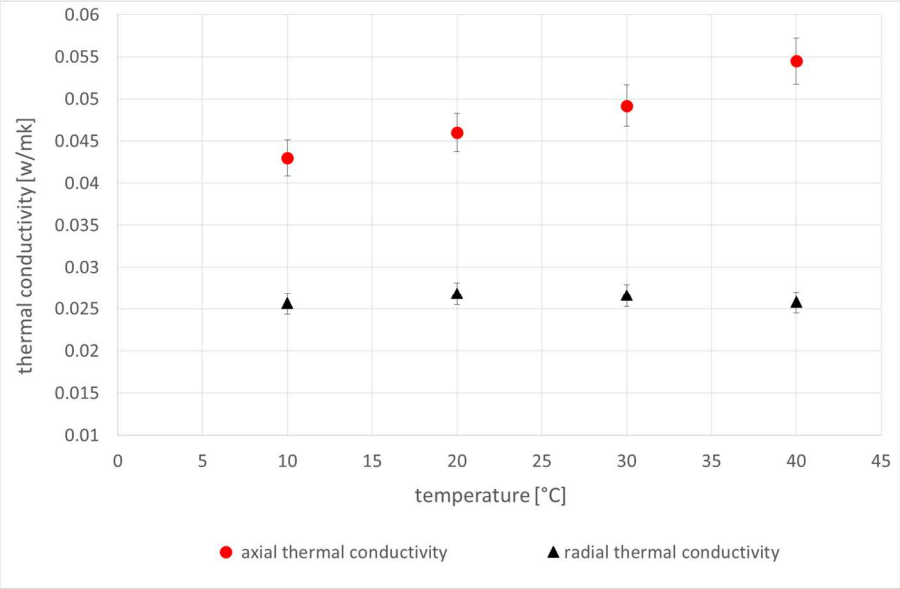

Figure 3-30: Hot Disk experimental values for glass wool during anisotropic tests

3-3-5-2 validation with Guarded Hot Plate (TLP 500 X1)

The most suitable technique for insulation materials taking into account the total heat transfer is the steady-state methods [21]. The guarded hot plate as other steady-state methods suffer from major drawbacks. They require a long time to establish a steady-state temperature gradient across the sample, and this temperature gradient is required to be large. Sample size is also required to be large and contact resistance between the thermocouple and the sample surface is considered a major source of error. Some material properties can be altered during the time to achieve steady state. A sample of material is placed between two plates (figure 3-31). One plate is heated and the other is cooled. The thickness of the sample and the heat input to the hot plate are used to calculate thermal conductivity.

According to ISO 8302, guarded hot plate (TPL 500X1) has been used to determine thermal conductivity of glass wool L1 against sample mean temperature (figure 3-32).

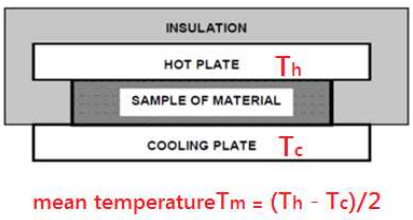

Figure 3-31: scheme of guarded hot plate

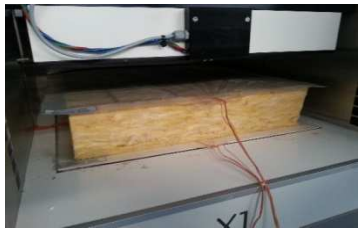

Figure 3-32: Image of sample inside guarded hot plate (TLP 500 X1)

Under steady state condition, thermal conductivity for homogeneous sample is calculated during passage the rate of flux through unit area for each temperature gradient perpendicular to the isothermal surface of the sample. Usually the heat flux is determined by the measurement of a power emitted in an electrical heater. The thermal conductivity value is often related to the average temperature.

Dimension of the sample is 246 x 250 x 60mm. In the case of glass wool, about 6 hours are necessary to achieve the stabilization of the temperature difference between the two external surfaces of the sample as required the ISO 8302 standard. This equilibrium is obtained by using 0.4W thermal flow. This procedure is repeated for successive mean sample temperatures of 10, 20, 30 and 40 °C.

Experimental results coming from Guarded Hot Plate technique have been inserted in the (figure 3-33). Measurement error bars of 3% for guarded hot plate (ISO 8302 standard) have been added in order to establish the coherence of these results.

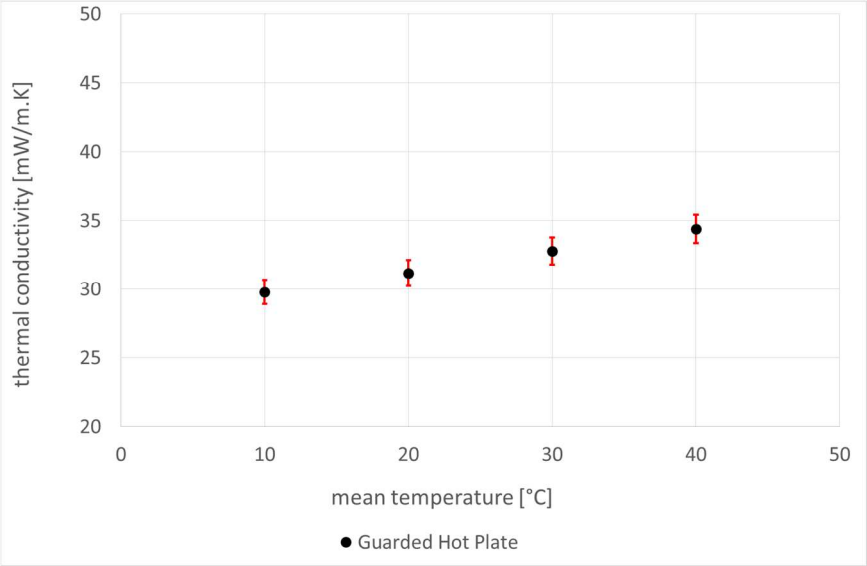

Figure 3-33: Guarded Hot Plate experimental values for glass wool

The results of the guarded hot plate and hot disk are closed together although the differences in the conditions (temperature, heat power and period of the test) as shown in figure (3-34).

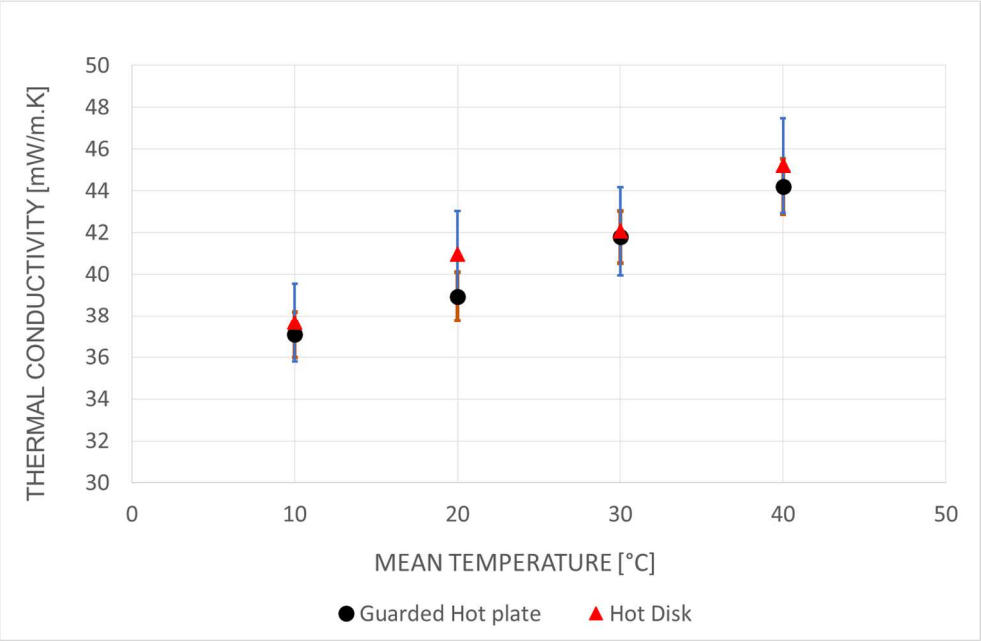

Figure 3-34: Guarded Hot Plate experimental values for glass wool

The summery of this chapter, study of morphological characteristics (density, porosity and specific surface) and crimping process for insulation materials is very important to know behaviour of these materials during use in building envelop.

Effect of the heterogeneity of structure (porous and fibrous) and influence of the process modifying the local orientation of fibers in a glass wool material has been studied. We have shown that the anisotropic factor is reduced and the final structure is finely divided. Thermal conductivity of the glass wool has been investigated experimentally by using steady state method (guarded hot plate technique) and transient plane method (hot disk technique). Hot disk technique has also been used to determine the effective thermal conductivities in the three directions inside the material. This procedure has established the quasi-isotropic character of the thermal conductivity of the crimped glass wool.

References chapter three

[1]: Halonen, L., Tetri E. & Bhusal, P. 2010. Guidebook on energy efficient electric lighting for buildings. Annex 45. Aalto University, School of Science and Technology, Department Electronics, lighting unit, http://www.ecbcs.org/docs/ECBCS, Annex 45, Guidebook.pdf, 15-9-2015.

[2]: Insulation for Sustainability, XCO2 conisbee Ltd, Consulting engineer, 1-5 Offord Street London N1 1DH, UK, E: mail@xco2.com W: www.xco2.com

[3]: Exploratory study with regard to Eco-design of thermal insulation in buildings, VITO, 2014.

[4]:Melchert Duijve,Comparative assessment of insulating materials on technical, environme ntal and health aspects for application in building renovation to the Passive house level, Utrecht University,2012.

[5]: VHK, Study on Amended Working Plan under the Eco-design Directive. Study prepared for the European Commission under DG ENTR Service Contract SI2.574204, 2011.

[6]: EN 15804, Sustainability of construction works - Environmental product declarations - Core rules for the product category of construction products. Comité Européen de Normalisation. Brussels, Belgium, 2011.

[7]: Preventing Moisture and Mold Problems: Design and Construction Guidelines, CH2M HILL, 2003 Handbook of Fundamentals, ASHRAE, Atlanta, GA, 2009.

[8]: Extrait de “Hygro-Thermal Properties of Sheep Wool Insulation, T.M. Tuzcu, Thesis of Delft University of Technology, 2007.

[9]: A method of manufacture of the glass wool. Federation of industry glass; Belgium.

[10]: F. Bartholomew. Fiberglass: A point on building new materials. BRGM-REM.

[11]: F. Achchaq, Etude hydro-thermique de matériaux isolants fibreux. PhD thesis, Université de Picardie Jules Verne, France, Amiens, décembre 2008.

[12] :J-F Witz, S Roux, F Hild, Mechanical and thermal behaviour Thermomechanical Behaviour Prediction of Glass Wool by Using Full-Field Measurements, Experimental Analysis of Nano and Engineering Materials and Structures, pp 669-670, ISBN: 978-1-4020-6238-4, 2007.

[13]: F. Achchaq, K. Djellab, H. Beji, L. Marmoret, Hydric, morphological and thermo-physical characterization of glass wools: From macroscopic to microscopic approach, Construction and Building Materials, 23, pp 3214–3219, 2009.

[14]: L. Marmoret, M. Lewandowski, A. Perwuelz, An Air Permeability Study of Anisotropic Glass Wool Fibrous Products, Transport in Porous Media, ISSN 0169-3913, Vol. 86, N°2, 2012

[15]: S. Bergonnier, F. Hild, J.B. Rieunier, S. Roux ; Strain hétérogeneities and local anisotropy in crimped glass wool, Journal of Material Science, N°40, pp 5949–5954, 2005.

[16]: G. W. Jackson, D. F. James, The permeability of fibrous porous media, the Canadian journal of chemical engineering, volume 64. 1986.

[17]: L. Marmoret, F. Collet, H. Beji, Moisture adsorption of glass wool products, High Temperature High Pressure, Vol. 40, N°1, pp. 31–46, Old City Publishing Inc. 2011.

[18]: P. Schneider, Adsorption isotherm of microporous-mesoporous solids revisited, Applied Catalysis A: General, 129, pp 157-165, 1995.

[19]: S.A. Al-Ajlan, Measurements of thermal properties of insulation materials by using transient plane source technique, Applied Thermal Engineering, 26, pp 2184–2191, 2006.

[20]: R. Coquard, D. Baillis, D.Quenard Experimental and theoretical study of the hot-ring method applied to low-density thermal insulators, International Journal of Thermal Sciences, 47, pp 324–338, 2008.

[21]: T Kobari, J. Okajima, A. Komiya, S. Maruyama, Development of guarded hot plate apparatus utilizing Peltier module for precise thermal conductivity measurement of insulation materials, International Journal of Heat and Mass Transfer Volume 91, pp 1157–1166, 2015.

Chapter 4 : Thermal testing study with probe method

4-1 Introduction

Studies were carried out from the TP02 probe of Hukseflux®. Thermal probe is considered a well-adapted technique to determine thermal conductivity of powder, liquid and gas but in the case of porous materials there are some difficulties. Hukseflux indicates in the user manual guide of the TP02 that the probe can be used to characterize materials in the thermal conductivity range between 0.1 and 6.0 $W.m^{-1}.K^{-1}$. This is not the case of insulation materials. A material can be considered an insulant according to European standards (EN13162 to EN13171), if a declared thermal resistance higher than 0.15 $m^2.K/W$ or a declared thermal conductivity lower than 0.10 W/(m.K) at a measuring temperature of 10 °C is obtained. Second problem if the TP02 probe is used to characterize insulation materials comes from the expected accuracy at 20 °C of ± (3% + 0.02) $W.m^{-1}.K^{-1}$. Hukseflux has introduced fixed accuracy of 0.02 in the user manual guide to take into account the low accuracy of the mathematical procedure to determine the thermal conductivity. This analysis consists of a linear long term mathematical approximation equation applying on experimental temperature gradient kinetic values against logarithm of time. But considering glass wool thermal conductivity near 0.04 $W.m^{-1}.K^{-1}$, TP02 can't be considered useful for the moment.

So, firstly, we will study the usual for determining thermal conductivity. That consists of a linear assumption applied on the curve representing he temperature gradient of the probe against the logarithm of the time. Then, we will study the importance of using a new mathematical methodology using inverse technique to take into account not only the linear part of the curve but the entire S-shaped curve. Another way of improvement is to identify the drawback of Hukseflux probe for characterizing insulation materials. By using Comsol Multiphysics® simulation we have studied errors that can come from the components of the probe (composition, size ...), the contact resistance and power supply.

4-2 TP02 Hukseflux® probe

The choice of Hukseflux probe is due to the fact that their probes are very popular (indeed even the most used) for various applications (agriculture, mining, spatial, building…). Their versatility, simplicity of use and the fact that thermal probes eliminate moisture loss and migration within the material these probes have also gained much popularity in food and biomedical engineering applications. Their probes are representative of the last generation of thermal probes and Hukseflux purpose probes of different dimensions in function of applications and material to characterize.

4-2-1 Design of TP02 Hukseflux® probe

Our tests were carried out from the TP02 probe of Hukseflux® (Figure 4-1) with a length of 150 mm and a diameter of 1.5 mm. Hukseflux TP02® probe incorporates two thermocouple junctions in the needle. The hot joint (3) is located at 1/3 of the needle length and the cold joint (4) at the tip. The heating wire runs across 2/3 of the needle length. Temperature measurements are made via the hot junction positioned 50 mm from the base (thermocouple 3 in figure 4-1), the cold junction at the end of the probe (thermocouple 4 in figure 4-1). These thermocouples junctions are connected, producing a voltage output U_{sen}, proportional to the differential temperature of the two junctions. TP02 has a reference temperature sensor (Pt_{1000}) built into the base of the probe. This reference serves as a "cold junction" measurement for establishing the absolute medium temperature *T*. The base temperature (the Pt_{1000}) is used as a cold junction to compensate the temperature for the cold thermocouple junction at the tip. The main sensor signal is ΔT, the differential temperature, measured between the hot and the cold junctions by:

$$\Delta T = \frac{U_{sen}}{E_{sen}} \quad (4\text{-}1)$$

Where the temperature dependence *(ΔT)* of the thermocouple thermoelectric power is determined by E_{sen} $(\mu V.K^{-1})$ defined by measuring the base temperature *T* using the Pt_{1000} as:

$$E_{sen} = 39.40 + 0.05\,T - 0.0003T^2 \quad (4\text{-}2)$$

As an electric current of fixed intensity flows through the wire, the thermal conductivity can be derived from the resulting temperature change over a known time interval.

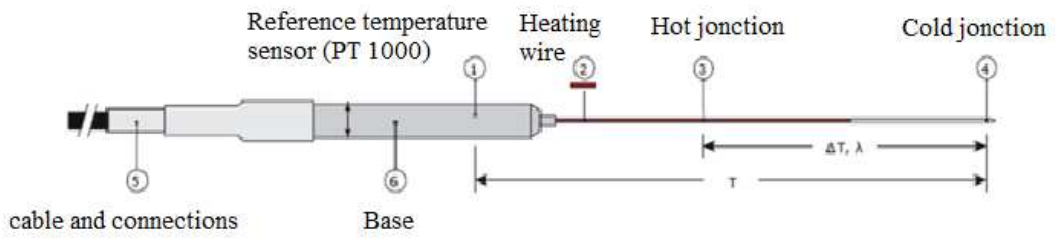

Figure 4-1: TP02 Hukseflux® probe

Hukseflux® TP02 has a length to radius ($L/2R_s$) ratio of 100 in order to reduce losses in the axial direction of the probe. It is composed of several layers of material in the radial direction, whose properties (Table 4-1).

Details of layer	Thickness [mm]	Thermal conductivity $[W.(m.K)^{-1}]$	Density $[kg.m^{-3}]$	Specific heat $[J.(kg.K)^{-1}]$
Constantan (hot wire)	0.065	19.50	8910	390
Glass pearl (insulant)	0.355	0.16	1600	800
Stainless steel (Outer face)	0.330	16.00	7900	500

Table 4-1: Thermal properties of the component layers of the Hukseflux® TP02 probe.

Hot wire heater is made from constantan. This material has been chosen because of its high electrical resistivity and its low temperature coefficient. The resistance of the constantan does not change much with the temperature. Constantan has an extraordinarily strong negative Seebeck coefficient above (0 Celsius) leading to a good temperature sensitivity. Therefore it's used for the purpose of making thermocouples. Stainless steel is mainly used due to its durability coming from its high resistance of humidity. This property is important because this metal is used for the outer face of the probe.

4-2-2 TPSYS02 control interface

TP02 may be supplied separately by a so-called home apparatus or by using TPSYS02 control interface. We have used this interface (figure 4-2) to feed the TP02 probe by the power.

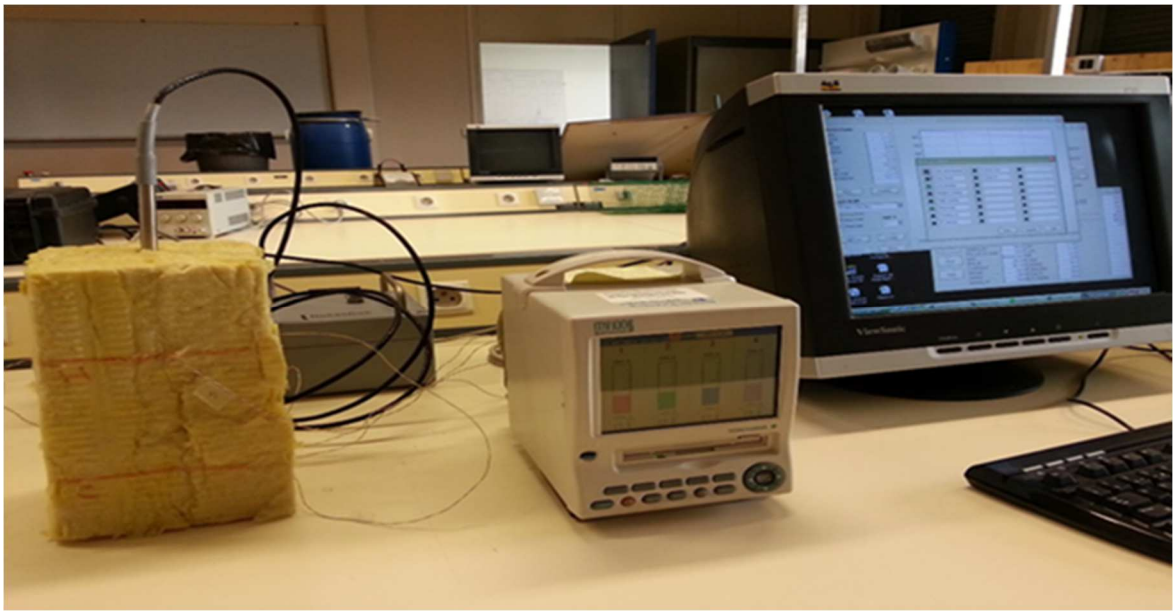

Figure 4-2: image of probe TP02 Hukseflux ® and the TPSYS02 control interface

The TPSYS02 control interface allows the power setting test conditions and visualization of measurement during time data acquisition (figure 4-3). An electric power per unit length Q is kept constant during the duration of the test. The thermal conductivity system TP02sys is manufactured and designed for supplying three heat power levels: high heat flow of 4.44 $W.m^{-1}$, medium heat flow of 2.64 $W.m^{-1}$ and low heat flow of 0.87 $W.m^{-1}$.

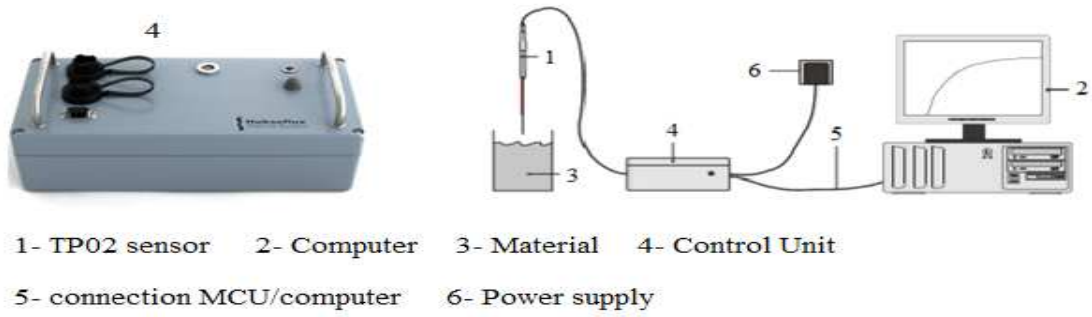

Figure 4-3: Scheme of probe TP02 Hukseflux ® and the TPSYS02 control interface

4-2-3 Calibration process by Glycerol

Glycerol has been chosen to calibrate the experimental process. This fluid is considered by Hukseflux as a reference material. Fluids are interesting to calibrate because they present no contact resistance and no porosity. Test has been done in a tube of 2.2 cm diameter. According to glycerol thermal diffusivity of 9.10^{-8} $m^2.s^{-1}$, a maximum time (t_{max}) of 180s has been determined [4] and [5]. Linear variation of increase temperature against logarithm of

time is observed (Figure 4-4). Applying the 4.44 Wm^{-1} high flow, a slope of 1.1863 is obtained for time between t_{trans}=78s and 165s.

The method of determination of thermal conductivity from thermal probe is based on the equation 2-28:

$$\lambda = \frac{Q}{4\pi}\left[\frac{ln(t_2/t_1)}{T(t_2)-T(t_1)}\right] \quad (2\text{-}28)$$

The slope value (Q/4πλ) allows the determination of the thermal conductivity of the medium.

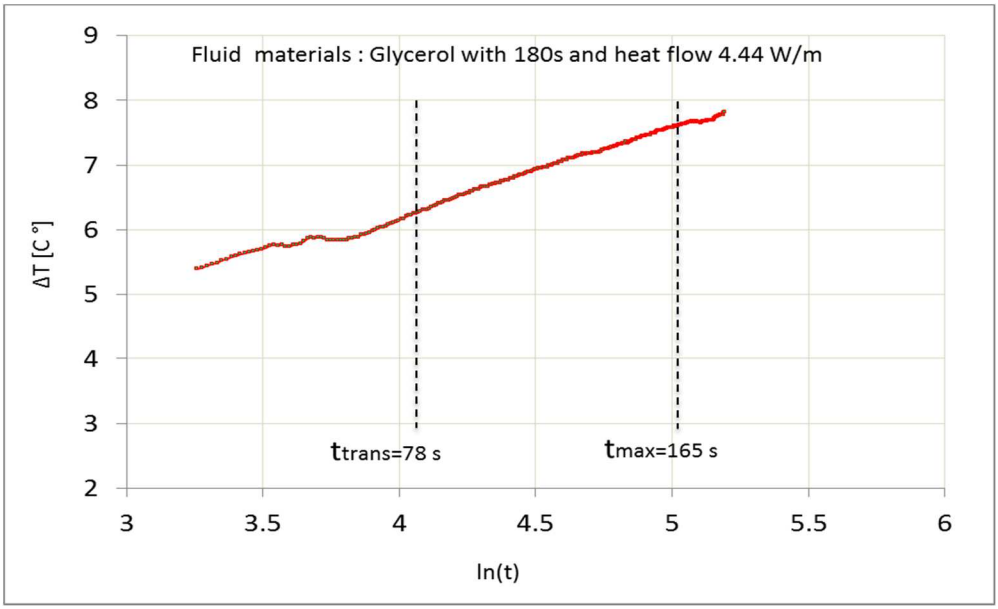

Figure 4-4: Variation of temperature against natural logarithm time for glycerol

Maximum time and heat flux values have been modified. Thermal conductivity reference value (handbook) for glycerol at 25 ° C is 0.29 W (m.K) $^{-1}$. Considering the expected accuracy defined by Hukseflux at 20 degrees of ± (3% + 0.02) $W.m^{-1}.K^{-1}$, experimental values are consistent with the reference value. However, the lower heat flux generates the most important difference with the reference value (table 4-2).

Test time [s]	High heat flux [4.44W.m^{-1}]	medium heat flux [2.64 W.m^{-1}]	Low heat flux [0.87 W.m^{-1}]
60	0.30± 3%	0.31± 3%	0.34± 3%
120	0.30± 3%	0.31± 3%	0.33± 3%
180	0.29± 3%	0.30± 3%	0.34± 3%
240	0.28± 3%	0.30± 3%	0.32± 3%

Table 4-2: Experimental results for thermal conductivity (W (mK) -1) of glycerol

Experimental kinetic by using TP02 probe Hukseflux is linear for glycerol (a fluid), so the equation 2-28 can be easily used to determine thermal conductivity.

4-2-4 Comsol Multiphysics® simulation

Hukseflux® TP02 probe was modelled with Comsol Multiphysics® software to compare experimentally and by simulation the temperature response of the probe. In Comsol, a sensor has been positioned at the probe-material interface representing hot temperature measurement. Comsol Multiphysics® software has been used to validate experimental test and to study the influence of parameters that cannot be accessible experimentally such as the length / diameter ratio and components of the probe.

The first step is to define the design space and geometries with the thermal characteristics of a known material (reference material). Thus, we can see the evolution of heat in our reference material and check with the results of the study of practical cases. The procedure then move to the steps of the modelling process to define materials Geometry, thermal properties these materials and the various operative transfers (figure 4-5).

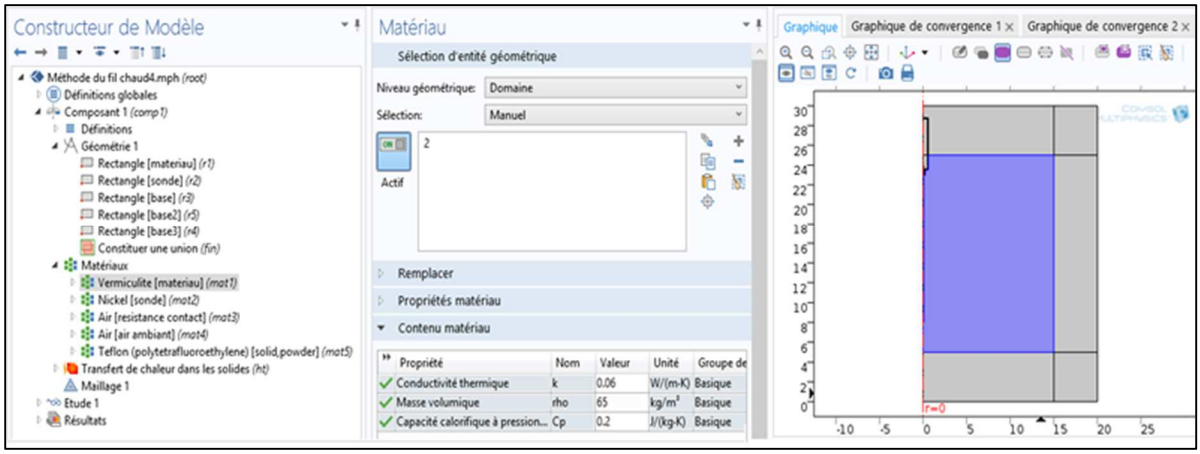

Figure 4-5: Representation of the user interface COMSOL

During start up the modelling of Comsol Multiphysics® software, the composition of the layers of the probe has been drawn in details and then the module was selected from the existing library. Each layer or component of the TP02 probe has been reproduced making possible the study of the effect of changing components of the probe (figure 4-6). Physical characteristics of materials have been found in the database of the software.

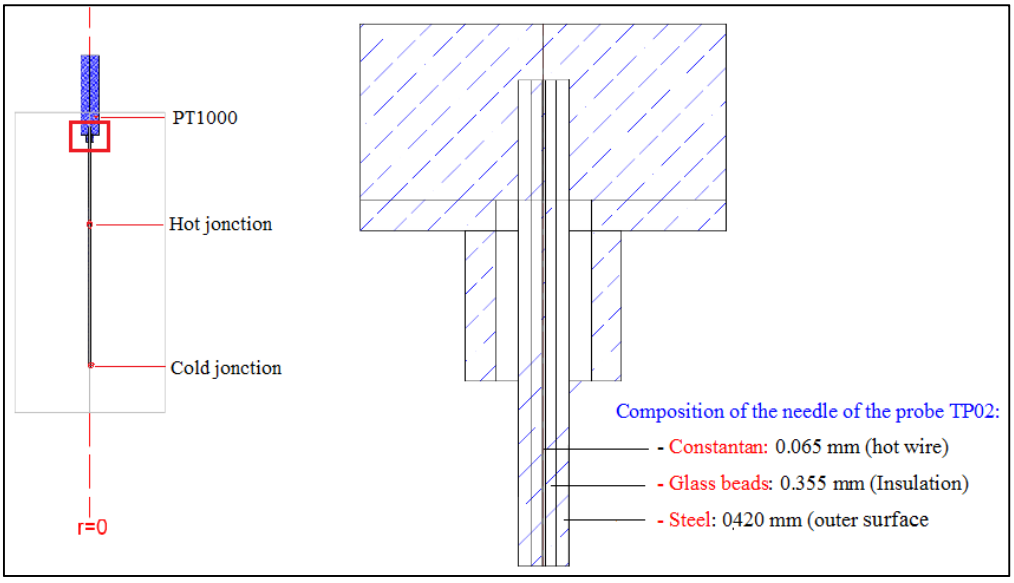

Figure 4-6: Axisymmetric 2D modelling of the hot wire Hukseflux TP02.

Axisymmetric module 2-D performing the study in a plane (2D) has been selected. In this module, the radial and the axial directions of the heat transfer are followed and an axis-symmetry in the middle of the probe is considered (Figure 4-7). An automatic mesh (Free Triangular) is realized by Comsol representing the normal size of each (Figure 4-8). To represent experimental conditions, a 1 mm air gap has been considered in order to take into account the contact resistance between the probe and sample.

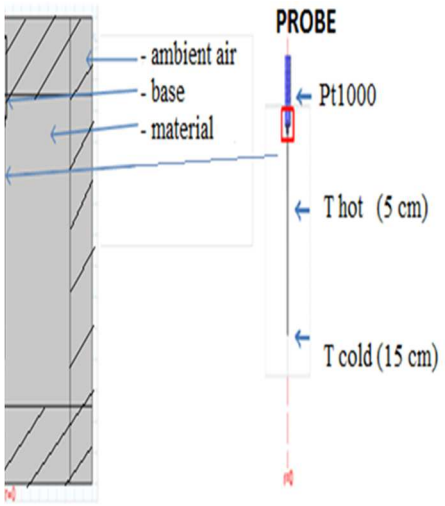

Figure 4-7:Probe and its environment

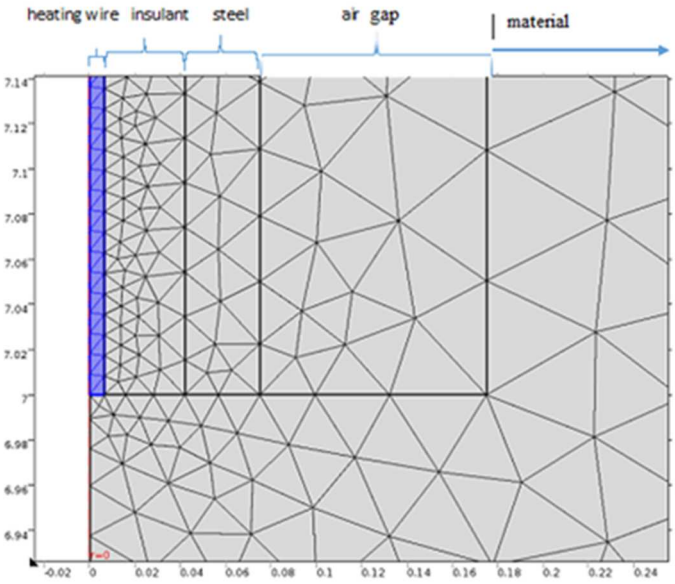

Figure 4-8: Mesh used in COMSOL model.

Thermal probe Hukseflux TP02 inserted into a cylindrical sampling medium is modelled using COMSOL, as shown in Figure (4-9). The glowing part in the axial center is the thermal probe Hukseflux TP02 heated by a very fine heating wire (constantan). The material properties and dimensions used for the COMSOL model are shown in table 4-3. Also, the cylindrical sampling medium is Ø60 mm × 250 mm to ensure that the radial infinite medium condition is achieved during the heating period of the thermal probe Hukseflux TP02 whose theoretical dimensions are Ø1.50 mm × 150.0 mm.

Materials properties and dimensions used in COMSOL	λ [w/m.K]	ρ [kg/m^3]	C_p [J/kg.K]	R [mm]
Constantan	19.5	8910	390	0.065
Glass pearl	0.16	1600	800	0.355
Steel	16	7900	500	0.33
Air boundary	0.0234	1.0	1005	1.00
material	0.0387	60	1015	60.00

Table 4-3: Parameters and values used for the simulation in Comsol

.

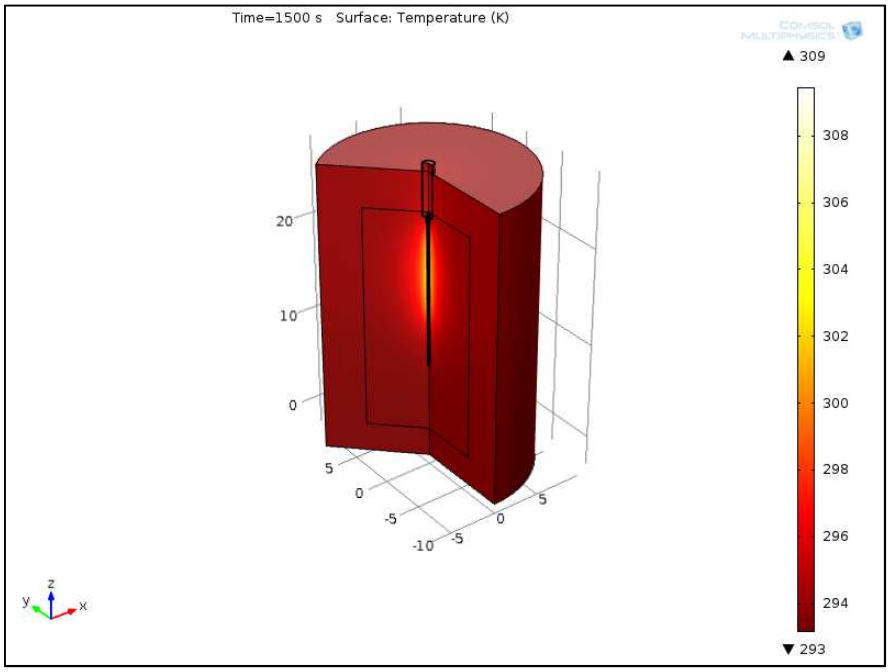

Figure 4-9: COMSOL model during Thermal probe Hukesflux TP02 inserted into sampling medium.

The same power heat flow (0.87 Wm^{-1}) corresponding to the low experimental heat flux and maximum time (1500s) allowed by the TPSYS02 interface have been chosen with time step 0.01 s. To define the boundary conditions, ambient air of 20 °C has been considered

surrounding the sample and at the surface of the probe heat power per unit area of the cross section of the probe (65545468 $W.m^{-3}$) have been introduced corresponding to the experimental heat flow used. The reason for using COMSOL is to reduce the computational time and power besides studying the influence of parameters that cannot be accessible experimentally.

4-3 Prospective errors by using thermal probe

Equation 2-28 has been referred to the classical solution is obtained with the following assumptions and simplifications:

a. Homogeneous material with physical properties considered constants,
b. Medium considers as infinite with reference of the size of the probe,
c. No consideration of the design of the probe,
d. No radiation and bulk flow in the medium,
e. The length to radius ratio of the probe is greater than 50,
f. Thermal contact between the probe and the medium is ignored,
g. Radius of the probe must respect the following condition: $\boldsymbol{u = \frac{r^2}{4\alpha t} \ll 1}$

Above assumptions and simplifications will be discussed in the following paragraph in order to check their applicability in order study.

4-3-1 Error associate to homogeneous material assumption

Three diameters (2 mm, 8 mm and 10 mm) glass beads have been studied (Figure 4-10) to study influence of the porosity on the thermal conductivity. The gaps between the glass beads (air) have an effect on the porosity and on the contact resistance between the probe and glass beads.

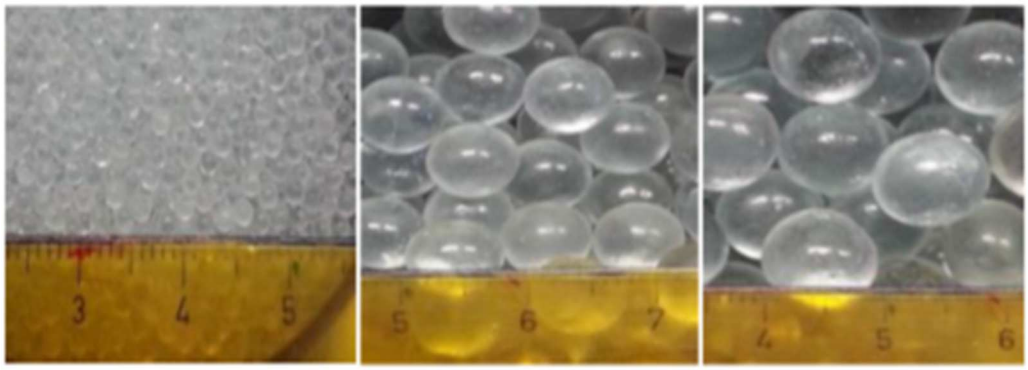

Figure 4-10: Glass beads 2, 8 and 10 mm diameters

For each bead type, the total porosity by water saturation (Table 4-4) is determined in a well-defined volume. Porosity increases with diameter of glass beads. These experimental values of porosity are in agreement with the literature [6] and [7].

Glass beads diameter [mm]	2	8	10
Total porosity [%]	36.55	40.30	41.00

Table 4-4: variation of the porosity of the glass beads with diameter.

Test has been done in a tube of 10 cm diameter for all tests and the probe of Hukseflux ® inserted inside the center of the samples vertically (figures 4-11 and 4-12). Low heat power (0.87 W/m) has been used in the experimental tests with time (600s) controlled by the TPSYS02 interface to evaluate effect porosity on the curve of variation of the temperature with the logarithm time.

Figure 4-11: Image of 2 mm glass beads during the test

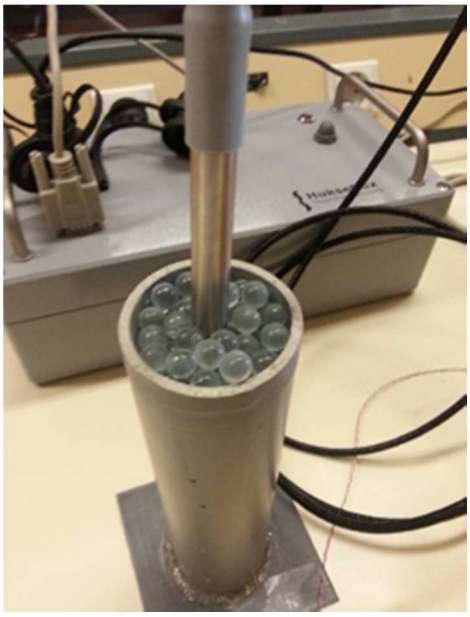

Figure 4-12: Image of 10 mm glass beads during the test

For 2mm diameter glass balls, a linear curve is observed but, non-linear variation in form of S-shaped curves is obtained for glass diameters of 8 and 10 mm (Figure 4-13). The S-shaped form can be assigned to heat transfer conduction and thermal inertia contrasts in the air and in the glass bead and the edge effect. Taking into account all these phenomena, thermal conductivity can be considered as an equivalent value.

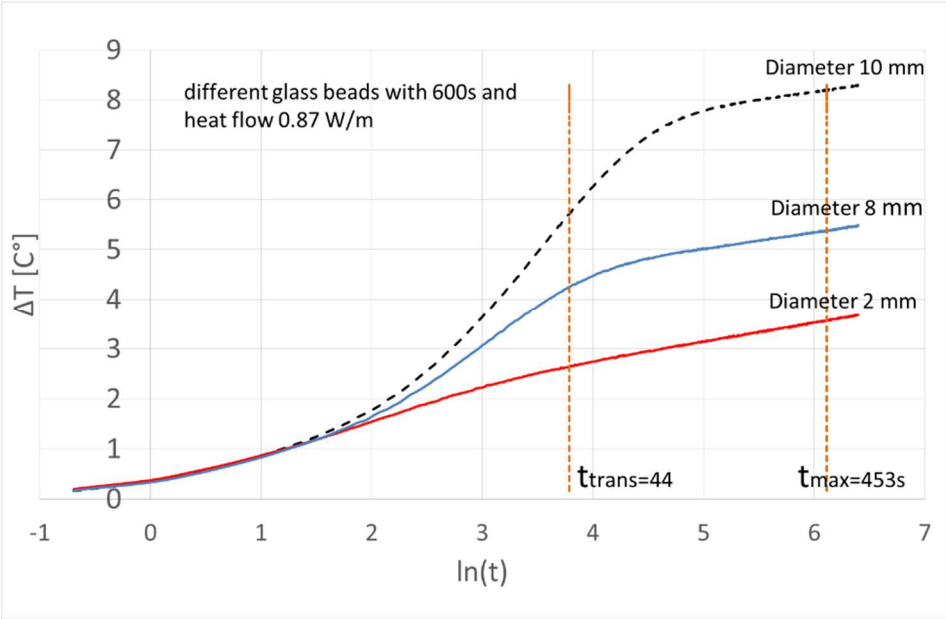

Figure 4-13: Variation of temperature against natural logarithm time for the different glass beads diameter with heat flow 0.87 W/m.

Thermal conductivities have been found from the S-shaped curve time period between t_{trans} and t_{max} defined respectively by equation 2-29 and equation 2-30. Thermal conductivity's values decrease when porosity increases which is scientifically checked. Coherent value has been found in literature [6] and [7] with our experimental values for 2mm glass bead diameter. But, for 8 and 10 mm diameters no value has been found in literature. So, measurement using guarded hot plate has been done for 8 mm diameter (table 4-5).

Glass beads diameter [mm]	Thermal conductivity (measured) [W (mK) $^{-1}$]	Thermal conductivity (reference) [W(mK) $^{-1}$]
2	0.18 ± 3%	0.17 [6] and 0.20 [7]
8	0.16 ± 3%	0.14*
10	0.09 ± 3%	

(*) Determined in the laboratory by using the guarded hot plate method

Table 4-5: Experimental results for thermal conductivity of glass beads.

The effect of the porosity on the thermal conductivity has been investigated well during study different insulation materials.

4-3-2 Errors associate with probe design

4-3-2-1 Error associate with length / diameter (L / D) of the probe

Blackwell [1] has defined a length to diameter (L/D) minimum ratio of 25 in order to reduce heat losses in the axial direction of the probe. For L/D ratio equal to 25, we observe (Figure 4-15) important axial heat losses in the base-material interface (upper part of the probe) and in the other direction (end of the probe). For L/D ratio of 100 (figure 4-14) corresponding to TP02 probe used for experimental runs, we just observed axial heat losses in the upper part of the probe due to the stainless steel (this metal is used to make the base of the probe). It would be preferable to use a more thermally insulating material for this base. As we note that heat is foremost loss from the upper part of the probe, we suggest to follow the temperature from the measurement of the Pt_{1000} and to keep its increase lower than 1 °C.

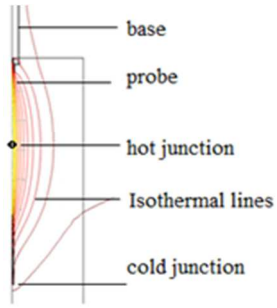

Figure 4-14:L/D ratio =100

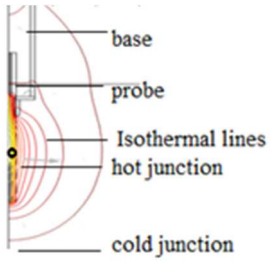

Figure 4-15:L/D ratio = 25

We investigated by Comsol Multiphysics® for different ratios of length to outer diameter (L/D) as shown in figure (4-16) to reach to the best value. We noticed that decreasing this value less than 100 gives us unreal value for thermal conductivity in spite of the increase in the variation in temperature, this result is in agreement with the previous studies for Hooper and Lepper [13].

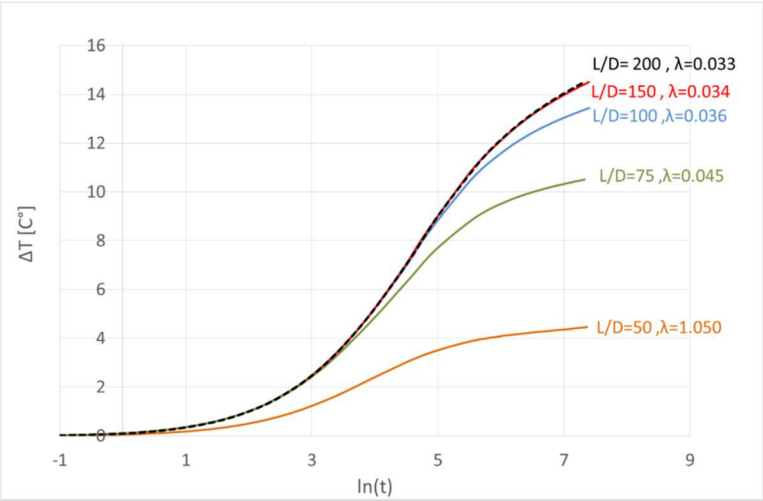

Figure 4-16: value of thermal conductivity for different ratio (L/D)

4-3-2-2 Error associate with the choice of components for the probe

Hukseflux has used stainless steel as components for the outer surface of the probe at the interface probe-studied material. This metal has the advantage of a lower thermal diffusivity increasing inertia during the heat transfer. Many metals have been selected in order to evaluate their influence. Table 4-6 present their electrical and thermal properties.

Materials	Density ρ [kg.m^{3}]	Electrical properties		Thermal properties		
		Resistivity 10^{-8}. ρ [Ω. m]	Temperature Coefficient 10^{-3}. α [K^{-1}]	Thermal conductivity λ [W.m^{-1}.K^{-1}]	Specific heat C_P [J.kg^{-1}.K^{-1}]	thermal diffusivity a [mm².s^{-1}]
Stainless Steel	7900	6,90	3.000	16	500	40
Copper	8960	1,55	4,041	390	390	116
Aluminium	2700	2,50	4,308	237	880	100
Nickel	8890	6,80	5,866	91	460	222
constantan	8910	49,00	0,074	19.5	390	56

Table 4-6: electrical and thermal properties of metals.

But we observed important temperature increase even if a low heat flux is produced (Figure 4-17). To reduce S-shaped form and to increase temperature at the outer surface of the probe, nickel can be used as Laurent [20] concluded. But, physical characteristics of copper seem to be more interesting.

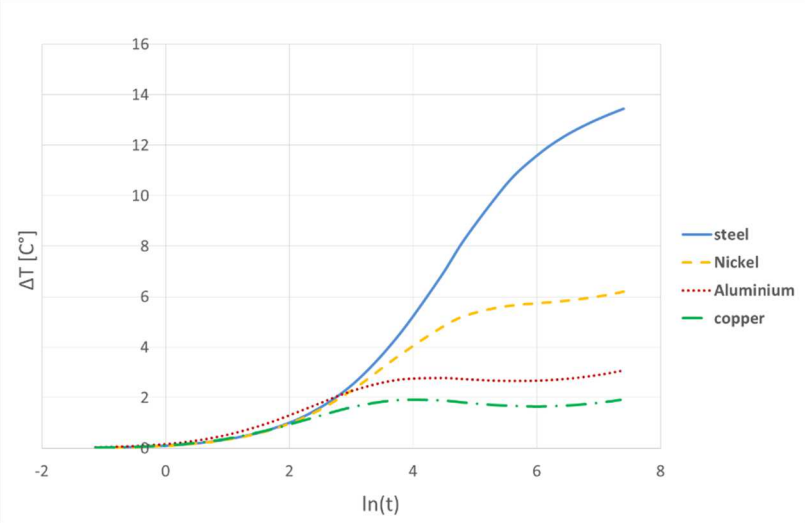

Figure 4-17: Metal outer surface of the probe for glass wool with low power 0.87 W/m at test time =1500s

As mentioned earlier hot wire heater is made from constantan. Influence of the hot wire metal has been investigated to know its effect on the shape of the curve of variation of temperature with the logarithm time. It is observed that the variation of the temperature was not affected very much by changing the metal of the hot wire (figure 4-18). This material has been chosen because of its high electrical resistivity and its low temperature coefficient as shown previously in table 4-6.

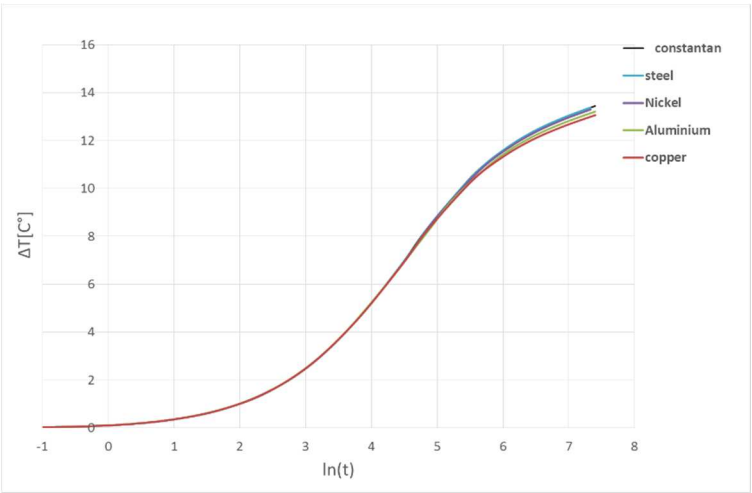

Figure 4-18: Metal the hot wire of probe for glass wool with low power 0.87 W/m at test time =1500s

3-3-2-3 Error associate with neglected thermal contact resistance

Between the outer surface of the probe and studied material, contact resistance must be taking into account especially for insulation materials. Influence of the contact resistance is considered by introducing air layer thicknesses of 0 mm (no contact resistance), 1 mm and 2

mm (large contact resistance). We observe (Figure 4-19) that the contact resistance has no influence on the slope for long time investigation (for *lnt>6*). The effect is relatively not sensible on S-shape curve for low heat flux and test time of 1500s.

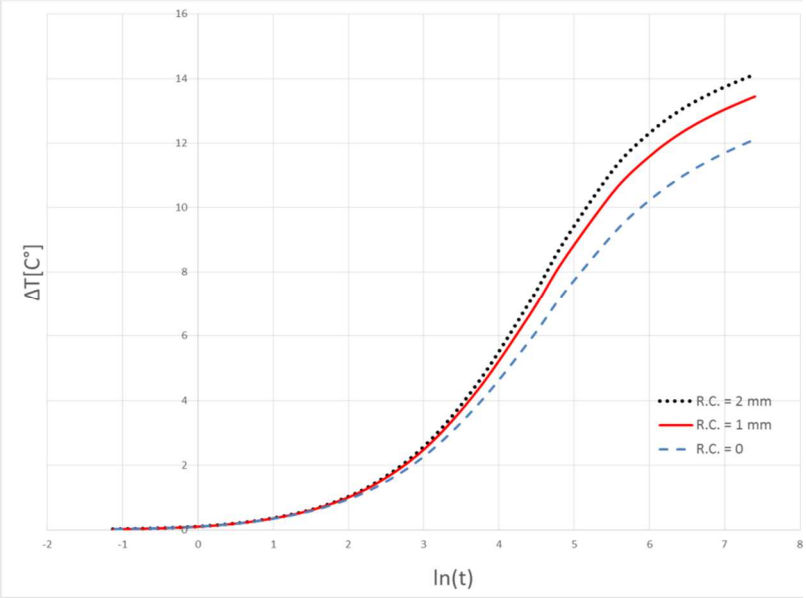

Figure 4-19: Effect of the thickness of the air gap for glass wool with low power 0.87 W/m at test time =1500s

3-3-2-4 Error associate with power supply

According to the TP02 probe of Hukseflux® specifications, temperature increase at the outer surface of the probe must be less than 1°C. By using the lower heat flux, experimentally we can't respect a temperature increase less than 1°C. ASTM Standard D 5334-08 [3] recommended for soil and soft rock that the temperature in the medium must be less than 10 °C in 1000s. To reduce effect of radiative transfer inside fibrous media especially, temperature variation of 5°C maximum must be checked. Van der Held in 1952 [14], [15] observed that the radiation occurs easily in materials which have high porosity. Temperature variation can be reduced by limiting energy and therefore by decreasing the heat flux and the time. Woodside in 1958 [16], Eschner et al in 1974 [17], Pilkington in 2008 [18] and R. Coquard in 2006 [19] also observed this phenomenon.

According to Comsol Multiphysics® simulation (Figure 4-20), temperature increase less than 1°C is only obtained for heat flux lower than 0.07 $W.m^{-1}$. But, this heat power can't be produced by TP02sys interface (the lower heat power level is 0.87 W/m). We can note also that this 0.07 $W.m^{-1}$ heat flux reduces the S-shaped form of temperature against natural

logarithm of the time and the finally obtained thermal conductivity 0.0347 $W(m.K)^{-1}$, is coherent with the reference value (0.035 $W(m.K)^{-1}$).

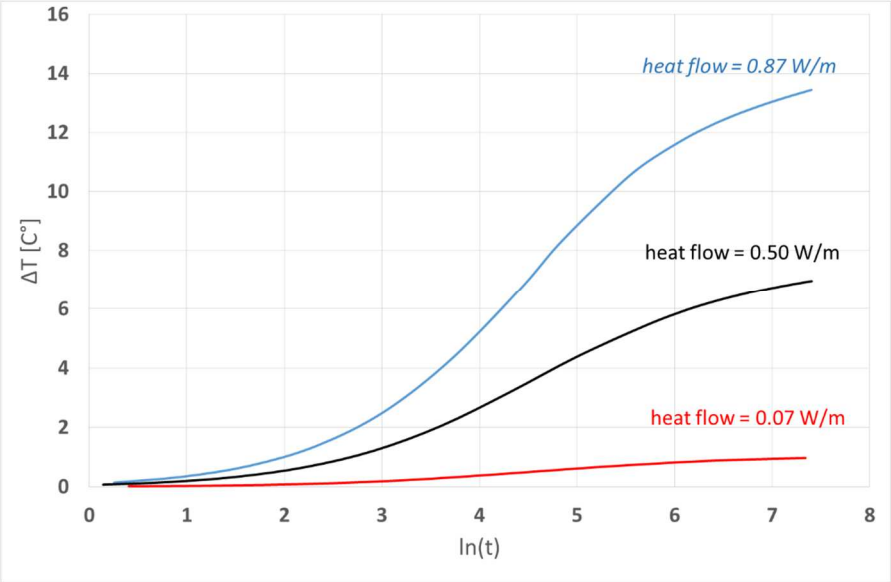

Figure 4-20: Results for very low heat flow on glass wool

4-4 Thermal characterisation of insulation materials

Insulation materials representative of the main categories of sold insulation have been chosen: powdery mineral insulator (vermiculite) or panel (glass wool) and synthetic insulation of chemical (XPS). Vermiculite is a powdered material having a porosity of about 90% and the size of the grains is between 1 and 4 mm. The glass wool is a structured material with fiber assemblies thereby obtaining a higher porosity (about 96%) [8]. Extruded polystyrene has a porosity similar to the glass wool but the pores are closed thereby reducing the transfer of heat into the air (Table 4-7). The maximum time (1500s) allowed by the TPSYS02 control interface has been selected. This value respects maximum time conditions (Equation 2-30) in chapter 2.

Insulation material	Diffusivity [$m^2.s^{-1}$]	Porosity [%]	t_{trans} [s]	t_{max} [s]
Vermiculite	$69 .10^{-8}$	90	10	527
Glass wool	$63.5 .10^{-8}$	96	11	573
XPS	$56 .10^{-8}$	96	13	650

Table 4-7: properties and time intervals (t min, t max) for thermal characterization insulation materials

As before for glass beds, low heat flux has been applied on 10 cm diameter cylindrical form samples. Due to the more important value of porosity, gradient of temperature is higher for

insulation materials than for glass beds. It is appropriate to be careful because the radiative phenomena can intervene in this case for glass wool.

Note that Hakansson et al in 1988 [9] already observed the non-linearity of the *ΔT/ln t* curve for thermal conductivity less than 0.07 W/ (m.K). He attributes the origin of the S-shaped curve to the thermal diffusivity of the samples. For Pilkington and Grove [10] this non-linearity depends on the pores of the cellular structure of the materials. They remark the shape of the curve is S-shape for polyisocyanurate foam (PIR) ($0.018<\lambda<0.025$ W/ (m.K)) and linear for the polytetrafluoroethylene (PTFE) (thermal conductivity of 0.25 W/ (m.K)). For Batty et al. [11], the structure of the material is less important than the contact resistance. They reveal the importance of the contact resistance between the probe and the glass wool fibers compared to the contact between the fibers.

4-4-1 Effect of contrast capacity ratio

In addition to these parameters, the non-linear variation in form of S-shaped curves is affected by the contrast capacity ratio of the thermal mass of the materials to the thermal mass of the probe (M) where $M = (\rho.C_p)_{material} / (\rho.C_p)_{probe}$ [12]. This ratio is very low for insulation materials (0.014 for glass wool, 0.012 for XPS and 0.025 for vermiculite) while this ratio is important 0.78 for glycerol (linear variation). Non-linear variation in S-shaped form appears for each curve of insulation material (Figure 4-21).

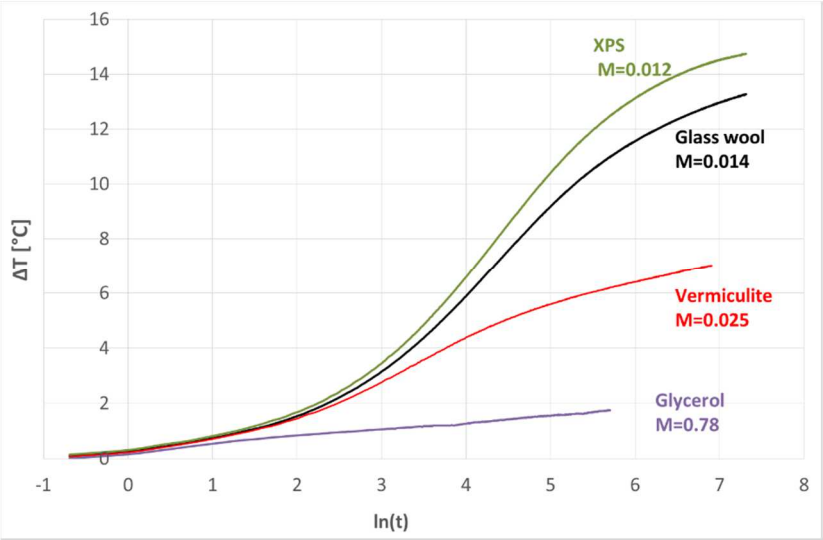

Figure 4-21: experimental kinetic different insulating materials at time 1500s, low flow 0.87 Wm-1

To determine thermal conductivity, we have defined three cases. First case (time 1), the entire kinetic has been selected to determine the slope (0 < ln (t) < end). Second case (time 2), according to Vos [2], we consider the part between t_{trans} and $t_{max.}$ Third case (time 3), according to ASTM recommendation [3], we chose t_1 and t_2 to obtain the best straight line between t_{trans} and t_{max}. In the particular case of glass wool (Figure 4-22), the straight line is obtained for t_{trans} and t_{max} respectively equals to 11s and 573s according to the Vos [2]. The experimental value for thermal conductivity which has obtained when selecting the time (t_{trans} < ln (t) < t_{max}) for the glass wool is (λ= 0.026 $W.m^{-1}.K^{-1}$). The best points have been selected (t_1 and t_2) equals to 30s and 150s respectively according to the ASTM recommendation [3]. The experimental value for thermal conductivity which has obtained when selecting the time (t_{t1} < ln (t) < t_2) for the glass wool is (λ= 0.021 $W.m^{-1}.K^{-1}$). The experimental value for thermal conductivity which has obtained when selecting the time (0 < ln (t) < end) for glass wool is (λ= 0.035 $W.m^{-1}.K^{-1}$) according to the all kinetic of the curve.

Despite the experimental results have a good consistency with the literature values (Table 4-8) when selecting the time (0 < ln (t) < end), but according to the linear asymptote of $\Delta T/\ln(t)$, thermal conductivity calculated from the slope ($Q/4\pi\lambda$) in equation 2-28 not satisfy the methodology of the equation 2-28.

Insulation material	Thermal conductivity (measured)[$W(mK)^{-1}$]	Thermal conductivity (reference)[$W(mK)^{-1}$]	Reference
Vermiculite	0.071 ± 3%	0.076 (*)	(0 < ln (t) < end)
Glass wool	0.033 ± 3%	0.035 (**)	
Extruded p .(XPS)	0.029 ± 3%	0.028 (**)	
Vermiculite	0.045 ± 3%	0.076 (*)	Vos [2]
Glass wool	0.026 ± 3%	0.035 (**)	
Extruded p .(XPS)	0.023 ± 3%	0.028 (**)	
Vermiculite	0.052 ± 3%	0.076 (*)	ASTM [3]
Glass wool	0.021 ± 3%	0.035 (**)	
Extruded p .(XPS)	0.018 ± 3%	0.028 (**)	

(*) Determined at the laboratory by using the guarded hot plate method
(**) Technical agreement value issued from the manufacturer of the product

Table 4-8: measured and reference thermal conductivity values of insulation materials

The kinetic of the thermogram is not linear so equation 2-28 could not reasonably be used. Values of the thermogram has been selected between t_{trans} and t_{max} according Vos [2], between t_1 and t_2 according ASTM recommendation [3] and between t_0 and t_{end} according to

our suggestion are unsatisfying the methodology of the equation 2-28. So, there is a necessity of finding a new methodology to determine thermal conductivity.

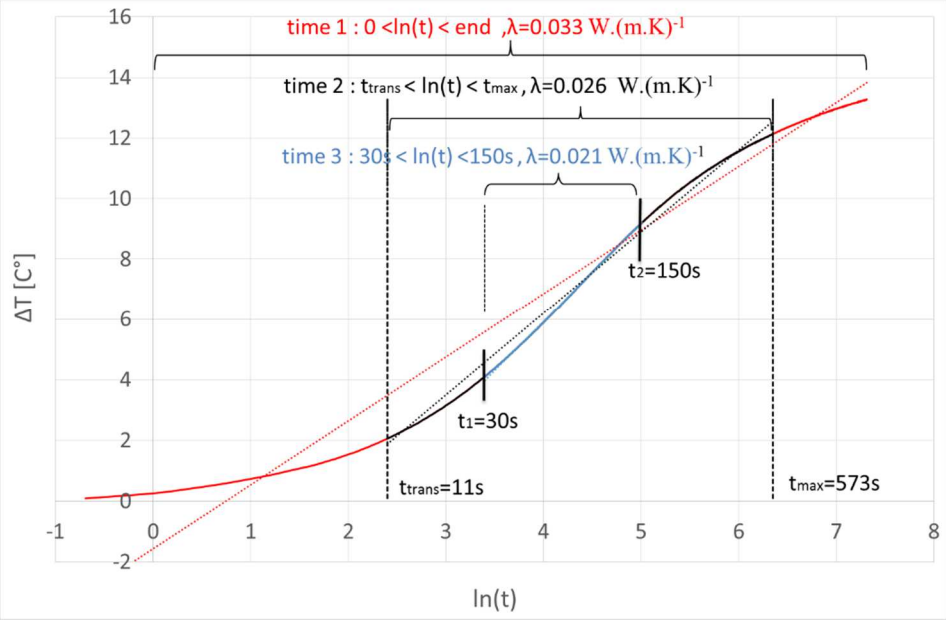

Figure 4-22: three ways to select ln (t) on the S-curve to find thermal conductivity for glass wool.

The glass wool is a structured material with fiber assemblies and has been chosen to study experimentally different conditions. The experimental values of thermal conductivity of the glass wool is change according to the heat power value and to the direction of heat flow.

4-4-2 Effect of heat power

TP02 probe of Hukseflux® have three heat power (high 4.44 W/m, medium 2.64 W/m and low 0.87 W/m). To reduce effect of radiative transfer inside fibrous media especially, temperature variation must minimum. Glass wool has been chosen to study effect of heat power supply on the thermal conductivity. According to the TP02 probe of Hukseflux® specifications, temperature increase at the outer surface of the probe must be less than 1°C. Figure (4-23) illustrates that the differences in the temperature during the experimental test for glass wool is more than 1 °C (13 °C for low flow, 37 °C for medium flow and 63 °C for the high flow), that means experimentally we can't respect temperature increase less 1°C and will achieve this condition just in modelling of Comsol Multiphysics®.

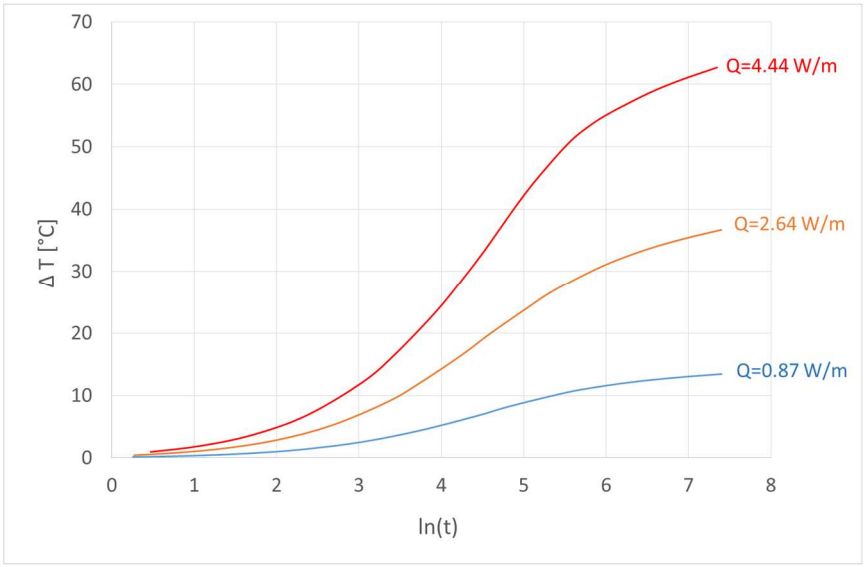

Figure 4-23: variation of temperature with logarithm time for different heat power

The value of thermal conductivity increases with heat power from (0.033 W/m.K to 0.038 W/m.K). This result was in agreement with the results of [Woodside] in 1958, [Eschner et al] in 1974, [R. Coquard] in 2006 and [Pilkington] in 2008.

4-4-3 Effect of direction of the thermal flow

The direction of the flow inside the fibrous insulation materials has an effect on the thermal conductivity for these materials. Two samples of yellow glass wool (density 68 kg/m^3) with dimensions (10 ×10 ×30) cm have been cut in different direction (figures 4-24 and 4-25) to evaluate effect the direction of the flow according to the fibrous structure.

Figure 4-24: Parallel (longitudinal) heat flow *Figure 4-25: Perpendicular heat flow*

Low flow (0.87 W/m) with maximum time (1500s) allowed by the TPSYS02 control interface has been used to study the effect of heat flow on the structure of the fibrous. The variation of the temperature changes according to the direction of flow to the fibrous besides the value of thermal conductivity which change from (0.032 W/m.K) for the parallel heat

flow to (0.034 W/m.K) for the perpendicular heat flow as shown in figure (4-26). These results are in agreement with Batty [11] 1984 and Pilkington [18] 2008.

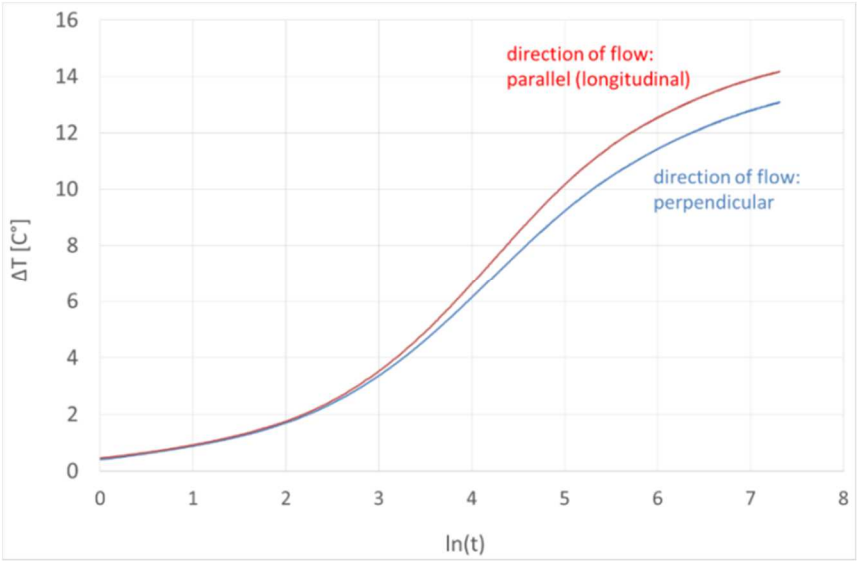

Figure 4-26: Variation of the thermal conductivity according to the direction of flow

The experimental values of thermal conductivity of the glass wool are changed according to the heat power value and the best results can be obtained when the heat power is low. According to the TP02 probe of Hukseflux® specifications, temperature increase at the outer surface of the probe must be less than 1°C. Experimentally we can't satisfy this condition with TP02 probe of Hukseflux® and it will achieve this just in modelling of Comsol Multiphysics®.

4-4-4 Effect of thermal properties of the medium

The temperature variation with the logarithm of the time is non-linear for insulation materials as mentioned previously. This variation has been investigated for different thermal characteristics (conductivity and specific heat). The base material is always the glass wool, this material has been used in this investigation with low power 0.87 W/m at test time 1500s. In the case of Figure 4-27, the thermal conductivity varies from 10 to 0.01 [$Wm^{-1}.K^{-1}$]. It is observed that the variation of the temperature increase with lowest thermal conductivity. The shape of temperature variation with the logarithm time has become more curvature and more clearer than 0.5 [$Wm^{-1}.K^{-1}$].

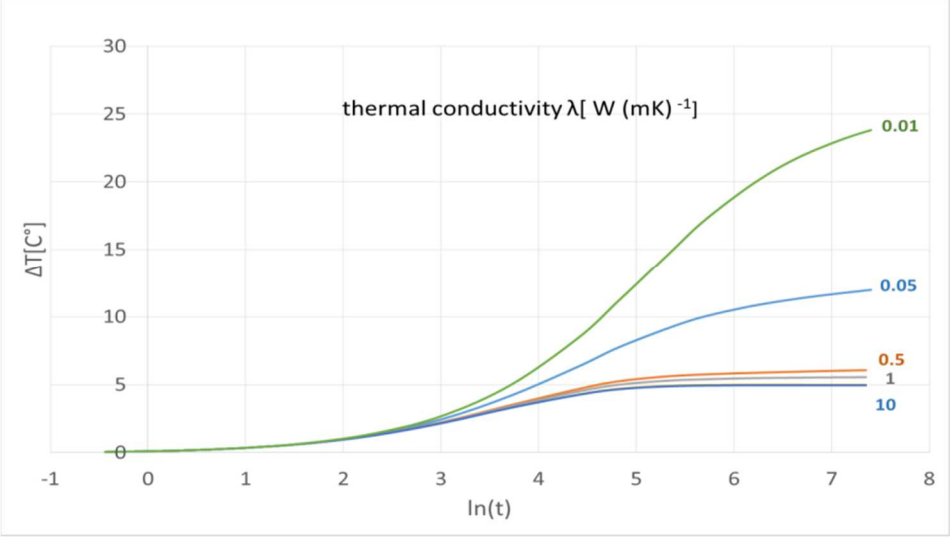

Figure 4-27: influence of thermal conductivity

In the case of the figure 4-28, the thermal capacity varies from 100 to 10000 [$J.kg^{-1}.K^{-1}$]. It is observed that the variation of the temperature is less clear than the thermal conductivity. The method of calculation (Equation 2-28) does not refers to the specific heat and the kinetics slope of the temperature variation with logarithm time remains the same for long time.

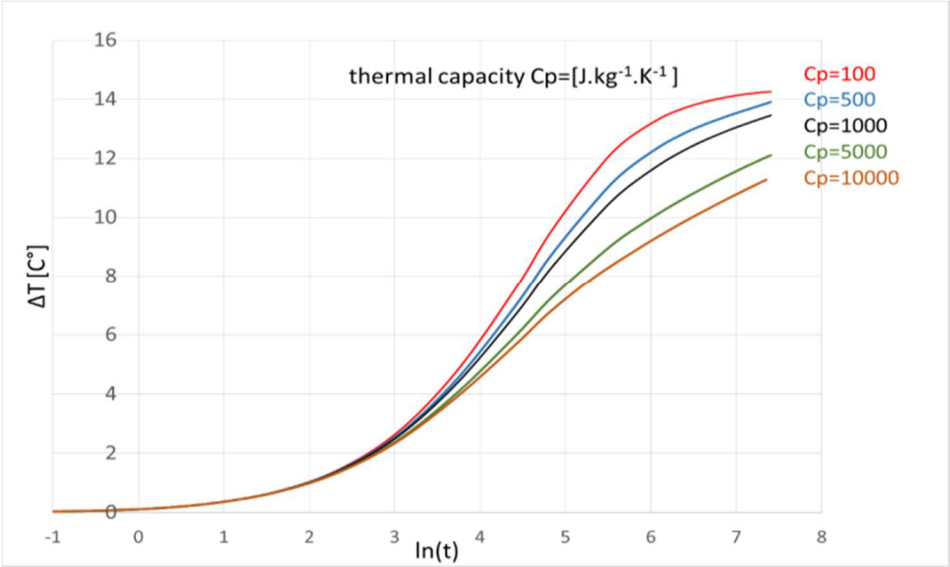

Figure 4-28: influence of thermal capacity

4-5 New mathematical analysis

In order to reduce the assumptions and simplifications, we have considered the temperature response of the heat source over time with heat is maintained at a constant rate can be described by Carslaw and Jaeger solution:

$$\Delta T = -\frac{Q}{4\pi\lambda} Ei\,[u] \tag{2-21}$$

Where $u = \frac{r^2}{4\alpha t}$ (2-22)

The exponential integral function (E_i) can be expressed by a series expansion [65]:

$$-E_i(-u) = \int_u^{\infty} \left[\frac{e^{-u}}{u}\right] du \tag{2-23}$$

Some authors have purposed innovative methodologies. Van Loon et al. [20] applied a revised model of the probe based on that of Jaeger to determine simultaneously the thermal conductivity, the volumetric heat capacity and the contact resistance. Zhang [21] tested the parameters introduced by Van Loon and demonstrated the model needs to be as complete and precise as possible. He demonstrated identification from Van Loon model can only be applied for long time approximations. André et al. [22] developed an analytical solution for the time dependent problem of heat transfer based on the quadrupole method. To determine thermal diffusivity or the volumetric heat capacity, other methods can be used by dual probe techniques [23]. Two thin parallel needles are built, one serving as a heater and the other as a temperature sensor.

4-5-1 Theoretical aspects

The general solution for temperature distribution at the external boundary of the probe can be expressed in terms of dimensionless parameters; Fourier's number (Fo), Inertia contrast (Ω) and Biot's number (Bi) as:

$$\frac{\lambda.T}{q} = G(Fo, \Omega, Bi) = \frac{8.\Omega^2}{\pi^3} \int_0^{\infty} \frac{1-\exp(-Fo.x^2)}{x^3.\Delta(x)}\, dx \tag{4-3}$$

Where $\Delta(x) = \left[x.J_o(x) - \left(2.\Omega - \frac{x^2}{Bi}\right) J_1(x)\right]^2 + \left[x.Y_o(x) - \left(2.\Omega - \frac{x^2}{Bi}\right) Y_1(x)\right]^2$ (4-4)

J_0 and J_1 are the Bessel functions of the first kind of order 0 and 1 while Y_0 and Y_1 are Bessel functions of the second kind of order 0 and 1. In the following paragraphs, dimensionless parameters are defined.

4-5-2 Sensibility analysis

Sensitivity analysis has been studied in order to check if unknown parameters are uncorrelated. Sensibility analysis of the parameter estimation problem (Figure 4-29) shows the thermal conductivity of the medium is the parameter of highest sensitivity. This parameter is sufficiently uncorrelated from the other parameters and the sensitivity analysis justifies the model reduction embedded in the direct model from equation 4-3. Inertia contrast is sensible at very short time (before 500 s). Sensibility of this parameter is very low compared with the 2 other parameters. Sensibility analysis identify also the necessity of considering simultaneously dimensionless parameters (Fo, Ω, Bi).

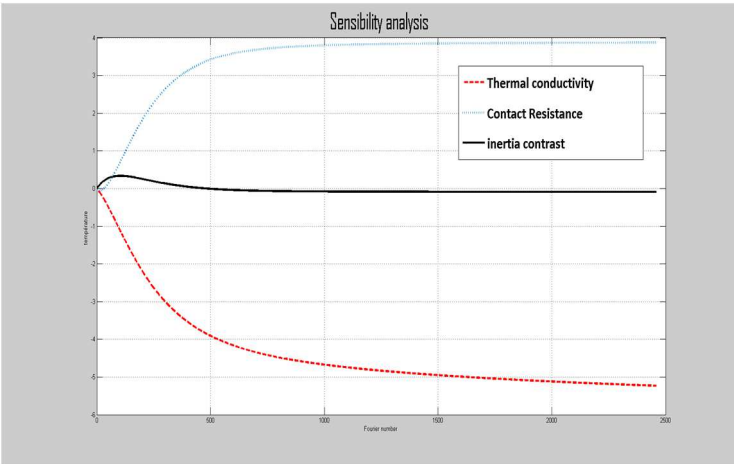

Figure 4-29: Sensibility analysis of the parameter estimation problem

4-5-3 Results

Estimated parameters determined by this process have been presented in table 4-9. Contact resistance can't be unheeded, its value corresponds to an air thickness of 0.5 mm. Dimensionless number can be compared to literature values. Laurent [23] bring out the necessity of producing a low Biot number and propose the maximal value of 0.25 to reduce the effect of S-curve. Our value is a half less than this value. Laurent considers also useful to reduce inertia contrast if Fourier number is important (which is the case for this test). Laurent concludes an inertia contrast of 2.5 is too important instead of 0.25 which is better. Our value is less than 0.25. Thermal conductivity (λ = 0.0391 $W.m^{-1}.K^{-1}$, table 4-9) is very close to reference values (λ = 0.035 $W.m^{-1}.K^{-1}$, table 4-8).

dimensionless parameters		estimated parameters	
Biot number :	Bi=0.2291	Contact resistance :	$R_c = 0.020$ m².K.W^{-1}
Fourier number :	0<Fo<4377	Thermal conductivity :	$\lambda = 0.0391$ W.m^{-1}.K^{-1}
Inertia contrast :	Ω=0.018	Thermal diffusivity :	a = 5.16 10^{-7} m².s^{-1}

Table 4-9: estimated parameters for glass wool

Main results from Matlab are presented in (figures 4-30) for glass wool characterization. Experimental values, already presented in (figure 4-31), are compared with estimation results curve. Fitting curve obtained by optimization process describe below is consistent with experimental values. Differences between experimental and estimation values can be assigned to the exact composition of the probe and contact between the components in the probe.

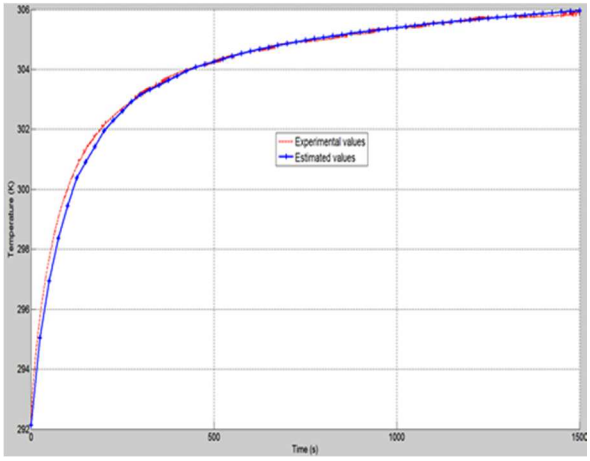

Figure 4-30: ΔT against time

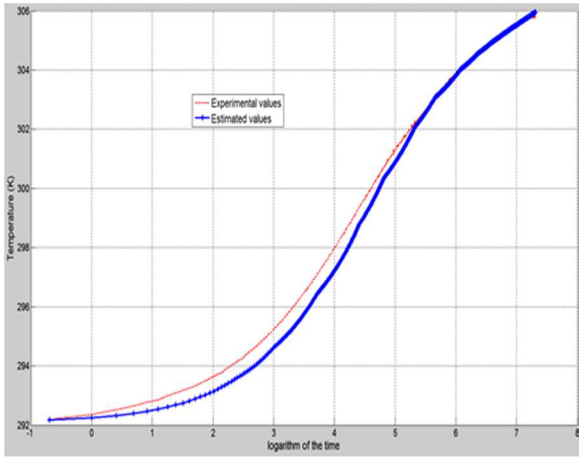

Figure 4-31: ΔT against logarithm of time

New studies by coupling Comsol Multiphysics and Matlab are in development by collaboration with Evry University.

4-6 Conclusion of the chapter

Applying long time approximation relation (equation 2-28) to determine thermal conductivity requires that the experimental kinetic representing the temperature increase vs. log time is linear. Experimental kinetic is linear for glycerol (a fluid) but as soon as the porosity of studied material is growing, S-shaped curve appears. Method becomes debatable. Due principally to important porosity, a sigmoid curve is obtained for insulation materials. We conclude traditional methodology can't be used for insulation materials. Analytical

simulation with development of a program Matlab has allowed simultaneously determining thermal conductivity and thermal diffusivity. Consistent results have been obtained.

Decreasing heat power reduces non-linear variation and provides thermal conductivity values with a good accuracy compared to reference values. We conclude that it is important to carry out tests over long time (>1500s) with a very low heat flux (<0.1 W.m-1). It is also important to check that temperature increase at the hot junction is less than 5 ° C. These conditions cannot be achieved with the control interface associated to Hukseflux TP02.

The length to diameter (L/2Rs) ratio of the probe is an important value to reduce axial heat flux along the probe and consequently error in thermal conductivity determination. A L/2Rs ratio of 100 is enough to neglect heat loss in the lower part of the probe. Making the probe by ourselves will be important to investigate in order to know the exact position of the thermocouples and how the probe has been precisely.

Comsol Multiphysics® has been used to study the influence of parameters that are not accessible experimentally such as the components of the probe, the contact resistance and the thermal properties of materials. Although the slight difference in the variation of temperature with the logarithm time for glass wool materials between experimental and Comsol curve, the simulation approach has been considered validated.

We noticed that decreasing the value of (L/D) less than 100 give us unreal value for thermal conductivity. To reduce S-shaped form and to increase temperature at the outer surface of the probe, copper can be used and we observe that the outer surface of the metal more influential than the hot wire metal. We conclude that the contact resistance has no influence in the slope for long time investigation for the S-shaped form of temperature against natural logarithm of the time. During Comsol Multiphysics® simulation, temperature increase less than 1°C is only obtained for heat flux lower than 0.07 $W.m^{-1}$. We note also the variation of the temperature increase with lowest thermal conductivity and it is less clear for thermal capacity because the method of calculation (Equation 2-28) not refer to the specific heat.

According to these conclusion we can built a new design for the probe, its properties are shown in the table (4-10).

Length (mm)	Diameter (mm)	Outer surface metal	Hot wire metal	Heat power (W/m)	Base materials
150	1.5	Copper	Constantan	0.07	Glass pearl

Table 4-10: properties of suggestion probe

Copper was selected as outer face because the electric current pass through it without loss and heat transfer quickly. Copper has low reactivity and it is considered antibacterial metal. Also, besides above properties, copper has good corrosion resistance, it resists to saline solutions, alkaline solutions and organic chemicals. Copper tough enough but for increase the strength, copper metal can be plated with stainless steel to prevent corrosion during long time to use specially in experimental moist material.

References of chapter four

[1]: Blackwell JH, A transient-flow method for determination of thermal constants of insulating materials in bulk, Part 1-Theory, Journal of Applied Physics, Vol. 25, N. 2, pp.137-144, 1954.

[2]: Vos B, Analysis of thermal-probe measurements using an iterative method to give sample conductivity and diffusivity data, Appl. Sci. Res., pp. 425–438, 1955.

[3]: ASTM D 5334 – 08, Standard Test Method for Determination of Thermal Conductivity of Soil and Soft Rock by Thermal Needle Probe Procedure, Approved 2008.

[4]: Humaish H, Ruet B, Marmoret L , Beji H, Thermal characterization of highly porous materials by the hot wire method, in proceeding of the French Thermal Society (SFT) congress, La Rochelle, France,Vol.23, 2015.

[5]: Ruet B, Humaish H, Marmoret L, Beji H, Assessment of thermal probe technique for determination of effective conductivity of building insulation materials, 20th European Conference on Thermophysical Properties (ECTP), Porto, Portugal, 2014.

[6]: Testu A., "Caractérisation thermique dans les milieux granulaires, caractérisation à cœur et en proche paroi", phD of Lorraine Polytechnic National Institute, France, 2005.

[7]: Huetter ES, Koemle NI, Kargl G, Kaufmann E, Determination of the effective thermal conductivity of granular materials under varying pressure condition, Journal of Geophysical Research, Vol.113, ref. E 12004, 2008.

[8]: Achchaq F, Etude hygrothermique de matériaux isolants fibreux (in French), PhD Picardie Jules Verne University, 2008

[9]: Hakansson B, Andersson P, Backstrom G, Improved hot-wire procedure for thermophysical measurements under pressure, Review of Scientific Instruments, Vol.59, n°10, pp.2269-2275, 1988.

[10]: Pilkington B, Grove S, Thermal conductivity probe length to radius ratio problem when measuring building insulation materials, Const. and Build. Materials, Vol.35, pp 531–546, 2012.

[11]: Batty WJ, O'Callaghan PW, Probert SO, Assessment of the thermal-probe technique for rapid, accurate measurements of effective thermal conductivities, Applied Energy, Vol.16, pp. 83-113, 1984.

[12]: Murakami, EG, Sweat VE, Sastry SK, Kolbe E, Datta A, Recommended design parameters for thermal conductivity probes for non-frozen food materials, Journal of Food Engineering, Vol. 27, pp. 109-123, 1996.

[13]: Hooper FC, Lepper FR, Transient heat flow apparatus for the determination of thermal conductivities, Transactions American Society of Heating and Ventilation Engineers v .56, pp.309-324, 1950.

[14]: Van der Held EFM, The contribution of radiation to the conduction of heat, Applied Scientific Research, Section A, Vol. 3, pp 237-249, 1952.

[15]: Van der Held EFM, The contribution of radiation to the conduction of heat: boundary conditions, Applied Scientific Research, Section A, Vol. 4, pp 77-99, 1953.

[16]: Woodside W, Calculation of the thermal conductivity of porous media, Canadian Journal of Physics, Vol. 36, pp. 815-823, 1958.

[17]: Eschner A, Grosskopf B, Jeschke P, Experiences with the hot-wire method for the measurement of thermal conductivity of refractories, Vol. 98, N.9, (in German) - cited in Davis WR, Downs A, The hot wire test- a critical review and comparison with the BS 1902 panel test, Transactions British Ceramic Society, Vol. 79, pp.44-52, 1974.

[18]: Pilkington B, In situ measurements of building materials using a thermal probe, phD, University of Plymouth, England, 2008.

[19]: Coquard R, Baillis D, Quenard D, Experimental and theoretical study of the hot-wire method applied to low-density thermal insulators, International Journal of Heat and Mass Transfer, Vol. 49, pp. 4511–4524, 2006.

[20]: W.K.P Van Loon, I.A Van Haneghem, J Schenk, A new model for the non-steady state probe method to measure thermal properties of porous media, Int. J. Heat Mass Transfer, Vol. 32, N.8, pp 1473-1481, 1989

[21]: X. Zhang, A. Degiovanni, and D. Maillet, «Hot Wire measurement of thermal conductivity of solids: a new approach, High Temp. - High Press. 25, pp: 577 – 584, 1993.

[22]: S. André, B. Rémy, F.R Pereira, N Cella, A. J Silva Neto, Hot wire method for thermal characterization of materials: inverse problem application, Engenharia Termica, N.4, pp 55-64, 2003.

[23]: Laurent JP, Contribution à la caractérisation thermique des milieux poreux granulaires (in French), phD of Grenoble Polytechnic National Institute, France, 1986.

Chapter 5 : Experimental measurement for heat transfer in wall

5-1 - Introduction

The European Union has planned to decrease the energy use for heating of buildings with 50% during the next two decades. The major part of the energy consumption related in heating of buildings and production of hot water. To reduce this energy in buildings different requirements have been studied related by types of insulation materials and its thickness, method of the building envelope and structural elements of the buildings. Heat transfer in thermal insulation materials generally occurs by conduction through building elements such as walls, roof, ceiling, floor, etc. heat transfer also by convection through the gas molecules of porous materials and radiation through the pores. A large part of the heat transfer in buildings takes place through the external walls. The thermal performance of a wall depends on the geometrical dimensions, thermal materials properties and weather condition. Different techniques are available for estimating the performance of walls and classified under Steady State methods and dynamic methods.

A guarded hot box is a method used to determine the amount of heat transfer through a wall by controlling the temperature on both sides of the wall. The guarded hot box consists of two boxes one representing the hot climate (inside condition) and other representing cold climate (outside condition). There are different standards that can be used to analyze the data from a guarded hot box such as Russian Standard GOST 26602.1-99, British standard EN ISO 8990 and American standard ASTM C 236 – 89 which is more suitable for a wide range of non-homogenous samples.

In this study the thermal performance of glass wool against dynamic solicitations in temperature has been studied by using guarded hot box in realistic climatic building envelopes conditions.

Building envelopes are subjected to thermal and hydric stresses that are not constant during days and seasons. In situ measurements are difficult (and often impossible) to control one-self due to coupled effects of heat and mass transfer coming from environment (sun, wind, rain,…). Such as dynamics solicitations in temperature and humidity are difficult to

reproduce in laboratory. Guarded Hot Box (GHB) apparatus can be considered as an interesting help to create realistic climatic conditions.

First objective of this study in this chapter to determine thermal resistance and thermal conductivity of the glass wool against temperature and compare the results with other techniques (guarded hot plate and hot disk). So a comparison has been done in order to validate measurements. It can be considered as preliminary step to take control of the apparatus. **Second objective** is to determine thermal storage capacity of the glass wool wall against temperature and humidity gradients. Flowmeter method already used in laboratory and guarded hot plate method has been adapted on GHB method. Thermal balance calculation must be undertaken to evaluate the importance of various heat flow inside GHB apparatus. These thermal properties can be also compared with Hot Disc results. Time delay and damping have been also determined to characterize thermal storage capacity of glass wool wall. **Third objective** is to study of heat and mass transfer (in simple cases) and a comparison with Wufi® data. Temperature and humidity gradients regulated in each cell of GHB can generate moisture transfer, air movement and superficial or interstitial condensation. To study these phenomena Wufi® can be considered well-adapted software. A comparison of results from GHB (experimental) and Wufi (simulated) have been investigated.

During this study, experimental tests were carried out from the Guarded hot box (THERMO 3R). This Guarded hot box has been chosen because of: (i) the area of the surface specimen (120×120) cm more than the area of the metering box (80×80) cm, so the heat loss around the edges of the test specimen (Flanking loss) has not happened compared with the Calibrated Hot Box (CHB). (ii) All the external walls of the Guarded Hot Box (THERMO 3R) are insulated with polyurethane with thermal conductivity (0.021 w/mk), this value is small compared with our materials (glass wool 0.04 w/mk). (iii) The wall that is fixed between the two cells is representing the realistic condition for the wall. (iv) Small area of the form of the specimen wall in guarded hot box (THERMO 3R) compared with other (GHB) leads to reduction the time of the experimental tests to reach the thermal balance.

5-2 General description of THERMO 3R

THERMO 3R is a device for measuring thermal transfers, through a flat vertical wall based on the Guarded Hot Box (GHB) principles. The apparatus includes two cells: cold cell temperature regulated (representing weather climatic conditions) and hot cell temperature

(representing interior climatic conditions) (figure 5-1). The outer envelope of each zone is covered by metal enclosure dimensions 1200x1200x600 mm inside a second envelope (inner shell) covered by steel dimension 1000x1000x500 mm is the warm-up area. The two shells are isolated by 100 mm polyurethane. In the hot zone cell, a box of dimensions 800x800x300 mm envelope delimits the measured zone. The area between this measurement zone and the inner shell is called guarded zone.

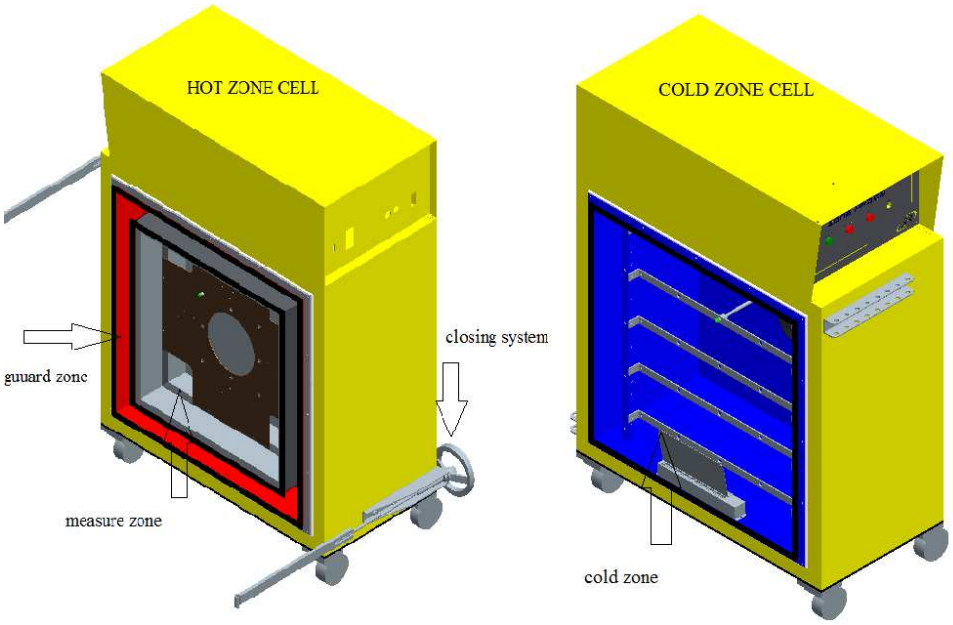

Figure 5-1: Image of hot zone and cold zone for Guarded Hot Box (GHB) THERMO 3R

The wall to be studied is placed between the two cells (figures 5-2). The heat that moves from one cell to another must pass through the wall. The walls to study must have dimensions (1200mm width and 1200mm height) with thickness from 10 to 300 mm in order to be installed with the frame of the guarded hot box. They can be composed of several layers of superposed materials, but each layer must be uniform over the entire surface of the wall. The outer surfaces must be flat, smooth and parallel. Particular attention must be paid to the achievement of hollow walls in blocks. The trolley caster wheels allow to place and maintain a wall between the two chambers to test the Thermo3. For this study, wall from glass wool has been manufactured by attached two parts from the sample. Dimension of the each part was (125 *60) cm and dimension of the frame metal of the equipment 3R was (120*120) cm. The excess part was cut to fit the frame metal for of the equipment 3R (figure 5-3).

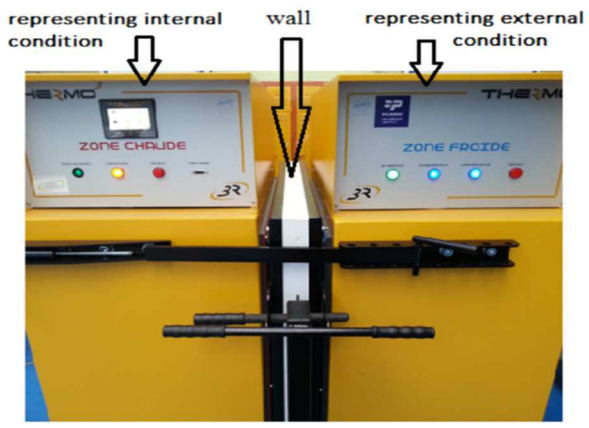

Figure 5-2:image of (GHB) thermo 3R cells and tested wall

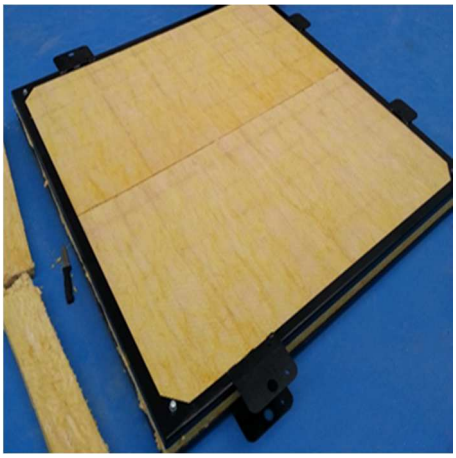

Figure 5-3: scheme of (GHB) thermo 3R cells and tested wall

5-2-1 Cold zone cell

The cold zone has a 450W piece refrigeration unit, a heat exchanger (cold) connected to the cold area, a hot heat exchanger connected to the outside. The group uses refrigerant R404A. Condensate generated by the heat exchangers is collected in a stainless steel tank through the piping of the hot gas at the compressor outlet which causes the immediate evaporation (figure 5-4). The refrigeration unit is equipped with a safety thermostat set at -20 °C. The Ventilation of the cold zone is formed by the condenser chiller. It draws air from the back of the enclosure, made it through the exchanger and then blowing cold air in the cold zone. It thus ensures uniformity of the temperature of the zone.

Figure 5-4: image of cooling unit

Figure 5-5: image of tangential fan

The air blown into the cold zone passes through a baffle making significant speed variations on the wall. Therefore it can be considered that the air near the wall is so still that the natural convection is not disturbed by ventilation. A tangential fan is optional to model the forced convection, figure (5-5). It is located at the bottom of the freezer against the wall and sends air the latter along the bottom to the top. The cold zone is standard equipped with 8 digital

temperature sensors distributed throughout the volume and on the wall of study. It can also accommodate a humidity sensor (optional). The sensors use a digital bus to 3 son and a communication protocol (One Wire) identifying them and read their measurement (figures 5-6 and 5-7).

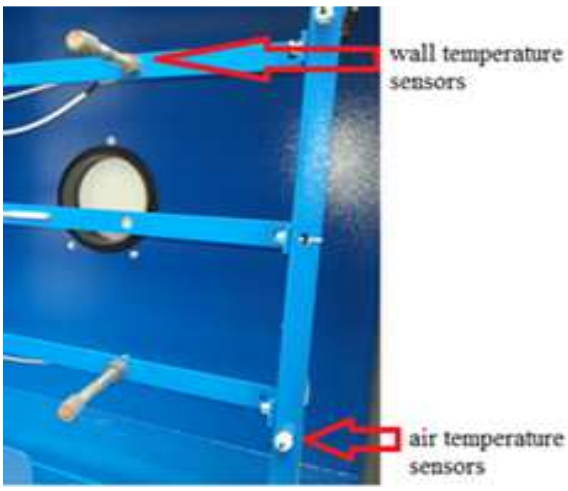

Figure 5-6: Image of cold temperature sensor

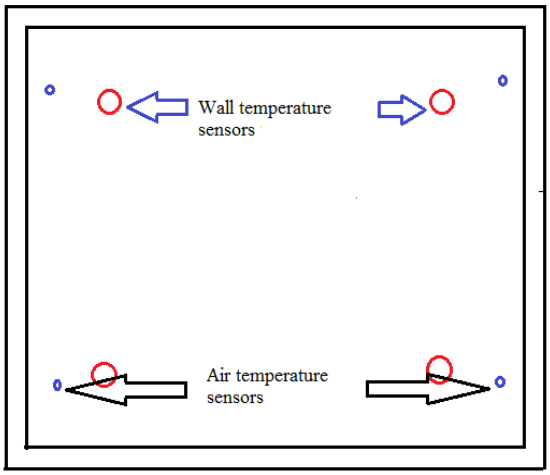

Figure 5-7: Scheme of cold zone sensors

5-2-2 Hot zone cell

The thermal energy in the measurement area and the guarded area is formed by electric resistors (200W per zone) extra low voltage (48VDC). A pulse width modulation controller controls the power fed to each zone. The current and the voltage are measured by the CPU and used to calculate the actual power of each zone. The hot zone is equipped with a safety thermostat set at 50 ° C. The ventilation of measurement zones and guard zone is provided by a fan in each zone. It ensures the homogeneity of temperatures, without accelerating the natural convection. The measurement area and custody are equipped as standard with 8 digital temperature sensors each, distributed throughout the volume of the wall and to study. It can also accommodate a humidity sensor (optional). The sensors use a digital bus to 3 son and a communication protocol (One Wire) identifying them and read their measurement as shown in figure 5-8. The sensor is designed for using with the Poseidon, Ares, HWg-STE and other HW group products (see appendix B).

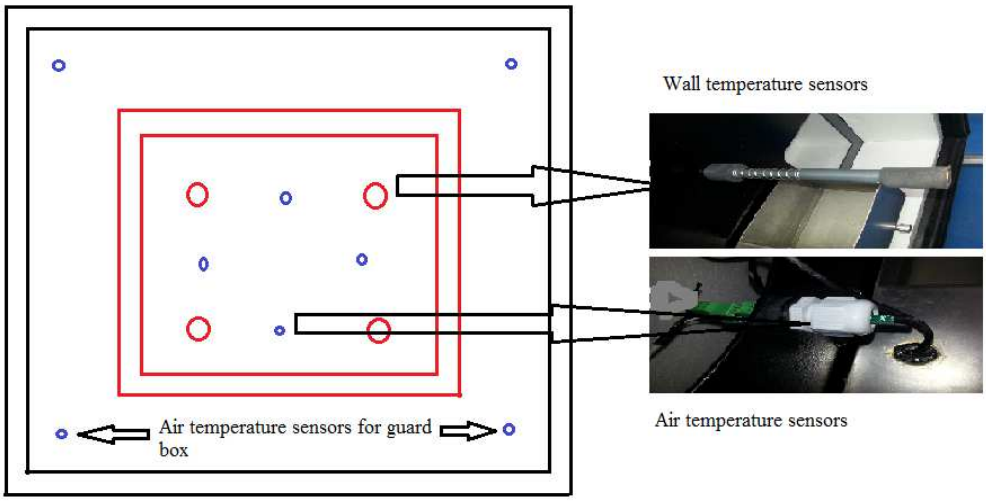

Figure 5-8:Images of wall and air temperature sensors inside hot cell

5-3 Calibration of Guarded hot Box

The similar temperature of the ambiance inside the measure zone (so called also metering box) and guarded box allows to neglect the heat loss The previous condition and uniform temperature on the both side of the specimen are representing the ideal solution.

5-3-1 calibration of measured hot cell

The power provide by the measured zone (Q_{in}) is representing the summation of the heat flow through the wall plus heat flow exchange between measurement area and guard area. The power (Q_{in}) is electrical power by heating system. The heat flow exchange between measure area and guard area it's equal to the summation of heat transfer parallel to the test specimen (Q_p) and through measuring wall (Q_w). If all the input heat will transfer through the test specimen that means the heat transfer parallel to the test specimen and through measuring wall are equal to zero. In reality this has not happened and the heat losses in the Guarded Hot Box (GHB) will be described in both of cells (hot cell and cold cell).

Heat flow balance in the measure zone of the hot cell (figure 5-9) can be described as:

$$Q_{ts} = Q_{in} - Q_p - Q_w \quad (5\text{-}1)$$

Where:

Q_{ts} : Heat transfer through test specimen [W]
Q_{in}: Total power input [W]
Q_p : Heat transfer parallel to test specimen [W]
Q_w : Heat transfer through metering box walls [W]

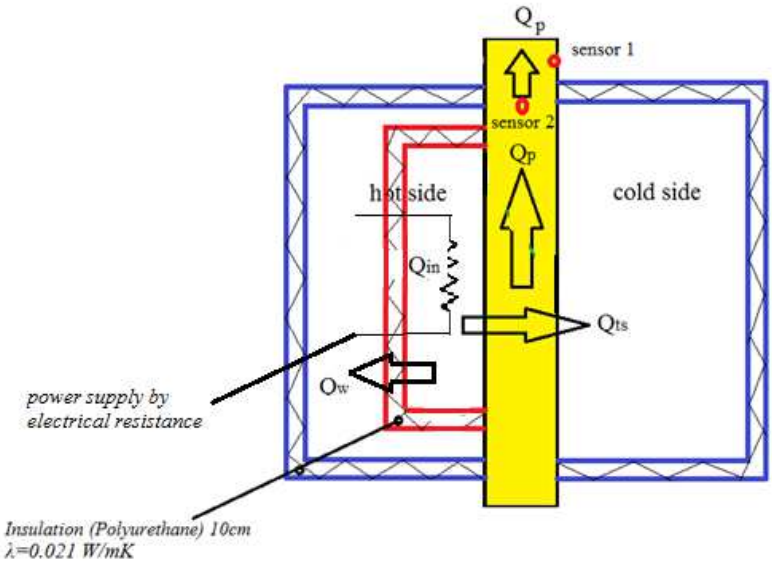

Figure 5-9: Guarded Hot Box Losses [6]

5-3-1-1 Influence of the heat loss by test specimen outside GHB (Q_p)

Heat flow (Q_p) corresponds to the flux transfer inside the specimen and loss at surrounding external surface of his area in the ambiance of the laboratory. To prove the importance of Q_p, two thermocouples (Sensor 1 and sensor 2) have been installed as shown in figure 5-9 (thermocouples type T made of copper and constantan with range of temperature -200 °C to + 400°C). Sensor 2 is placed inside the specimen and sensor 1 measures the temperature of the laboratory (outside the GHB). The data logger (MV100 by YOKOQAWA) has been used to store the temperature as shown in figure 5-10 (a). Cells have been regulated as shown in the figure 5-11.

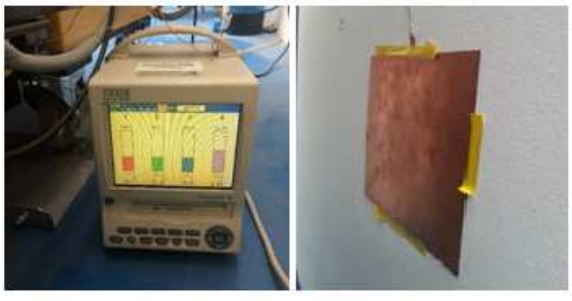

Figure 5-10: Data logger and flowmeter used in experimental

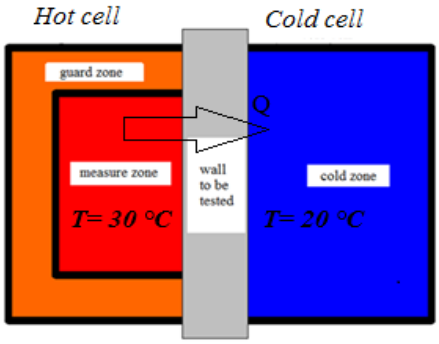

Figure 5-11: Condition of the two cells

We observe (figure 5-12) the temperature inside the specimen is similar to the room temperature (from morning to the afternoon). The effect of hot cell GHB temperature regulated at 30° is not sensible. So we can conclude that the heat loss Q_p from measured zone to ambiance of the room can be neglected. If it was not the case, sensor 1 and sensor 2 variation are not similar. Usually, tests are realized on walls with concrete or wood for example and specimen to test can be insulated on the surrounding surface but in our case, as we study an insulant, this can't be done.

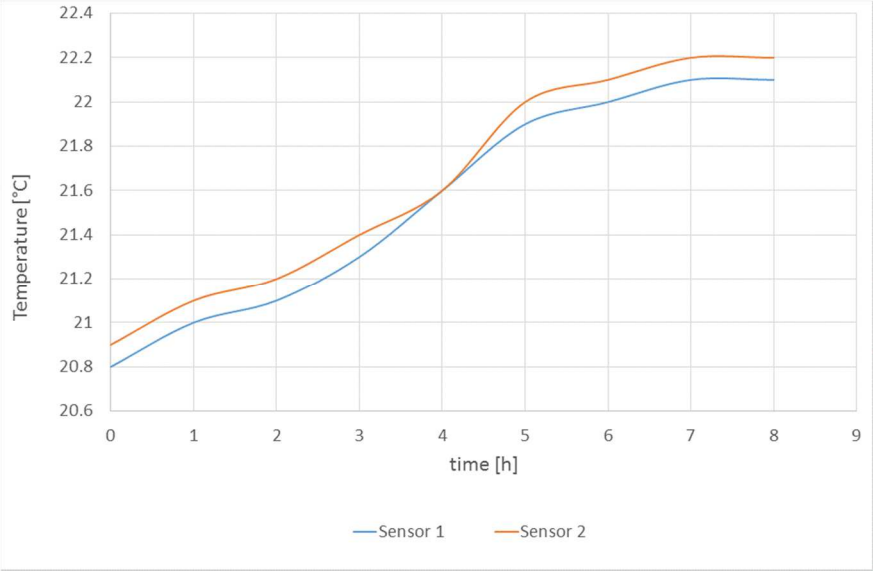

Figure 5-12: Variation of temperature inside and outside the specimen

5-3-1-2 Influence of the heat loss by wall of measure zone of GHB (Q_w)

After neglected Q_p, the heat transfer through specimen (Q_{ts}) from the measured hot box can be obtained by:

$$Q_{ts} = Q_{in} - Q_w \quad (5\text{-}2)$$

To determine Qts, we have installed one flowmeter with sensitivity 264 µV/ (w/m²) on the hot surface of the specimen in contact with measured zone. Q_{in} is calculated by Thermo 3R according to methodology described in appendix C. The value of Q_w has been calculated by using the expression:

$$Q_w = \frac{S.\Delta T}{R_w} \quad (5\text{-}3)$$

Where:

S : Surface area of the metering box [m²]
ΔT: Temperature differences between measured box and guarded box [°C]
R_w: Thermal resistance of the wall of the measure box [m² K/w].

ΔT is obtained from sensors of the THERMO3R in guarded zone and measured zone ambiances. The value of the cold cell is still regulated at 20 °C and temperature of the hot cell changes at 30 °C, 40 °C and 50 °C. Calculated value in table 5-1 corresponds to the use of equation 5-2. Knowing, by experimental data, Q_{ts} an Q_{in}, it is possible to deduce Q_w. A slight difference is obtained coming from the accuracy of temperature measurement, from the fact that temperature measurement is taken by values in ambiance and not in surface of the wall and from the fact that Q_p is assimilated negligible (which is not exactly the case).

Hot cell T [°C]	Cold cell T [°C]	ΔT [°C]	Experimental value of Q_w [W] by eq. (4-2)	Calculated value of Q_w [W] by eq.(4-3)
30	20	10	0.02	0.04
40	20	20	0.05	0.10
50	20	30	0.09	0.17

Table 5-1: Comparison between experimental value and theoretical value Qw

We observed in figure 5-13 at the beginning of the kinetics the hug variation of the flow Q_{in} in the first hour of the test. We are in unsteady state period. There is a need of an important flow to obtain a stabilised temperature in cells. As soon as the thermal equilibrium is obtained a stabilised flow is observed. We can conclude that Q_w can be neglected. When steady state is reached, Q_w is near (or under) 0.1 W while Q_{in} and Q_{ts} is near 8W. So, for the hot cell, equation (5-2) can be expressed as:

$$Q_{ts} = Q_{in} \tag{5-4}$$

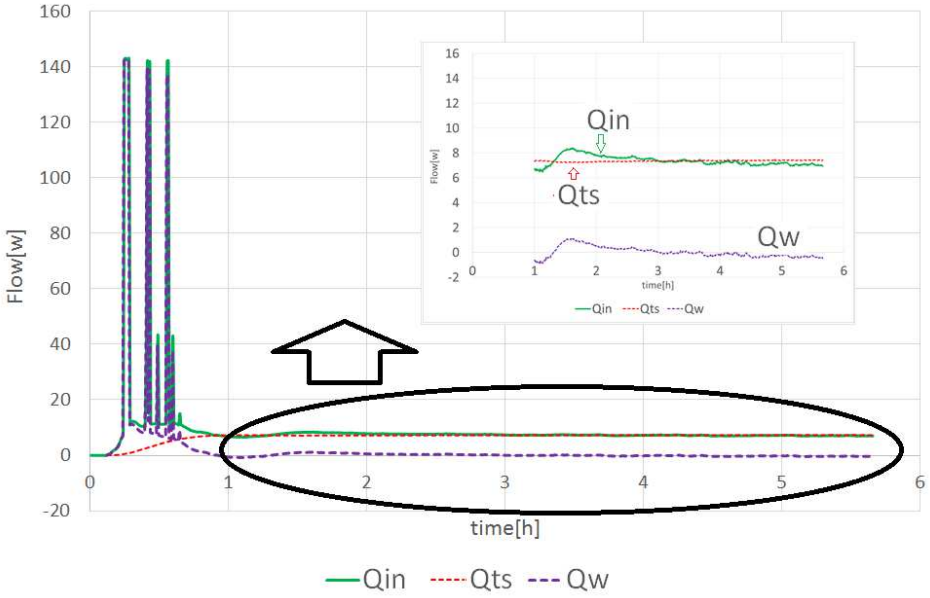

Figure 5-13: Heat losses by wall of measure zone during the experimental test

5-3-2 calibration cold cell

There is no guarded zone in the cold cell. We can identify other heat flow source in this cell. The heat flux Q_w, corresponds to the flow transfers from room laboratory to the cold cell. The heat flux Q_c corresponds to the power supplied by the cold group to regulate the temperature.

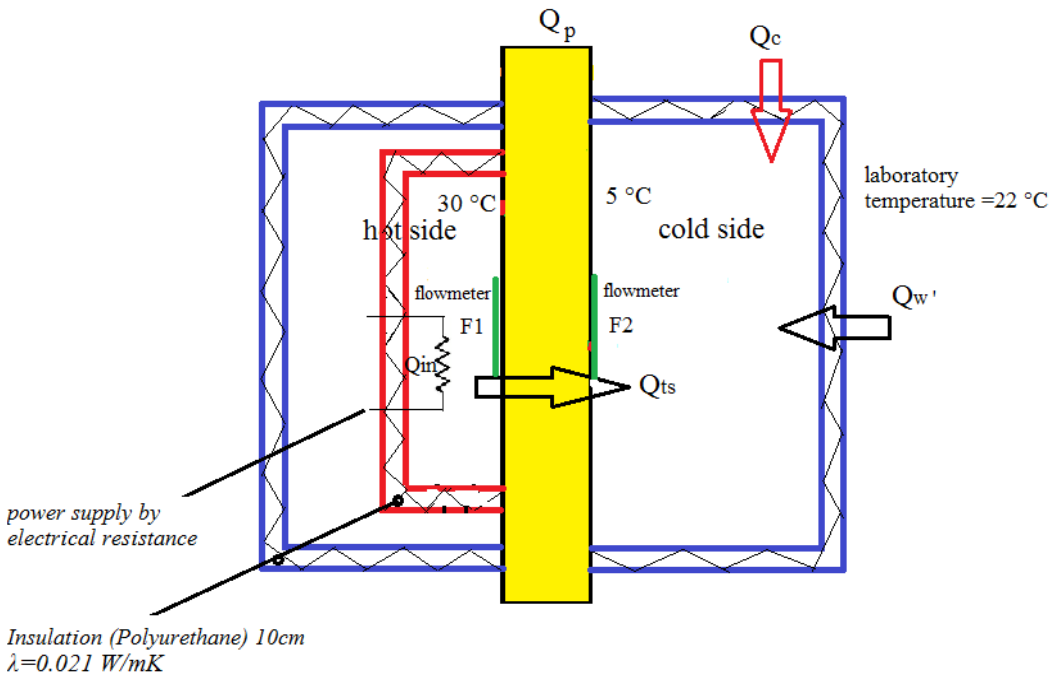

Figure 5-14: Losses occur in cold cell

As the heat flow is supplied in hot box by electrical resistance and we want to study heat flow in cold zone, there is a need of measuring the flow on each side of the specimen. To that two flowmeters were used. These flowmeters measure temperature and flow during the test. The sensitivity of flowmeters respectively placed in the hot and in the cold surface of the specimen is 250 µV/ (w/m²) and 264 µV/ (w/m²) with accuracy 0.1 °C.

5-3-2-1 Cold group OFF

When Cold group is OFF, Q_c equal to 0W so we are in the same case as the previous study. We can consider the relation if the flow $Q_{w'}$ is neglected:

$$Q_{ts} = Q_{in} \quad (5\text{-}4)$$

We can remark also that, if the steady state is reached, $Q_{ts}=F_1=F_2$ (F_1 and F_2 correspond to the flowmeter measurements which are described in figure 5-14).

The experimental test has been done during the Cold group OFF with the same conditions shown in figure 5-14 (temperature and position of flowmeter). We observe in the figure (5-15), the flux reached to the steady state after (4.5 h) when flux value in the hot cell equal to the flux value in cold cell (F1=F2).

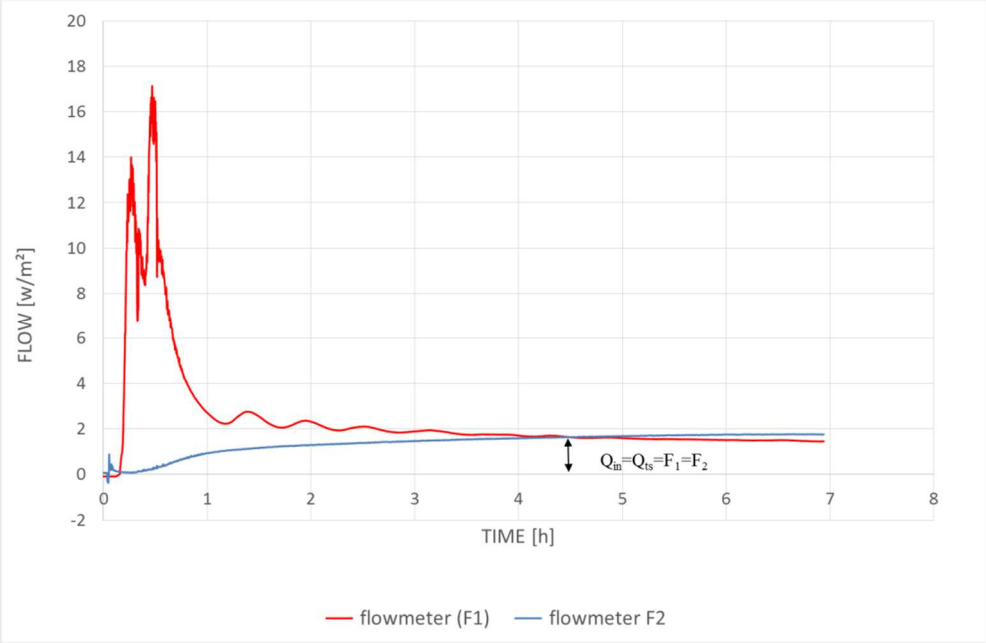

Figure 5-15: Heat flow losses occur in cold cell when cold group is OFF

5-3-2-2 Cold group ON

When Cold group is ON, we must take into account the power supply of this group (denoted Q_c). The heat losses can be expressed as:

$$Q_{ts} = Q_{in} - [Q_{w\prime} + Q_c] \quad (5\text{-}5)$$

When steady state is reached, Flowmeters F_1 and F_2 measure the flow transfers inside the specimen. They integrate in their measurement not only (as when Cold group is OFF) the effect of power supplied by the electrical resistance in the hot box (Q_{in}) but also the power supplied by cold group (Q_c).

In the same temperature conditions as before (when cold group is OFF), we have studied heat flow when Cold group is ON. We observe (figure 5-16) variations on the flowmeter curve placed on the specimen surface inside cold cell (F2). This is due to power (Q_c) supplied by cold group to regulate the temperature of the cold cell. It is interesting the base of this wavering corresponds to the flowmeter 1 (F1).

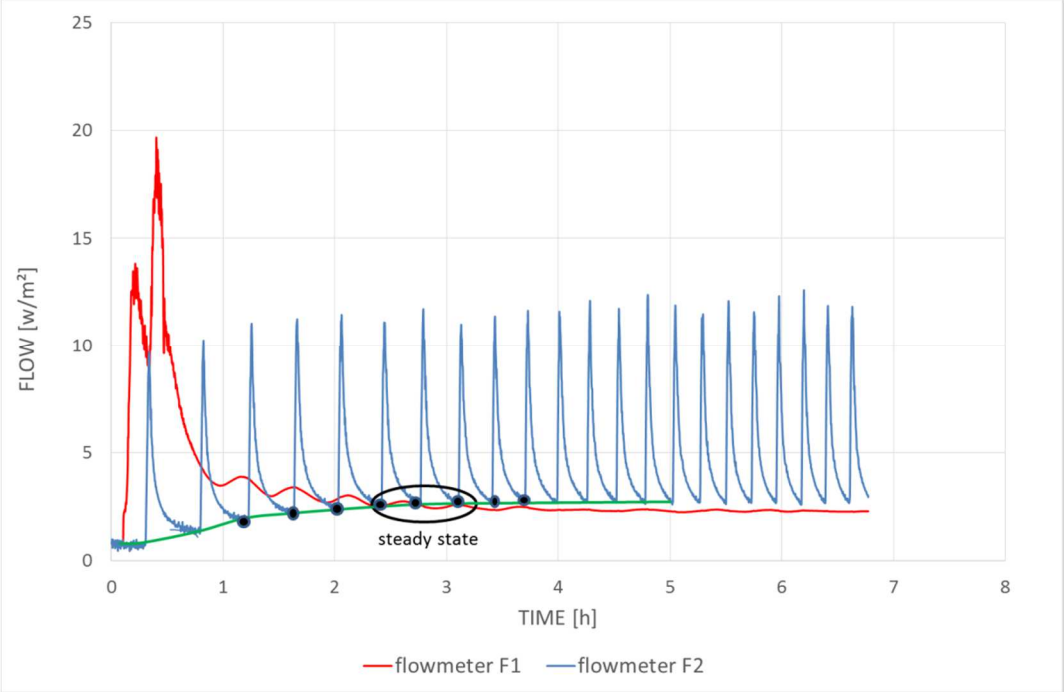

Figure 5-16: Heat flow losses occur in cold cell when cold group is ON

The flux reached to the steady state when cold group is ON (figure 5-17) at 3 h. This time is weaker than when cold group is OFF (4.5 h). The flow is bigger when cold group is ON (2.60W) than when it is OFF (1.65W). This difference is due to power supplied by cold group to regulate the temperature in cold cell but also power supplied by electrical resistance to compensate the cold group effects.

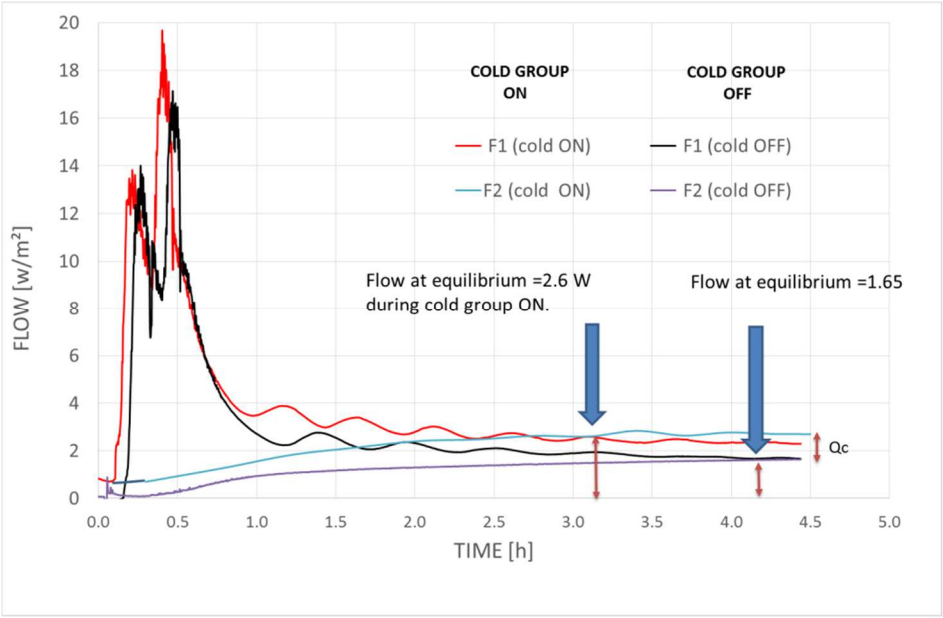

Figure 5-17: Comparison of heat flow losses when cold group OFF and ON)

5-4 thermal resistance

Thermal resistance is determined when steady state is reached. There is a need of determining with a good accuracy the flow in the specimen and the flow (Q_{ts}) must be constant. So, thermal resistance of the specimen can be calculated by using relation:

$$R_{ts} = \frac{A_{ts}\ (T_{hot\ ts} - T_{cold\ ts})}{q_{ts}} \quad (5\text{-}6)$$

Where;

R_{ts} = test specimen thermal resistance [m² K/w]
A_{ts} = test specimen area [m²]
$T_{hot\ ts}$= hot side test specimen surface temperature [k]
$T_{cold\ ts}$= cold side test specimen surface temperature [k]

We have seen, in the previous calibration paragraph, how the heat flow (Q_{ts}) can be determined with precision by using flowmeters. Flowmeters give also temperature in each side of the specimen. THERMO-3R presents a lot of temperature placed in the surface of the specimen.

There is a need of purposing a methodology for defining the minimum time to consider that steady state is reached. We will describe ASTM recommendation that describe a methodology to calibrate the system. Then we will determine thermal resistance of our glass wool against temperature and humidity. Finally, a comparison with experimental results from guarded hot plate and hot disc has been done.

5-4-1 Calibration process

To calibrate the process, we have chosen a wall provides by THERMO-3R to realise typical exercises for student. The wall (figure 5-19) is composed of three layers (table 5-2):

Designation	units	Plaster BA 13	Glass wool	Plaster BA 13
Surface	m^2	0.64	0.64	0.64
Thickness	mm	13	90	13

Table 5-2: details of the wall during calibrate guarded hot box

This wall has been used to measure thermal resistance of the wall and deduce the thermal conductivity of the glass wool. Temperature conditions of the test are: 30 °C in the hot cell and 5 °C in the cold cell (figure 5-18).

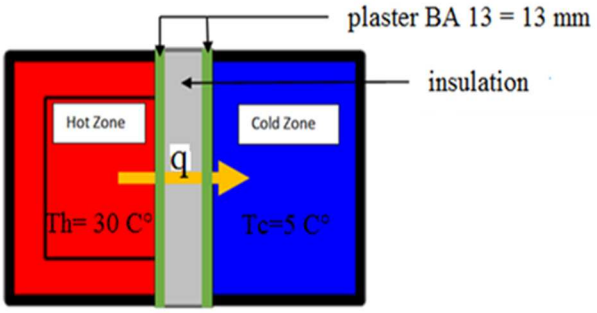

Figure 5-18: cross section of the wall with the cells

Figure 5-19: image of calibrate wall

5-4-1-1 Time minimum for steady state by ASTM recommendation

ASTM recommendations [1] consist of two periods:

- First period: to reach steady state conditions (test shall be more than 4 h in duration), the average surface temperature must not vary more than ± 0.06 C° and the average power in the meter area must not vary more than ± 1%.
- Second period: continue the test (at least 8 h), two or more successive 4-h periods produce results that do not differ by more than 1%.

a. First period

Data shall be collected at intervals of 1 h or less. The thermal equilibrium is reached after 2 h. We can draw the cold wall temperature, hot wall temperature and flux with the time during the test time (figure 5-20).

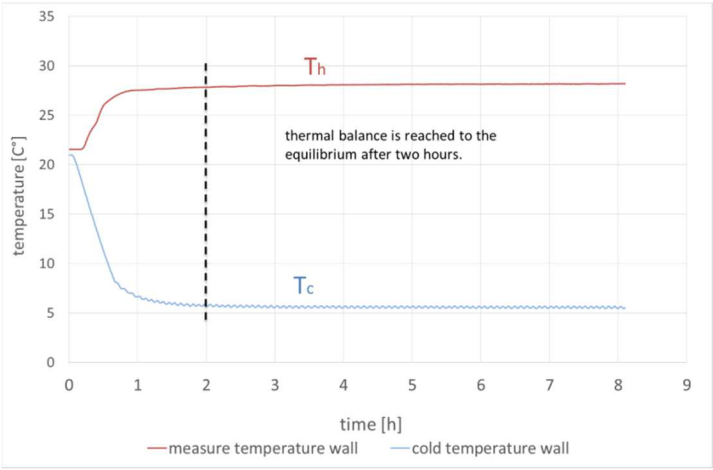

Figure 5-20: variation of Wall temperatures (° C) with the test time (h) during steady state period

The variation of temperature illustrated in the table 1 in the appendix A is 0.074 °C from (0 to 3h. So ASTM recommendations are not respected. From 2 to 6h, variation of temperature is less than 0.06 °C (table 2 in Appendix A) respecting ASTM recommendations. During the same period, average power in figure 5-21 varies more than 1% (table 3 in Appendix A).

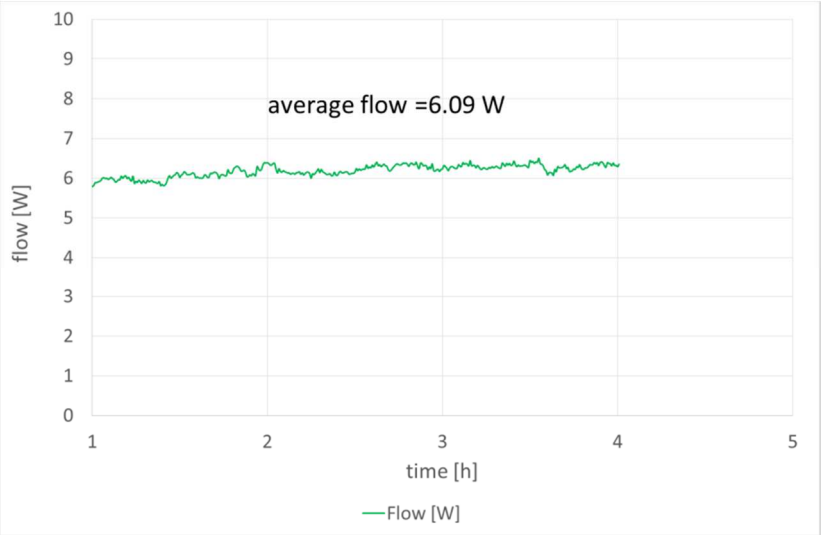

Figure 5-21: variation of flux (w) during first period

b. Second period

If we continue the test during 8h, we observe the flow is stabilised (figure 5-22). The difference during two periods of 4 h is less than 1%. So ASTM requirement has been achieved (Table 4 in Appendix A).

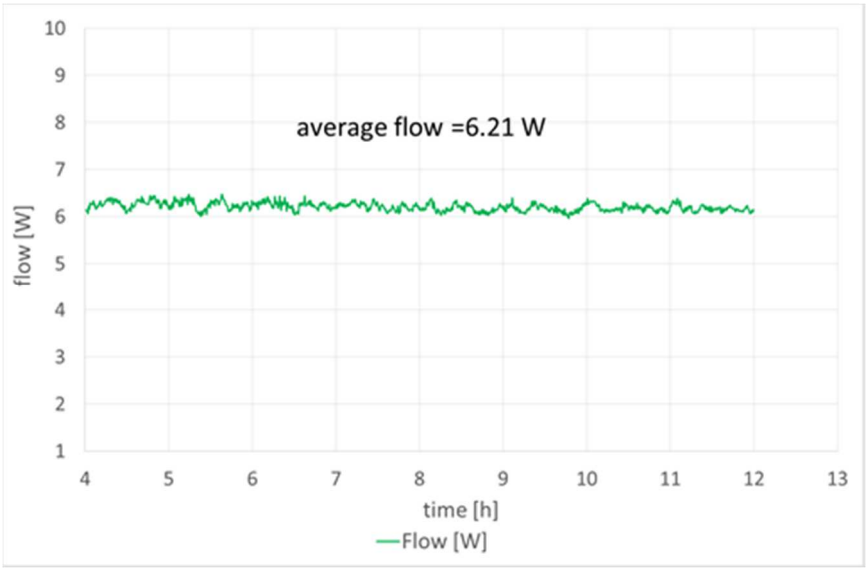

Figure 5-22: variation of flux (w) with the test time (h) during second period

5-4-1-2 Determination of thermal resistance

To check the validity of the experimental procedure, we have calculated the total thermal resistance of the wall by using the thickness and the thermal resistance of each layer. The calculated thermal resistance is 2.315 $m^2K.W^{-1}$.

Considering the time of the first period respecting ASTM recommendation, experimental value for the thermal resistance is 2.330 $m^2K.W^{-1}$ (figure 5-23). Deviation 0.64% from these two values is obtained. During the second period (figure 5-24), the experimental value for the thermal resistance is 2.305 $m^2K.W^{-1}$ with deviation of 0.43% from the theoretical value.

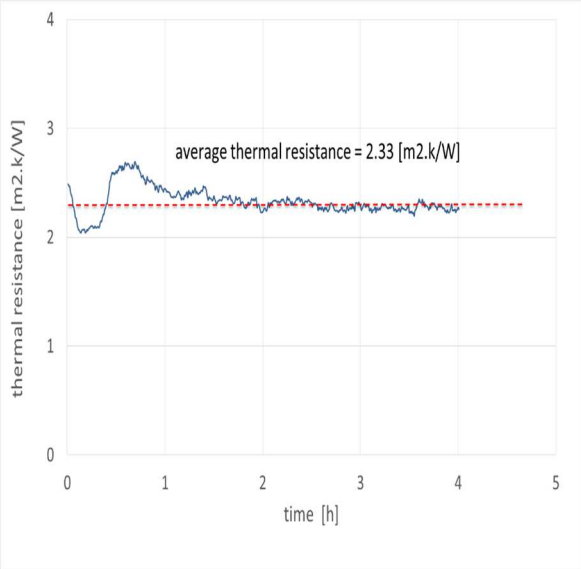

Figure 5-23: Thermal resistance ($m^2K.W^{-1}$*) during the first period (ASTM)*

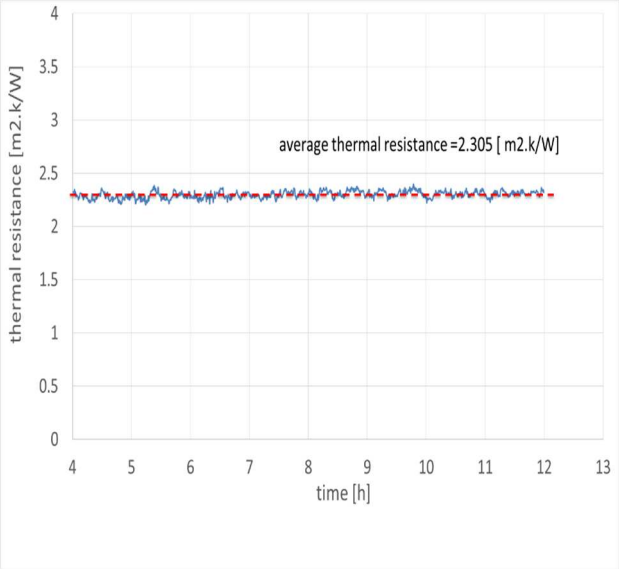

Figure 5-24: Thermal resistance ($m^2K.W^{-1}$*) during the second period (ASTM)*

5-4-2 Thermal resistance of glass wool

Once, the procedure has been validated, we want to determine thermal resistance of the glass wool and study the influence of temperature and humidity. We possess panels of glass wool of 125x60 cm with 10 cm thickness. Considering that frame metal of the equipment THERMO-3R is 120x120 cm, we decide to associate two panels side by side (figure 5-25). Density of glass wool is (68 $kg.m^{-3}$) and porosity (96%).

The wall is placed between the hot cell and the cold cell in THERMO-3R. The data logger kind YOKOQAWA (mV 100) is used to evaluate the temperature for the two sides of the wall (figure 5-26).

The flowmeter has been placed at the center of the surface of the wall in the hot side with sensibility 273 µV/ (w/m²) to evaluate the rate of flow during the test (figure 5-27).

Figure 5-25: manufacturing glass wool wall and fixing it on the frame.

Figure 5-26: the wall between two cells.

Figure 5-27: flowmeter to evaluate the flux rate.

5-4-2-1 Experimental results

The cold cell temperature is regulated at 5 °C and hot cell temperature is fixed to obtain an average temperature between these two cells of 10 °C, 15 °C, 20 °C and 25 °C. We observe that temperature has an effect on the thermal resistance. As soon as temperature increases, thermal resistance decreases (figure 5-28) or thermal conductivity increases (figure 5-29).

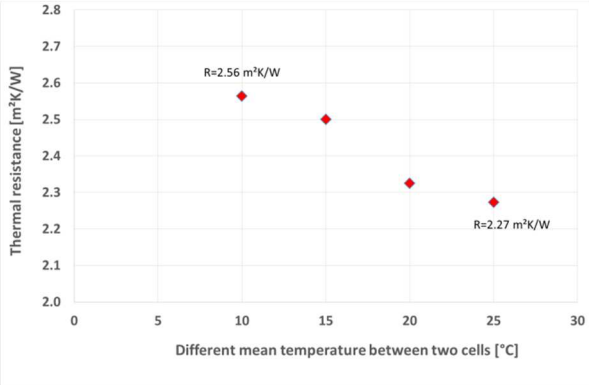

Figure 5-28: Thermal resistance against temperature

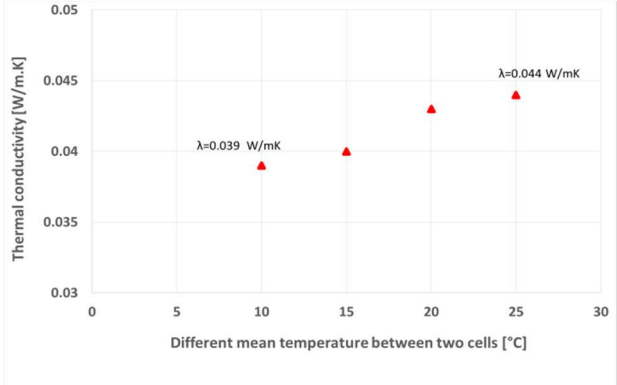

Figure 5-29: Thermal conductivity against temperature

5-4-2-2 Validation with experimental results from other techniques

Thermal resistance and thermal conductivity has been determined by various techniques such as guarded hot plate method (steady state) and hot disk method (transient state). As mentioned earlier in chapter three the steady-state technique (guarded hot plate method) is suitable for insulation materials although its drawbacks (long time to establish a steady-state

temperature gradient across the sample, temperature gradient and Sample size are required to be large and contact resistance between the thermocouple and the sample surface). According to ISO 8302, guarded hot plate (TPL 500X1) has been used to validate thermal conductivity of glass wool under steady state condition, typically with accuracy ± 1% (max. ± 3%, according ISO 8302). Thermal conductivity for homogeneous sample is calculated during passage the rate of flux through unit area for each temperature gradient perpendicular to the isothermal surface of the sample. Hot disk method (TPS 2500, ISO 22007-2) with accuracy 5% for thermal conductivity is distinguished mainly by the short time and by the low flow in comparison with steady state techniques.

We can notice that in the case of guarded hot plate (GHP) and guarded hot box (GHB), thermal resistance is determined after reaching steady state. Moreover, these techniques need the establishment of gradient of temperature between the two sides of the specimen and the temperature correspond to the mean value calculate from these two temperatures. We can consider that GHP and GHB determine global resistance of the specimen. Hot Disc (HD) is transient technique. Specimens have been placed inside an oven and temperature is constant HD determine local resistance of the specimen. When material is heterogeneous, difference in results can come from this fact. It is necessary to define a representative elementary volume (ERV) of the material. Taking into account accuracies of techniques, experimental results are consistent (figure 5-30). It is very important to observe that local result with HD is consistent with global values with GHP and GHB. Dimension of the HD probe can be considered sufficiently large with respect to the ERV.

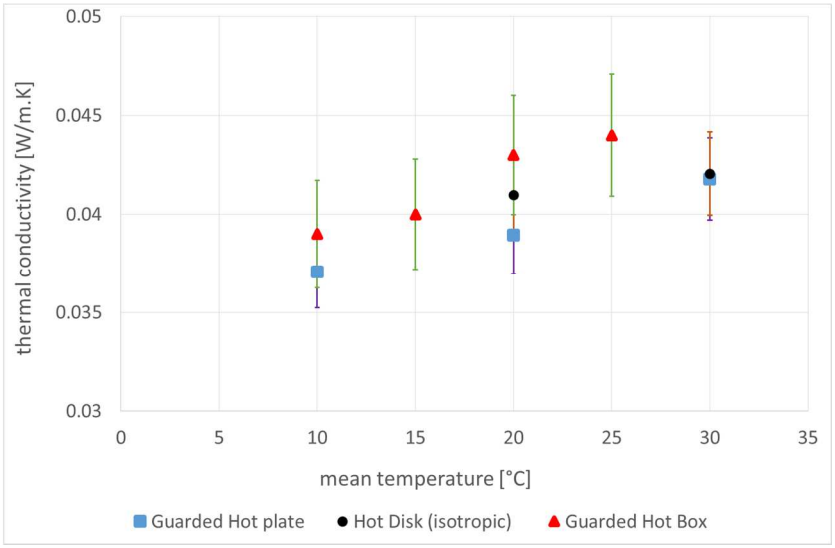

Figure 5-30: variation of thermal conductivity with the temperature for different methods

5-4-3 Effect of humidity

The presence of moisture in the insulation materials of building envelope reduces efficiency of these materials and impacts thermal performance. Despite the evolution of construction quality, moisture problems still pose the biggest challenge due to increases the risk of interstitial condensation inside insulation materials. The effect of humidity on the thermal properties of insulation materials (glass wool) has been investigated by using guarded hot box (GHB).

The wall contains two panels (figure 5-31) of crimped glass wool of 10 cm thickness with density (68 kg/m3) and porosity (96%) has been fixed in frame of GHB (figure 5-33).

Figure 5-31: crimp wall

Figure 5-32: fixing flowmeter

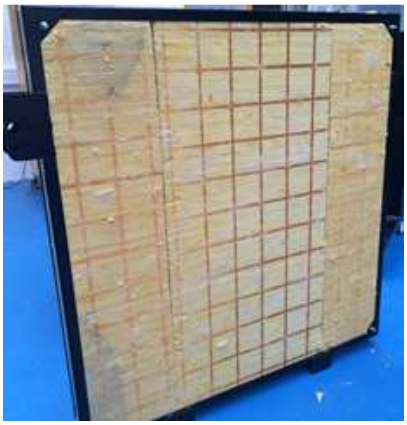

Figure 5-33: in frame (THERMO 3R)

Hot cell of the GHB is regulated at 30°C and cold cell at 20°C. Humidity of the two cells are identical in order to avoid mass transfer between them and thus complicating the problem. Humidity is regulated at 50%, 75% and 95%. Two flowmeters has been placed in the hot and in the cold surface of the specimen with sensitivity 250 µV/ (w/m²) and 264 µV/ (w/m²) respectively and accuracy 0.1 °C (figure 5-32). We want to obtain humidity value less than 50%. But for many reasons, it is difficult to get this relative humidity in the laboratory. It is possible for HD because this technique has been installed inside a climatic chamber and the measure is just obtained on a sample of small dimension. Sorption curve shows that humidity less than 40% has no effect on water content (see chapter 3, paragraph 3-3-4).

Guarded hot plate techniques can't be used for this study to determine thermal conductivity. Only HD and GHB techniques have been used. Consistent values have been obtained by these techniques (figure 5-34). We can note that thermal conductivity values by HD technique don't change significantly for humidity less than 50% respecting previous remark from sorption curve.

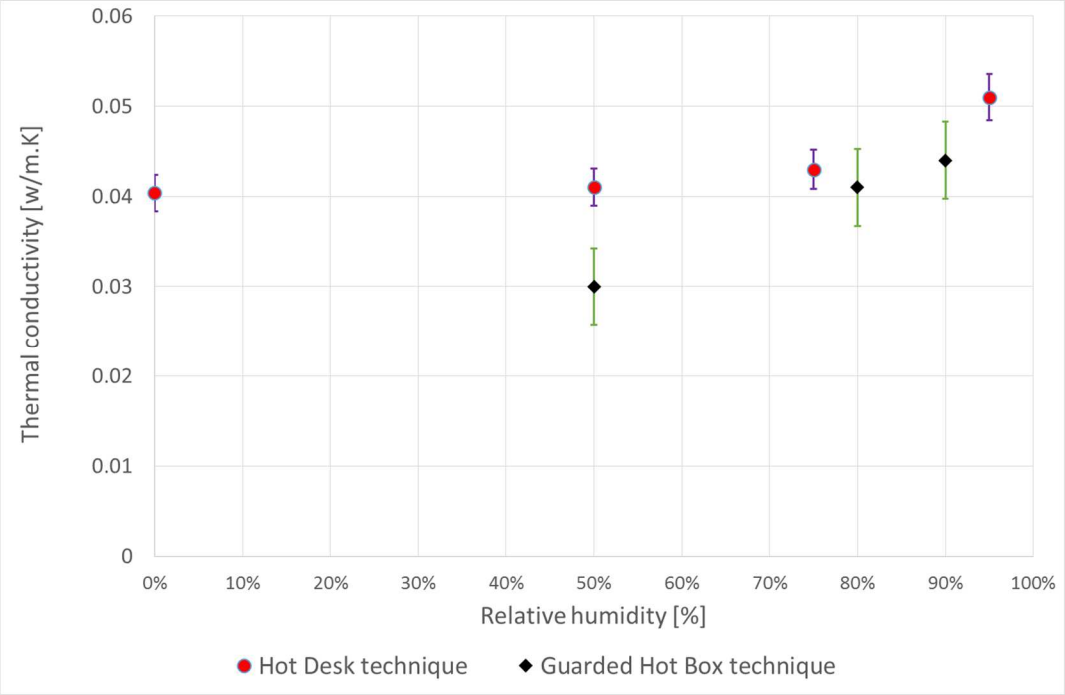

Figure 5-34: variation of thermal conductivity with humidity

5-5 Thermal capacity of the glass wool by flowmeter method

The specific heat capacity can be determined by using the expression:

$$C_p = \frac{\int_0^t (f_{hot} - f_{cold})dt}{\rho.d.\Delta T} \quad (5\text{-}7)$$

Where:

C_p: Specific heat capacity (J/kg.K),
f_{hot}: Hot surface flow (W/m²),
f_{cold}: Cold surface flow (W/m²),
ρ: Density (kg/m3),
d: Thickness of the wall (m),
ΔT: Different temperature between two surfaces (K).

The “difficulty” of the method is to determine the integral part of the equation 5-7. The originality of the method concerns the method to calculate this integral [2]. This integral is obtained by calculating the flow on the hot surface minus the flow on the cold surface. This calculation corresponds to the hatched zones of the figure 5-35.

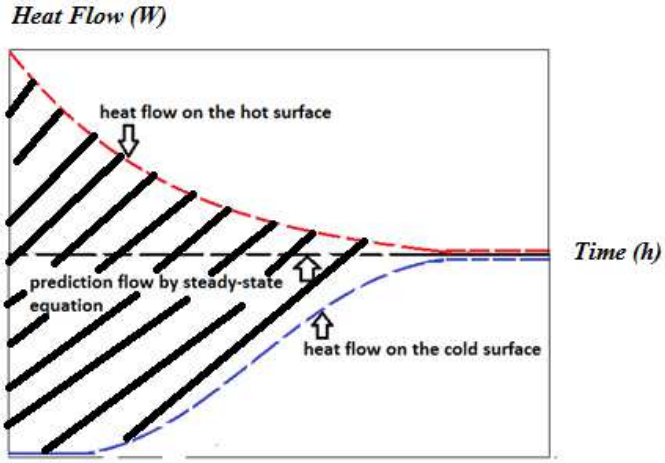

Figure 5-35: Example of heat flow to explain the principles of flowmeter method

So, in a first we will present validated results of flowmeter method with the results that have been obtained with Hot Disc. Second, study effect of gradient of temperature for glass wool and effect of the cold group on the results of thermal capacity.

5-5-1 Validation of the method

We have used the same wall as presented before in figure 5-31 in guarded hot box (THERMO 3R). One flowmeter has been fixed in each side (hot side and cold side surfaces) of the wall. The sensitively of the hot surface flowmeter and cold surface flowmeter is respectively 250 µV/ (W/m²) and 264 µV/ (W/m²) with accuracy 0.1 °C. Regulated temperatures are respectively in the hot cell 30°C and in the cold cell 20°C. We observe that steady state is obtained after 4 hours and the flow at equilibrium is equal to 1.52 W/m² (figure 5-36).

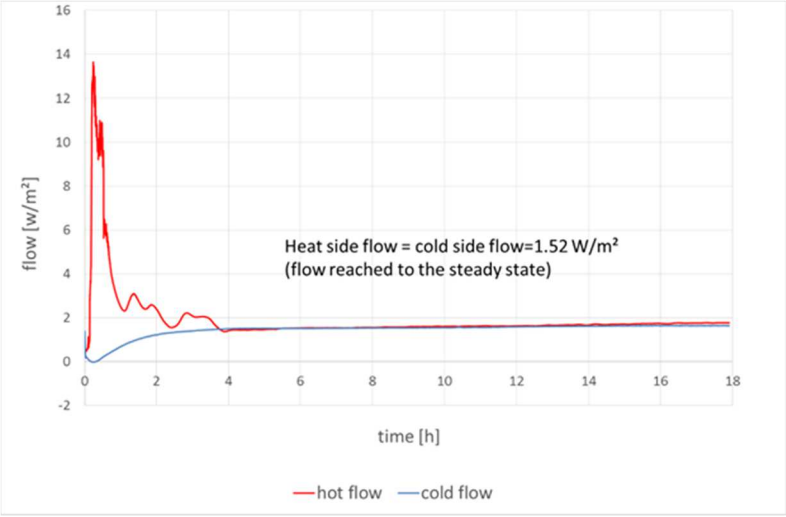

Figure 5-36: Heat flow for glass wool to validate flowmeter method

To validate the flowmeter method, we have compared results from this method and those with Hot Disc technique .Knowing the density and the thermal conductivity of the material we have deduced he thermal capacity. Table 5-3 illustrate the results of GHB consistent with the results of HD

Temperature [°C]		Mean value [°C]	Thermal capacity [J/kg.K] by GHB	Thermal capacity [J/kg.K] by HD
Hot cell	Cold cell			
30	20	25	615	485
40	20	30	790	700
50	20	35	940	1020

Table 5-3: Compare the results of GHB with HD

5-5-2 Effect of temperature

Cold cell temperature is fixing to 20°C. But we change the temperature of the hot cell at 30 °C, 40°C and 50°C to study its influence. We can observe that flowmeter placed on the specimen surface in contact with hot cell measure important variation of flow for 50°C. As cold group is OFF, these variations can only come from power supplied by electrical resistance in hot cell. To obtain 50°C in the hot cell and maintain the temperature gradient with cold cell there is a need of power supply.

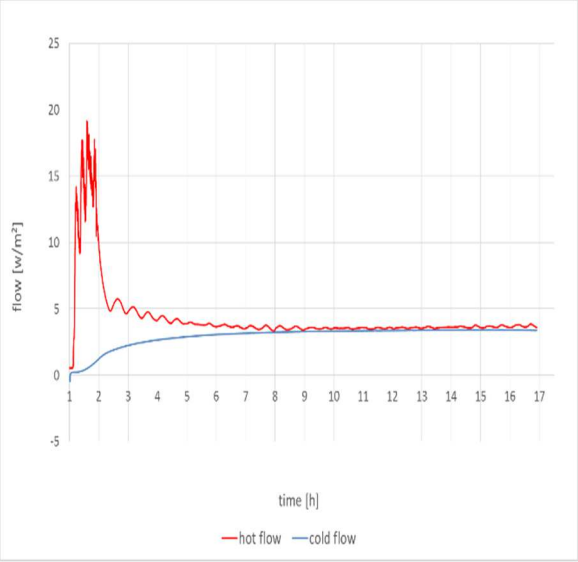

Figure 5-37: flux with time when the hot cell temperature 40°C

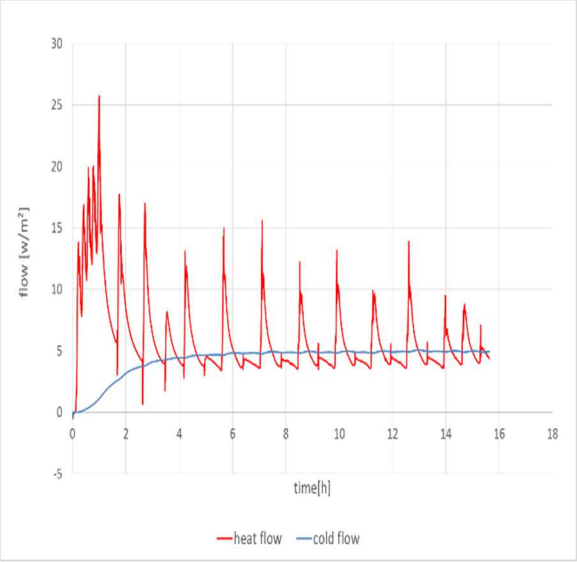

Figure 5-38: flux with time when the hot cell temperature 50°C

Thermal capacity is influenced by temperature. We observe (table 5-3) that thermal capacity increased with temperature. Another interesting point is the time to establish the steady state. We observe in figure 5-39 that this time increased with temperature. This time can be determined by extracting from graph (experimental procedure in figures 5-37 and 5-38). This time is obtained when the flow from the flowmeter placed on the hot side is the same than those on the cold side.

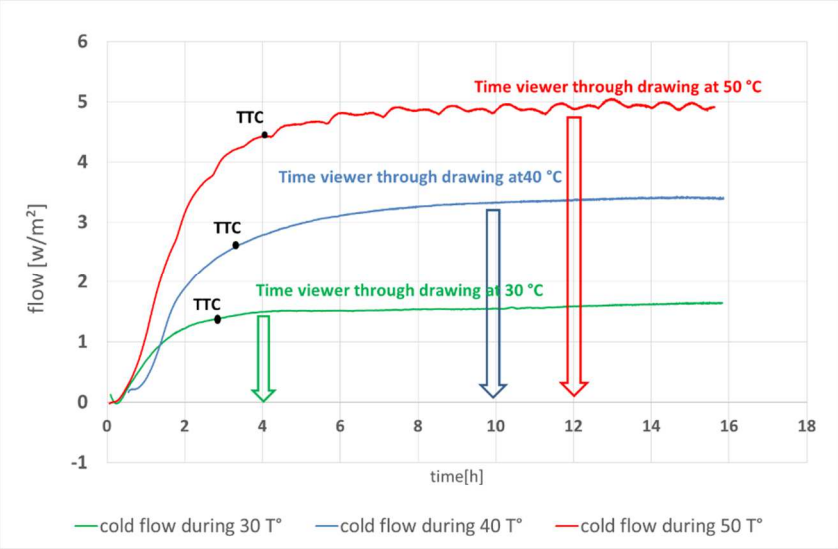

Figure 5-39: Cold flow for different temperatures of the hot cell (30, 40 and 50°C)

5-5-3 Effect of thermal time constant

A mention previously in chapter 2 (section 2-2-4), thermal time constant (TTC=τ) is a time, it takes heat to propagate through the wall. To determine time to reach the steady state, it is possible to consider 5τ according to the figure 2-5. Thermal time constant (TTC) has been obtained from equation 2-11 for different temperature by the sum of the cumulative heat capacity multiplied by the thermal resistance of each layer. The experimental time to establish steady state is obtained from figure 5-39 by visual analysis. Theoretically, lumped system approximation suggests to determine this time by considering equal to 5τ. But this approximation is applicable if $B_i \leq 0.1$ and we obtained high Biot number ($B_i > 13$) as shown in table 5-4. So the lumped system can't be used in our case. This explains that experimental and theoretical times to the steady state are not consistent. We don't find method to establish steady state time theoretically.

Gradient of temperature [°C]	Experimental time to establish steady state [h]	TTC [h] from equation 2-11	5τ [h]	Biot number (B_i) [-]
10	4	2.98	14.9	13.2
20	10	3.48	17.4	13.4
30	12	4.03	20.15	13.5

Table 5-4: Compare between TTC and experimental steady state time with different temperature

5-5-4 Effect of the Cold group

As mention previously in section (5-3-2-2) group cold ON, when steady state is reached, Flowmeters F_1 and F_2 measure the effect of power supply by the electrical resistance in the hot box (Q_{in}) and also the power supply by cold group (Q_c) as explain in equation (5-5).

The effect of the power supply by cold group must take into account. The experimental test has been done for different case (cold group OFF and cold group ON) with different temperature. The experimental test has been done for ordinary glass wool (76 kg/m3) with dimension (120 ×120) cm with thickness 5 cm (two layer each one thickness 2.5 cm) as shown in figure (5-40). Two flowmeters have been fixed in two sides (hot side and cold side) (figure 5-41) to measure the flow rate during the test. The sensitivity of the hot surface flowmeter and cold surface flowmeter was 250 μV/ (w/m²) and 264 μV/ (w/m²) respectively with accuracy 0.1 °C. The sample fixing in the frame of the guarded hot box (THERMO 3R) (figure 5-42). The test has been done for different temperature in the hot side of the THERMO 3R equipment (30 °C, 40°C and 50°C) and fixing the cold side temperature with (20°C).

Figure 5-40: layers of the glass wool sample

Figure 5-41: fixing flowmeter

Figure 5-42: layers in frame of the guarded hot box

Table 5-5 illustrate the results of the thermal capacity for the glass wool with different temperature for two cases.

T_h	T_c	Δ T [°C]	Thermal capacity [J/kg.K] (cold OFF)	Thermal capacity [J/kg.K] (cold ON)	Percentage of deviation [%]
30	20	10	600	550	8.33
40	20	20	700	675	3.57
50	20	30	830	760	3.14

Table 5-5: thermal capacity during cold group OFF and Cold group ON

Table 5-6 illustrates the results of the heat flux for two cases (cold group OFF and cold group ON). During cold group OFF, as mentioned previously in section (4-3-2-1) group cold OFF the flux $Q_{in}=Q_{ts}=F1=F2$. But when the cold group ON, our observation that the flux has been risen due to effect of the Q_c. during cold group ON, the flux coming from cold cell tend to rising the electrical power Q_{in} in hot cell.

T_h	T_c	Δ T [°C]	Flow (Q_{in}) [W] (cold OFF)	Flow (Q_{in}) [W] (cold ON)	Percentage of increasing of flux Q_{in} [%]
30	20	10	1.35	2.65	49 %
40	20	20	2.90	7.30	60 %
50	20	30	4.80	10.50	54 %

Table 5-6: variation of the flux during cold group OFF and Cold group ON

We can conclude that the effect of the cold group on the variation of the flux more than its impact on the value of thermal capacity.

5-6 Time lag and decrement factor

5-6-1 Definition of these parameters

During heat transfer through the wall (figure 5-43), the time for the heat wave to go from the hot surface to the cold surface of the specimen is called ‘‘time lag’’. The decreasing ratio of its capacity during transfer process is called ‘‘decrement factor’’ [4]. These factors are very important to define the heat storage capabilities of wall materials [5].

The time lag is calculated by using the equation (5-9) [7]:

$$t_{lag} = t_{T-hot(\max)} - t_{T-cold(\max)} \quad (5\text{-}9)$$

Where:

$t_{T-hot(\max)}$: The time that the hot surface temperature is being maximum.

$t_{T-cold(\max)}$: The time that the cold surface temperature is being maximum.

Decrement factor is calculated by using the equation (5-10) [7]:

$$D_f = \frac{A_h}{A_c} = \frac{T_{hot(\max)} - T_{hot(\min)}}{T_{cold(\max)} - T_{cold(\min)}} \quad (5\text{-}10)$$

Where:

$T_{hot(\min)}$: Minimum hot surface temperature.

$T_{cold(\min)}$: Minimum cold surface temperature

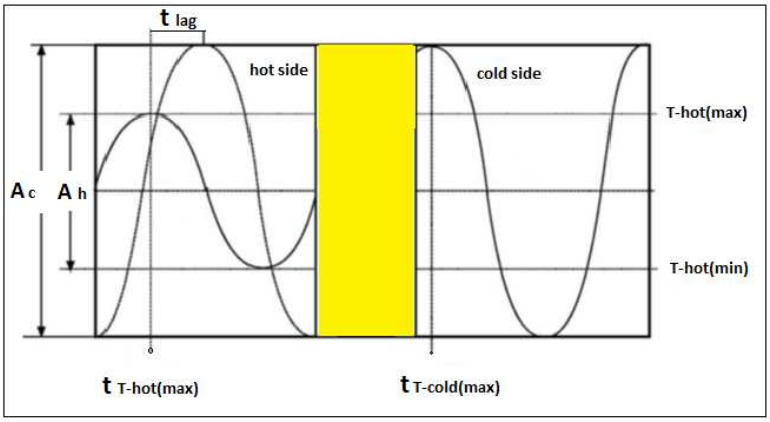

Figure 5-43: Representation of time delay and dimensionless factor [6].

Time lag does not impact on energy use directly but its impacts on the time of energy use, while decrement factor directly impacts on energy use. In general insulation materials have high time lag and low decrement factor compare with other building materials.

5-6-2 Experimental values

To study the effect of the thickness of the specimen on the time lag and the decrement factor, we have considered following thickness: 5 cm (2 panels), 7.5 cm (3 panels) and 10 cm (4 panels). The test has been done with variation of the flow (2 W for maximum flow and 0 W for minimum flow) and fixing the cold temperature in cold cell of the guarded hot box with (T_{cold}= -5 °C) inside. We change the thickness of the sample in each test to obtain different thickness with the same condition (figure 5-44).

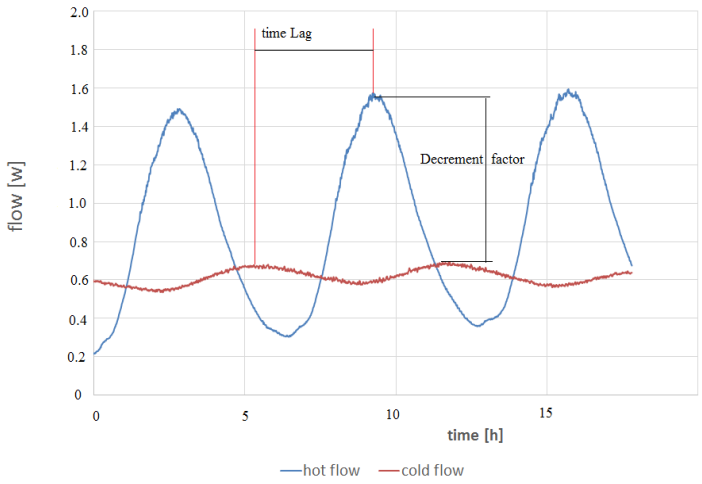

Figure 5-44: Time lag and decrement factor for thickness 5 cm.

We observe that time lag and decrement factors are sensible to the thickness (figures 5-45 and 5-46).

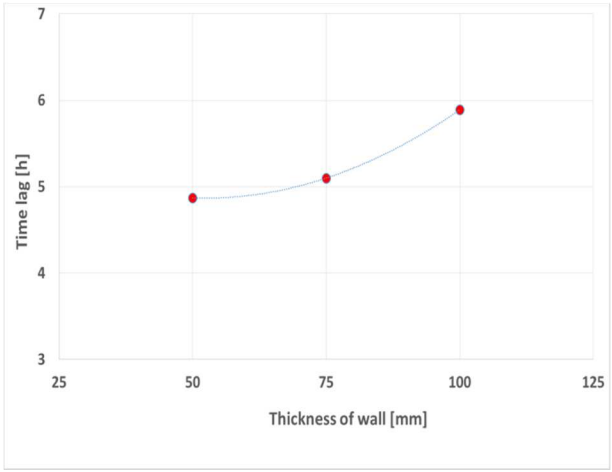

Figure 5-45: Time lag against thickness

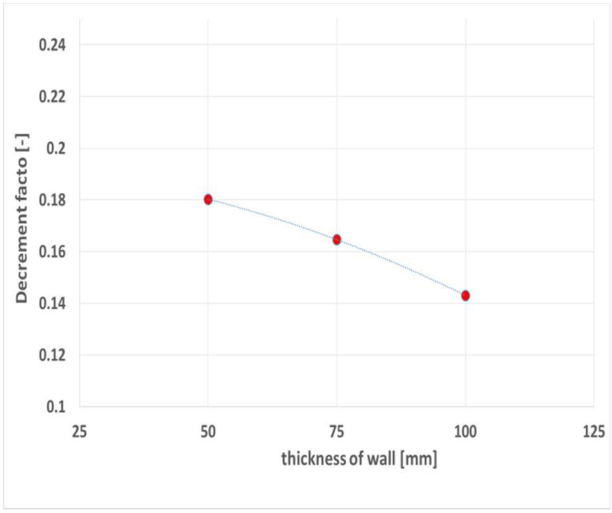

Figure 5-46: Decrement factor against thickness

We have synthetized experimental results in table 5-7 for the 3 thickness. We have also compared our results for glass wool with those Ozel [9] on insulation materials (glass wool) these results are in agreement for time lag and decrement factor.

Thickness [cm]	Experimental results		Ozel results [9]	
	Time lag [h]	Decrement factor [-]	Time lag [h]	Decrement factor [-]
5	4.8	0.18	5.1	0.20
7.5	5.1	0.17	5.5	0.15
10	5.9	0.14	6.4	0.10

Table 5-7: variation of the time lag and decrement factor with thickness

5-7 WUFI simulation

The influence of the humidity on the composition of walls materials can be investigated by guarded hot box. The most important thermal properties for insulation materials is thermal conductivity and thermal capacity which are function of the humidity. Increasing the moisture inside insulation materials tends to esthetical degradation of the finishing and mold growth besides to the damage these materials thus reducing the basic functions. Assessments of hygrothermal results can be done by using by dew point assessment (Glaser Method) according to the standard: IS EN 13788 (2002) or by hygrothermal numerical simulation according to the standard: IS EN 15026 (2007).

Glaser method is used during steady state conditions and does not takes into account hygroscopic sorption and liquid transport besides moisture in construction, precipitation and rising damp.

The modern simulation numerical models such as WUFI [Kunzel 1995] [10] is used to overcome limitation of Glaser method. WUFI can be used for assessing risk of (interstitial condensation, driving rain moisture, mould growth, freeze-thaw) and provide good solution to moisture transport and assessment problems for buildings. It establishes temperature and moisture profiles through the building wall. WUFI provides a substantial database of materials and properties for the designer and climatic data relative to different cities in the world.

We will study the interest of using WUFI to complete the objectives of this thesis. Firstly, we will analyse the database of WUFI. Then we will validate results of WUFI with experimental results obtained by Guarded Hot Box. Finally, we explain interest of using WUFI simulation for this study.

5-7-1 Database in WUFI

WUFI takes into account enthalpy during moisture movement, short-wave solar radiation and long-wave night radiation. Convection heat transport by air flows has been neglected in simulation of WUFI. The vapour diffusion transport mechanisms included in WUFI but also the convection vapour transport by air flows has been ignored. The liquid transport mechanisms include capillary conduction and surface diffusion.

The couple transport for heat and moisture requires defined well the material parameters. WUFI needs some data to calculate the quantities. Data of usual materials are present in database.

It is also possible to insert new materials for specific materials. We have inserted some properties of glass wool L1 measured in the chapter 2 (paragraph 3-3-4). These properties included:

5-7-1-1General information:

The basic values (list below) for general parameters are inserted (figure 5-47).

Basic Values	
Bulk density [kg/m³]	76
Porosity [m³/m³]	0.97
Specific Heat Capacity, Dry [J/kgK]	615
Thermal Conductivity, Dry ,10°C [W/mK]	0.04
Water Vapour Diffusion Resistance Factor [-]	3.17

Figure 5-47: Basic properties

• Bulk density= 76 [kg/m³].

• Porosity= 0.97 [m³/m³]

• Specific heat capacity of dry material =615 [J/kgK],

• Thermal conductivity of dry material =0.04 [W/mK],

• Water vapour diffusion resistance factor of dry material =3.17 [-]

5-7-1-2 Moisture storage function

The basic data are required as a minimum for each calculation; otherwise, the transport equations, are not fully defined. The hydric properties are necessary to fully describe the hygrothermal situation. The hydric properties such as moisture storage function [kg/m³] have been inserted as a table. These properties have been inserted because data base of WUFI® didn't have the properties of our material as shown in figures 5-48.

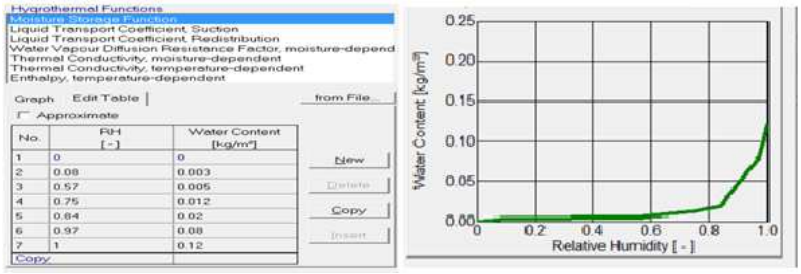

Figure 5-48: Storage moisture database

5-7-1-3 Thermal conductivity

Thermal conductivities against temperature and water content have been inserted also into database of WUFI as shown in figures (5-49 and 5-50). Normalized water content used is the water content divided by the maximum water content (multiplied by 1000kg/m^3, density of water).

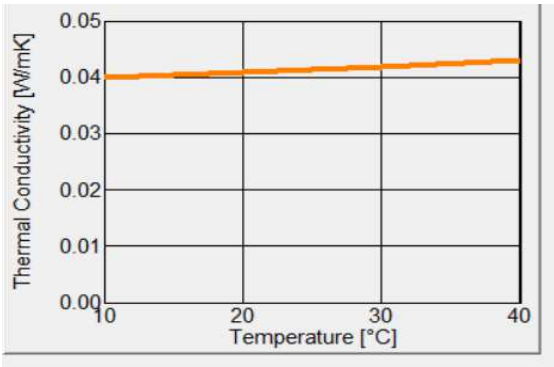

Figure 5-49: Thermal conductivity with temperature

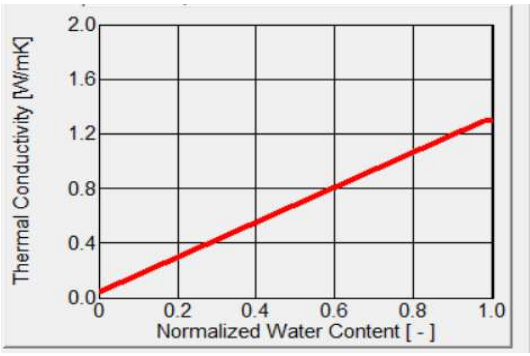

Figure 5-50: Thermal conductivity with water content

We have studied in chapter 4 the possibility of using thermal probe to thermally characterize insulation material in use (or in situ). We want to know if WUFI presents an interest for this type of study. It seems obvious that for a long term (5 years or more) using in a building envelope the insulation must have lost all its shape and insulation ability.

After studying the database of WUFI, we conclude that the assessment of these results with respect to thermal and hygric performance, long-term stability, aging, specific damage risks etc. is still outside the scope of simulation programs.

5-7-2 Validation with experimental test

We want to compare experimental values from Guarded Hot Box (GHB) and simulation results from WUFI. Same conditions of test must be fixed in GHB as in WUFI. Firstly, we wait for obtaining stabilised temperature (20°C) and humidity (60%) in the two cells (figure 5-51). Then, conditions on temperature (5 °C) and humidity (80%) in the cold cell (only) are modified (figure 5-52). In realistic condition, hot cell represents indoor condition and can be stabilized by regulation and cold cell is outdoor condition which changes during time.

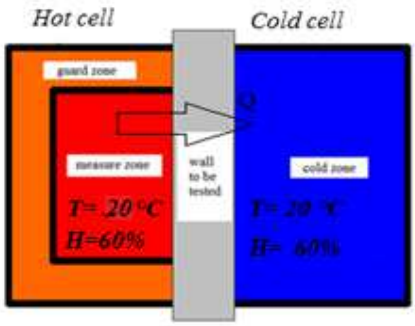

Figure 5-51: Initial conditions

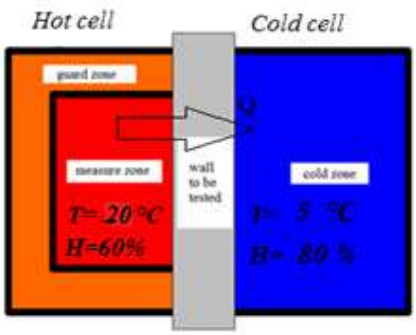

Figure 5-52: Experimental conditions

5-7-2-1 Experimental results

Humidity and temperature sensors values in the hot cell and cold cell give are presented in figure 5-53 and 5-54 respectively. There is a need of 2 hours to reach equilibrium in each cell. We observe important variation of humidity in the cold cell but not in the hot cell.

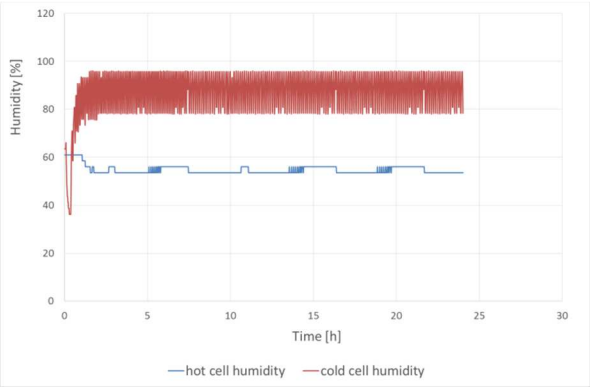

Figure 5-53: Variation of humidity

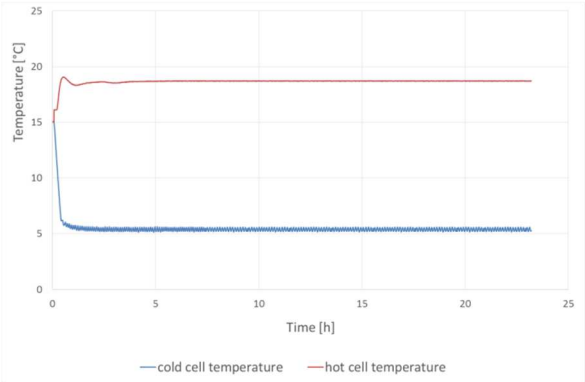

Figure 5-54: Variation of temperature

This observation must be due to the humidifier apparatus and associated regulated system. Principles of cell humidification are not the same. In the hot cell, it is obtained by evaporating the water (figure 5-55) and in the cold cell by ultrasound (figure 5-56). In the ultrasound apparatus, it is possible to change the power supply of vapour emission, that what we must do next time.

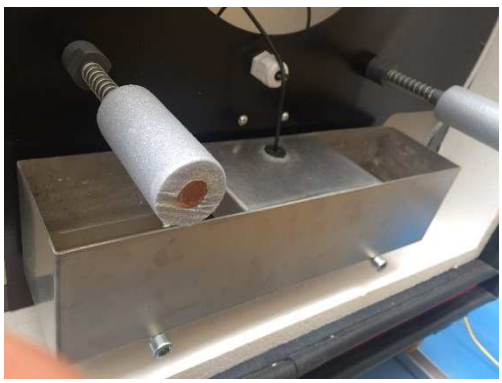

Figure 5-55: Evaporating humidifier (hot cell)

Figure 5-56: Humidifier by ultrasound (cold cell)

5-7-2-2 WUFI results

We have inserted two layers (2.5 cm) of the glass wool (figure 5-57) to compose the wall. Physical characteristics of glass wool have been already described in previous database paragraph. The boundary conditions for the interior and exterior surfaces of the layers included (figure 5-58):

• The initial conditions are 80% relative humidity and 20 °C temperature,

• 90°inclination to represent a wall,

• The orientation and height above ground has been ignored because we use internal wall,

• Time step of 1 h and period of simulation of 24 h.

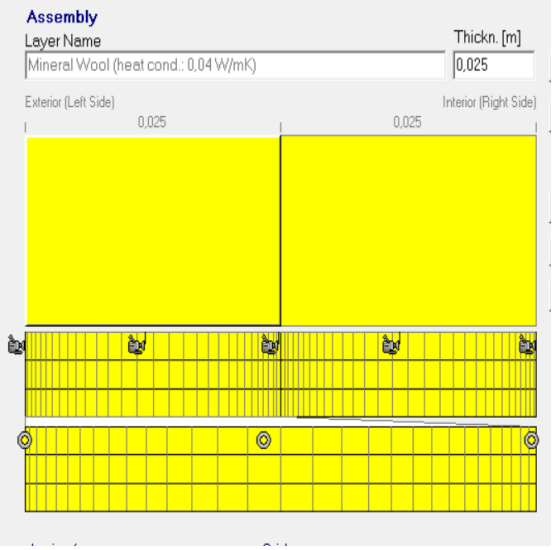

Figure 5-57Insert layers in WUFI view

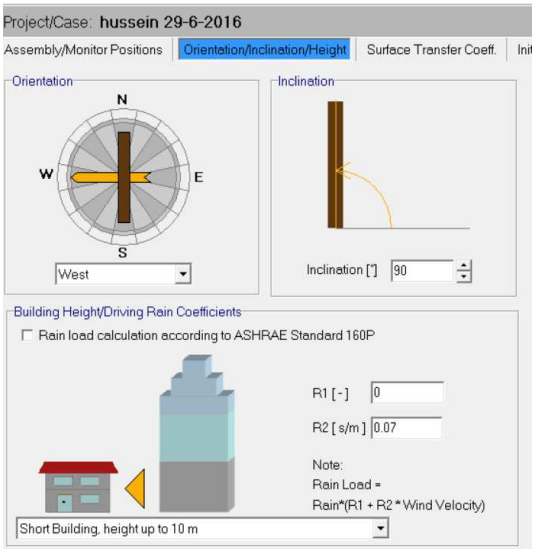

Figure 5-58: : Orientation conditions

Indoor and outdoor conditions have been introduced in order to respect same experimental conditions in hot and cold cell of the GHB (figures 5-59 and 5-60).

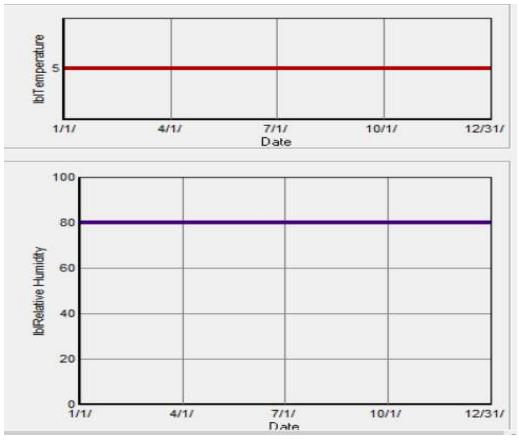

Figure 5-59: Outdoor climate conditions in WUFI

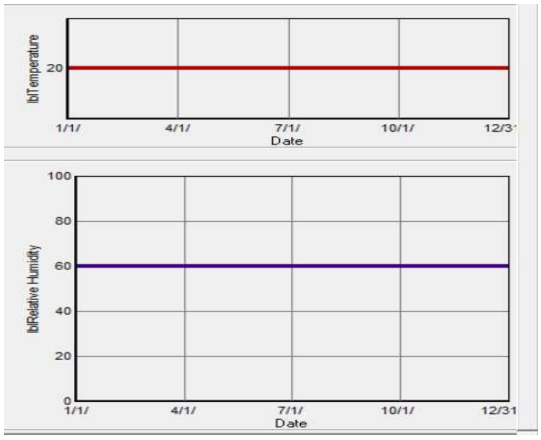

Figure 5-60: Indoor climate conditions in WUFI

5-7-2-3 Comparison between experimental and WUFI simulation results

Comparison between the experimental and simulation results have been done. (Figures 5-61) between internal (WUFI) and hot cell (experimental) and (figure 5-62) between external

(WUFI) and cold cell (experimental). We observe results are closed. Difference can be due to the experimental regulation of humidity and the effect of temperature gradient.

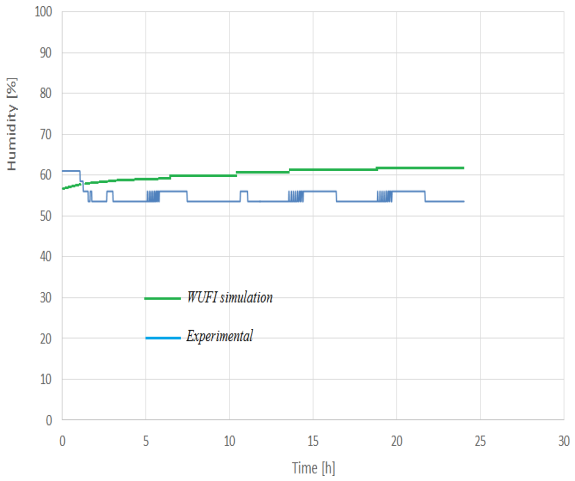

Figure 5-61: Internal (WUFI) and hot cell (experimental) humidity

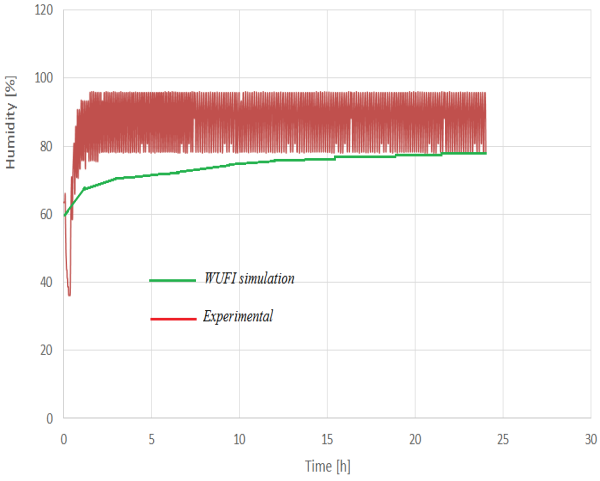

Figure 5-62: External (WUFI) and cold cell (experimental) humidity

5-7-3 Interest of using WUFI simulation for the study

WUFI is interesting to study the heat and moisture transfer inside construction elements with realistic solicitation in temperature and humidity. Our objective is to evaluate the possibilities of using WUFI to improve the experimental work of this thesis.

Firstly, we have observed, in the database paragraph, that thermal and hydric performance for long-term stability, aging, specific damage risk is still outside the scope of simulation program. So the use of thermal probe in situ (or in use) can't be directly compared with WUFI.

Then, validation procedure by comparison experimental and WUFI simulation results have identified the lack of performance of the regulation of humidity in cold cell of the GHB. There is a need of more experimental values. So, further we must introduce temperature and humidity inside the wall at different thickness to establish a profile.

Finally, realistic climatic conditions can be introduced in WUFI simulation for external temperature and humidity values. Moreover, long time study (many years) can be done. Even if long-term performance of thermal characteristics is not taking into account by the software, WUFI can be used to check temperature and humidity profiles inside the wall during time study.

5-8 Conclusion of the chapter

Guarded hot box (GHB) THERMO 3R has been used to determine thermal properties for insulation materials (glass wool). This equipment is suitable for measuring thermal properties for vertical walls and can be considered as an interesting help to create realistic climatic conditions. Two sides of guarded hot box (GHB) THERMO 3R have been calibrated by using multilayer wall (plaster + insulate + plaster). Hot side cell has been calibrated to measure the losses that occur through the specimen and through the wall of the measure zone while cold side has been calibrated to measure the losses through the walls of cold side to the outside. The calibration has been done according to the ASTM recommendations (Standard Test Method for Steady-Stat~ Thermal Performance of Building Assemblies) Designation: C 236 - 89 (Reapproved 1995). The results of thermal properties of glass wool materials (thermal resistance and thermal conductivity) that have been obtained by guarded hot box (GHB) THERMO 3R is close to the results obtained by guarded hot plat and hot disk.

The results of the thermal capacity for glass wool have been obtained by using flowmeter method with different conditions. These thermal properties have been compared also with Hot Disc results. Time delay and damping have been also determined to characterize thermal storage capacity of glass wool wall.

To study phenomena of heat and mass transfer, WUFI (simulated) have been investigated to compare the experimental results for glass wool. Due to the importance of assessing the age of insulating material, WUFI (simulated) during the long time have been done for glass wool. The database base of WUFI does not mention to change thermal properties of materials during aging of materials, so not important use WUFI in the meantime, but may be for future some simulation improved to focus on this point.

In general guarded hot box (GHB) THERMO 3R is considered feasible equipment to evaluate thermal properties of insulation materials.

References of chapter five

[1]: Standard Test Method for Steady-Stat thermal Performance of Building Assemblies by Means of a Guarded Hot Box 1, Designation: C 236 - 89 (Reapproved 1995).

[2]: M. Rahim, O. Douzane, A.D. Tran Le, T. Langlet, Effect of moisture and temperature on thermal properties of three bio-based materials, Construction and Building Materials 111, 119–127(2016).

[3] : K. W. Childs, G. E. Courville and E. L. Bales "THERMAL MASS ASSESSMENT", Oak Ridge National Laboratory, September 1983.

[4]: Duffin RJ. A passive wall design to minimize building temperature swings. Solar Energy; 33(3/4):337–42, 1984.

[5]: Asan H, Sancaktar YS. Effects of Walls' thermophysical properties on time lag and decrement factor. Energy and Buildings; 28:159–66, 1998.

[6]: Önder, K., R. Yumrutas., & O Arpa. (2009). Theoretical and Experimental Investigation of Total Equivalent Temperature Difference Values for Building Walls and Flat Roofs in Turkey. Applied Energy, 86, 737–747.

[7]: OzelM., Pihtili K., Optimum location and distribution of insulation layers on building walls with various orientations, *Building and Environment*, Vol. 42, pp. 3051-3059, 2007.

[8]: Asan H., Numerical computation of time lags and decrement factors for different building materials, *Energy and Buildings*, Vol. 41, pp. 615-620, 2006.

[9]: Ozel M., Pihtili K., Investigation of the effect on time lag and decrement factor of insulation thickness on the walls of various orientation (in Turkish), *Firat University Journal of science and engineering*, Vol. 17, pp. 287-298, 2005.

[10]: Künzel, H.M., Simultaneous Heat and Moisture Transport in Building Components: One- and twodimensional calculation using simple parameters, Fraunhofer-Informationszentrum Raum und Bau. IRB Verlag. Stuttgart, (1995).

Chapter 6: Conclusions, remarks and recommendations for future research

6-1 Overview

In this thesis, different successful experimental tests were reported and interpreted, to determine thermal conductivity of insulation materials by using (transient method) cylindrical probe technique. All experimental tests were implemented using Non-Steady-State Probe for Thermal Conductivity Measurement (Hukseflux® TP02) Needle length 150 mm and diameter 1.5 mm. Other techniques have been used to evaluate the experimental results, steady state method (guarded hot plate technique) and transient method (hot disk technique).
To assess heat transfer through the wall and to study thermal characteristics of building insulation materials, guarded hot box has been used with different conditions.

6-2 Assessment of cylindrical probe technique.

Applying long time approximation relation to determine thermal conductivity by using probe technique requires that the experimental kinetic representing the temperature against logarithm of time is linear. Experimental kinetic is linear for glycerol (a fluid) but as soon as the porosity of studied material is growing, S-shaped curve appears. Due to the porosity, a sigmoid curve is obtained for insulation materials and the method becomes debatable. We conclude traditional methodology can’t be used for insulation materials.

Analytical simulation with development of a program Matlab has allowed simultaneously determining thermal conductivity and thermal diffusivity. Consistent results have been obtained.

Decreasing heat power reduces non-linear variation and provides thermal conductivity values with a good accuracy compared to reference values. During use Comsol Multiphysics®, we observe that reduction heat flux less than (<0.1 $W.m^{-1}$) provides a good accuracy for thermal conductivity and less than (<0.07 $W.m^{-1}$) makes temperature increase less than 1°C. These conditions cannot be achieved with the control interface associated to Hukseflux TP02.

Comsol Multiphysics® has been used to study the influence of parameters that are not accessible experimentally such as the components of the probe, the contact resistance and the thermal properties of materials. Although the slight difference in the variation of temperature with the logarithm time for glass wool materials between experimental and Comsol curve, the simulation approach has been considered validated.

The length to diameter (L/2Rs) ratio of the probe is an important value to reduce axial heat flux along the probe and consequently error in thermal conductivity determination. We noticed that decreasing the value of (L/2Rs) less than 100 give us unreal value for thermal conductivity. We conclude that using copper metal in outer face of the probe reduce S-shaped form and increase temperature at the outer surface of the probe. We observe that the outer surface of the metal more influential than the hot wire metal.

We note also the variation of the temperature increases with lowest thermal conductivity and it is less clear for thermal capacity because long time approximation equation does not refer to the specific heat.

According to these conclusions, we recommend to use a copper metal for outer surface of probe instead steel as the actual design of the TP02 probes. The dimensions of the probe must respect the ratio (L/2Rs) equal to 100 and its length not less than 150mm. The hot wire of the probe made from constantan and the base from glass pearl to prevent heat loses through the base. The control interface associated with the probe should be supplied power less than (<0.1 $W.m^{-1}$).

6-3 Assessment of guarded hot box technique during the heat flux through the wall

To measure thermal properties (thermal resistance, thermal conductivity and thermal capacity) for insulation materials especially in the vertical wall, guarded hot box THERMO 3R has been used. Different effects have been studied, ambient temperature, differences the temperature between two cells (hot and cold), time lag and decrement factor and humidity. The results was closed to the results of the references and results obtained by other method. Guarded hot box (GHB) THERMO 3R is representing suitable to measure thermal properties for vertical walls and can be considered as an interesting help to create realistic climatic conditions.

Two sides of guarded hot box (GHB) THERMO 3R have been calibrated by using multilayer wall. Hot side cell has been calibrated to measure the losses that occur through the specimen and through the wall of the measure zone while cold side has been calibrated to measure the losses through the walls of cold side to the out.

Experimental of thermal resistance has been done according to the ASTM recommendations (Standard Test Method for Steady-Stat~ Thermal Performance of Building Assemblies) Designation: C 236 - 89 (Reapproved 1995). The results of thermal properties of glass wool materials (thermal resistance and thermal conductivity) that have been obtained by guarded hot box (GHB) THERMO 3R is close to the results obtained by guarded hot plate (steady state) and hot disk (transient state).

The results of the thermal capacity for glass wool have been obtained by using flowmeter method with different conditions. These thermal properties have been compared also with Hot Disc results. Time delay and damping have been also determined to characterize thermal storage capacity of glass wool wall.

To study phenomena of heat and mass transfer, WUFI® (simulated) have been investigated to compare the experimental results for two sample (multilayer wall and glass wool). The assessing the age of insulating material is importance to evaluate the performance these materials during the life cycle. The database base of WUFI does not mention to change thermal properties of materials during aging of materials, so not important use WUFI in the meantime, but may be for future some simulation improved to focus on this point.

6-4 Recommendations for future research

According to the TP02 probe of Hukseflux® specifications, temperature increase at the outer surface of the probe must be less than 1°C, this condition does not validate during the experimental tests. Temperature variation can be reduced by limiting energy and therefore by decreasing the heat flux. For the future work, to reduce the S- shape of the kinetics and reduce the variation of the temperature, we recommend building new probe that has outer surface from copper not steel as the actual design of the TP02 probes. This probe can feed with low heat power (less than 0.07 W/m) not as actual design of TP02 (minimum power 0.87 W/m) to reduce the S-shape of the curve and to reduce the variation of the temperature less than 1 C°.

As mentioned, the transient method (probe technique) can be used in site to measure thermal conductivity of insulation materials due to its speed to get the results and not to destroy the sample in addition to taking into account the conditions of the site such as moisture.

According to the guarded hot disk THERMO 3R, distilled water that is used in hot cell and cold cell has been evaporated during (three days to five days) according to the ambient weather. in the future work we can find constant source to the distilled water during the experimental tests to carry out long time experimental. Long-time experiments are important to evaluate the results with WUFI® simulation.

Different wall from different buildings materials with various insulation materials can be manufacturing to evaluate heat and mass transfer during different conditions with Guarded hot box THERMO 3R.

Appendix A: ASTM recommendations

Evaluate the temperature according to ASTM

1- First period

Average of hours	Average Hot wall temperature [°C]	Differences between each two hours [°C]	According to ASTM	
Average first hour	27.9775	-0.0740	> 0.06	✗
Average second hour	27.9035	-0.0299	< 0.06	✓
Average third hour	27.8736	0.0089	< 0.06	✓
Average forth hour	27.8825			

Table1: variation of temperature for the first period

2- Second period

Average of hours	Average Hot wall temperature [°C]	Differences between each two hours [°C]	According to ASTM	
Average first hour	27.8876	-0.0003	< 0.06	✓
Average second hour	27.8873	-0.0002	< 0.06	✓
Average third hour	27.8871	-0.0033	< 0.06	✓
Average fourth hour	27.8838	-0.0109	< 0.06	✓
Average fifth hour	27.8728	-0.0287	< 0.06	✓
Average sixth hour	27.8442	-0.0103	< 0.06	✓
Average seventh hour	27.8338	-0.0076	< 0.06	✓
Average eighth hour	27.8263			

Table 2: variation of temperature for the second period

Evaluate the flux according to ASTM

1- First period

Average of hours	Average flux for each hour [W]	Differences between each two hours [%]	According to ASTM	
Average first hour	5.7873	4.2281	> 1%	✗
Average second hour	6.0428	2.8614	> 1%	✗
Average third hour	6.2208	1.2138	> 1%	✗
Average forth hour	6.2973			

Table 3: variation of flux during first period

2- Second period

	Average flux for each hour [W]	Differences between each two hours [%]	According to ASTM	
average first hour	6.2811	-0.3957	< 1%	✓
average second hour	6.2563	-0.1320	< 1%	✓
average third hour	6.2481	-0.4111	< 1%	✓
average fourth hour	6.2225	-0.8318	< 1%	✓
average fifth hour	6.1711	-0.0933	< 1%	✓
average sixth hour	6.1654	0.3381	< 1%	✓
average seventh hour	6.1863	-0.1998	< 1%	✓
average eighth hour	6.1740			

Table 4: variation of flux during second period.

Appendix B : Temperature and humidity sensors

1- Temperature sensors

HW group

Temp-1Wire - Temperature sensor

Digital temperature sensor for indoor and outdoor usage. The sensor is designed for using with the Poseidon, Ares, HWg-STE and other HW group products.

You can have several parallel sensors on one RJ11 sensor port. Each one sensor is identified by a unique serial number.

Temp-1Wire 1m
-10 to +80°C

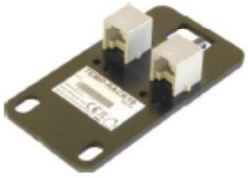

Temp-Rack19
-10 to +80°C

Temp-1Wire 3m
-10 to +80°C

Temp-1Wire-Outdoor 3m
-50 to +125°C

Temp-1Wire-Flat 3m
-30 to +60°C

Technical parameters

- Temp. sensor resolution — 0.1 °C
- Temp. measuring accuracy — **± 0.5** °C in range from -10°C to +85°C; ± 2.0 °C (-50°C to +125°C)
- Communication — 1-Wire bus (Data, GND, +5V) - RJ11
- Operating temperature range — -40°C to +85°C
- **Temp-1Wire Rack19**
  - Probe dimension & cable — 83 x 44 x 18 mm, 2x RJ11, cable 3m included
  - Montage drill — 2x Ø6mm

- **Temp-1Wire-Outdoor 3m**
  - Probe dimension — Ø 5.7mm, 60mm long, stainless steel
  - Cable probe — silicon cable 3m

HW group www.HW-group.com

Sensors & Accessories

HTemp-1Wire 3m

Temp-1Wire 1m

Temp-1Wire-Flat 3m

T-Box

HTemp-1Wire Outdoor 3m

Temp-Rack19

HTemp-1Wire Box2

T-Box

Temperature & Humidity sensors & Accessories	
HTemp-1Wire 3m	*Temperature & Humidity sensor (-30 to +80°C, 0 to 100% RH). 3 meter long cable with 1-Wire connector RJ11, encased in black covering.*
HTemp-1Wire Box2	*Temperature & Humidity sensor (-10 to +80°C, 0 to 100% RH). Boxed sensor designed for internal use, 2x RJ11 daisy-chainable 1-Wire, 3m cable included.*
HTemp-1Wire Rack19	*Temperature & Humidity sensor (-10 to +80°C, 0 to 100% RH). 1U rack mount housing, 2x RJ11 daisy-chainable 1-Wire, 3m cable included. Sensor designed for 19" rack cabinets.*
Humid-1Wire 1m / 3m / 10m	*Humidity sensor (0 to 100% RH) on a 1m / 3m / 10m long cable with 1-Wire connector RJ11, encased in black covering.*
HTemp-1Wire Outdoor 3m	*Temperature & Humidity outdoor sensor (-30 to +85°C, 0 to 100% RH). 3 meter long cable with 1-Wire connector RJ11. Sensor encased in outdoor metal tube.*
T-Box	Hub for connecting 1 to 5 sensors to 1-Wire bus (5x RJ11), 10 cm connecting cable.
T-Box2	Hub for connecting 1 or 2 sensors to 1-Wire sensors (RJ11), 3 m connecting cable.
Temp-1Wire 1m / 3m / 10m	*Temperature sensor (-10°C to +80°C), on a 1 / 3 / 10 meter long cable with 1-Wire connector RJ11, encased in white covering.*
Temp-1Wire-Outdoor 3m	*Temperature outdoor sensor (-50°C to +125°C) - Multi-purpose watertight (IP67) sensor probe, stainless steel 17241 with PVC cable 3m, 1-Wire connector RJ11.*
Temp-1Wire-Flat 3m	*Temperature sensor for freezers (-30 to +60°C), watertight (IP67) stainless steel 17241 probe, flat cable 3m, 1-Wire connector RJ11.*
Temp-Rack19	*Temperature sensor (-10 to +80°C), 1U rack mount housing, 2x RJ11 daisy-chainable 1-Wire, 3m cable included. Sensor designed for 19" rack cabinets.*

Connectors

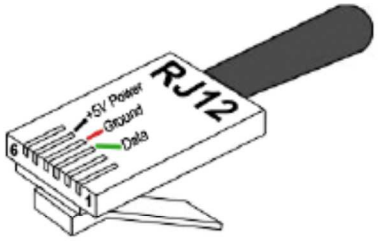

RJ12	RJ11			
3	2	Data	<->	Data 1-Wire
4	3	GND	---	System Ground
5	4	+5V	---	Power supply

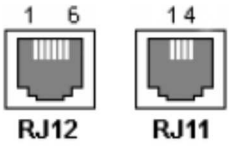

Sensors wiring examples

Star topology – 60m in total:

You can use the T-Box or T-Box2 splitters to connect more sensors to one device active port.

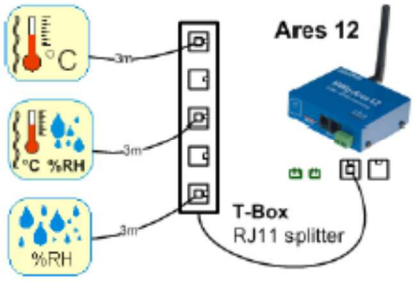

Daisy-chained – 60m in total:

There are two RJ11 female connectors on some sensors.

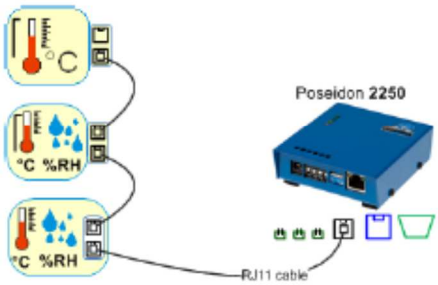

4x active port, 4x60m:

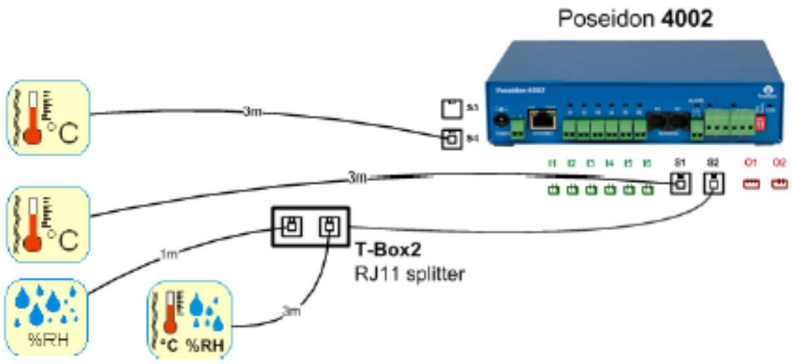

2- humidity sensors

Humid-1Wire

A simple digital humidity sensor, communicating over 1-wire bus (MicroLan). The sensor is designed for using with the Poseidon family products.

You can have several parallel sensors on one bus, each one is identified by a unique serial number. The humidity sensor uses an integrated measuring element with accuracy of ±2% RH.

Connectors

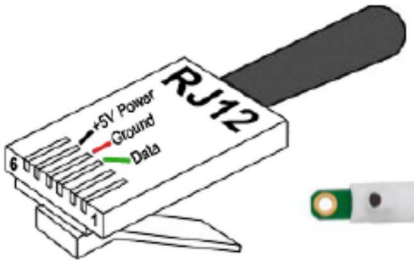

RJ12	RJ11			
3	2	Data	<->	Data 1-Wire
4	3	GND	---	System Ground
5	4	+5V	---	Power supply

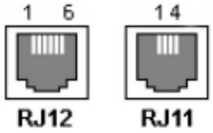

Technical parameters

- **Sensor range** **0-100% RH** (Relative Humidity)

- RH Accuracy ±2% RH, 2-80%RH non-condensing, 25 °C
- RH Linearity & Hysteresis <2% RH typical, ±2% RH span maximum
- RH Repeatability ±0.2% RH
- RH Response Time, 1/e 15 sec in slowly moving air at 25 °C
- Communication 1-Wire bus (Data, GND, +5V) - RJ11 male

- Probe dimension & cable 78 x 9.5 x 6 mm, cable 3m
- Montage drill Ø3mm
- Operating temperature range -40°C to +85°C

Similar sensors	
Humid-1Wire 1m / 3m / 10m	*Humidity sensor for indoor usage, RJ11 connector, 1m / 3m / 10m cable.*
HTemp-1Wire Outdoor 3m	*Temperature & Humidity outdoor sensor, 3m cable RJ11 connector.*
HTemp-1Wire 3m	*Temperature & Humidity sensor, 3m cable RJ11 connector.*
HTemp-1Wire Box2	*Temperature & Humidity sensor, 2x RJ12 female (can be daisy-chained). Boxed version designed for internal usage*
HTemp-1Wire Rack19	*Temperature & Humidity sensor, 2x RJ12 female (can be daisy-chained). Designed for 19" rack cabinets usage.*

Connectors

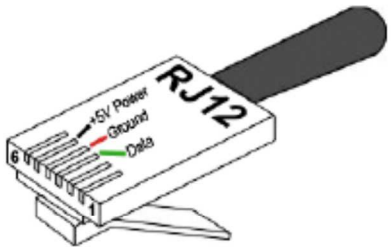

RJ12	RJ11			
3	2	Data	<->	Data 1-Wire
4	3	GND	---	System Ground
5	4	+5V	---	Power supply

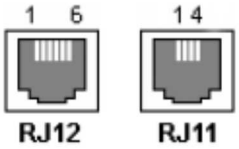

Sensors wiring examples

Star topology – 60m in total:

You can use the T-Box or T-Box2 splitters to connect more sensors to one device active port.

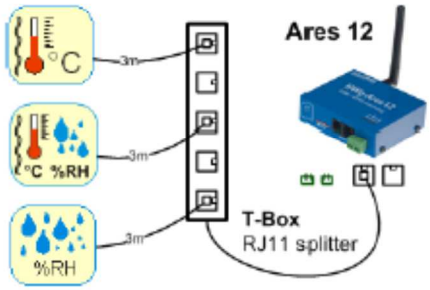

Daisy-chained – 60m in total:

There are two RJ11 female connectors on some sensors.

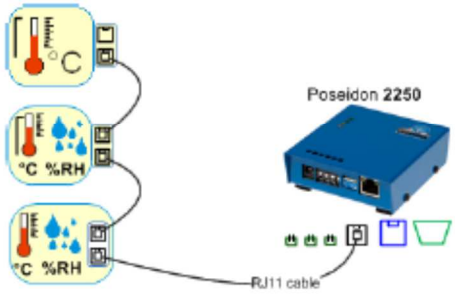

4x active port, 4x60m:

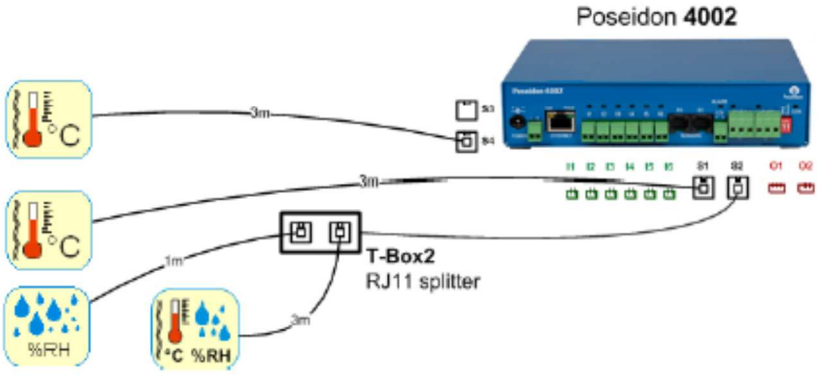

Appendix C : Heat power from electrical resistance of thermo3R

Les résistances de chauffage sont alimentées par un régulateur à découpage 1kHz, à alimentation continue.

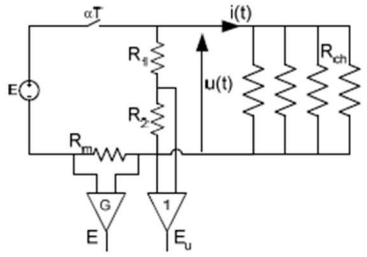

L'unité centrale mesure la tension moyenne aux bornes des résistances de chauffage à l'aide de ponts diviseurs et de convertisseurs analogiques numériques.

$$u(t) = \frac{R_1 + R_2}{R_2}.E_u(t)$$

Le courant qui parcours les résistances de chauffage est mesuré aux bornes de résistances séries de précision et amplifié d'un facteur G.

$$i(t) = \frac{G}{R_m}.E_I(t)$$

Après filtrage des signaux, on obtient des valeurs moyennes du courant et de la tension qui parcourent les résistances de chauffage.

$$I_{moy} = \frac{1}{T}\int_0^T \frac{G}{R_m}.E_I(t).dt \qquad U_{moy} = \frac{1}{T}\int_0^T \frac{R_1+R_2}{R_2}.E_U(t).dt$$

$$I_{moy} = \frac{1}{T}.\frac{G}{R_m}.E_{Imax}\int_0^{\alpha T} dt \qquad U_{moy} = \frac{1}{T}\frac{R_1+R_2}{R_2}.E_{Umax}\int_0^{\alpha T} dt$$

$$I_{moy} = \alpha.\frac{G}{R_m}.E_{Imax} \qquad U_{moy} = \alpha.\frac{R_1+R_2}{R_2}.E_{Umax}$$

$$I_{moy} = \alpha.I_{max} \qquad U_{moy} = \alpha.U_{max}$$

Avec :

$\alpha = \frac{T_{ON}}{T}$	Rapport cyclique du hacheur
U_{moy}, I_{moy}	Valeur moyenne de la tension, du courant
U_{max}, I_{max}	Amplitude de la tension, du courant

Les résistances étant très peu selfiques, le courant est haché comme la tension. Pour déterminer la puissance électrique injectée, il faut connaitre le rapport cyclique du hacheur.

$$P_e = \frac{1}{T}\int_0^T u(t).i(t).dt$$

$$P_e = \frac{1}{T}\int_0^{\alpha T} u(t).i(t).dt$$

$$P_e = \alpha.U_{max}.I_{max}$$

$$P_e = \frac{1}{\alpha}.U_{moy}.I_{moy}$$

Attention : Les voltmètres standards, en particulier les voltmètres numériques, ne sont pas adaptés à la mesure de tensions hachées à 1kHz. Utilisez de préférence un oscilloscope ou un wattmètre.

Régulation thermique

Coté froid

La régulation de température dans la zone froide est de type « Tout ou rien » à consigne et hystérésis réglables :

Si : $T_f \geq C_f + hyst$ Démarrage du groupe froid

$T_f \leq C_f - hyst$ Arrêt du groupe froid

avec :

T_f	Température de la zone froide
C_f	Consigne de température froide
$hyst$	Hystérésis

Lorsque le groupe froid est arrêté, le ventilateur de l'évaporateur fonctionne pour assurer le dégivrage.

Coté chaud en température

L'actionneur de chauffage étant proportionnel, la régulation de température dans la zone chaude est de type « PID » à consigne réglable :

Tel que : $\varepsilon_c = C_c - T_c$

$$Ch = K_p.\varepsilon + K_I.\sum \varepsilon + K_D.\frac{d\varepsilon}{dt}$$

avec :

T_c	Température de la zone chaude
C_c	Consigne de température chaude
ε_c	Ecart de température mesuré
Ch	Commande de l'actionneur chauffage
K_p	Gain proportionnel
K_I	Gain intégral
K_D	Gain dérivé